Hee Anthony Kong

A Thesis submitted for the Degree of

Doctor of Philosophy

University College London

University of London

October 2007

Cell Biophysics Laboratory

Protein Phosphorylation Laboratory

Lincoln's Inn Fields Laboratories

Cancer Research UK London Research Insti

&

Molecular Oncology Laboratory

Weatherall Institute of Molecular Medicine

University of Oxford

ProQuest LLC
789 East Eisenhower Parkway
P.O. Box 1346
Ann Arbor, MI 48106-1346

To my parents

"We shall not cease from exploration

And the end of all our exploring

Will be to arrive where we started

And to know the place for the first time"

T S Eliot (1888-1965)

Abstract

The decision to treat cancer patients with Iressa (Gefitinib, tyrosine kinase inhibitor of EGFR) and Herceptin (Trastuzumab, monoclonal antibody for HER2) is frequently based on EGFR or HER2 receptor over-expression. However, even in these selective groups of patients, the response rate is poor and unpredictable. The underlying mechanisms contributing to drug resistance, as well as predicting the success of these drugs in cancer patients are still poorly understood. One of the reasons for poor response rates based on HER (ErbB) levels is that over-expression *'per se'* fails to consider receptor activation for example through autocrine expression of one of its several ligands. Over-expression as a criterion for treatment fails to account for patients having receptor activation without up-regulation. It was hypothesized that using Förster Resonance Energy Transfer (FRET) to measure the functional status of EGFR in tumour arrays should provide more quantitative prognostic information than using immunohistochemistry alone. After validating a high throughput fluorescence lifetime microscopy (FLIM) system in a series of cell lines, it was shown that EGFR phosphorylation, reflected in high FRET efficiency, is correlated with worsening Disease Free Survival (DFS) in a set of head and neck tumour arrays.

The FRET methodology was applied further to assess the phosphorylation of HER2 and other HER family receptors in various breast cancer cell lines in relation to Iressa and Herceptin treatments. Monotherapy with Iressa while targeting EGFR and decreasing phosphorylation of HER3, induced proteolytic cleavage of HER4 and dimerisation between HER2 and HER4, leading to HER2 phosphorylation, as a result of ligand release. Therefore the activation of alternative pathways like HER2 and HER4 may mediate resistance to Iressa. It was also demonstrated that Herceptin while targeting HER2, parodoxically induced the phosphorylation of all HER receptors due to antagonist-induced ligand secretion. Therefore, it has been shown that Iressa and Herceptin treatment in breast cancer cells induces activation of alternative HER pathways, thus providing an insight into possible mechanisms of resistance for targeted therapies in breast cancer. The results suggest alternative treatments to

overcome resistance to these targeted therapies in patients.

FRET was also applied to assess HER2 phosphorylation in a set of HER2 positive breast tumour arrays using automated FLIM. It was shown that FRET maybe used to stratify HER2 positive breast cancer patients into different prognostic groups. It is proposed to utilise this assay for prospective stratification of patients in randomised trials of EGFR and HER2 inhibition. The methodology shows great promise and can also be applied to assess the activation of other signalling pathways (e.g. PKB and MAPK) in relation to various cancer treatments.

Acknowledgements

First and foremost, I would like to thank my supervisors Dr. Banafshe Larijani, Prof Peter Parker and Prof Adrian Harris for giving me the opportunity to pursue this interesting and challenging project. I would like to thank all of them for their patience and tireless support, and most importantly for teaching and guiding a beginner in science like me. I would like to thank Banafshe for the many hours that she dedicated to train me in laboratory skills, the use of the FLIM methodology, as well as presentation and writing skills. I want to thank Peter who despite being extremely busy had always found time for me and for his input in suggesting some of the crucial experiments done in this project. And for Adrian, who is always full of useful and interesting ideas, I want to thank him for his many useful suggestions as well as his advice in linking science and oncology for my project.

I would like to thank all the past and present members of Cell Biophysics Laboratory for making the period of my PhD very enjoyable and for the many hours that we shared and talked about our daily lives. I am particularly grateful to Veronique for her scientific advice, for her help in writing the papers, for her encouragement and support; Richard for teaching me western blot, for proof-reading my papers and for his British sense of humour (although I didn't always understand!); Marie, for her advice in IT skills and for organising get-together events for the lab (we had fabulous times in her house...); Natali, for her support and a listening ear; Damien, for his advice in physics and FLIM; Parbin for her help and company in the beginning of my PhD; as well as Prabhat, Thomas, Trung, Tina, Venassa and Fabrice for their friendship.

I would like to thank our consultant engineer, Pierre Leboucher (College de France) for the automation of FLIM done in collaboration with Banafshe, making it possible to process the tumour arrays in a high throughput manner and thus making my life easier! I am also grateful to many other colleagues and friends at the London Research Institute for their help and support, especially Li Khun for her friendship and for many hours of gossiping over the coffee times; Kirsty Allen and Lola Martinez (FACS laboratory) for their help in flow cytometry and cell viability experiments; Richard Whelan (Protein

Phosphorylation Laboratory), Emma Nye and especially Bradley Spencer-Dene (Experimental Pathology Laboratory) for their help in xenograft experiments; Darren Harvey (Cell Services) for preparing the cells; Yvonne Harman and Erin Fortin for their help in student issues; Peter Sheeham and David Bacon for their help in thesis writing. I also want to thank various colleagues from Weatherall Institute of Molecular Medicine (University of Oxford): Russell Leek for his help in the immunostaining and scorings of the tumour arrays; Stuart Winter for collecting the head and neck clinical data; Leticia Campo and Rekha Wadeka for preparing the tumour arrays.

I am indebted to Cancer Research UK for giving me a clinician training fellowship to support this PhD and for a pilot project award to fund part of the project. I am also grateful to Jo's trust for awarding me a James Maxwell fellowship that helped to pay part of the cost of my computer used for my PhD.

I want to thank all my friends for being there for me, particularly Joe for his uncomplaining help in numerous occasions when I was just too busy to do anything and for his unconditional and unselfish friendship; Howard who spent hours listening to me complaining about the whole world and stood by me throughout the difficult time of my PhD; Walter, for making me laugh and for being a true friend who speaks the truth even when it hurts; Pan for offering me a shoulder to cry on when things were difficult; Richard, for his advice on life issues; Anita, Fiona and Shareen for keeping me informed on the medical world of gossips.

And finally I thank my family (mum and dad, Joseph, Philip and Lina) for their support and encouragement even though they are so far away.

Abbreviations

ADAM: A disintegrin and metalloproteinase

APC gene: Adenomatosis polyposis coli gene

APMA: 4-Aminophenylmercuric acetate

AR: Amphiregulin

ASCO: American Society of Clinical Oncology

ATP: Adenosine triphosphate

BRCA 1 and BRCA2: Breast cancer genes

BSA: Bovine serum albumin

BTC: Betacellulin

CAP: The College of American Pathologists

CCD: Charged-coupled device (CCD)

CDK2: Cyclin-dependent kinase 2

CYT-1: Cytochrome c1, component of the mitochondrial respiratory chain

DAB: Diaminobenzidine

DAG: Diacylglycerol

DFS: Disease-free survival

2-D histograms: two-dimensional histograms

DMF: N, N-Dimethylformamide

DMEM: Dulbecco's modified eagle's medium

DMSO: Dimethylsulfoxid Methyl sufoxide

D/P ratio: Dye to protein ratio

ECL: Enhanced chemiluminescence

EDTA: Ethylenediamine tetraacetic acid

EGFR: Epidermal growth factor receptor

EGF: Epidermal growth factor

EPR: Epiregulin

Erk: Extracellular signal regulated kinase

ErbB family: Epidermal growth factor receptor family (were originally named because of their close homology to the erythroblastoma viral oncogene protein sequences, v-erbB)

FBS: Foetal bovine serum

FISH: Fluorescence *in-situ* hybridisation

FRET: Förster Resonance Energy Transfer

FLIM: Fluorescence Lifetime Imaging Microscopy

5-FU: 5 Fluoracil

Grb2: Growth factor receptor-bound protein 2

H&E stain: Haematoxylin & Eosin stain

HRP: Horseradish peroxide

HERA trial: Herceptin adjuvant trial

HB-EGF: Heparin-binding epidermal growth factor

HER: Human epidermal growth factor receptor

HRG: Heregulin

HNSCC: Head and neck squamous cell carcinoma

IHC: Immunohistochemistry

IP: Immunoprecipitation

IP3: Inositol triphosphosphate

MAPK: Mitogen-activated protein kinase

MCP: Micro-channel plate (MCP)

NBF: Neutral buffer formalin

NICE: National Institute of Centre of Excellence

NRG: Neuregulin

NSCLC: Non-small cell lung cancer

OS: Overall survival

PDK1: Phosphoinositide-dependent protein kinase-1

PBS: Phosphate buffered saline

PDGF: Platelet-derived growth factor

PFA: Paraformaldehyde

PH domain: Pleckstrin homology domain

PI3K: Phosphatidylinositol 3-kinase

PLC: Phospholipase C

PKC: Protein kinase C

PKB: Protein kinase B

PTEN: Phosphatase and Tensin homolog

PTB: Phosphotyrosine binding domain

PVDF: Polyvinylidene difluoride

Rb gene: Retinoblastoma gene

Ras: A G protein (a small GTPase)

RTK: Receptor tyrosine kinase

SCID mice: Severe combined immune deficiency mice

SDS-PAGE: SDS polyacrylamide gel electrophoresis

STAT: Signal transducer and activator of transcription

SW-AOM: Standing-wave acousto-optic modulator

Src: Oncogene of the chicken Rous sarcoma

SH2: Src homology 2

SH3: Src homology 3

SOS: Son-of-Sevenless

TACE: Tumour necrosis factor-α converting enzyme

TGF-α: Transforming growth factor α

TKI: Tyrosine kinase inhibitors

TMAs: Tumour microarrays

TPA: Tissue plasminogen activator

UV: Ultra-violet

UICC: Union Internationale Contre le Cancer (International Union Against Cancer)

VEGF: Vascular endothelial growth factor

YOP: *Yersinia enterocolitica* phosphatase

Table of Contents

List of Figures

Chapter 5

Chapter 6

List of Tables

Chapter 3

Chapter 6

1 Introduction

1.1 Background

Cancer treatments are becoming increasingly complicated as basic science research has led to the introduction of new biological agents or targeted therapies for clinical use. These agents bring great promise to cancer patients since they were developed to target specific abnormal signalling pathways in cancers, in contrast to the conventional radiotherapy and chemotherapy which are non-specific and affect both cancer and normal cells. However, the challenge remains of how to identify appropriate patients who will benefit from such agents. Moreover, many questions remain unanswered, including the best method of using these drugs in combination with radiotherapy, chemotherapy and endocrine therapy; what kinds of patients should receive these drugs; which are the appropriate biomarkers to predict response; the mechanisms of primary and secondary resistance to these drugs and how to prevent the onset of resistance in responders.

Dysregulation of epidermal growth factor receptors (HER or ErbB) receptors has been implicated in various epithelial cancers (Yarden and Sliwkowski, 2001). Drugs that target epidermal growth factor receptor family (ErbB or HER receptors` family) including EGFR (ErbB-1 or HER1) inhibitors and HER2 (ErbB2) monoclonal antibodies are among the very first generation of targeted therapies that were translated from basic science research into clinical use (Herbst, 2004). These drugs are gaining an increasingly important role in the treatment of various cancers, particularly the HER2 monoclonal antibody Herceptin (Trastuzumab) in breast cancer (Piccart-Gebhart et al., 2005; Romond et al., 2005)

The decision to treat cancer patients with EGFR inhibitor and HER2 monoclonal antibody have been based on EGFR and HER2 receptor over-expression (or gene amplification) respectively (Arteaga, 2002; Yaziji et al., 2004). More recently, EGFR inhibitors have been given to patients without

measuring EGFR concentration since the response of EGFR inhibitors do not necessarily correlate with the response to the drugs (Chung et al., 2005). The criteria of Herceptin treatment is still currently based on HER2 over-expression shown by immunohistochemistry (IHC) or HER2 gene amplification determined by fluorescence in situ hybridization (FISH) (Yaziji et al., 2004). However, despite the selection of these patients based on IHC and FISH, only about one third of these patients respond to Herceptin monotherapy (Vogel et al., 2002). Aside from the costs of the drugs and unpredictable response, up to 5-10% patients may have worsening cardiac function if given this drug with chemotherapy (Piccart-Gebhart et al., 2005). Therefore, to select the "right" patients who will benefit from this drug while sparing the "non-responders" from potential drug-induced cardiac problems is of utmost importance.

The present methods to select patients for HER receptor inhibitors based on immunohistochemistry (IHC) or fluorescence in situ hybridization (FISH) measure only receptor concentration without measuring the functional status of the receptors. Moreover, these methods are poor predictors for response to targeted therapies. There is a need for a better biomarker to predict response than the present methods. One specific approach is to measure the phosphorylation status of HER receptors since a number of mechanisms other than over-expression of HER receptors may cause increased activation and phosphorylation of HER receptors, including over-expression of ligands, dimerisation with other HER receptors to induce potent signalling as well as constitutively activated mutant HER receptors (Arteaga, 2002; Dei Tos AP, 2005). This may explain why the response to these drugs as monotherapy based on receptor concentration alone has been disappointing and the response rate rarely sustains long periods of time among the responders.

This thesis is based on a translational project that was performed using an interdisciplinary approach, integrating clinical oncology with cell biology, biophysics, chemistry as well as engineering and software interface for high throughput processing of the tumour samples. The project employed Förster Resonance Energy Transfer (FRET) (Lakowicz, 1999; Valeur, 2002) monitored by high throughput Fluorescence Lifetime Microscopy (FLIM) (Larijani, 2006) to answer some of the clinical questions regarding HER

receptors and the targeted therapies created by the introduction of these drugs from basic science research into clinical use. FRET has been shown to have many applications including the studies of protein-protein interaction, activities of protein kinases as well as study of protein conformation changes (Calleja et al., 2007). It was postulated that FRET could be exploited to assess the phosphorylation status of HER receptors in tumour arrays in comparison with the current IHC method. Although IHC staining for phosphorylated HER receptors is possible, being a single antibody method the results may be affected by various factors including non-specific staining and its specificity may be affected by the usage of high antibody concentration (Dei Tos AP, 2005). The FRET assay developed in this study uses a two-site assay overcomes the non-specificity problems encountered in the one-site assay used in immunohistochemistry.

In this thesis, FRET in combination with classical biochemistry were performed to assess the phosphorylation status of HER receptors in relation to targeted therapies in cell lines. The responses of HER receptors and mechanisms of resistance to EGFR and HER2 inhibitors were investigated in breast cell lines. In addition, a high throughput method was established in tumour arrays to assess phosphorylation status of EGFR and HER2 in relation to the prognosis of cancer patients.

In this chapter, the general aspect of tumour carcinogenesis and cellular signalling related to HER receptors will be discussed before an in-depth discussion of HER receptors and their inhibitors. The chapter will proceed to discuss the present methods of selection criteria for targeted therapies using IHC and FISH together with the principle of FRET monitored by FLIM before concluding with the aims and objectives of this thesis.

1.2 Carcinogenesis and cellular signalling

The continuous improvement in cancer treatment and the arrival of targeted therapies against HER receptors result from basic understanding of the cellular

carcinogenesis processes. To understand the importance of HER receptors and the targeted therapies against these receptors, one needs to put in context HER receptors in the overall carcinogenesis processes and cellular signalling. Carcinogenesis results from successive mutations in specific cellular genes, leading to the activation of oncogenes and inactivation of tumor suppressor genes. (Bertram, 2000). The mutations at the gene level may result in the over-expression of certain proteins or reduction of inhibitory proteins and may lead to dysregulation in the normal cellular signalling process as well as abnormal proliferation of the cells (Vogt, 1993).

1.2.1 Oncogenes and tumour suppressor genes

Normal cells are tightly regulated for their signalling and proliferation. The main difference of a normal cell and a tumour cell is that the latter may proliferate in an uncontrolled manner, due to either mutations in and/or dysregulation of multiple genes (Grander, 1998) However, not all mutations contribute to carcinogenesis since most cells that harbour such genes are destined for repair or elimination (e.g. through apoptosis) (Polverini and Nor, 1999). The genes that contribute to tumourigenesis can be divided into two categories: oncogenes and tumour suppressor genes (King, 2000). Each gene in a cell contains two alleles and mutation of one of these may transform the normal "proto-oncogene" to an activated, transforming, dominant oncogene. An oncogene represents a gain-of-function mutation that may results in the production of a protein product that is constitutively active and not regulated in the normal way, resulting in tumourigenesis (King, 2000; Tannock et al., 2005). By contrast, tumour suppressor genes are recessive and require the loss or the inactivation of both alleles before malignant transformation (King, 2000; Tannock et al., 2005). Hence a tumour suppressor gene represents a loss-of-function mutation. Carcinogenesis may result from either the activation of oncogene (s) or the inactivation of tumour suppressor gene (s) or both (Hanahan D, 2000).

An oncogene activation resulting from the mutation or deregulation of a proto-oncogene, produces protein products leading to tumourogenesis (Vogt, 1993). There are many ways that these oncogenes may be activated. For example, some retroviruses may incorporate their viral form of the oncogenes into the host DNA, in which regulatory viral sequences alter host gene activity resulting in the deregulated activity of the protein product (King, 2000). Chromosomal translocation may also lead to constitutive expression and activation of oncogenes, e.g. in Burkitt's lymphoma, the reciprocal translocation of chromosome 8 with chromosome 14 resulting in the myc gene being transcribed by the active immunoglobulin regulatory region (Taub et al., 1982). Lastly the amplification of the genomic locus containing a proto-oncogene can also lead to oncogene activation since multiple copies of the gene are produced and the encoded protein is highly expressed disrupting a particular regulatory balance (Tannock et al., 2005). For example HER2 gene amplification has been shown in human breast cancer and correlates with the poor prognosis in breast cancer patients (Slamon et al., 1987).

The mutations and deregulation of oncogenes act in a dominant manner and are associated with sporadic tumours. By contrast most inherited cancers are a consequence of the mutations or inactivation of tumour suppressor genes (King, 2000). Tumour suppressor genes are recessive at the somatic level and require the loss or the inactivation of both alleles before malignant transformation. In 1971, Knudson investigated the epidemiology of familial retinoblastoma (a hereditary form of retinal cancer) and found that patients with familial disease were more likely to develop a more severe, bilateral or multifocal disease at an earlier age of onset compared to sporadic cases of retinoblastoma (Knudson, 1971). He proposed that two mutations or two hits were required for retinoblastoma (Knudson's two hit hypothesis). In familial cases, the first mutation is transmitted through the germline and is present in all cells but the tumour develops when the second mutation occurs somatically (Knudson, 1971; Tannock et al., 2005). In sporadic cases both mutations have to occur within the same somatic cell, this being more probable event may explain the late onset of the disease (Knudson, 1971; Tannock et al., 2005). His hypothesis highlights the cooperation between inherited and somatic mutations and deregulation in human cancers. The retinoblastoma gene Rb is

the tumour suppressor gene implicated in retinoblastoma and loss of retinoblastoma gene Rb is a frequent event in human cancers, including breast cancers (Lee et al., 1988). Other tumour suppressor genes that are involved in human carcinogenesis include p53 gene (Vousden and Prives, 2005), PTEN (Depowski et al., 2001; McMenamin et al., 1999) and BRCA1 and BRCA2 genes (Suthers, 2007). The p53 gene is the gene most frequently altered in human cancers and loss of p53 activity appears to be important for malignant progression (Vousden and Prives, 2005). Loss of pTEN is associated with poor prognosis and outcomes for several cancers including breast cancer and prostate cancers (Depowski et al., 2001; McMenamin et al., 1999). Mutations of BRCA1 and BRCA2 are associated with increased risk of cancers (Chen and Parmigiani, 2007), with the cumulative lifetime risk in developing breast cancer being 50-60% and the equivalent risk of ovarian cancer is 20-40% (Suthers, 2007).

The oncogenes and tumour suppressor genes can generate carcinogenesis on their owns. However, more commonly synergism occurs between cooperating oncogenes and tumour suppressor genes, e.g. APC, K-ras and p53 mutations in colon carcinogenesis (King, 2000). Therefore, oncogenes and tumour suppressor genes cooperate in carcinogenesis (Grander, 1998).

1.2.2 Cellular signalling

Tumour oncogenes and tumour suppressor genes may result in the over-expression of certain proteins or reduction in the expression of others and thus may lead to dysregulation of the normal cellular signalling process with consequent abnormal cellular proliferation (Grander, 1998). For example, EGFR gene amplification may lead to over-expression of EGFR and ligand-independent cellular dysregulation and proliferation (Chung et al., 2006; Nicholson et al., 2001). Cellular signalling is normally a well-regulated process through an elaborate network of intracellular signals transmitted by changes in the protein phosphorylation of the receptors (King, 2000). The regulation is typically controlled by growth factors which are secreted

polypeptides that trigger cascades of signalling processes within cells via their interaction with specific transmembrane receptor tyrosine kinases (RTKs) (Blume-Jensen and Hunter, 2001). There have been a large number of growth factors or ligands identified with diverse functions including cell growth, proliferation, differentiation, survival and metabolism although only a few has been associated with carcinogenesis (Tannock et al., 2005). These growth factors have variable specificities for these RTKs receptors in different cells and thus create diverse signalling processes between them (Robinson et al., 2000). They are usually small monomeric (single chain) polypeptides (e.g. EGF) although they can exist as dimeric polypeptides (e.g. PDGF) (Tannock et al., 2005). They interact with specific domains of the RTKs in the extracellular domain to cause intracellular signalling (Cho et al., 2003; Franklin et al., 2004).

Receptor protein tyrosine kinases (RTKs)

HER receptors belong to the receptor protein tyrosine kinases (RTKs) which represent a large family of molecules (Yarden and Sliwkowski, 2001). More than 60 of them have been identified and they are also subdivided into different families according to the their distinct structural components (van der Geer et al., 1994). Most of the RTKs consist of extracellular domains which are connected to the intracellular (cytoplasmic) domains by single short hydrophobic helix transmembrane components (Robinson et al., 2000). The cytoplasmic domain is comprised of regulatory sequences and a conserved kinase domain. The kinase domain is capable of phosphorylating tyrosine residues of a protein by catalysing the transfer of a phosphate group from adenosine trisphosphate (ATP) onto the protein substrate. The regulatory sequences contain sites of tyrosine phosphorylation and usually regulate catalytic activities as well as signal transmission (Robinson et al., 2000). Without the growth factor, the intracellular kinase domain is usually inactive and is held in a repressed conformation by intramolecular interactions. Upon the binding of growth factor or ligand, the extracellular domain undergoes conformational changes that facilitate dimerisation between the receptors (Cho et al., 2003). The dimerisation of two receptors bring their catalytic domains

together, resulting in intermolecular transphosphorylation of tyrosine residues within the catalytic domain and in the noncatalytic regulatory sequences of the cytoplasmic domain (Schlessinger, 2002). The phosphorylation of key residues within the kinase activation loop induces the alignment of the catalytic site and allows access to ATP and protein substrates (Robinson et al., 2000). The phosphorylation of tyrosine residues in non-catalytic regions creates docking sites for downstream signalling molecules that are essential for signal transduction.

Carcinogenesis may result from abnormal RTKs which are ligand independent and deregulated with increased catalytic activity. For example, the amplification of HER2 oncogene results in the over-expression of HER2 RTKs (Slamon et al., 1987) that increase the concentration of active dimers in generating continuous and uncontrolled cellular signalling.

Formation of protein complexes and activation of downstream pathways

Upon ligand binding, a network of downstream signalling pathways of RTKs is created through interaction of specific proteins (Tannock et al., 2005) (Figure 1.1). The activation of RTKs creates a number of docking sites for cytoplasmic proteins including those that contain SH2 (Src homology 2), PTB (phosphotyrosine binding domain), SH3 (Src homology 3) and PH (Pleckstrin homology) domain (Figure 1.1) (Tannock et al., 2005). These proteins mediate the formation of signalling complexes following the activation of receptor tyrosine kinases. Different SH2 domains recognise specific tyrosine phosphorylated motifs in the non-catalytic regions (Songyang et al., 1993). The PTB domains recognise phosphotyrosine in a specific sequence motif where amino acids on the amino terminal side of the tyrosine are critical for binding specificity (van der Geer and Pawson, 1995). SH3 can bind to proline rich motifs in target proteins and the interaction is not dependent on changes induced by phosphorylation. They function in the assembly of multiprotein complexes, and as regulatory domains in intramolecular interaction. A number of PH domains interact specifically with membrane phosphoinositides and recognise specific phosphoinositides such as PtdIns(3,4,5)P3 that are transiently produced following growth factor receptor activation (Bazley and Gullick, 2005).

The activated RTKs may associate with phospholipase C (PLCγ) via the SH2 domain, hydrolysing phosphatidyl inositol (PIP2) into inositol triphosphate (IP3) and diacylglycerol (DAG) (Figure 1.1) (Tannock et al., 2005). Many activated growth factor receptors also result in the activation of PI-3 kinases, comprises a catalytic subunit p110 and a regulatory subunit p85, leading to the activation of PKB and PDK1 via PH domain, the refined mechanisms of which have recently been proposed by Calleja et al (2007) (Calleja et al., 2007).

The binding of growth factors to RTKs results in the phosphorylation of the intracellular domain on tyrosine residues, which are targets of the adaptor proteins (Figure 1.1) (Tannock et al., 2005). The adaptor proteins (e.g. growth factor receptor bound-2, grb2) are composed entirely of SH2 and SH3 domains without catalytic activity (Bazley and Gullick, 2005). They however interact with signalling enzymes which do not contain SH2 domains, thereby coupling them to tyrosine kinase signalling complex (Pawson and Scott, 1997). Each of these adaptor molecules has a different capacity to form protein complexes due to binding specificities of its SH2 and SH3 domains, resulting in an organised network of protein-protein interactions within the extensive intracellular signalling network (Tannock et al., 2005). The adaptor protein grb2 plays an important role in the activation of the small GTPase protein, Ras. The Ras protein is a central transducer of growth factor receptor signals and it is a membrane-associated molecule that is activated when bound to the guanine nucleotide GTP (Downward, 2006). The SH2 domain of grb2 associates with the some of the receptors when activated while the SH3 domains are bound to SOS (Son-of-Sevenless), which is a guanine nucleotide exchange protein that activates Ras (Figure 1.1) (Bazley and Gullick, 2005). The small GTPase Ras cycles between the inactive GDP bound state and the active GTP bound state and Ras is activated when SOS promotes the exchange of GDP for GTP (Downward, 2006). The activation of Ras leads to the downstream signalling including activation of the extracellular signal regulated kinase 1 and 2 (ERK1/2) (mitogen activated protein kinase MAPK signalling pathways) (Figure 1.1).

The formation of protein complexes and activation of downstream pathways described above is common to a large family of RTKs and its dysregulation may lead to carcinogenesis processes. HER receptors are among the most

important RTKS implicated for human carcinogenesis (Nicholson et al., 2001) and the specific details of HER receptors will be described in the next section.

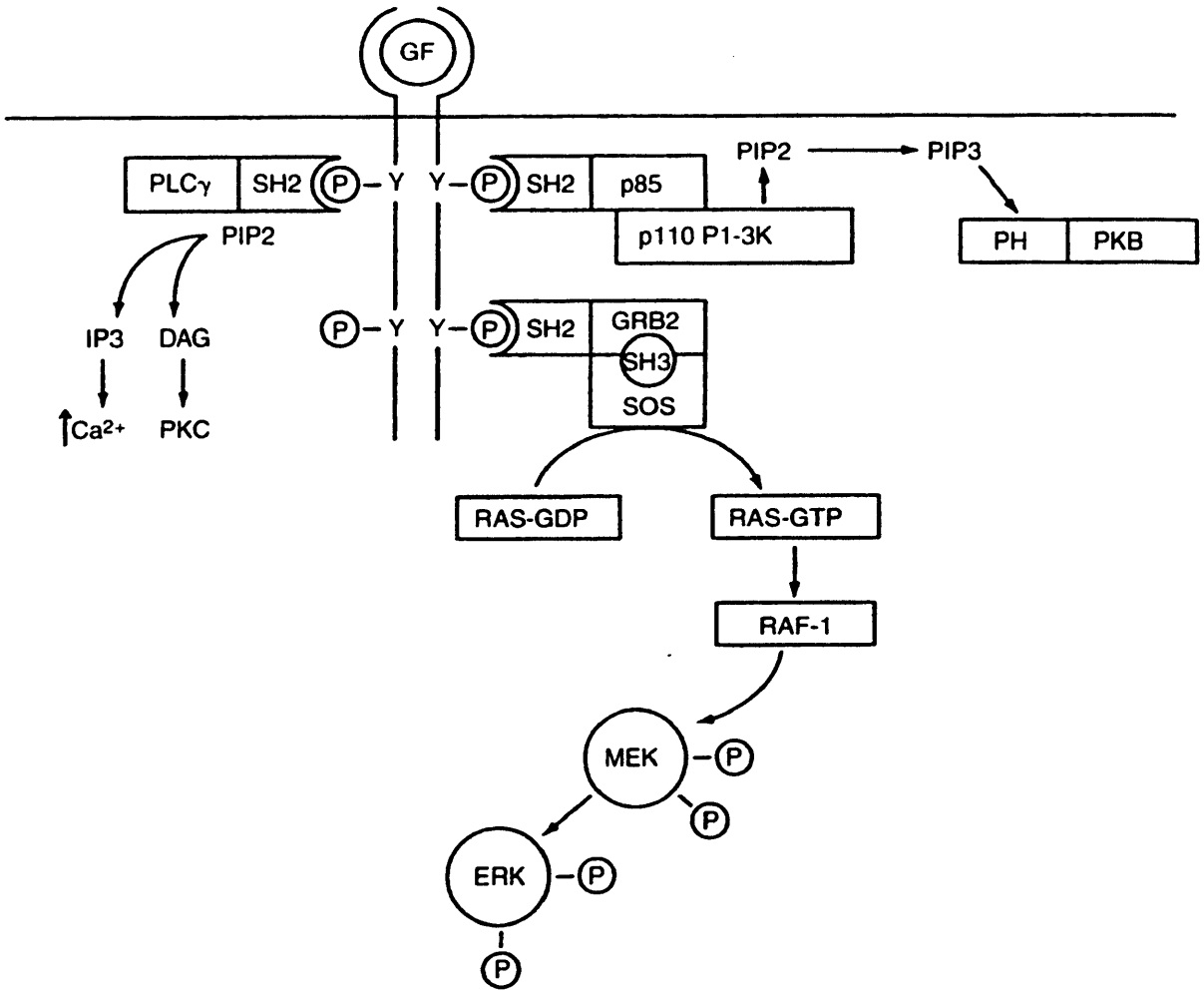

Figure 1.1: Receptor protein tyrosine kinases and recruitment of cytoplasmic signalling molecules. See list of abbreviations. Figure taken from Tannock et al 2005.

1.3 HER (ErbB) family

The epidermal growth factor (HER or ErbB) family comprises four receptors: EGFR (also known as HER1 or ErbB1), HER2 (ErbB2), HER3 (ErbB3) and HER4 (ErbB4) (Bazley and Gullick, 2005). ErbB receptors were originally named because of their close homology to the erythroblastoma viral oncogene protein sequences, v-erbB (Downward et al., 1984). These receptors belong to subclass I of the superfamily of RTKs which are transmembrane receptors with an intrinsic ability to phosphorylate their tyrosine residues in the cytoplasmic domains to transduce signals (Citri and Yarden, 2006). However, HER2 and HER3 are not autonomous since HER2 has no known ligand and the kinase activity of HER3 is defective (Yarden and Sliwkowski, 2001). These two receptors can form heterodimeric complexes with each other as well as other HER receptors to generate potent signals (Olayioye et al., 2000).

A number of ligands can activate HER receptors (see table below). These ligands include epidermal growth factor (EGF), amphiregulin (AR), transforming growth factor-α (TGFα) for EGFR; betacellulin (BTC), heparin-binding EGF (HB-EGF) and epiregulin (EPR) for EGFR and HER4; neuregulin (NRG) 1-4 (also called heregulin or neu differentiation factor) for HER3 and HER4 (NRG-1 and NRG-2 bind to HER3 and HER4 but NRG-3 and NRG-4 bind to HER4 only) (Olayioye et al., 2000) (Figure 1.2A). However, no direct ligand for HER2 has been identified.

HER receptors	**Ligands**
EGFR	- EGF, AR, TGFα - BTC, HB-EGF and EPR (co-ligands with HER4)
HER2	- No direct ligand
HER3	- NRG (heregulin) 1-2 (co-ligands with HER4)
HER4	- NRG (heregulin) 1-4 (co-ligands with HER3); - BTC, HB-EGF and EPR (co-ligands with EGFR)

The ligands determine which receptor dimers are formed and thus influence the activation of various signalling pathways (Beerli and Hynes, 1996). The HER receptors are able to dimerise (homodimerisation) or interact with different receptors (heterodimerisation) upon ligand binding (Bennasroune et al., 2004). The homo- or hetero-dimerisation of the receptors results in the activation of the intrinsic tyrosine kinase domain and autophosphorylation of specific tyrosine residues in the C-terminus. Depending on the pattern of phosphorylated tyrosine residues in the C-terminus, different subsets of SH2- and PTB-binding signalling molecules are recruited to the activated receptors (Figure 1.2B). The specific characteristics of each HER receptor will be discussed below.

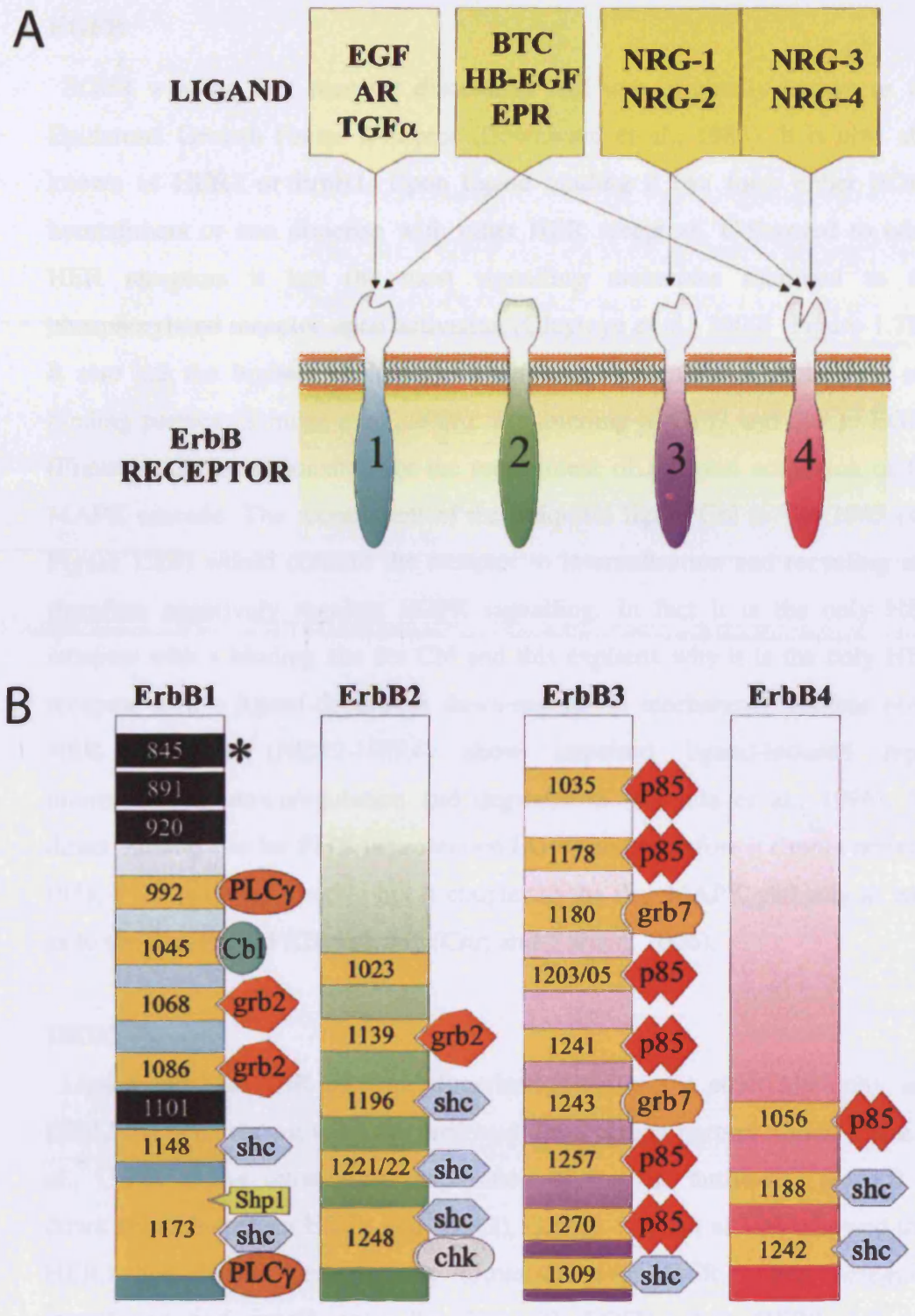

Figure 1.2: A, HER (ErbB) receptors and their ligands. **B,** Specific phosphotyrosine residues and binding sites of signalling molecules to the cytoplasmic domains of HER receptors. For ErbB1, the sites for the Src kinase are in black, including Y845 in the kinase domain (indicated by asterick) (Figures taken from Olayioye et al 2000)

EGFR

EGFR was the first receptor discovered and was originally known as the Epidermal Growth Factor Receptor (Downward et al., 1984). It is now also known as HER1 or ErbB1. Upon ligand binding it can form either EGFR homodimers or can dimerise with other HER receptors. Compared to other HER receptors it has the most signalling molecules recruited to the phosphorylated receptor upon activation (Olayioye et al., 2000) (Figure 1.2B). It also has the highest percentage of tyrosine residues with more than one binding partner (Schulze et al., 2005). The binding of Grb2 and Shc to EGFR (Figure 1.2B) is responsible for the recruitment of Ras and activation of the MAPK cascade. The recruitment of the ubiquitin ligase Cbl to Tyr 1045 (see Figure 1.2B) would commit the receptor to internalisation and recycling and therefore negatively regulate EGFR signalling. In fact it is the only HER receptor with a binding site for Cbl and this explains why it is the only HER receptor with a ligand-dependent down-regulation mechanism whereas other HER receptors (HER2-HER4) show impaired ligand-induced rapid internalisation, downregulation and degradation (Baulida et al., 1996). No direct binding site for PI3K is present on EGFR and therefore it cannot activate PI3K-PKB pathway directly but it couples to the Ras-MAPK pathway as well as to the Ras-PI3K-PKB pathway (Citri and Yarden, 2006).

HER2

Ligand induced HER receptor dimerisation follows a strict hierarchy and HER2 has been shown to be the preferred dimerisation partner (Graus-Porta et al., 1997). Using intracellular expression of specific antibodies (scFV0 to down regulate surface EGFR and HER2), Graues-Porta et al 1997 showed that HER3 and HER4 preferentially dimerised with HER2 upon heregulin stimulation and would only dimerise with EGFR when HER2 was not available partner (Graus-Porta et al., 1997). In addition, they showed that EGF and betacellulin induced HER3 activation was dramatically impaired in the absence of HER2, suggesting that HER2 mediates lateral transmission between other HER receptors. They also showed that HER2 enhanced and prolonged MAPK signalling in response to various ligands. Over-expression of HER2

may cause ligand independent activation as well as activation of EGFR (Worthylake et al., 1999). HER2 containing dimers have defective endocytosis and enhanced recycling properties (Lenferink et al., 1998; Sorkin et al., 1993).

HER3

HER3 is kinase defective but it can form functional dimers with other HER receptors. Upon dimerisation and tyrosine phosphorylation of its cytoplasmic domain, HER3 can recruit PI3K to six distinct sites (Y1035, 1178, 1203/05, 1241, 1257 and 1270) and Shc to one site (Figure 1.2B). Together with HER2 it can generate downstream signalling both through the Ras-Erk pathway for proliferation, and through the PI3K-PKB pathway for survival (Citri et al., 2003). Wallasch et al (1995) showed that the tyrosine phosphorylation of HER2 and HER3 receptors upon heregulin stimulation did not occur when the kinase-inactive HER2 mutation was co-expressed with HER3 in cells; whereas HER2/HER3 transphosphorylation was stimulated by heregulin when HER2 was coexpressed with the kinase-inactive HER3 receptor mutant (Wallasch et al., 1995). Therefore, activation of the signalling potential of the HER2/HER3 dimer upon heregulin stimulation is due to unidirectional transphosphorylation of HER3 by the HER2 kinase.

HER4

HER4 shares recognition and signalling features with EGFR, including common ligands (betacellulin, HB-EGF and epiregulin) and an ability to recruit GRB2, Shc and STAT5 (Citri and Yarden, 2006). An isoform of HER4 (CYT-1) can also activate PI3K (Elenius et al., 1999). Moreover, it has been shown that proteolytic cleavage of HER4 occurs in cells at a low basal level and can be increased by TPA, heregulin, or other growth factors that bind HER4 (Zhou and Carpenter, 2000) (Figure 1.3). The ectodomain cleavage of HER4 is mediated by tumour necrosis factor-∝-converting enzyme (TACE), a transmembrane metalloprotease. Proteolysis produces a membrane-anchored fragment (80 kD) which consists of the entire cytoplasmic and transmembrane domain (Carpenter, 2003; Vecchi and Carpenter, 1997). The m80 HER4 fragment from ectodomain cleavage was found to associate with full length HER2 (Cheng et al., 2003). In addition, the transmembrane m80 was found to

be cleaved by γ-secretase and the soluble fraction (S80) was found to be associated with STAT5A as well as translocated to the nucleus to influence transcription (Ni et al., 2001; Williams et al., 2004). The growth factor-dependent HER4 cleavage seems to involve endocytosis while TPA-dependent cleavage does not (Figure 1.3) (Carpenter, 2003).

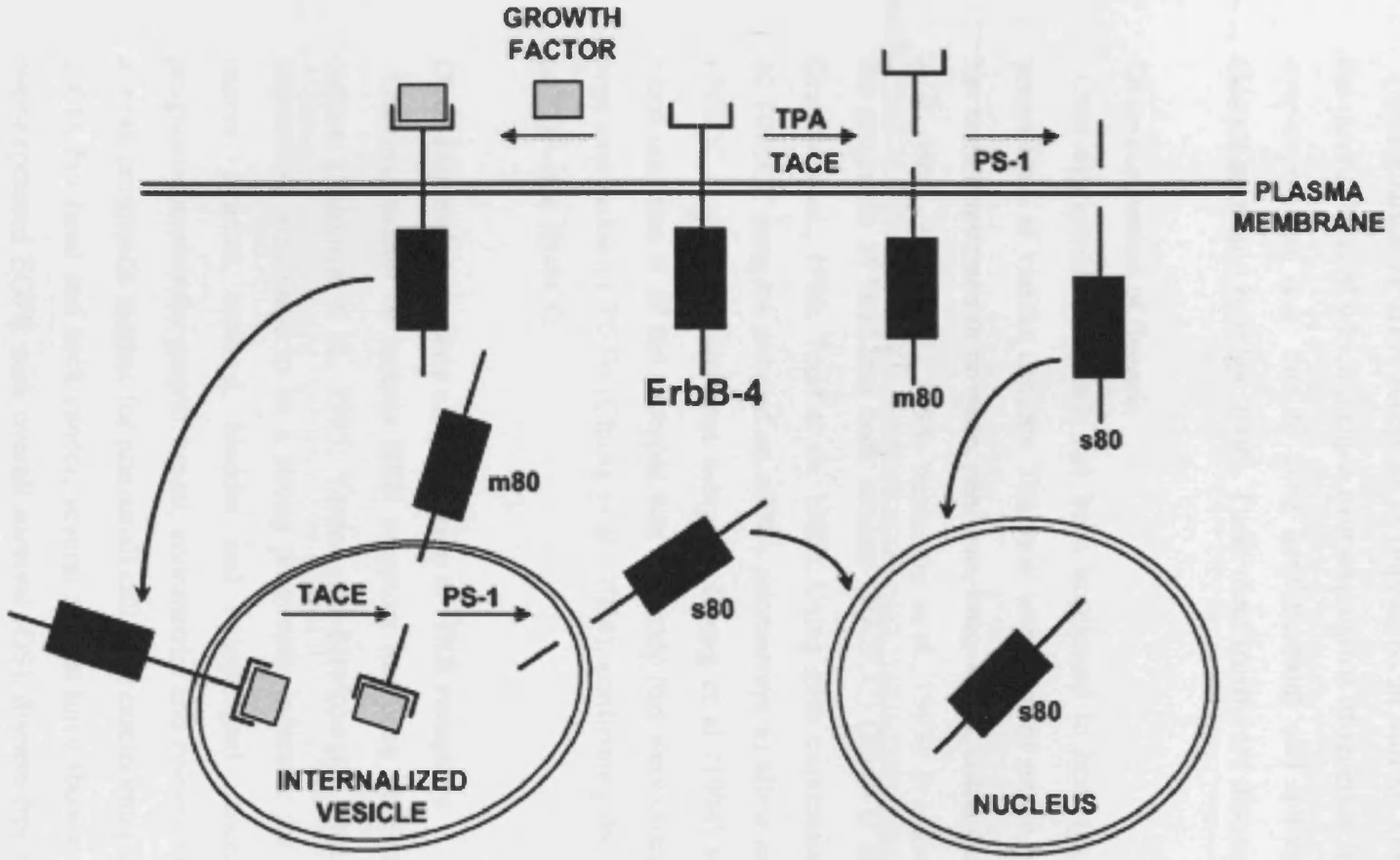

Figure 1.3: Proteolytic cleavage pathway for HER4 (ErbB4). The ectodomain cleavage of HER4 can occur upon TPA treatment or growth factors that bind to HER4. This process is mediated by TACE, producing a membrane-anchored fragment, m80, consisting of entire cytoplasmic and transmembrane domain. The transmembrane m80 was then cleaved again by gamma-secretase (PS-1). Growth factor-dependent HER4 cleavage seems to invlove endocytosis, while TPA-dependent HER4 cleavage does not although either route produces m80 which is found in the nucleus (Figure taken from Carpenter et al 2003).

1.4 HER receptors and cancers

Dysregulation of HER receptors is implicated in various epithelial cancers, the mechanisms of which include over-expression of receptor ligands, receptor over-expression (e.g. due to gene amplification) and activating mutations (Mendelsohn and Baselga, 2006). These mechanisms are discussed below.

Over-expression of ligands

Over-expression of ligands has been implicated in both the prognosis and progression of various cancers. The most important of which is TGF-α which has been implicated in prostate, pancreas, lung, ovary, colon cancers (Salomon et al., 1995; Scher et al., 1995; Yamanaka et al., 1993). It is also implicated in the prognosis of head and neck cancers (HNSCC) (Endo et al., 2000; Rubin Grandis et al., 1996; Todd et al., 1989). Using gene expression patterns from 60 HNSCC samples assayed on cDNA microarrays to allow categorisation of HNSCC tumors into different subtypes, Chung et al (1994) showed that the worst outcome of all the subtypes was the group that were characterised by the high expression of TGFα (Chung et al., 2004), confirming the prognostic role of TGF-α in HNSCC.

Over-expression or gene amplification of HER receptors

Over-expression of various HER receptors has been implicated in various cancers (Salomon et al., 1995; Yarden and Sliwkowski, 2001). EGFR over-expression was found to be a strong prognostic indicator for head and neck cancer, ovarian, cervical, bladder and oesophageal cancer; a moderate prognostic marker for gastric, breast, endometrial and colorectal carcinoma but a weak prognostic marker for non-small cell lung carcinoma (Nicholson et al., 2001). For head and neck cancer, several studies have shown a correlation of over-expressed EGFR with overall survival (OS), disease-free survival (DFS), increased loco-regional recurrence and decreased sensitivity to radiation treatment in these patients (Ang et al., 2002; Dassonville et al., 1993; Gupta et al., 2002; Sheridan et al., 1997). Gene amplification of EGFR was also shown

to be associated with prognosis of head and neck cancer (Chung et al., 2006). The amplification of HER2 was first shown to be a significant predictor for both overall survival and time to relapse in breast cancer patients (Slamon et al., 1987). The protein expression of HER2 was also found to correlate with the prognosis of breast cancer patients (Hartmann et al., 1994; Marks et al., 1994; Rosen et al., 1995; Ross and Fletcher, 1999).

Mutation of HER receptors

Several mutations involving HER receptors have been reported. One of the commonest mutations in EGFR is the deletion of a section of the extracellular domain resulting in a constitutively active receptor, e.g. in glioblastoma (Moscatello et al., 1995) although the mutation is rare in breast cancers and other cancers (Rae, Scheys et al. 2004). Mutations of EGFR, either small, in-frame deletions or amino acid substitutions (including L858R) clustered around the ATP-binding pocket of the tyrosine kinase domain, have been detected in human lung cancer (Lynch et al., 2004). They seem to increase the kinase activity and predict a dramatic response to Iressa (Lynch et al., 2004). The mutations are associated with bronchioloalveolar pathology that arise in non-smoker, and in individuals of East Asian descent (Paez et al., 2004). However, EGFR kinase domain mutations rarely present in other types of cancers although they have been reported in a few cancer types including small cell lung cancer, ovarian, oesophageal and pancreatic carcinoma (Kwak et al., 2006; Okamoto et al., 2006; Schilder et al., 2005). In head and neck cancer, where the majority of patients have over-expression of EGFR most Caucasian patients do not have the mutations seen in non-small cell lung cancer, except in a small proportion of patients from certain ethnic origins (Loeffler-Ragg et al., 2006). Furthermore, the activating mutations in EGFR exons are also uncommon in sporadic breast cancer (Generali et al., 2007). HER2 mutation (including a $G776^{YVMA}$ insertion in exon 20) has also been found in lung cancer, resulting in constitutive activation of HER2 and EGFR. The mutations rendered the cells resistant to EGFR tyrosine kinase inhibitors but the cells remained sensitive to HER2 inhibitors (Wang et al., 2006). However, the HER2 kinase domain mutations are only found in a small proportion of

patients in gastric carcinoma, colorectal and breast cancer (5% or less) (Lee et al., 2006).

1.5 HER receptors and targeted therapies

Since over-expression of ligands as well as the HER receptors are implicated in the carcinogenesis, various targeted therapies against these HER receptors are increasingly used in various cancers. These include inhibitors of EGFR and HER2 receptors and the mechanisms of these drugs and their clinical use will be discussed in this section.

In order to understand how these inhibitors work on EGFR and HER2 receptors, the crystal structure of HER receptors needs to be discussed. HER receptors comprise an extracellular domain, transmembrane region, a small intracellular juxtamembrane domain preceding a cytoplasmic protein tyrosine kinase domain, and a C-terminal tail, on which the phosphotyrosine-binding molecules are recruited (Cho et al., 2003). The extracellular region of about 630 amino acids, consists of four subdomains: I, II, III and IV (Cho et al., 2003) (Figure 1.4a). The subdomains I (L1) and III (L3) are leucine-rich repeats and subdomains II (CR1 or S1) and IV (CR2 or S2) are laminin-like, cysteine-rich domains. The crystal structure revealed that ligands bind to domain I and III. Domain II mediates inter-receptor dimerisation via its long-finger-like projection although it is in intramolecular contact with domain IV when the receptors are not activated. The unliganded receptors exist in an autoinhibited ('closed') form but become 'open' upon ligand stimulation when domains I and III are brought close together, breaking the domain II and IV interaction and allowing domain II to participate in dimerisation of the receptors. The only exception is HER2 receptor since its extracellular domain is always in the 'open' conformation with the projection of domain II ready for dimerisation even when monomeric (Figure 1.4a) (Franklin et al., 2004). This fixed 'open' conformation of HER2 in the absence of ligand binding (mimicking the ligand-bound form in the EGFR structure) may account for

why it is the preferred dimerisation partner for other HER receptors (Cho et al., 2003).

EGFR inhibitors

The two principal classes of EGFR inhibitors are monoclonal antibodies that bind to the extracellular domain (e.g. Cetuximab) and quinazoline small molecular inhibitors of the intracellular kinase domain (e.g. Gefitinib and Erlotinib) (Mendelsohn and Baselga, 2003).

Cetuximab is a human-murine monoclonal antibody to EGFR. Cetuximab has been most extensively investigated compared to other existing anti-EGFR monoclonal antibodies. For EGFR to change its conformation resulting in the extension of the dimerisation arm of domain II, ligand must engage sites on both domain I and III for high affinity binding (Mendelsohn and Baselga, 2006). Cetuximab binds to extracellular domain III of EGFR occluding the ligand binding on this domain and prevents the receptor from adopting the conformation required for dimerisation. Therefore it blocks activation of receptor tyrosine kinase by the ligands. Cetuximab has been used in cancers of colon and head and neck. It has been shown to have a modest activity in chemotherapy refractory colon carcinoma that express EGFR with a partial response rate of 9% (Saltz et al., 2004). In a randomised trial, 329 patients were assigned to either Cetuximab monotherapy or Cetuximab in combination with chemotherapy for treatment of EGFR expressing metastatic colon carcinoma that are refractory to standard Irinotecan (topoisomerase-1 inhibitor) chemotherapy (Cunningham et al., 2004). The response rate for Cetuximab monotherapy was 10% and that of the combination therapy was 23%. In head and neck cancer, a phase III trial which randomly assigned 424 head and neck cancer patients to receive either radiation therapy alone or radiation with concurrent Cetuximab showed that Cetuximab nearly doubled the median survival in these patients (Bonner et al., 2006). Cetuximab is now licensed for treatment of colon carcinoma and head and neck cancer.

Gefitinib (ZD 1839, Iressa) and Erlotinib (Tarceva) are reversible tyrosine kinase inhibitors of EGFR. These low molecular weight inhibitors act intracellularly by competing with ATP for binding to the tyrosine kinase domain of EGFR and thus inhibiting the enzymatic activity (Mendelsohn and

Baselga, 2006). It has been shown that these inhibitors may induce inactive EGFR homodimers and EGFR/HER2 dimers and thus prevent EGFR mediated transactivation of EGFR and HER2 activities (Arteaga et al., 1997; Geyer, 2006; Lichtner et al., 2001). It has also been shown that they inhibit PI3K and PKB pathways via inhibition of EGFR/HER3 (Engelman et al., 2005). Moreover, they are also effective in HER2 over-expressing breast cancer cells through the inhibition of EGFR mediated lateral heterodimerisation (Anderson et al., 2001; Anido et al., 2003; Moulder et al., 2001). Both Iressa and Tarceva have been used in non-small cell lung carcinoma (NSCLC) with some modest response. Patients with advanced stage NSCLC, who had progressed on first-line or second chemotherapy were randomised to either Tarceva or placebo (Shepherd et al., 2005). NSCLC patients who received Tarceva had a statistically significant increase in overall survival by 2 months compared to those who received placebo alone although the response rate was only 8.9%. Iressa has also been used in NSCLC patients with a similar response rate to Tarceva but the difference in overall survival compared to placebo was not statistically significant (Fukuoka et al., 2003; Kris et al., 2003). Some of these patients have mutations around the ATP-binding pocket of tyrosine kinase domain which render these patients highly sensitive to Iressa (Lynch et al., 2004). Iressa has been tested in a phase II trial in head and neck cancer (HNSCC) and the response rate was about 10% (Cohen et al., 2003).

HER2 inhibitors

The drugs that target HER2 are a monoclonal antibody that binds to HER2 in the extracellular domain, Trastuzumab (Herceptin); inhibitor of HER2 dimerisation that also acts extracellularly, Pertuzumab; and the small molecular inhibitor targeting the tyrosine kinase activities of EGFR and HER2, Lapatinib.

Herceptin binds to the juxtamembrane region of HER2 of domain IV (Cho et al., 2003) (Figure 1.4b). There have been several proposals of mechanisms of Herceptin to explain its clinical benefits but the precise mechanisms of action are still not known. The current proposed primary mechanisms of action for HER2 include HER2 receptor downregulation and inhibition of aberrant receptor tyrosine kinase activity (Cuello et al., 2001; Sliwkowski et al., 1999).

There was also suggestion of immune mediated mechanisms from the interaction of Herceptin's human Fc region with immune effector cells, resulting in the stimulation of natural killer cells and activation of antibody-dependent cellular cytotoxicity (Clynes et al., 2000; Cooley et al., 1999). More recently it was shown that Herceptin increased PTEN membrane localization and phosphatase activity by reducing PTEN tyrosine phosphorylation via Src inhibition (Nagata et al., 2004). Moreover, PTEN deficiency is predictive for Herceptin resistance (Nagata et al., 2004). Other proposed mechanisms include inhibition of basal and activated HER2 ectodomain cleavage in breast cancer cells (Molina et al., 2001), and increased $p27^{Kip1}$ levels and interaction with CDK2, resulting in decreased CDK2 activity (Lane et al., 2001). Unlike Pertuzumab, Herceptin does not prevent dimerisation of other receptors with HER2 (Agus et al., 2002). Herceptin was first shown to increase an objective response, longer time to disease-free progression and longer survival for metastatic breast cancer patients where tumours over-express HER2 receptors (Slamon et al., 2001). More recently however, Herceptin has been given as an adjuvant treatment in non-metastatic HER2 positive breast cancer patients since several trials have shown an improvement of disease-free survival and overall survival for Herceptin given to this group of patients in the early course of the disease before any sign of recurrence (Piccart-Gebhart et al., 2005; Romond et al., 2005; Smith et al., 2007).

Pertuzumab binds to different epitopes in the extracellular domain of HER2 from Herceptin. It binds near the centre of domain II, preventing HER2 receptor dimerisation with other HER receptors and thus blocking the signalling from dimerisation (Franklin et al., 2004). It has been shown to prevent dimerisation of HER2/HER3, which was not the case in Herceptin (Agus et al., 2002). This may explain why it may be effective against cancers that may not over-express HER2 (Agus et al., 2002). HER2 undergoes proteolytic cleavage upon activation by 4-aminophenylmercuric acetate (APMA), a well-known matrix metalloprotease activator, resulting in the release of the extracellular domain and the production of a truncated membrane-bound fragment, p95 (Molina et al., 2001). Herceptin inhibits basal and induced HER2 cleavage and prevention of the production of an active truncated HER2 fragment (Molina et al., 2001). Pertuzumab however does not

inhibit this proteolytic cleavage of HER2. Pertuzumab had been used in ovarian carcinoma and prostate carcinoma, with no clinical significant activity as a single agent in hormone-resistant prostate cancer (Agus et al., 2007; de Bono et al., 2007) and a response rate of 4.3% in heavily treated advanced ovarian carcinoma patients (Gordon et al., 2006).

Lapatinib is a potent dual tyrosine kinase inhibitor of EGFR and HER2. Unlike other reversible 4-anilinoquinazoline inhibitors of EGFR like Iressa and Erlotinib (Tarceva), Lapatinib is bound to an inactive-like conformation of EGFR and HER2, reducing the rate of inhibitor dissociation from the intracellular domains of these receptors, so that the autophosphorylation of these receptors recovers very slowly in tumour cells after treatment (Wood et al., 2004). Lapatinib was found to reduce growth of human breast cancer xenografts in athymic mice and the combination of Lapatinib and Herceptin was synergistic in exerting anti-proliferative effects in HER2-over-expressing cell lines (Konecny et al., 2006). Moreover, it retained significant *in vitro* activity against breast cell lines treated in long-term Herceptin-containing culture medium, providing a rationale of its use in patients who are clinically resistant to Herceptin. In a randomised trial, women with advanced HER2-positive breast cancer women who had progressed on chemotherapy and Herceptin, were randomly assigned to either Capecitabine (oral 5-FU chemotherapy) alone or Capecitabine with Lapatinib and the results showed that combination of Lapatinib and Capecitabin increased median time to progression in these patients (Geyer et al., 2006).

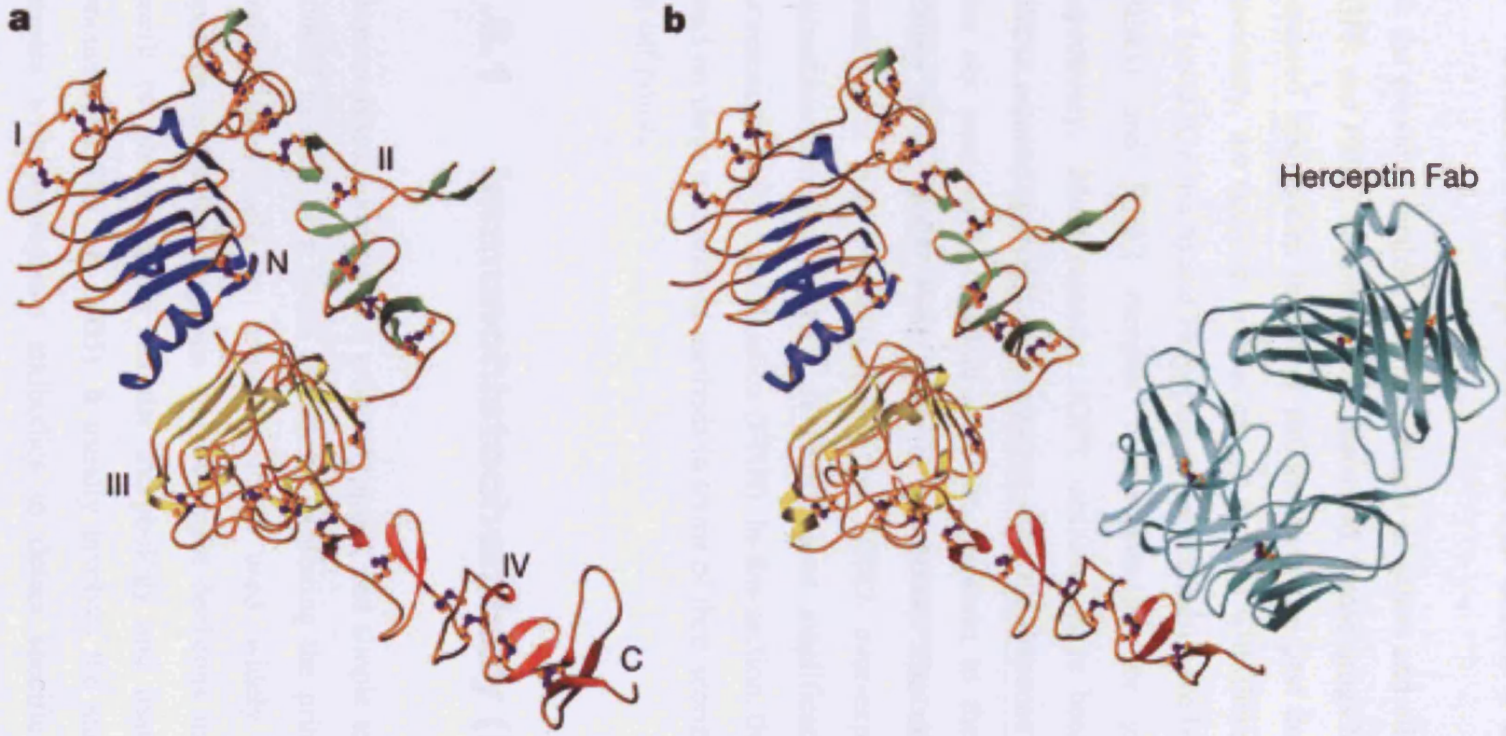

Figure 1.4: Crystal structure of HER2 receptor. A, Four domains of HER 2 receptors. **B,** Herceptin's binding site on HER2 receptor (Figures taken from Cho et al 2003).

1.6 Current methods of assessing HER receptors: IHC and FISH

In the previous section, the mechanisms of action and clinical use of various EGFR and HER2 inhibitors were discussed. These drugs have been used with increased frequencies in cancer patients over the past decade. As discussed previously, the decision to treat cancer patients with these targeted therapies, e.g. Iressa (Gefitinib) and Herceptin (Trastuzumab) have been based on EGFR (HER1) and HER2 receptor over-expression (or gene amplification) respectively. More recently, EGFR inhibitors have been given to patients without measuring EGFR concentration since the response of EGFR inhibitors does not necessarily correlate with the response to the drugs or survival (Chung et al., 2005; Perez-Soler et al., 2004). The criteria of Herceptin treatment is still currently based on HER2 over-expression shown by immunohistochemistry (IHC) or HER2 gene amplification determined by fluorescence *in situ* hybridization (FISH). In this section, the discussion will be based on these two present methods in terms of their scoring systems and their cut-off points.

1.6.1 Immunohistochemistry (IHC)

Immunohistochemistry is a relatively quick and simple technique to localize proteins in cells of a tissue section by exploiting the principle of antibodies binding specifically to antigens. It is used widely in histopathology departments for the diagnosis and treatment decisions in cancer. It has the benefit of preserving the cellular morphology and tissue integrity of the tumours (Dei Tos AP, 2005). It usually involves the staining of the tissue samples with appropriate antibodies to detect specific antigens and the antibody-antigen interaction can then be visualised by a variety of methods. For example, an antibody may be conjugated to an enzyme, such as peroxidase (Press et al., 1994), that can catalyse a colour-producing reaction or

alternatively an antibody can be tagged to a flurophore, such as rhodamine. The antibodies used for specific detection may be either polyclonal or monoclonal. The monoclonal antibodies are considered to have greater specificities since polyclonal antibodies are a heterogeneous mix of antibodies that recognise several epitopes.

Both direct and indirect methods can be used in IHC. The direct method utilises only one labelled antibody reacting directly with the antigen in tissue section (Ramos-Vara, 2005). However, this method may have low sensitivity due to little signal amplification and it is not used widely compared to the indirect method. In the indirect method, the unlabelled primary antibodies recognise a specific antigen of interest while the labelled secondary antibodies react with the primary antibodies (Ramos-Vara, 2005). The secondary antibodies recognise immunoglobulins of a particular species and are conjugated to a reporter or fluorophore (Press et al., 1994). For example, a biotinylated secondary antibody may be coupled with streptavidin-horseradish peroxidase which reacts with 3,3'-Diaminobenzidine (DAB) to produce a brown staining (Walker, 2006). The indirect method has greater sensitivity since the signal may be amplified through several secondary antibody reactions with different antigenic sites on the primary antibody (Ramos-Vara, 2005).

1.6.1.1 EGFR scoring by IHC

The EGFR IHC scoring is based on the assessment of proportion of positively stained tumour cells as well as the intensity of the observed staining using an antibody detecting EGFR antigen. IHC has been used in many studies to measure EGFR expression and many investigators have developed various algorithms to score them by either proportion of staining or intensity of staining or a combination of both methods, resulting in a variety of scoring systems (Chung et al., 2005; Cunningham et al., 2004; Hirsch et al., 2003; Kersemaekers et al., 1999). An example of a scoring system is illustrated in the table below and Figure 1.5 (Chung et al., 2005):

Score	Criteria
0	No membranous staining in any of the tumor cells
1+	Membranous staining in less than 10% of the tumor cells with any intensity or in less than 30% of the tumor cells with weak intensity
2+	Staining in 10% to 30% of the tumor cells with moderate to strong intensity or staining in 30% to 50% of the tumor cells with weak to moderate intensity
3+	Staining in more than 30% of the tumor cells with strong intensity or more than 50% of the tumor cells with any intensity

The scoring systems are not strictly quantitative despite the numerical scoring being assigned to them since the assessment of the intensity and the actual percentage of staining may represent only a rough estimate by the scorers and such visual interpretation of the stained samples may be subjective and may vary between individuals (Walker, 2006). In addition, the choice of antibodies and IHC protocol is not consistent and may cause variation in the sensitivity to detect EGFR expression (Dei Tos AP, 2005). Therefore, current EGFR scorings by IHC for epithelial cancers may vary between laboratories. The variation may be partially controlled by using a panel of tissue control slides and consensus scoring system by several observers (Adams et al., 1999). However, a standardised scoring system is urgently needed to allow direct comparison between studies and laboratories (Adams et al., 1999; Dei Tos AP, 2005).

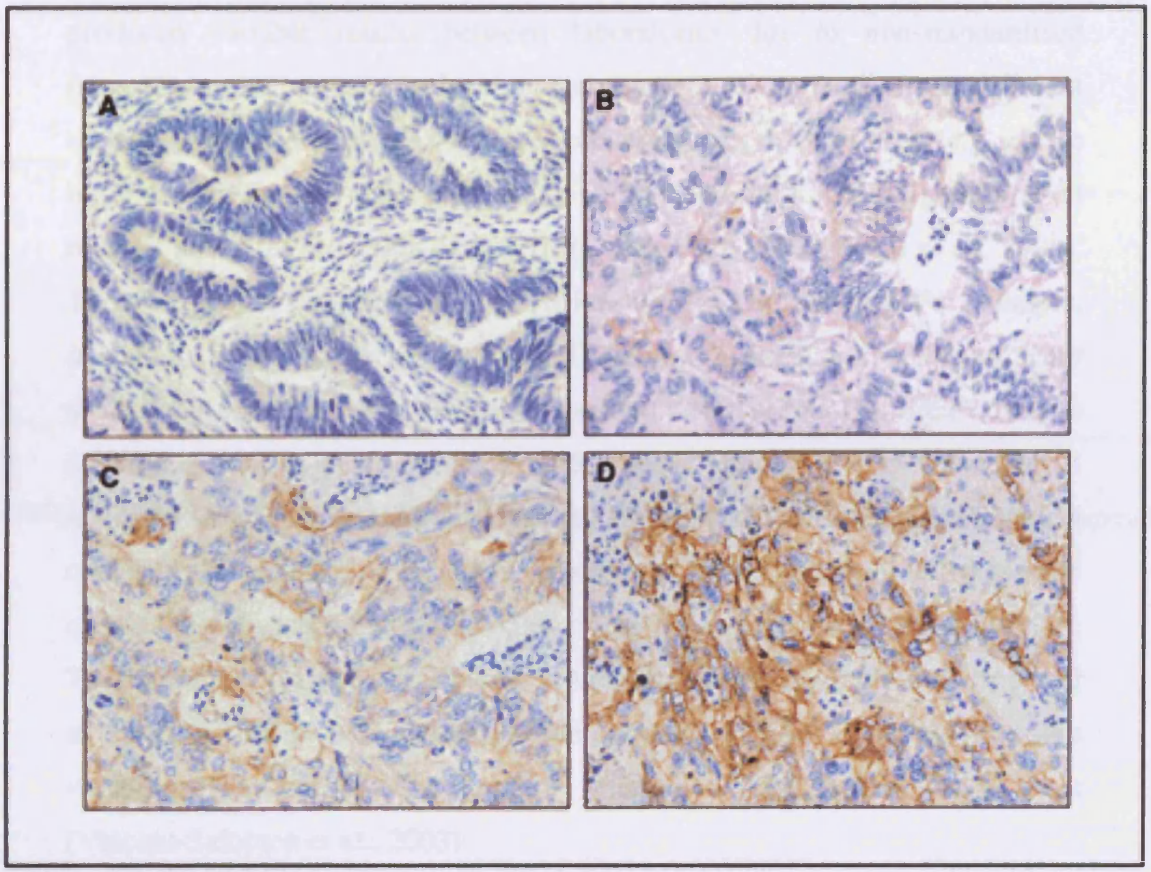

Figure 1.5: EGFR scoring by immunohistochemistry in colorectal carcinoma. A, 0. B, 1+. C, 2+. D, 3+ (Figure taken from Chung et al 2005)

1.6.1.2 HER2 scoring by IHC

Like EGFR scoring, assessment of HER2 over-expression by IHC has also produced variable results between laboratories due to non-standardised procedures (the antigen-retrieval process, usage of antibodies) or different scoring systems. For antigen-retrieval processes, the solution used (e.g. citrate buffer or EDTA and their pH), the duration of heating and antigen-retrieval may all affect the detection of the HER2 antigen by IHC (Yaziji et al., 2004). The other major variable is the anti-HER2 used for IHC staining. For example, in a study by Mitchell et al (1999), R60 (rabbit polyclonal antibody) uniformly stained cell membranes in paraffin-embedded tissue sections of breast cancers containing two to five copies of HER2 gene. However, 4D5 (monoclonal antibody to HER2) stained the majority of these sections with more than 5 copies of the gene and lastly TA-1, another anti-HER2 antibody failed to stain even cells with more than five copies of the gene (Mitchell and Press, 1999). The HercepTest (Dako, Carpinteria, CA) using A0485 antibody was proposed as the standardised IHC method to overcome the problems between inter-lab variations. The scoring system uses the intensity of HER2 staining as its basis (Vincent-Salomon et al., 2003):

Scoring	Criteria
0+	Absence of membranous staining,
1+	> 10% stained cells with a weak staining intensity
2+	> 10% stained cells with moderate staining intensity
3+	> 10% stained cells with a strong intensity

The College of American Pathologists (CAP) also issued its own guideline and a tumour is considered to be HER2 over-expressed if it scored 2+ or 3+ using the Herceptest reporting system or if > 60% cells had a moderate or strong membranous staining (Fitzgibbons et al., 2000). Beside the variability from the IHC procedures, the question also arises as to whether HER2 protein

may still be intact after fixation and being made into paraffin sections and this will be discussed in greater details in Chapter 6.

1.6.2 Fluorescence *In Situ* Hybridization (FISH)

Fluorescence *in situ* hybridization (FISH) has been used to detect HER2 amplification for selecting breast cancer patients for Herceptin treatment (Wolff et al., 2007). It is a cytogenetic technique which detects and localises specific DNA sequences on chromosomes using complementary probe sequences (Fan et al., 1990). The procedures involve constructing a fluorescence probe that hybridizes specifically to its target on the chromosomes before adding it to a sample DNA (Fan et al., 1990). The sample is denatured to separate the complementary strands within the DNA double helix structure. The fluorescence probe hybridises with the sample DNA at the target sites as it re-anneals back into the double helix. The fluorescence probe signal is visualised through a fluorescence microscope and the sample DNA can then be scored for the presence or absence of the signal. FISH has been used in many other applications in addition to detection of HER2 gene amplification, e.g. to diagnose specific chromosomal abnormalities in genetic counselling (Fan et al., 1990).

Fluorescence *in situ* hybridization (FISH) can directly detect amplification of HER2 genes within the cells and this may be assessed by various methods, including INFORM assay (commercial kit from Oncor Inc, Gaithersburg-Maryland, USA) or PathVysion assay, the HER2 DNA probe kit from Vysis (Wang et al., 2000). In the INFORM assay, the cells were counted for HER2 gene signal in each specimen (Wang et al., 2000). Gene amplification is considered when there are more than four HER2 gene copies per nucleus. For PathVysion, the cells are counted for both HER2 gene and chromosome 17 centromere (Wang et al., 2000). The result is reported as the ratio of the average number of the HER2 gene to that of the chromosome 17 centromere. When the specimens with a signal ratio of less than 2 they are considered as "non-amplified" and when the signal is 2 or greater, they are classified as

"amplified" (Wang et al., 2000). The difference of HER2 gene amplification by FISH from HER2 expression determined by IHC methods will be discussed in the next section.

1.6.3 IHC versus FISH in HER2 assessment

As discussed in the background (Section 1.1), the current criteria to choose breast cancer patients for Herceptin treatment is based on either HER2 over-expression by IHC or HER2 gene amplification by FISH (Wolff et al., 2007). The usage of IHC versus FISH for testing HER2 levels is however the subject of debate (Seelig, 1999; Wiley and Diaz, 2004). Although both methods are supposed to measure HER2 level, the two methods are essentially different with IHC measuring its protein level and FISH, the gene level. The gene amplification of HER2 is supposed to be the surrogate marker for protein expression of HER2, but this difference of measuring gene level or protein level may produce disparity between the two methods (Wang et al., 2000). For example, IHC 2+ patients have been found to contain significant amount of FISH negative patients (Kakar et al., 2000) and patients with polysomy of chromosome 17 may also produce high HER2 over-expression detection from IHC without true HER2 gene amplification (Salido et al., 2005). When the two methods are discordant, e.g. IHC-positive/FISH-negative or IHC-negative/FISH-positive, it may cause problems in decision-making for Herceptin treatment. Gene amplification of HER2 was first shown to correlate with relapse and survival of breast cancer patients in 1987 (Slamon et al., 1987). Initially assessment of HER2 gene amplification was found to be superior to IHC (Pauletti et al., 2000). However, FISH is more expensive and labour-intensive than IHC. In addition, there is a lack of clinical data regarding negative gene amplification and response to Herceptin; Herceptin acts at the protein level and not gene level. IHC assesses HER2 at the protein level and therefore it is potentially more directly relevant for assessment of patients for Herceptin treatment. However, HER2 assessment by IHC has produced

variable results, e.g. HercepTest (Dako, Carpinteria, CA) (Section 1.6.1.2) for IHC was found to have high false-positive results (Kakar et al., 2000). The discrepancy of IHC methods may be due to the choice of antibody, technical procedures, tissue fixation, cut-off levels and subjective interpretation and analysis between assessors and centres (Yaziji et al., 2004). Although the two methods may be discordant in their results, one study showed a close correlation of the two methods if quality control and quality assurance was in place (Yaziji et al., 2004). This particular study recommended IHC to be used first and then to perform FISH for intermediate over-expression of HER2.

Determining a cut-off point for high HER2 concentration is also problematic for both IHC and FISH. In IHC, there is a problem of using the criteria either based on the intensity of the membranous staining or the percentage of stained cells. One study recommended reporting IHC-HER2 as a continuous variable and selecting patients for Herceptin based on high percentage of positive tumour cells (Vincent-Salomon et al., 2003). In FISH, the choice of using different FISH ratios to classify "amplification of HER2" (see Section 1.6.2) affects whether it correlated with shorter survival (Kakar et al., 2000). The recent American Society of Clinical Oncology (ASCO) / College of American Pathologists (CAP) defined HER2 positive or negative based on either IHC (see Section 1.6.1.2) or FISH (gene copies or FISH ratio, see Section 1.6.2):

HER2 status	**IHC or FISH criteria**
HER2 positive	- IHC 3+ (Uniform, intense membranous staining of > 30% of invasive tumour cells) - FISH > 6 HER2 gene copies per nucleus or - FISH ratio > 2.2 (the ratio of HER2 gene signals to chromosome 17 signals)
HER2 negative	- IHC 0-1+ - FISH < 4 HER2 gene copies per nucleus - FISH ratio < 1.8
Equivocal HER2	- IHC 2+ - FISH 4-6 gene copies per nucleus - FISH ratio 1.8-2.2

The panel recommended extra testing for equivocal cases: IHC 2+ to have FISH test and FISH equivocal cases, to either retest or count additional cells or test with IHC. Nevertheless, not all centres adopt the recommendations, especially those centres outside the USA since they may use their own HER2 systems, creating variability in the definition of HER2 status between centres.

Therefore, the current methods using IHC and FISH to select patients for Herceptin have a variable scoring systems and cut-off points which are not standardised between centres; a tumour that is "HER2 positive" may be negative under the criteria used by another centre and this may cause problems in patient selection for Herceptin treatment. However, more important and urgent issues are how these tests that are supposed to select correct patients for targeted therapies for Herceptin perform as predictive markers for such therapies. These issues will be discussed in the next section.

1.7 HER receptor concentration and response to targeted therapies

Increasingly targeted therapies have been used in all types of cancers. Although the EGFR and HER2 inhibitors are meant to target the over-expression of receptors, the response to these drugs has been disappointing based on receptor concentration criteria monitored by IHC or FISH.

The two phase II head and neck cancer trials revealed a relatively low response rate (around 10%) of patients to Cetuximab despite the fact that the majority of the patients had a 2 to 3+ staining for EGFR (Baselga et al., 2005; Herbst et al., 2005). Iressa had a similar low response rate of about 10% in head and neck cancer (Cohen et al., 2003). In non-small cell lung carcinoma, a similar poor response rate was noted for Iressa (Fukuoka et al., 2003; Kris et al., 2003) unless the patients had mutations around the ATP-binding pocket of the tyrosine kinase domain which rendered these patients highly sensitive to Iressa (Lynch et al., 2004; Paez et al., 2004). However, these mutations are

associated with brochioloalveolar pathology that arise in non-smokers, and in individuals of East Asian descent (Lynch et al., 2004; Paez et al., 2004). EGFR kinase domain mutations are rarely present in other types of cancers. In head and neck cancer, where the majority of patients have over-expression of EGFR most Caucasian patients do not have these mutations seen in non-small cell lung cancer, except in a small proportion of patients from certain ethnic origin (Loeffler-Ragg et al., 2006). In two colon cancer two trials the relationship between the expression of EGFR and response rate to Cetuximab was examined and a relationship was not found (Cunningham et al., 2004; Saltz et al., 2004). In fact another trial has reported objective responses to Cetuximab in chemotherapy-refractory colorectal cancer even when EGFR expression was not detected by IHC (Chung et al., 2005). When the tyrosine kinase inhibitors of EGFR were first used, they were given to patients with over-expression of EGFR. However, it was found that the EGFR level does not necessarily predict the response to targeted therapy (Parra et al., 2004) and now they may be administered to patients irrespective of EGFR expression (Shepherd et al., 2005).

Chung et al (2004) found, by molecular classification of HNSCC using patterns of gene expression, that the poorest outcome group was the group with tumours characterised by the high expression of TGF-$\propto$ with evidence of activation of EGFR pathway (Chung et al., 2004). In addition, another study has shown that it is the over-expression of multiple receptors, mainly EGFR, with other HER receptors (HER2-4) that correlates more with metastatic disease (Bei et al., 2004). Based upon our understanding of the behaviour of these receptors, these studies indicate that not only is the actual level of EGFR expression important, but specifically the activation/phosphorylation state of these receptors.

Despite the selection of HER2 positive breast cancer patients based on IHC and FISH, only about one third of these patients respond to Herceptin given as monotherapy (Vogel et al., 2002). It was also shown that non-HER2 over-expressing tumours may also respond to Herceptin through its activation via heregulin over-expression (Arteaga, 2006; Menendez et al., 2006). One of the reasons accounting for poor predictive value using receptor concentration is that over-expression per se fails to consider receptor activation e.g. through

autocrine expression of one of the several ligands. In addition, over-expression as a criterion for treatment fails to account for patients having receptor activation without up-regulation through other HER receptors since it is the preferred dimerisation partner for other HER receptors (Graus-Porta et al., 1997). Therefore, it may be assumed that some patients without HER2 over-expression may have a highly active HER2 receptor and may also benefit from HER2 inhibitors like Herceptin. Therefore, like EGFR inhibitors, it is assumed that assessing HER2 phosphorylation may be a better predictor for response to Herceptin treatment.

In summary, this section discussed the poor relation between the expression of EGFR and HER2 receptors and the response to targeted therapies. It is therefore of critical importance to determine how EGFR and HER2 activation status, rather than concentration, track with response to these and related EGFR and HER2-directed treatments. The next section will discuss various methods that can be used to assess the phosphorylation status of HER receptors.

1.8 Assessment of HER receptor phosphorylation status

To assess phosphorylation status of HER receptors, various methods can be used, including IHC, eTag or FRET methods. IHC that is currently used to determine the expression of HER receptors (Section 1.6.1) may also be used to monitor the phosphorylation status of HER receptors in tumours. However, using IHC methods to detect phoshorylated HER receptors will have the same limitations relating to EGFR and HER2 scorings by IHC (Section 1.6.1.1 and 1.6.1.2). And not being a two-site assay, it specificity may be influenced by background staining and high antibody concentration and thus it is difficult to be optimise quantitatively to obtain reliable results. Using eTag reporters (fluorescence molecules) conjugated to different HER antibodies, the eTag assay platform have been shown to be potentially useful in assessing HER activation and dimerisation (Chan-Hui et al., 2004). The amount of released

eTag reporter is said to be proportional to HER concentration. The problem with such assays is that it depends on fluorescence intensity which may be influenced by multiple factors including dye concentration, background fluorescence, photo-bleaching, and concentration of antibodies conjugated to fluorescence reporters. Moreover, it does not provide any spatial data which is of critical importance when assessing HER receptors in the tumours. A more quantitative method would be required that is not affected by the problems encountered in IHC and eTag.

FRET is measured by variation in the changes of lifetime and is independent of dye concentration and fluorescence intensity (Larijani, 2006). It was proposed that FRET may provide spatial data about the interaction between the HER antibodies and may be used to assess phosphorylation status of HER receptors as well as dimerisation of HER receptors. For these reasons, FRET was chosen to assess HER receptor activation in relation to cancer treatments in this thesis. The principle of FRET will be discussed below.

1.9 Principles of Förster Resonance Energy Transfer

In this thesis, Förster Resonance Energy Transfer (FRET) monitored by Fluorescence Lifetime Imaging Microscopy (FLIM) was exploited to assess the phosphorylation of various HER receptors. Since the thesis aims to present a translational project, using FRET as a tool to assess HER receptor activation in cells and tumour arrays, in-depth discussion on the photophysics of the flurophores, mathematic calculations of FRET and physics of FLIM instruments will not be given here and may be obtained from other sources (Lakowicz, 1999; Larijani, 2006; Valeur, 2002). The relevant details of FRET and principles relevant to the project will be described below.

1.9.1 Fluorescence

When the electrons of the molecules of a fluorophore are excited to a higher energy state, the absorbed energy can be released by the emission of a photon (radiative) before returning to the ground state, resulting in two types of luminescence: fluorescence and phosphorescence (Larijani, 2006). Fluorescence occurs when there is immediate release of energy (between the states of the same spin state of the electrons, e.g. S1 to S0) through the emission of a photon (Figure 1.6). If the spin states of the initial and final energy levels of the electrons are different (e.g. from T1 to S0), the emission of the photon is called phosphorescence (Figure 1.6). Fluorescence is statistically much more likely to happen than phosphorescence and the lifetimes of fluorescent states are very short (1-10 nanoseconds) and phosphorescence greater (1×10^{-4} seconds to minutes or even hours). The two processes may be illustrated using the Jablonski diagram (Figure 1.6). However, not all the excited electrons of the fluorescent molecules return to the ground state via luminescence since many other non-radiative competing processes may occur. These include internal conversion to the ground state (a non-radiative transition between energy states of the same spin state, e.g. via heat); intersystem crossing to triplet state (a non-radiative transition between different spin states where energy may be dissipated); collisional quenching (when the excited state fluorophore is deactivated upon contact with other molecules or the quencher) (Lakowicz, 1999; Larijani, 2006) and resonance energy transfer (RET or Förster resonance energy transfer, FRET). These radiative decay and non-radiative decay processes compete to depopulate the molecules in the excited state.

Fluorescence lifetime of a fluorophore is defined as the mean time the electrons of fluorescent molecules spend in the excited state before coming back to ground state or the probability of the molecule existing in the excited state. Fluorescence lifetime is thus affected by the rate of various radiative and non-radiative processes. Measuring the lifetime of a fluorescence probe may inform on the local environment of the molecule since the local environment may change the rate of non-radiative decay (Lakowicz, 1999; Valeur, 2002). Therefore fluorescence has been exploited to investigate structure and the dynamics of molecules in their microenvironment since the emission of

fluorescence molecules is sensitive to physical and chemical parameters such as pH, pressure, viscosity, electric potential, quenchers, temperature and ions (Larijani, 2006). Förster resonance energy transfer is one of the photophysical processes that are responsible for the de-excitation of fluorescent molecules and has been used as a reporter of molecular environment (Larijani, 2006). In this thesis FRET has been exploited to answer some important clinical questions regarding HER receptors and cancer treatment. The following sections will focus on various methods of FRET measurement and its application.

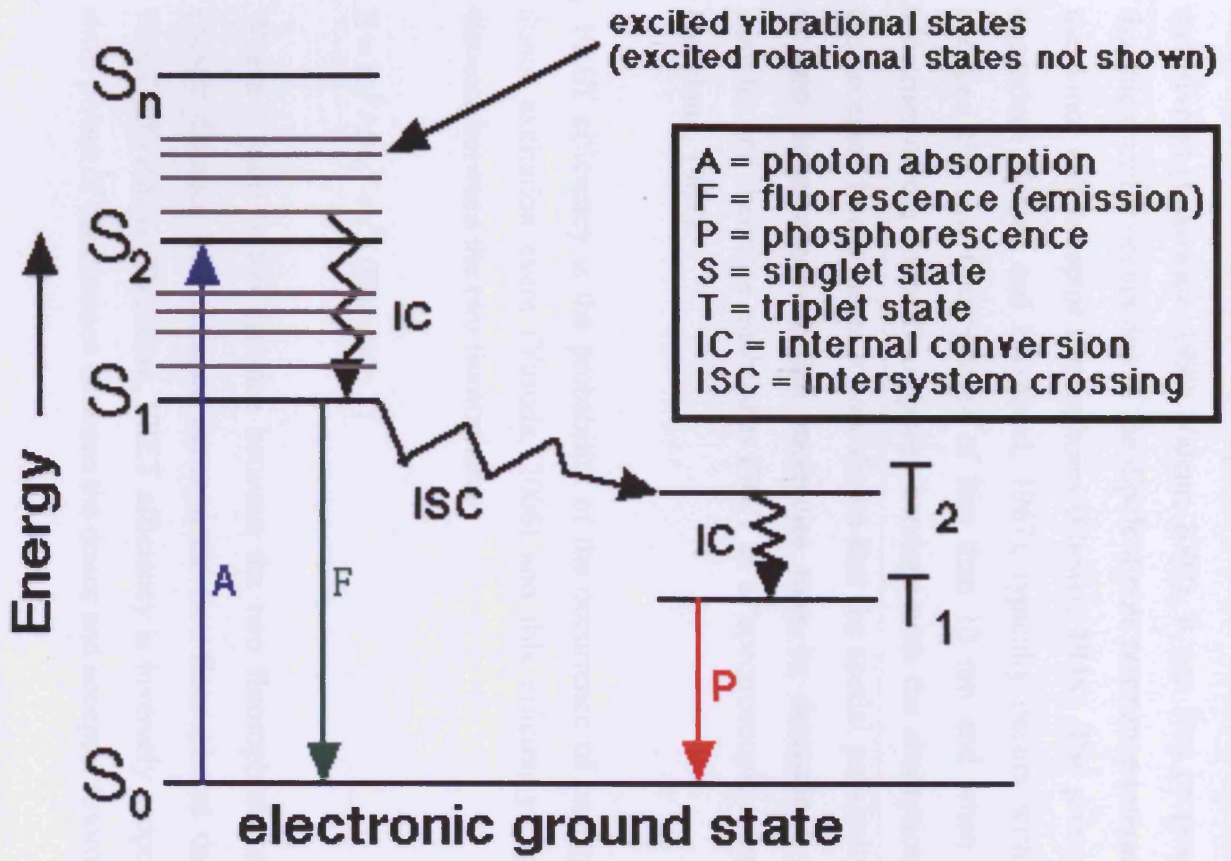

Figure 1.6: Jebloski diagram (Figure taken from http://www.shsu.edu/~chemistry/chemiluminescence/JABLONSKI.html, by Dr. Thomas G. Chasteen at Sam Houston State University, Huntsville, Texas).

1.9.2 Förster Resonance Energy Transfer

FRET is a process whereby the energy of an excited donor fluorophore is transferred to an acceptor fluorophore without emission of a photon (non-radiatively) (Lakowicz, 1999; Valeur, 2002). It was first proposed by Förster that the transfer occurs due to the dipole-dipole resonance interaction between the donor and acceptor fluorophores (Förster, 1948). The process is distance dependent (Stryer and Haugland, 1967), typically occurs with the distance between the two fluorophores of less than 10 nm and when the emission spectrum of the donor fluorophore overlaps with the absorption spectrum of the acceptor fluorophore. It was shown that the spatial proximity relationship of two fluorescence-labelled molecules may be determined in biological samples and therefore establishes FRET as a "spectroscopic ruler" (Stryer and Haugland, 1967).

FRET efficiency is the probability of the occurrence of energy transfer per donor excitation event (Yasuda, 2006) and this efficiency depends on the distance between the two fluorophores:

$E = R_0^6 / (R_0^6 + r^6)$ (Equation 1)

Where r (nm) is the distance between the two fluorophores and R_0 is the Förster distance (the distance between the two fluorophores that gives 50% FRET efficiency). Therefore, FRET efficiency is inversely proportional to the sixth power of the distance between the donor and acceptor fluorophores.

Reported Förster distance R_0 may typically range between 1-7 nm (10-70 Å) but up to 12 nm may be measured (Wu and Brand, 1994). The R_0 may be affected by various parameters given by the equation below:

$$R_0 = [\kappa^2 \times J(\lambda) \times n^{-4} \times Q]^{1/6} \times 9.7 \times 10^2 \quad \text{(Equation 2)}$$

Where κ^2 is the relative orientation of the transition dipoles of the flurophores, J (λ) is the overlap integral between the donor emission and acceptor absorption spectra, n is the index of refraction of the medium and Q is the quantum yield of the donor. From the equation it can be determined that the energy transfer rate depends on three parameters: (1) the overlap of the donor emission and acceptor absorption spectra; (2) the relative-orientation of the donor absorption and acceptor transitions moments; and (3) the refractive index (Jares-Erijman and Jovin, 2003). These factors as well as the distance r between the two fluorophores will influence FRET efficiency from the donor to the acceptor fluorophores.

1.9.3 Methods to measure FRET

FRET may be quantified and monitored by both steady-state and time-resolved methods (Wu and Brand, 1994). The steady-state methods include intensity-based measurements like ratiometric imaging and donor dequenching; and the time-resolved methods are comprised of fluorescence lifetime imaging microscopy (FLIM) and anisotropy imaging.

In the steady-state measurement, the fluorescence sample is illuminated continuously and the emission of photons is measured. The steady state is reached immediately when the sample is first exposed to light. The intensity of the fluorescence is measured and this depends on the concentration of the probe. The time-resolved measurements are used to measure intensity decays or anisotropy decays. For this type of measurement, the sample is exposed to a short pulse of light and the decays are recorded with a high-speed detection system.

The detection of FRET using intensity-based methods and time-resolved FLIM methods will be discussed in this section. Since anisotropy imaging is not used in this thesis, the details of anisotropy will not be explained in this section and may be obtained elsewhere (Lakowicz, 1999; Valeur, 2002).

1.9.3.1 Intensity-based methods

In the intensity-based methods (steady-state measurement), FRET is quantified using intensities of donor and acceptor fluorescence, and typically involving the decrease in donor fluorescence and increases in the acceptor fluorescence. FRET based on intensity-based methods can have many pitfalls including the insensitivity, high background and the signal is dependent on the concentration of the fluorophores (Parsons et al., 2004). Ratiometric imaging and donor quenching methods are two examples of intensity-based measurement and will be discussed below.

Ratiometric imaging

In this method, the donor fluorophore is selectively excited and the ratio of acceptor emission I_A and donor emission I_D is used to measure relative FRET efficiency (I_A/I_D) (Parsons et al., 2004). The donor and acceptor fluorescence can be separated by appropriate dichroic filters that detect the donor and acceptor fluorescence at different wavelengths. However, the excitation source may directly excite the acceptor and therefore the emission of the acceptor may not be due to the transfer of energy from the donor fluorophore (Lakowicz, 1999). In addition, the donor fluorescence may bleed through into the acceptor detection channels and make the FRET efficiency difficult to measure (Parsons et al., 2004). For the method to be reliable, the donor and acceptor stoichiometry needs to remain constant (Lakowicz, 1999). Otherwise correction for the spectral bleed through needs to be done.

Donor dequenching (acceptor photobleaching)

In this method, donor fluorescence is measured quantitatively while the acceptor fluorophore is photobleached selectively (Parsons et al., 2004). As a result, the donor is no longer quenched by the acceptor i.e. donor dequenching and the intensity of the donor increases (Lakowicz, 1999). FRET efficiency can be obtained using the equation below:

$$E = 1 - I_D/I_{DA}$$

Where I_D is the donor fluorescence intensity and I_{DA} is the donor fluorescence intensity after acceptor photobleaching (Parsons et al., 2004). The method may be used reliably when the bleed-through of the acceptor into the donor channel is negligible. It also does not depend on the relative concentration of the donor and acceptor fluorophores (Parsons et al., 2004).

1.9.3.2 Fluorescence lifetime imaging microscopy (FLIM)

FLIM is a time-resolved method and it may be monitored by either time-domain or frequency-domain measurements. FLIM measures fluorescence lifetime as a readout for FRET efficiency. Unlike the steady state methods where the intensity of the fluorophore may change in a way that is difficult to quantitate, a key advantage of using time-resolved method is that Fluorescence lifetime is relatively independent of fluorophore concentration, light scattering and the excitation intensity (Larijani, 2006). Therefore FLIM using either time-domain or frequency-domain measurements may be exploited to measure quantitatively the environmental factors that affect the excited state in fixed and live cells (Larijani, 2006).

Time-domain method

In the time-domain method, the fluorescence sample is excited with a short pulse of light (usually in the orders of tens to hundreds of picoseconds), producing a population of fluorophores in the excited-state, which will relax to the ground-state by emitting photons. The resulting emission decay in intensity may be reconstructed using various methods including multiple time gating method or time correlated single photon counting (TCSPC). The most common method is TCSPC and in this method the time delay between the emitted photon and the excitation pulse is recorded (Alcor D, 2007). An entire decay curve is built by plotting the number of photons versus delay time. The excitation profile needs to be measured so that a deconvolution may be done to separate the excitation pulse from the emission profile. The fluorescence lifetime of the fluorophore may be determined by fitting the decay curves

(Figure 1.7A) (Lakowicz, 1999). Recent advances have also enabled the use of multi-photon or confocal laser scanning microscopes to measure FRET, yielding highly improved spatial resolution, controlled depth of field and the potential to generate a three-dimensional reconstruction of FRET signals within a cell by acquiring multiple optical sections (Calleja et al., 2007; Parsons et al., 2004).

Frequency domain method

FRET data presented in this thesis is measured by frequency-domain FLIM. The fluorescence sample is excited by a continuous wave laser in a frequency-domain method as opposed to a pulsed laser in the time-domain method. The light source is modulated via an acousto-optical modulator and the sample is excited by a sinusoidally modulated light (Larijani, 2006). The emitted light appears as a sine wave but it is demodulated and phase-shifted from the excited light due to Stokes shift (with a lower energy) (Figure 1.7B). The phase shift and demodulation are used to obtain the lifetimes τ of the fluorophore from the equations below:

$$\omega\tau = \text{Tan}\,(\Phi)$$
$$\omega\tau = \sqrt{1/M^2 - 1}$$

where ω is the angular modulation frequency ($\omega = 2\pi f$), f is the modulation frequency, Φ is the phase difference and M is the demodulation. To obtain the maximum sensitivity, the angular modulation frequency should be roughly the inverse of the lifetime obtained. Therefore, the typical modulation frequencies are between 20 to 200 MHz since the lifetimes are usually between 1-10 ns. The FLIM instrument used in Cell Biophysics Lab uses a single modulation frequency of 80 MHz and the range of lifetime detected is between 1.5 ns to 2.6 ns.

The frequency-domain method is more rapid than the time-resolved method in detecting the lifetime of fluorescence although it is not the best tool to directly measure multiple exponential decays (Larijani, 2006). However, multiple-frequency FLIM instruments may be used to detect multiple

exponential decays that may arise due to heterogeneity of the local environment of the fluorophore (Larijani, 2006).

A

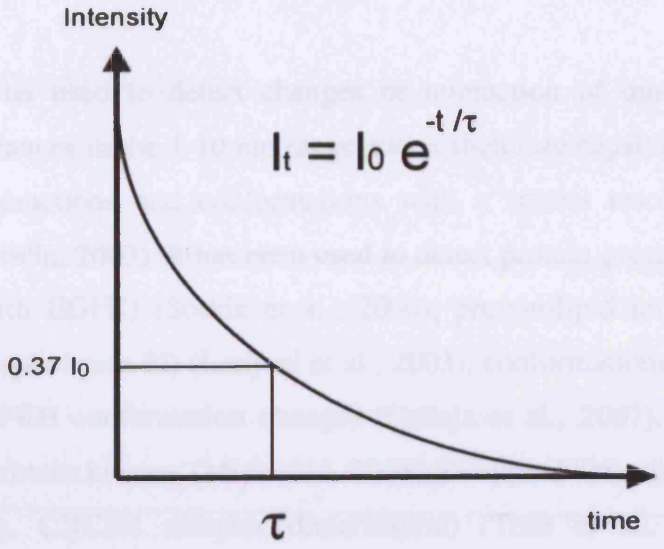

B

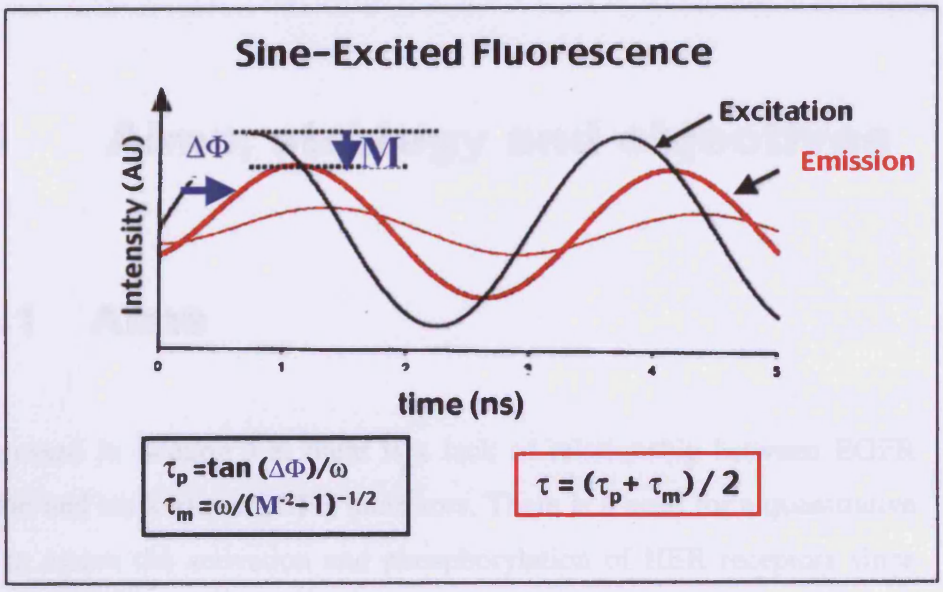

Figure 1.7: A, Time-domain method. B, Frequency-domain method
(Figures taken from Olympus microscope website)

1.9.4 Application of FRET

FRET may be used to detect changes or interaction of intra- and inter-molecular distances in the 1-10 nm range and is therefore capable of resolving molecular interactions and conformations with a spatial resolution (Jares-Erijman and Jovin, 2003). It has been used to detect protein-protein interaction (e.g. Grb2 with EGFR) (Sorkin et al., 2000), protein-lipid interaction (e.g. PITP and phospholipids PI) (Larijani et al., 2003), conformational change of a protein (e.g. PKB conformation change) (Calleja et al., 2007), study of the activities of protein kinases (Miyawaki, 2003; Yasuda, 2006), dimerisation of receptors (e.g. CXCR4 receptor dimerisation) (Toth et al., 2004), high throughput screening (Mere et al., 1999) and many other applications. In this thesis, FRET was exploited to assess the phosphorylation status of HER receptors in relation to cancer prognosis and treatments.

1.10 Aims, strategy and objectives

1.10.1 Aims

As discussed in Section 1.8, there is a lack of relationship between EGFR expression and response to EGFR inhibitors. There is a need for a quantitative method to assess the activation and phosphorylation of HER receptors since this may prove to be a better predictive marker for cancer prognosis and response to these inhibitors. The overall aim of this thesis was to establish a methodology whereby phosphorylation of HER receptors may be assessed by FRET monitored by high throughput FLIM and to apply such methodology to formalin-fixed, paraffin-embedded cancer tissues in relation to prognosis and treatments of various cancers. The ultimate long-term goal is to develop a validated methodology using various assays to assess activation of a whole

range of other pathways like PKB and MAPK activation in a high throughput manner in relation to cancer prognosis and treatments.

1.10.2 Strategy

To assess HER receptor activation state by FRET, a pair of anti-non-phosphoHER and anti-phosphoHER antibodies may be employed and conjugated to Cy3b and Cy5 respectively. The strategy is illustrated in Figure 1.8 using EGFR as an example. The hypothesis was that when EGFR was not phosphorylated, only EGFR-Cy3b would bind to the tyrosine kinase domain of EGFR. However, when the EGFR was phosphorylated, either from the autocrine loop (basal condition) or from exogenous ligand stimulation (e.g. by adding EGF), there would be autophosphorylation of the tyrosine residues of the C-terminal of EGFR resulting in the binding of pEGFR-Cy5 to the phosphotyrosine sites. This would bring the two conjugated antibodies into proximity, resulting in the quenching of the donor EGFR-Cy3b and a decrease in the lifetime of donor EGFR-Cy3b. Therefore, it was hypothesized that the decrease of lifetime could be used as a reporter of EGFR phosphorylation.

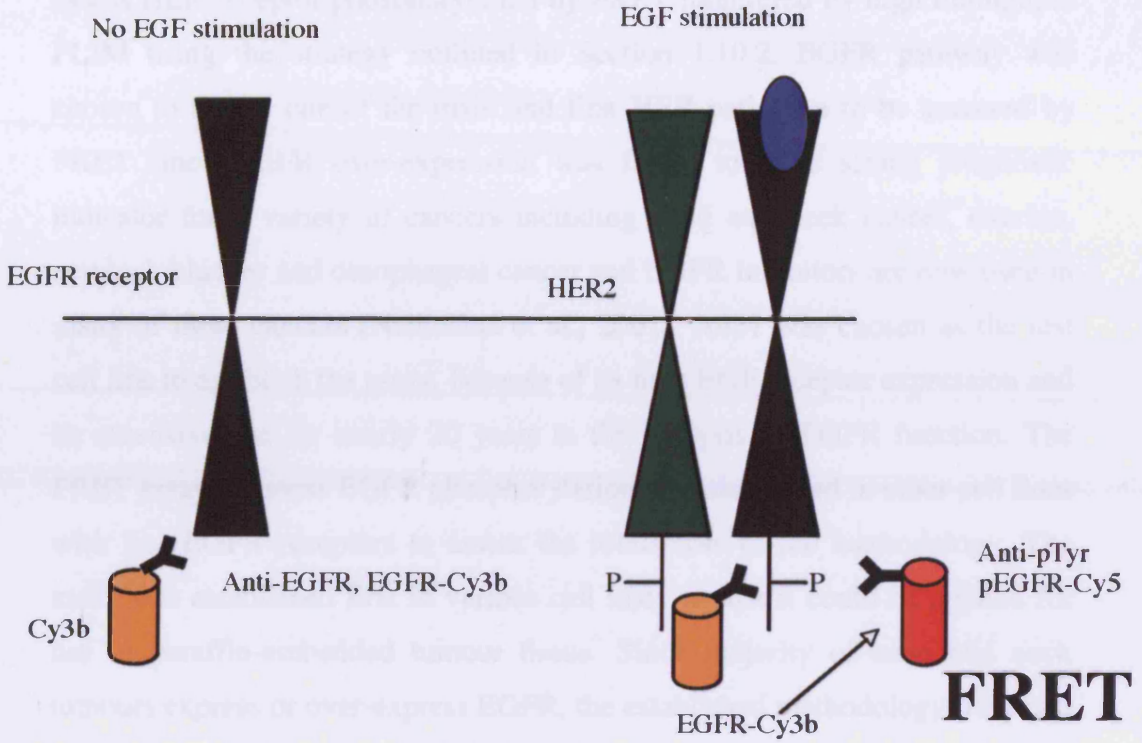

Figure 1.8: Strategy to assess EGFR phosphorylation by FRET.

1.10.3 Objectives

In this thesis, one of the first objectives was to develop an assay that can assess HER receptor phosphorylation by FRET monitored by high throughput FLIM using the strategy outlined in Section 1.10.2. EGFR pathway was chosen to be the one of the main and first HER pathways to be assessed by FRET since EGFR over-expression was found to be a strong prognostic indicator for a variety of cancers including head and neck cancer, ovarian, cervical, bladder and oesophageal cancer and EGFR inhibitors are now used in many of these cancers (Nicholson et al., 2001). A431 was chosen as the test cell line to establish the assay, because of its high EGF receptor expression and its extensive use for nearly 20 years in the analysis of EGFR function. The FRET assay to assess EGFR phosphorylation was also tested in other cell lines with less EGFR receptors to assess the robustness of the methodology. The assay was established first in various cell lines so that it could be applied for use in paraffin-embedded tumour tissue. Since majority of head and neck tumours express or over-express EGFR, the established methodology from cell lines was applied to an archive of formalin-fixed and paraffin-embedded head and neck tumour arrays as a test of principle. The EGFR phosphorylation determined by FRET was correlated with survival data of head and neck patients to assess the prognostic value of FRET assay. In addition, the prognostic value of FRET was compared with conventional IHC in the head and neck arrays.

The other main HER pathways to be chosen for assessment by FRET in this thesis is HER2 since it has been shown to be the preferred dimerisation partner (Graus-Porta et al., 1997) as well as a strong prognostic factor for breast cancer (Hartmann et al., 1994; Marks et al., 1994; Rosen et al., 1995; Ross and Fletcher, 1999). Therefore, one of the objectives of this thesis was to establish an assay to assess HER2 phosphorylation by FRET in cell lines and breast tumour arrays.

Both EGFR and HER2 play in role in the prognosis of breast cancers and thus both EGFR and HER2 inhibitors (alone or combination) have been used in

breast cancer patients (Geyer et al., 2006; Piccart-Gebhart et al., 2005; Polychronis et al., 2005; Romond et al., 2005; Smith et al., 2007). The intention was that the FRET will eventually be applied to prospective trials of HER receptor inhibitors in breast cancer patients (e.g. adjuvant Herceptin and Lapatinib trials (Geyer et al., 2006; Piccart-Gebhart et al., 2005; Romond et al., 2005; Smith et al., 2007)). Therefore, it was essential to first assess the responses of HER receptors in relation to EGFR and HER2 inhibitors in breast cell lines. Moreover, the mechanisms of action and resistance to these drugs are still poorly understood. Since FRET can be used to assess the phosphorylation status in vivo, it was used to monitor HER receptors' responses to these drugs in combination with classical biochemical analysis. The results from cell lines are also essential before such assay may be applied to prospective trials to assess responses of HER receptors by FRET in relation to HER receptor inhibitors.

It is often assumed that the phosphorylated antigens (including that of HER receptors) may survive the conventional IHC procedures for the tumours to be fixed and made into paraffin sections. However, if this was not the case, FRET could not have been used to assess the phosphorylation of these HER receptors. Therefore one of the objectives of the thesis was to investigate whether phosphorylated antigens may survive the conventional IHC procedures as well as the best way to fix and preserve the phosphorylated antigens. These results will be useful in providing guidelines for tumour fixation procedures of tumour samples used for FRET experiments in prospective trials. To assess the best way to preserve phosphorylated antigens (using HER2 phosphorylated antigens as a reporter), the MDAMB-453 breast tumours were grown in xenograft model. The tumours were fixed with either formalin or liquid nitrogen after varying the durations of delay in fixation. These tumours were subsequently assessed for their HER2 phosphorylation status using both conventional IHC and FRET.

Other than the potential problems with preservation of phosphorylated antigens, the optimisation of the established HER2 FRET assay from cell lines was necessary in archives of human breast tumour arrays before it may be applied to prospective trials. This would identify the difficulties of using such methodology in breast tumour arrays and to solve all the potential problems

before applying the assay to prospective trials. For this purpose, the established HER2 FRET methodology was applied to assess HER2 phosphorylation in archives of HER2 positive breast tumour arrays as well as mixed HER2 breast tumour arrays (consisting of both HER2 positive and HER2 negative cases).

In summary, the work of this thesis had the following objectives:

- **First,** the establishment of an assay that can assess EGFR phosphorylation by FRET monitored by high throughput FLIM.
- **Second,** the establishment of an assay that can assess HER2 phosphorylation by FRET in cell lines, and to assess the responses of HER receptors in relation to EGFR and HER2 inhibitors in breast cell lines.
- **Third,** the assessment of the best way to preserve phosphorylated antigens in xenograft breast tumours.
- **Fourth,** the establishment of HER2 phosphorylation by FRET in breast tumour arrays.

2 Materials and Methods

2.1 Materials

2.1.1 Mammalian Cell lines

A431, COS-7, MCF-7, SKBR3, MDMB-231 and MDAMB-453 cells were provided by the cell services at Cancer Research UK London Research Institute (CR-UK LRI) and MCF-12F cells were obtained from American Type Culture Collection (ATCC), USA.

2.1.2 Mice for xenograft work

Nude mice and Severe Combined Immune Deficiency (SCID) mice were obtained from Transgenic Lab at Cancer Research UK London Research Institute.

2.1.3 Tissue microarrays (TMAs)

Tissue arrays were prepared from formalin-fixed, paraffin-embedded tumour blocks derived by surgical resection from the Pathology Department, John Radcliffe Hospital, Oxford. Quality control for tumour specimens was undertaken and all slides were examined by at least one specialist consultant pathologist. It was not possible for each core to be uniformly involved by the tumour and naturally there was variation between the individual cores with the percentage of the tumour. The tonsil sections were provided as a reference point for slide orientation and contain heterogeneous tissues including squamous tissue, lymphoid and vascular tissues as well as supporting stromal

tissues. 500 μm cores were taken and transferred to an 8 x 15 core recipient array block using a Beecher Instruments Manual Tissue Arrayer-1 (Beecher Instruments Incorporated, Sun Prairie, WI). 5 μm sections were cut from each array block and made into slides which were stored at 4 ^{0}C.

The work was carried out with the approval of the Oxford Ethics Committee. For head and neck tumour arrays, 133 consecutive cases from the Ear Nose Throat department, Radcliffe Infirmary, Oxford, were analysed. Surgical approach was the primary approach always in these patients unless they were not encompassable in an appropriate surgical field. If, after primary surgery, margins were positive then radiotherapy was given to the patients. No chemotherapy was given to these patients. No primary radiotherapy cases are included here and patients who had previously been treated for HNSCC were also excluded. Two sets of breast arrays were used, one with a mixture of HER2 positive and HER2 negative cases (n=115) and the other set with only HER2 positive cases (n=55). All patients had conventional treatment including surgery, radiotherapy, chemotherapy and hormonal therapy according to their TNM staging and guidelines from medical oncology department at the University of Oxford.

2.1.4 Antibodies

Name	Species	Application	Source
Anti-EGFR, F4 (recognizing intracellular residues 985-996)	Mouse	WB 1: 10000	Cancer Research UK
Anti-phosphotyrosine, FB2	Mouse	WB 1: 500	Cancer Research UK
Anti-EGFR (Tyr845)	Rabbit	WB 1:1000	Cell Signalling
Anti-HER2	Rabbit	WB 1:1000	Cell Signalling

(intracellular)		IP 1:100	
Anti-phosphoHER2 (Tyr1248)	Rabbit	WB 1:1000	Cell Signalling
Anti-phosphoHER2 (Tyr1221/1222)	Rabbit	WB 1:1000	Cell Signalling
Anti-HER3 (monoclonal)	Mouse	WB 1:100	Sigma
Anti-phosphoHER3 (Tyr1289)	Rabbit	WB 1:1000	Cell signalling
Anti-HER4 83B10 (intracellular)	Rabbit	WB 1:1000	Cell signalling
Anti-HER4 111B2 (intracellular)	Rabbit	WB 1:1000	Cell signalling
Anti-HER4 (C-terminus)	Rabbit	IP 1: 25	Santa Cruz
Anti-phosphoHER4 (Tyr1284)	Rabbit	WB 1:1000	Cell signalling
Anti-phosphotyrosine (p-Tyr100)	Mouse	WB 1:2000	Cell signalling
Anti-Akt (PKB)	Rabbit	WB 1:1000	Cell signalling
Anti-phosphoPKB (Thr308)	Rabbit	WB 1:1000	Cell signalling
Anti-phosphoPKB (Ser473)	Rabbit	WB 1:1000	Cell signalling
Anti-p44/42 MAP Kinase	Rabbit	WB 1:1000	Cell signalling
Antiphospho-p44/42 MAP	Rabbit	WB 1:1000	Cell signalling

Kinase (Thr202/Tyr204)			
Anti-beta actin	Mouse	WB 1:20000	Sigma
Anti-pTEN	Rabbit	WB 1:2000	Santa Cruz
Anti-Human IgG	Mouse	WB 1:5000	Sigma
HRP-conjugated anti-mouse whole IgG	Sheep	WB 1:10000 (F4 and FB2); 1:2000 (for others)	Amersham (GE healthcare UK Limited)
HRP-conjugated anti-rabbit IgG	Goat	WB 1:2000	Amersham (GE Healthcare UK Limited)
Anti-human TGF-α	Goat	WB 1:2000 (0.05 μg/ml) Cell viability 1:40 (1 μg/ml)	Sigma
Anti-heregulin-α (Ab-1)	Goat	WB 1:10000 (0.1 μg/ml) Cell viability 1:100 (10 μg/ml)	Calbiochem
Anti-heregulin-1 precursor	Rabbit (human and mouse cross-reactivity)	WB 1:10000 (0.05 μg/ml)	Upstate
Anti-betacellulin	Mouse	WB 1:10000 Cell viability 1:25 (0.02 g/ml)	Sigma

2.1.5 Growth factors

Name	Species	Dose	Source

Epidermal Growth Factor (EGF)	Mouse	50-100 ng/ml	Sigma
Transforming Growth Factor-α (TGF-α)	Human	100 ng/ml	
Heregulin β*	Human	100 ng/ml	
Heregulin β1†	Human	100 ng/ml	
Betacellulin	Human	20 ng/ml	

* Heregulin β: Recombinant EGF domain of heregulin β3 (amino acid residues 178-241) of neuregulin 1 gene (Sigma product information).

† Heregulin β1: Recombinant EGF domain of heregulin β1 (amino acids 176 to 246) of neuregulin 1 gene (Sigma product information).

2.1.6 Inhibitors and drugs

Generic name	Trade name	Typical dose	Company
4-(3-Chloroanilino)-6,7-dimethoxyquinazoline	AG 1478; Tryphostin AG 1478	3 μM	Calbiochem
Gefitinib (ZD 1839)	Iressa	1 μM	Astrazeneca
Trastuzumab	Herceptin	40 μg/ml	Roche
TNF-α Protease Inhibitor-1 (TACE inhibitor)	TAPI-1	100 μM	Calbiochem

2.1.7 Solutions

PBS: 130.37 mM NaCl, 3.19 Mm KCL, 9.6 mM Na_2HPO_4, 1.75 mM KH_2PO_4, 1.1 mM $CaCL_2$, 1mM $MgCl_2$, pH 7.2

PBST: 0.2 % (v/v) Tween 20 (polyoxyethylene-sorbitan monolaurate) in PBS

Trypsin / versene: 0.05 % (w/v) trypsin, 0.02 % (w/v) EDTA, 27 Mm NaCl, 1.62 mM Na_2HPO_4, 0.3 mM KH_2PO_4, 0.0003% (v/v) phenol red

Cell lysis buffer: 20 mM Tris-HCl (pH 7.4), 150 mM NaCl, 100 mM NaF, 10 Mm $Na_2P_2O_7$, 10 mM EDTA, supplemented with 1% (v/v) Triton X-100 and 1 protease inhibitor cocktail tablet per 10 ml of cell lysis buffer

4xSDS sample buffer: 250 mM Tris-Cl (pH 6.8), 20 % (w/v) glycerol, 4 % (w/v) SDS, 0.01 % (w/v) Bromophenol Blue, 50 mM β-mercaptoethanol

8 % (v/v) SDS polyacrylamide resolving gel: 8 % (v/v) acrylamide mix, 0.375 M Tris pH 8.8, 0.1 % (w/v) SDS, 0.1 % (w/v) ammonium persulfate, 0.06 % (v/v) TEMED

5 % (v/v) SDS polyacrylamide stacking gel: 5 % (v/v) acrylamide mix, 0.126 M Tris pH 6.8, 0.1 % (w/v) SDS, 0.1 % (w/v) ammonium persulfate, 0.1 % (v/v) TEMED

Tris-glycine electrophoresis buffer: 25 mM Tris, 250 mM glycine, 0.1 % (w/v) SDS, pH 8.3

Tris-glycine transfer buffer: 24 mM Tris, 192 mM glycine, 20% (v/v) methanol

Stripping buffer: 500 mM glycine – acetic acid, pH 2.5

Ponceau S: 5% acetic acid (v/v), 2% Ponceau S (w/v) in water

Coumassie Blue stain: 40% (v/v) methanol, 10 % (v/v|) glacial acetic acid, 0.04 % (w/v) Coumassie Brilliant Blue R-250

4% PFA (paraformaldehyde): 8g PFA in 200 ml PBS

0.2% (v/v) Triton X-100: 50 µl of Triton X-100 in 25 ml PBS)

1 mg/ml Sodium borohydrate: 0.05g sodium borohydrate in 50 ml PBS

1% (w/v) BSA (Bovine Albumin): 0.5g in 50 ml PBS

Reaction buffer (for protein tyrosine phosphatase YOP): 50 mM Tris-HCL, 150 mM NaCl, 5 mM DTT, 2.5 mM Na_2EDTA, 100 µg/ml BSA

Mowiol: 10% (v/v) Mowiol, 25% glycerol, 100 Mm Tris-HCl, pH 8.5

OCT™: Polyvinyl alcohol (<11%), Carbowax (<5%), non-reactive ingredients (> 85%)

2.1.8 Reagents

Application	Reagents	Source
Cell culture	Foetal Bovine Serum	Bioclear
	Dulbecco's Modified Eagle Medium (DMEM)	Cancer Research UK
	Trypsin / versene	
Cell lysis	Protease inhibitor cocktail tablets	Roche
	Triton X-100 (t-Octylphenoxypoly-ethoxyethanol	Sigma
Protein assay	Bio-Rad Protein Assay	Biorad
SDS-PAGE	Acryl/Bis 30 % (v/v)	Amresco
	Tris, Ammonium Persulfate, TEMED	Sigma
	RPN 800 Molecular Weight Markers	Amersham
	4-12 % pre-cast gels	Invitrogen
	NuPAGE MOPS SDS running buffer x20	
Western blotting	Immobilon™-P PVDF membrane	Millipore
	ECL Western Blotting Detector System	Amersham
	30 % solution Bovine Albumin	Sigma
	Ponceau S solution	
	Medical X-Ray film	AGFA
	RPN800 Full range Rainbow Molecular Weight markers	GE healthcare

FRET	Cy3b	GE Healthcare
	Cy5	GE Healthcare
	DMF (N,N-Dimethylformamide)	Sigma
	4%PFA (paraformaldehyde)	Sigma
	Triton X-100 (t-Octylphenoxypoly-ethoxyethanol)	Sigma
	Sodium borohydrate	Sigma
	BSA (Bovine Albumin)	Sigma
	p-Nitrophenyl Phosphate	Calbiochem
	Protein Tyrosine Phosphatase, YOP (*Yersinia enterocolitica*)	Calbiochem
Cell viability	Trypan Blue (Vi-CELL™ Reagent Pak)	Beckman Coulter
	DMSO (Dimethylsulfoxid 99.8% Methyl sufoxide 99.8%)	Aldrich
Liquid nitrogen fixation	OCT	Sakura

2.2 Methods

2.2.1 Mammalian cell culture

A431, MCF-7, SKBR3, MDAMB-453 were routinely cultured as monolayers in Dulbecco's modified eagle's medium (DMEM) supplemented with 7.5 % (v/v) foetal bovine serum (FBS) at 37^0C CO_2 humidified atmosphere. The cells were obtained from Cancer Research UK cell services and were split before they were confluent. The cells were grown to a maximum of 30 passages before being discarded and new cells would be obtained from cell services. When splitting the cells, the cells were washed once with PBS to get rid of the dead cells and to clear the serum which contained inhibitors that would otherwise suppress trypsin. The cells were then incubated with 2 ml of trypsin/versene in a 10-cm plate for a maximum of few minutes before the trypsination was inhibited by adding 8 ml of 10% FBS. Following splitting the new cells were seeded at 1:10 - 1:20 dilution for MCF-7, SKBR3 and MDAMB-453 and 1:20 to 1: 40 dilution for A431 cells (since these cells have a faster proliferation rate).

2.2.2 Determination of protein concentration

Bio-Rad's protein assay (based on the Bradford's dye-binding procedure) was used to determine the protein concentration (Bradford 1976) before sample loading for SDS polyacrylamide gel eletrophoresis. Near confluent cells were first washed with cold PBS (4^0C) before adding lysis buffer (Section 2.1.7) for 10 minutes at 4^0C. The total protein concentration of the cell lysate was determined using the Coomassie Brilliant Blue G-250 dye that binds to basic/aromatic acid residues and changes its colour in response to various concentrations of the protein. Bovine serum albumin (BSA) was used as a

standard and a stock solution of 10 μg / μl was diluted with dH_2O (0.2, 0.5, 1.0, 1.5, 2.0, 3.0, 4.0 μg / μl) to produce a standard curve. The dye Reagent was first diluted with water (1:5 ratio) and 500 μl of this was transferred into each reaction vial. 2 μl of each standard solution or each cell lysate was mixed with 500 μl of diluted dye Reagent. After 10 minutes of incubation, a duplicate of each condition (200 μl) was loaded into a 96-well microtitre plate. The absorbance of the dye-protein complex was measured at 585 nm in a SpectraMax plate-reader from Molecular Devices and the protein concentration of the cell lysate was determined from the BSA standard curve (using lysis buffer as the blank measurement).

2.2.3 Immunoprecipitation

All experiments were performed using Protein G Agarose beads (Roche) which were washed with PBS for three times before each experiment to get rid of the storage ethanol. The cells were grown to near confluency before being lysed with lysis buffer (Section 2.1.7) on ice. The cell lysate was centrifuged for 5 minutes at, a speed of 20817 rcf (14000 rpm) in a 5417R centrifuge (from Eppendorf) before transferring the supernatant to a new reaction vial. The supernanatant was presorbed with beads for 2 hours at 4^0C. The mixture of cell lysate and beads was then centrifuged for 5 minutes at a speed of 20817 rcf (14000 rpm) before transferring the supernatant to another new reaction vial. The antibodies anti-HER4 (concentration 1:100, C-terminal; Santa Cruz) or anti-HER2 (concentration 1:100, intracellular; Cell signalling) were added to the supernatant and were incubated overnight at 4^0C. The next day, the immune-complex was collected by the addition of new beads and further incubation for 2 hours at 4^0C. The beads were washed thoroughly with lysis buffer before boiling with 1 x SDS. 40 μl was loaded in each lane in SDS-PAGE for western blot analysis.

2.2.4 SDS polyacrylamide gel electrophoresis (SDS-PAGE)

Following protein determination by Bradford Assay, the cell lysate was mixed with 4X SDS (with a reducing agent, β-mercaptoethanol). The SDS and cell lysate mixture was boiled for 10 minutes at 95^0C to dissociate the protein into their individual polypeptide subunits. Equal amounts of protein based on a Bradford Assay were then loaded onto an SDS-PAGE gel. In the first half of my PhD, the SDS polyacrylamide resolving and stacking gels (Section 2.1.7) were routinely made and SDS-PAGE was performed in a Tris-glycine electrophoresis buffer using a Biorad Mini Trans Blot electrophoresis cell. However, to improve the resolution, pre-cast gels were subsequently used to perform SDS-PAGE with 1x NuPAGE MOPS SDS running buffer and Invitrogen Novex Mini-Cell. The gels which contained separated polypeptides with the molecular marker were transferred onto the PVDF membrane for western blot analysis.

2.2.5 Protein transfer

Using the Biorad Trans-Blot Semi-Dry Transfer apparatus, the separated polypeptides and the molecular markers on the gel were transferred to Immobilon™-P PVDF membranes. For each gel, a PVDF membrane was initially equilibrated with methanol and two sets of Whatman paper (3mm, 4 pieces in each set) were immersed in Tris-glycine buffer before protein transfer. The gel was placed on top of the soaked PVDF membrane and both were then sandwiched between the two sets of Whatman papers. The transfer was performed using the Transfer apparatus at 12 V for 2 hours at room temperature. The membrane was then used for western blot analysis. To check for efficient protein transfer, the membrane was stained with Ponceau S solution and de-stained with water before western blot analysis.

2.2.6 Western blot analysis

After transfer, the PVDF membrane was washed with PBS first at room temperature for 5 minutes. The membrane was then incubated for 1 hour at room temperature or overnight at 4 ^{0} C with blocking buffer, 3% (v/v) BSA in PBS supplemented with 0.2% Tween-20 (PBST). Following blocking, the membranes were incubated with the appropriate primary antibody for 2 hours at room temperature, followed by four washes (15 minutes each) with PBST containing 1% (w/v) low fat milk powder. The membranes were then incubated with the appropriate HRP-conjugated secondary antibody (section 2.1.4) in PBST (containing 5% (w/v) low fat milk powder) for 1 hour at room temperature and another four washes with PBST (15 minutes each) containing 1% (w/v) low fat milk powder. The membranes were then washed twice with PBST and once with PBS before incubation with a 1:1 mixture of the Amersham ECL reagents for 2 minutes. The membranes were then put in Kodak BioMax MS cassette and exposed to photographic AGFA Cronex 5 Medical X-Ray Film for variable durations before being developed using an IGP Compact 2 Developer. All the western blot experiments were repeated at least three times and represented blots were shown in the results' section.

Western blot for experiments on growth factor stimulation and drug treatment in cell lines

The cells were grown to 80% -100% confluent in a 6-well cell culture plate after seeding 30,000 cells per well. The cells were grown for at least 24 hours before treated with drugs, e.g. 3 μM AG 1478, 1 μM Iressa and 40 μg/ml Herceptin for different durations according to the experiments (unless indicated otherwise, these will be the doses used for these drugs). The dosage for TAPI inhibitor, TAPI-1 was 100 μM. For growth factor experiments, the cells were treated with 50 ng/ml EGF, 100ng/ml heregulin β (β3 of NRG1, Section 2.1.5) and 100ng/ml heregulin-β1 (β1 of NRG1, Section 2.1.5) for 10 minutes following serum starvation of 16 hours. The cells were then obtained after 30-minute treatment with lysis buffer (Tris HCl, 20 mM; NaCl, 150 mM; NaF 100 mM; $Na_4P_2O_7$ 10 mM; EDTA 10 mM with 1% Triton and protease

inhibitor cocktail-Roche) and centrifuged at 4^0C to remove of the insoluble cell pellets. Polyacrylamide gel electrophoresis was carried out employing 10 μg of protein in each lane. Western blots were performed using primary antibodies mentioned above. A dilution of 1:1000 was used for the primary antibodies unless otherwise indicated in Section 2.1.4. Antibodies were incubated overnight at 4^0C. They were detected using horseradish peroxidase-linked secondary antibody (a dilution of 1:2000 sheep anti-rabbit IgG) and visualized with an enhanced chemiluminescent (ECL) system (Amersham).

2.2.7 Cell viability

To test cell viability, cells were grown in 24-well plates after seeding approximately 15,000 cells per well. The cells were left to grow for at least 24 hours before treatment with either 40 μg/ml Herceptin or 1 μM Iressa. For the Iressa experiments, a DMSO control (1:1000) was also performed. On the day of the experiment, the cells were trypsinised and diluted with PBS. The viable cells were counted in cell viability analyzer (Vi-cell ^{TM} XR, Beckman Coulter) using Trypan Blue to stain the dead cells. The viable cells for each condition were compared with the control.

2.2.8 Xenograft experiments

MDAMB-453 ($2.5\text{-}5\text{x}10^6$) and SKBR3 cells ($5\text{-}10\text{x}10^6$ cells) both in 100 μl serum-free medium were bilaterally injected subcutaneously into the flanks of SCID mice (n=2 for each cell type). SKBR3 cells were not tumourigenic in SCID mice but xenograft tumours were successfully grown in the bilateral flanks of the two SCID mice using MDAMB-453 cells. These two mice were killed using CO2 chamber after two months when the tumours grew to about 1cm^3. Only xenograft tumours from one mouse were used for tissue fixation experiments with either formalin (NBF) or liquid nitrogen.

The largest tumour measuring 1.1 cm was cut into three parts. One part was fixed immediately with formalin (NBP), one was left in the pot for 1 hour at 27^0 C before fixation with NBP, one was left in the pot for 1 hour at $4\ ^0$ C before fixation with NBP. The tumours fixed with formalin were processed and embedded into paraffin block before being sectioned and made into slides by the staff at the Experimental Pathology Department.

The second tumour measuring 0.8 cm was cut into two parts. One part was frozen within 15 minutes with liquid nitrogen and the other part was left in 20% sucrose/PBS solution (cryopretection solution) for 24 hours before fixation with liquid nitrogen. To prevent damage to the tumour tissues from sudden freezing by liquid nitrogen, the following steps were used in Experimental Pathology Department. The tumours were first immersed in OCT solution (Section 2.1.7) contained in an aluminium foil mould. The mould containing tumour tissues and OCT was then submerged for 5-10 seconds in thawing isopentane when it was semi-liquid and having first frozen by liquid nitrogen. OCT would crack if the mould was submerged in isopentane for a significant amount of time (instead of 5-10 seconds). The frozen tumour tissues in OCT were transferred immediately to – 70 ^{0}C for storage or to cryostat at – 20 ^{0}C for sectioning.

2.2.9 Antigen retrieval

Antigen retrieval was applied to cells fixed with 4% PFA or paraffin-embedded xenograft tumour slides or tissue microarrays (TMA) to recover the buried epitopes. Before the antigen retrieval, tumour slides or TMAs were de-waxed in Xylene and rehydrated through graded alcohols to water. For the cells fixed with 4% PFA, this additional step was not required. For antigen retrieval, 0.01M of citrate buffer (pH 6) was heated in an 800-watt microwave oven at full power for 4 minutes. The samples were then placed in the buffer and heated in the microwave for a further 4 minutes at full power. The citrate buffer was then topped up and microwave heated again for 4 minutes. The citrate solution and sections were then allowed to cool for 10 minutes before

handling. For IHC anti-pHER2 staining and HER2 FRET experiment, the New England Biolabs' protocol was used. This procedure is similar to the antigen retrieval process using citrate buffer, except that the tissue slides were brought to boiling in 1 mM EDTA pH8, followed by 15 minutes at a sub-boiling temperature.

2.2.10 Immunohistochemistry (IHC)

As discussed in the Introduction, the IHC scoring may vary depending on different laboratories and countries as well as the antibodies and the epitopes used. The scoring systems for TMAs in the histopathology department at the University of Oxford were previously validated by the department and they are based on either intensity or /and percentage of cell staining.

Intensity is scored as either 0 (negative staining); 1+ (weak intensity); 2+ (moderate intensity); or 3+ (strong intensity). Percentage of staining is scored as either 0 (negative staining); 1+ (1-10% staining); 2+ (11-50% staining); 3+ (51-80%) or 4+ (81-100%). These scoring systems are shown in the table below:

Scoring	Intensity	Percentage of staining
0	Negative staining	Negative staining
1+	Weak intensity	1-10% staining
2+	Moderate intensity	11-50% staining
3+	Strong intensity	31-80% staining
4+		81-100% staining

The score from intensity may be multiplied by the score from percentage of staining to give an overall score. The exact criteria may vary depending on antibodies used and may depend on the detected epitopes and tumours as well as locations of staining (membranous versus cytosolic versus nuclear).

For EGFR scoring reported in this study, F4 (anti-EGFR) antibody was used and intensity of the membranous staining (based on University of Oxford

histopathology department as classified above) is used. For HER2 scoring, HercepTest (DAKO) using A0485 (anti-HER2) antibody was used to screen for HER2 positivity (2+ and 3+) in breast tumour arrays. The scoring system of HercepTest based on intensity of anti-HER2 staining is illustrated in Introduction.

5 μm sections of TMAs were dewaxed in Xylene and rehydrated through graded alcohols to water. High temperature antigen retrieval was performed in 0.01 M citrate buffer pH 6 heated for 1 minute in a microwaveable pressure cooker. The sections were then cooled and washed in water. Following peroxidase block, sections were protein blocked for 15 minutes in 2.5% normal horse serum. The primary monoclonal antibody F4 (anti-EGFR) was incubated on the sections for 1 hour at room temperature with an antibody concentration of 10 μg/ml and then washed twice in PBS. The primary antibody was visualised using an HRP Vectorlabs Immpress Mouse Kit (Vector Laboratories, Burlingam, CA) and the sections were developed with diaminobenzidine (DAB). After washing in water, sections were mounted on cover slips with aqueous mounting medium.

2.2.11 FRET monitored by frequency-domain FLIM

FRET involves the transfer of energy from an excited donor molecule to a nearby (1-10 nm) spectrally overlapping acceptor. As discussed in the Introduction, various methods may be used to quantify FRET including FLIM used in this thesis. FRET can be quantified by measuring fluorescence lifetime of the donor, which is reduced as energy is non-radiatively transferred via a dipole-dipole interaction. Spatial aspects of fluorescence lifetime may be assessed by using FLIM (Larijani et al., 2003). In this thesis, the donor Cy3b lifetime variations were monitored in the frequency (phase) domain where the excitation light was sinusoidally modulated at 80.224 MHz to excite the sample. The emitted light oscillated at the same modulation frequency but with a phase shift and a decrease in amplitude (demodulation). Determining these

two parameters permitted measurement of phase (τ_p) and modulation depth (τ_m) of the fluorescence. The average lifetime, $<\tau>$, is the average of phase shift and relative modulation depth ($\tau_m + \tau_p$) / 2 of the emitted fluorescence signal. The efficiency of FRET can be mapped in a single cell by determining the excited state lifetime of the donor fluorophore at each pixel of the image. FRET efficiency is calculated as $E = 1 - [<\tau_{d/a}> / <\tau_d>] \times 100$, where $<\tau_{d/a}>$ is the lifetime map of the donor in the presence of the acceptor, and $<\tau_d>$ is the average lifetime of the donor in the absence of the acceptor (Larijani et al., 2003; Wu and Brand, 1994).

2.2.11.1 Frequency-domain FLIM system and set-up

The single frequency-domain FLIM used in this thesis at the Cell Biophysics Laboratory, consisted of several key components connected to an inverted microscope (Carl Zeiss Ltd) mounted on a 2x1m optical table (Technical Manufacturing Corporation) (Figure 2.1). The key components were:

(a) Light source. The light source was from Argon/Krpton monochromatic laser (Innova Spectrum 70C, Coherent UK Ltd) which was tuneable to select an appropriate wavelength for the excitation (e.g. 488 nm for GFP and 514 nm for Cy3b).

(b) Standing-wave acousto-optic modulator (SW-AOM; Intra-Action Corporation). The light source was sinusoidally modulated with SW-AOM at a modulation frequency of 80 MHz. Since the FLIM used was a single frequency set-up, the modulation frequency of 80 MHz was not changed and the maximum sensitivity of lifetime it could detect is around 2 ns (explanation in Section 1.9.3.2). Therefore, it was optimal for GFP (488 nm) or Cy3b (514 nm) since their lifetimes are around 2 ns in cells. The room temperature was kept close to 18^0 C to prevent thermal phase drift in AOM, which was essential for phase coherence between the fluorescent signal and the modulated gain of

the detector. With the help of an array of mirrors, the modulated light source was directed to an iris diaphragm to selectively isolate the central (zero-order) beam from the higher-ordered diffracted beams. The modulated central light beam was further directed into a multi-mode fibre light scrambler (a 1.5-metre step index silica fibre, 1-mm core, numerical aperture 0.37; Technical video Ltd) that disrupted the coherence of the laser light by vibrating the fibres at frequencies of around 100 Hz. This resulted in a randomly moving speckled illumination of the specimen and was subsequently integrated during detection.

(c) Frequency synthesisers (2023 Marconi). The AOM was driven by a frequency synthesiser (slave) to a resonance frequency of about 40.112 MHz and this produced the intensity oscillations in the laser light beam at 80.224 MHz (twice the driving frequency). The master frequency synthesiser driving the micro-channel plate (MCP) and the image intensifier head was set at 80.224 MHz which was the value that exactly double that driving the AOM (40.112 MHz).

(d) Phase-sensitive detection system. The resulting fluorescence was separated using a combination of dichroic beam splitter (Q565 LP; CHROMA technology Corp.) and narrow band emitter filter (BP 610 /75; Delta Lys and Optik). The fluorescence was imaged onto the photocathode of the image intensifier head (Hamamatsu C5825) which then focused the photoelectrons ejected from the photocathode onto the face of a MCP. An intensified light image was generated when the electron image at the output of the MCP hit the phosphor screen. The effective gain of the image intensifier was modulated at a frequency equal to that of the SW-AOM (80 MHz) for homodyne detection. The outputs from the two synthesisers were used to provide sinusoidal voltages sources for modulating both the excitation laser light via the SW-AOM and the gain of the image intensifier unit. The amplified image was then projected from the phosphor screen of the MCP onto the chip of a charged-coupled device (CCD) camera (Quantix, Photometrics). Two-by-two binning for cell experiments and three-by-three binning for tumour arrays were typically set as the readout of the CCD. The gain was adjusted according to the fluorescence intensity of the sample and it was usually set either two or three.

(e) Other components. 100-W Mercury arc lamp (Carl Zeiss Ltd) was used as a source of illumination for acceptor fluorophores and to bleach the acceptors as required. A variable density filter wheel was used to select the intensity of the excitation light.

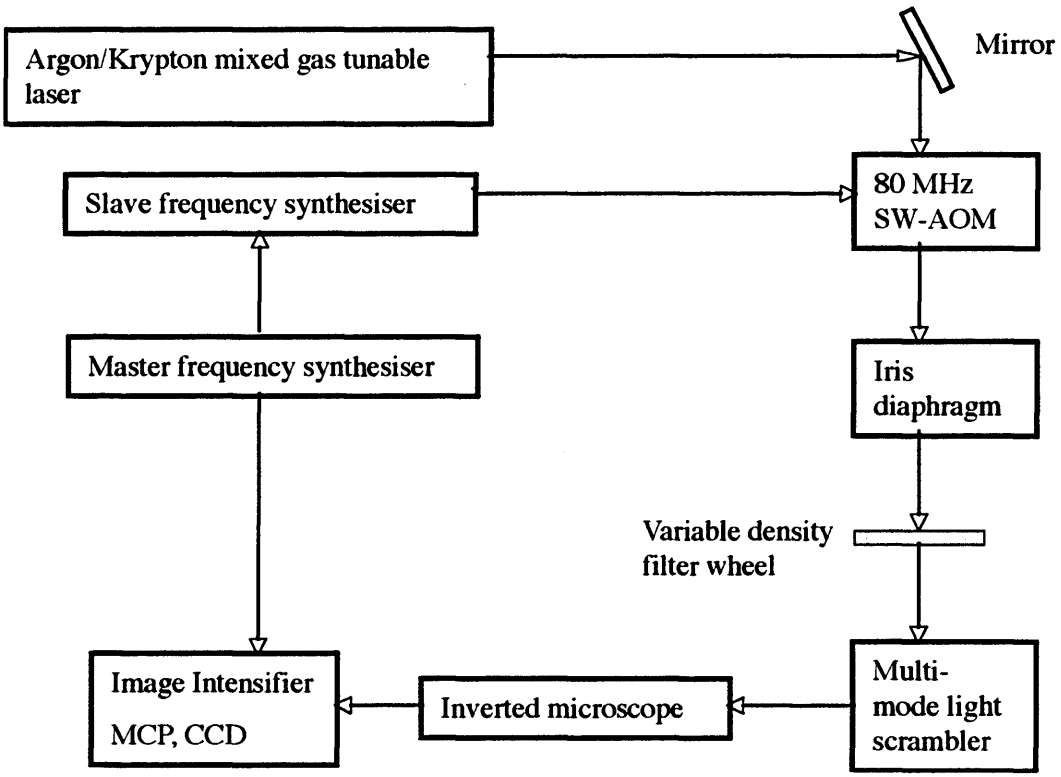

Figure 2.1: Simplified schematic diagram of frequency-domain FLIM at the Cell Biophysics Lab.

2.2.11.2 Image acquisition and data analysis

All images (a cycle of 16 phase-dependent images) were taken using a Zeiss Plan-APOCHROMAT ×100/1.4 NA phase 3-oil objective for cell experiments and using x10/0.5 NA phase 1 objective for TMAs experiments. Before proceeding to obtain the lifetimes of donor Cy3b, a reference image (a cycle of 16 phase-dependent images, each separated by 22.5°C) using a scattering foil was first obtained. Before taking images of the foil, the intensity of the 514 nm laser line was reduced to minimum using the variable density filter wheel. The reference measurement taken with this scattering foil was used to determine the phase setting at which the maximum intensity was reached in the image series. This was used to calibrate the phase of the master frequency synthesizer that must be set at a maximum in order to acquire a phase-dependent FLIM data. The phase value was set to zero degree on the master frequency synthesizer and another cycle of 16 phase images from the foil was taken and saved as a zero lifetime reference. This procedure was repeated every hour to ensure that the phase of the master frequency synthesizer remained at zero during the experiments. The reference measurement from foil also revealed a modulation value, indicating the modulation of the excitation laser source. The modulation value was approx 0.50 for the experiments done in this thesis. In addition, an arbitrary value of intensity (which is saturated at a value of 4095 counts) may be obtained with the scattering foil. If the intensity of the scattering foil was low (less than 1000 counts) or the modulation value was not near 0.50, it was due to the misalignment of the laser. The FLIM therefore needed to be optimised and aligned using the scattering foil before performing any experiments. In addition, when the wavelength of the tunable laser source was changed (between 488 nm and 514 nm), it was also essential to check that the laser alignment by assessing the modulation and intensity values of the scattering foil.

To obtain the lifetimes of donor Cy3b in cells or tumour cores, the intensity of the excitation light was restored to a maximum using the variable density filter wheel and the Cy3 filter set (excitation, HQ 545/30 band pass filter,

dichroic mirror, Q565 long pass; emission, HQ610/751 band pass filter; Chroma) was moved into excitation path. Two contiguous series of 16 phase-dependent images (one forward and one reverse cycle, 45 degree phase-stepped) and a background image from the samples were taken. The exposure time of the acquisition was chosen depending on the fluorescence intensity and may vary from 50 to 1000 ms. To acquire acceptor images, the laser source was switched to 100-W mercury arc lamp using a rotating mirror and the Cy5 filter set (excitation, HQ620/60 band pass filter; dichroic mirror, Q660 long pass; emission, HQ 700/75 band pass filter; Chroma) was set in the detection path.

Using these images from acquisition and the zero lifetime reference from the foil, the donor lifetimes (phase τ_p and modulation τ_m parameters) were obtained using IPLab Spectrum software (version 3.1.2c Scanalytics, Inc.) based on Fourier transformation. An average of the lifetime phase and modulation is calculated for each pixel ($[\tau_p + \tau_m]/2$) although these independent parameters cannot be averaged if the τ_p and τ_m do not have close values (Alcor D, 2007). To help visualization, the average lifetime map may be represented with pseudo-colour scale (higher lifetimes in blue and shorter lifetimes in red). However, since the pseudo-colour scale may differ for each set of experiments, it is essential to consider the values of the lifetimes in each experiment. Previously, the determination of the correct thresholding and the average lifetime map was done by the operator manually. In collaboration with Pierre Leboucher at College de France, an automatic analysis of the data was implemented, resulting in an increased speed in the non-biased data analysis and improved reproducibility of the results (Alcor D, 2007).

2.2.11.3 Choice of fluorophores and conjugation of fluorophores to antibodies

As discussed in the Introduction, FRET efficiency depends on several parameters including the quantum yield of fluorescence of the donor and the overlap between the emission spectra of the donor and the absorption spectra

of the acceptor (Section 1.9.2). Therefore, a suitable pair of donor and acceptor fluorophores needed to be chosen for FRET experiments. The FLIM instrument used in Cell Biophysics Lab uses a modulation frequency of 80 MHz and the maximum sensitivity of lifetime to be detected is around 2 ns (explanation Section 1.9.3.2). Cy3b was chosen as a donor fluorophore because of its near 2 ns lifetime as well as being a fluorophore that has high quantum yield (source from GE healthcare, formerly Amersham). Cy5 was chosen as the appropriate acceptor for Cy3b since the emission spectrum of Cy3b overlaps with the absorption spectrum of Cy5, which makes FRET possible between the pair. Both Cy3b and Cy5 have good photo-stability and therefore they are a suitable pair of fluorophores for FRET experiments.

F4 (anti-EGFR or anti-ErbB-1), anti-HER2 (anti-ErbB-2) and anti-HER4 (ErbB-4) were conjugated to Cy3b (donor fluorophore) and FB2 (anti-phosphotyrosine), anti-phospho-HER2 and pTyr-100 (anti-phosphotyrosine) were conjugated to Cy5 (acceptor fluorophore). The resulting pairs of F4-Cy3b / FB2-Cy5, HER2-Cy3b / pHER2-Cy5, HER4-Cy3b / pTyr-Cy5 were used to assess EGFR and HER2 phosphorylation as well as HER4 proteolytic cleavage respectively. 100 µl of N, N-Dimethylformamide (DMF) was added to 1 mg Cy3b to make a 10 mg/ml stock solution (15 mM). The stock 10 mg/ml Cy3b was diluted in DMF 10 fold to 1 mg/ml (1.5 mM). 50 µl of Cy3b / DMF from a stock of 1 mg/ml was added drop by drop into 450 µl anti HER receptor antibody / 50 µl Bicine (1M, pH 8) with continuous stirring. The final concentration of conjugated anti-HER receptor antibodies with Cy3b was approximately 100 µg/ml (150 µM). The solution was stirred in the dark for 2 hours. To conjugate FB2, anti-HER2 and anti-pTyr-100 with Cy5, 20 µl of DMF was added to a Cy5 vial. Cy5 dye in DMF was then added drop by drop to 450 µl antibodies (FB2, anti-HER2 and anti-pTyr-100) / 50 µl Bicine (1M, pH 8) while stirring. The solution was stirred in the dark for 2 hours. The conjugated antibodies were separated from free dyes by column chromatography (desalting column, Bio-Rad). The matrix of the column excluded solutes greater than 6000 Daltons (i.e. conjugated antibodies with Cye dyes) and retained the smaller contaminants (free dyes). The column was first washed and equilibrated with 3 x 5 ml PBS before the loading. The

labelled antibody and unconjugated Cy3 were eluted with PBS. The labelled antibody was collected and the dye/protein ratio was measured by UV/visible spectroscopy: detection of the antibodies' concentrations at 280 nm; F4-Cy3b, HER2-Cy3b and HER4-Cy3b at 561 nm; and FB2-Cy5, pHER2-Cy5 and pTyr-Cy5 at 650 nm wavelength. An example is given in Figure 2.2. The D/P ratios (aiming for 1-2) were calculated using the protocols provided by GE Healthcare (formerly Amersham Biosciences) for Cy^{TM}3B and Cy5 mono-reactive dyes:

D/P = [(Absorption A_{max}) x (Antibody Extinction Coefficient)] / [(A_{280} – correction factor x A_{max}) x (Cy Dye Extinction Coefficient)]

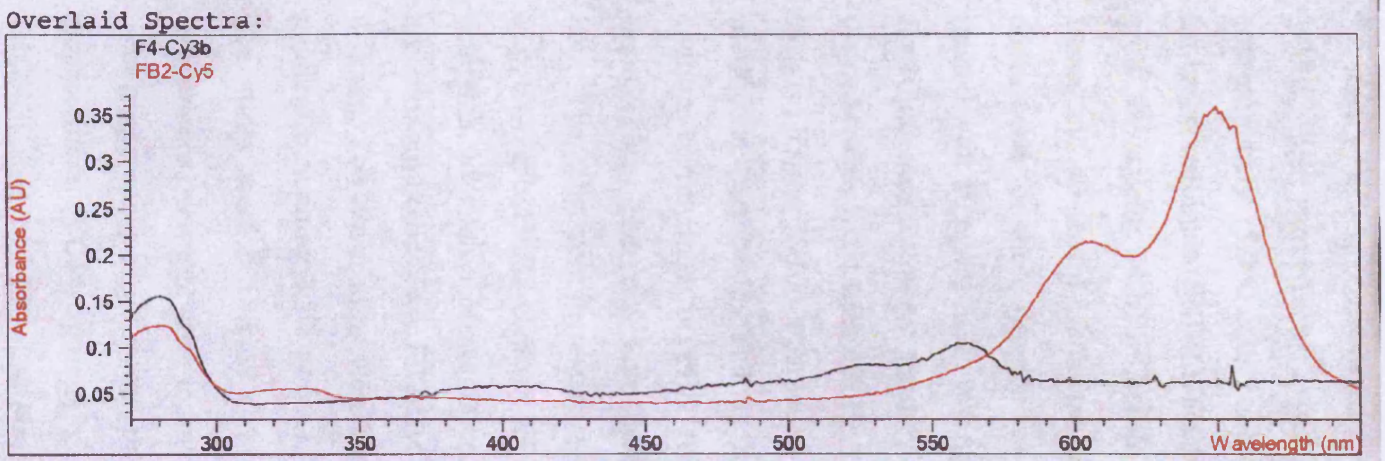

#	Name	Abs<280nm>	Abs<561nm>	Abs<650nm>
1	F4-Cy3b	0.15607	0.10443	6.5709E-2
2	FB2-Cy5	0.12283	7.8170E-2	0.35708

Figure 2.2: Dye/protein ratios (D/P) of F4-Cy3b and FB2-Cy5 were determined by UV spectroscopy. 50ul of F4-Cy3b was put in a cuvette and the absorbance of F4 was determined at 280 nm wavelength, and Cy3b at 561 nm by the UV spectroscopy. For FB2-Cy5, the absorbance of FB2 was determined at 280 nm and that of Cy5 at 650 nm by the UV spectroscopy. PBS solution was used as "blank " before measuring D/P ratios of F4-Cy3b and FB2-Cy5. The D/P ratios were then calculated by the formulas supplied by GE Healthcare (see text for details).

2.2.11.4 *In-situ* FRET experiments

Cells were grown in 24-well plates with cover slips after seeding approximately 15,000 cells per well for A431 cells and 30,000 cells per well for breast cell lines (SKBR3, MCF-7 and MDAMB-453). The cells were left to grow for at least 24 hours before treated with drugs, 3 μM AG 1478, 1 μM Iressa and 40 μg/ml Herceptin (unless indicated, otherwise this will be the doses used for these drugs). For growth factor experiments, the cells were treated with 50 ng/ml EGF, 100 ng/ml heregulin β and 100 ng/ml heregulin-β1 for 10 minutes following serum starvation of 16 hours. Following stimulation, the cells were fixed with 4% PFA at room temp for 10 minutes. 500 μl of 0.2 % (v/v) Triton X-100 was added in the well for 5 minutes to make the cell membrane permeable. This is followed by incubation with 1mg/ml fresh sodium borohydrate in PBS for 10 minutes to quench the background fluorescence. The cells were then blocked with 1% w/v BSA in PBS for 1 hour. The cells were incubated and labelled with conjugated donor antibodies (e.g. F4-Cy3b, HER2-Cy3b or HER4-Cy3b) for 2 hours. For cells that required detection with the acceptor fluorophores, further incubation with conjugated acceptor antibodies (e.g. FB2-Cy5, pHER2-Cy5 or pTyr-Cy5) was done for 2-4 hours. The cover slips were mounted on the slide with Mowiol mounting medium containing 2.5% (w/v) 1,4-diazabicyclo (2.2.2) octane as an anti-fade. The slides were left at 37^0C incubator for 1 hour and then left at room temperature overnight prior to image acquisition.

For phosphatase experiments, the protein tyrosine phosphatase from *Yersinia enterocolitica* (YOP), 50 units of phosphatase in 50 μl reaction buffer (50mM Tris-HCL, pH 7.2, 150 mM NaCl, 5mM DTT, 2.5 Mm Na_2EDTA, and 100 μg/ml BSA as recommended by Calbiochem) was used for each coverslip on the laboratory film (Parafilm "M") after fixing with 4% PFA. The rest of the procedures are the same as above.

2.2.11.5 FRET Data Interpretation and Statistical analysis

For FRET experiment, at least three to five measurements of lifetimes from single cell(s) were obtained from each condition and the results were represented in either two-dimensional (2-D) histograms or scatter diagrams.

Two-dimensional histograms

The two-dimensional histograms showed both the phase (τ_p) and modulation (τ_m) measurements for lifetimes for all recorded pixels and they quantified the reduction of the phase and modulation lifetimes of donor Cy3b when there was FRET. The error bars represent the standard deviations from all the measurements ($n > 3$ or 5).

Scatter diagrams of average lifetimes of donor

An average lifetime was obtained from the average of phase and modulation components of the lifetimes and the distribution of average lifetimes of donor fluorophore (e.g. EGFR-Cy3b) from each condition was shown as scatter diagrams. The basal condition was defined as the basal phosphorylation of the HER receptor, indicated by the decrease of lifetime of the donor in the presence of the acceptor without growth factor stimulation or drug treatment. The basal phosphorylation was due to autocrine ligand release of the cancer cells (Van de Vijver et al., 1991). The enhanced decrease in the average lifetime indicated further phosphorylation of the receptor due to its dimerisation with its partners. The medians of these measurements were displayed in the scatter diagram. Mann-Witney test was used to compare the medians of the average lifetimes between the basal condition and those stimulated with ligands or treated with drugs.

2.2.11.6 FRET experiment for tissue microarrays (TMAs)

To label the tumour arrays with conjugated donor antibodies (F4-Cy3b, HER2-Cy3b), the arrays were immersed with 0.2 % (v/v) Triton X-100 for 5 minutes to permeabilise the membrane. This was followed by incubation with 1mg/ml fresh sodium borohydrate / PBS for 10 minutes to quench background fluorescence. 1% w/v BSA in PBS was used for blocking. The tumour arrays were incubated with the donor (either F4-Cy3b or HER2-Cy3b) for 2 hours and the acceptor (either FB2-Cy5 or pHER2-Cy5) for 2 hours. The arrays were then mounted on a glass cover with Mowiol mounting medium containing 2.5% (w/v) 1,4-diazabicyclo (2.2.2) octane.

Automation of frequency-domain FLIM and high throughput processing for TMAs

The advantage of frequency-domain FLIM is its speed in acquiring images compared to time-domain FLIM. The frequency-domain FLIM was programmed by our consultant engineer Pierre Leboucher (College de France, Paris) and my primary supervisor Banafshe Larijani to process the TMAs and to analyse the data in a high throughput manner. This was achieved by writing a special script ("APierre") in the computer so that the motorized stage driver unit (x,y,z) which controlled the stage of the inverted microscope would be automated. Before processing the tumour arrays, the tumour cores were first mapped in IPLab Spectrum (Signal Analytics). The stage was first initialized and the first cell (in this case, first tumour core) was selected. The motorized stage driver unit needed to be set at zero value for this first cell by pressing "perform stage" on this first cell. The other tumour cores could then be mapped and the mapping of the tumour cores on the slide was named and saved in the slide mapping file. Following the mapping of the tumour cores, the processing of the tumour array was done automatically by "APierre" script after selecting the saved file. To analyse the data automatically, a copy of the foil from the experiment was saved in the desktop of the computer. The file (containing the list of data to be analysed) in IPLab was first opened. The data to be analysed was put in the same named folder and the data was analysed under "script automation 01.00" by pressing "run script". This automation of the data analysis listed all the parameters of lifetimes (phase, modulation and average) and the intensity of the donor fluorophore as well as number of pixels

and bad data analysed in an excel sheet which could then be exported into other files.

The automation of frequency-domain FLIM is essential if the FRET methodology is going to be applied for wide clinical use for. The first proof of principle for the automated high throughput FLIM was done in HNSCC tumour arrays described in chapter 3. However, the automation of FLIM as well as the analysis of the data at cell biophysics Lab are continuously being improved and upgraded by Pierre Leboucher and Banafshe Larijani.

HNSCC tumour arrays

HNSCC tumour arrays were labelled with donor F4-Cy3b and acceptor FB2-Cy5 to assess EGFR phosphorylation of the tumour cores. Using the automated FLIM system, each tumour core was mapped according to the position on the arrays. All images (a cycle of 16 phase-dependent images) of the tumour cores were taken using a Zeiss Plan-APOCHROMAT ×10 / 0.5 NA phase 1. The readout of the CCD was set for three-by-three binning and the gain was set at two. Images from each tumour core were acquired automatically from the arrays according to their positioning. The phase, modulation and average lifetimes of each tumour core were calculated automatically and the average FRET efficiency for each tumour core was obtained. Average FRET efficiency for each tumour core was correlated with survival data. A pilot study was first carried out to assess the first set of arrays with the automated system. To validate the pilot study, a new set of arrays were prepared with new antibodies and fluorophores and the arrays were processed with automated FLIM. In the validation study, the system was programmed to run two loops so that two lifetime measurements were taken from each tumour core (n = 2, i.e. 574 tumour cores in total). However, in any one array a patient would have a duplicate sample, so for each patient the final lifetime represents an average of four measurements. In total 1114 tumour core recordings were made and analysed in the validation study.

To obtain the EGFR status by FLIM, the donor intensity was calculated. For each tumour core, images were acquired and an intensity distribution histogram was plotted using Matlab version 7 and the median of the intensity distribution was calculated by Matlab 7. This median was normalised to the

background intensity. The average of two median intensity values from the two tumour cores of the same patient was used in each array. Thereafter these values were used to correlate with immunohistochemistry stains and average FRET efficiency.

Breast tumour arrays

The breast tumour arrays were labelled with donor HER2-Cy3b and pHER2-Cy5 to assess HER2 phosphorylation of the tumour cores. The tumour cores were mapped and processed automatically like HNSCC tumour arrays. In HNSCC tumour arrays the signal-to-noise ratio was not a problem when assessing EGFR phosphorylation in these tumour cores since almost all HNSCC tumours contain high EGFR. The problem only arrived when a particular tumour core contained very little tumour tissue or contained mostly stromal tissue. In breast cancer, less than a third of the breast tumours over-express HER2. Assessing HER2 phosphorylation was a problem for some of the breast tumour cores with low HER2 expression and for tumour cores with very little tumour tissues since inadequate signal-to-noise ratio was reached for some of the tumour cores. These specific problems were encountered and the details are described in Chapter 5.

Statistical analysis for TMAs

Disease-free Survival (DFS) is defined as the length of time after treatment during which no cancer is found and overall survival (OS) is a defined period of time that the subjects in a study have survived since diagnosis or treatment. All statistical analyses were done using Graphpad Prisms 3cx (Macintosh Version) except the univariate and multivariate analysis for prognostic factors which were done using 'R' (see below). The Kaplan-Meier survival curves were used to compare between the groups and a log-rank test was used to assess the hazard ratios. For the univariate and multivariate analysis of the prognostic factors, the data was analysed by fitting cox proportional hazard models to the data, using top 10% FRET efficiency as the group indicator with a common baseline hazard function, and including immunohistochemistry, UICC tumour stage, grade, necrosis, age and sex variously as covariates. To fit the models, the 'coxph' function was used from the 'survival' package within

R. R is a language and environment for statistical computing and is available as Free Software under the terms of the Free Software Foundation's GNU General Public License in source code form.

3 Assessing EGFR activation and phosphorylation state in cells and head and neck tumour arrays

3.1 Introduction

As discussed in the Introduction, the current methods of measuring EGFR levels including immunohistochemistry (IHC) cannot be unequivocally endorsed as predictive of patient prognosis or response to treatment (Arteaga, 2002). Therefore there is a need for a quantitative method to be set up to measure EGFR and its activation status. To achieve this, Förster Resonance Energy Transfer (FRET) monitored by Fluorescence Lifetime Imaging Microscopy (FLIM) was exploited as a reporter for EGFR (ErbB1 or HER1) phosphorylation and as a molecular prognostic tool to identify HNSCC patients who show over-expression and/or phosphorylation of the EGFR. To establish an assay to assess EGFR phosphorylation, a suitable pair of donor (Cy3b) and acceptor fluorophores (Cy5) were conjugated to F4 (anti-EGFR cytoplasmic domain antibody) and to FB2 (anti-phosphotyrosine antibody) respectively to monitor FRET between the fluorophores detected by FLIM upon EGF stimulation. The main aim was to establish a FRET method to evaluate EGFR phosphorylation in cell lines, which was applicable to paraffin sections. The assay was tested in a few cell lines and a series of optimisations were done to ensure that the assay was robust. The results presented in this chapter illustrate that the FRET associated with the co-incident binding of the labelled monoclonals was specific. These established reagents have been applied to head and neck tumour arrays using a high throughput automated FLIM. Using this highly selective FRET assay in tumour arrays, increased FRET efficiency (indicating high levels of EGFR phosphorylation) was shown to correlate with disease recurrence and prognosis of the patients. The EGFR

status determined by IHC or by average fluorescence intensity was also correlated with EGFR activation by FRET.

3.2 Results

3.2.1 Establishment of an assay to assess EGFR phosphorylation by FRET in cell lines

To develop a phosphorylation state readout with suitable specificity for the EGFR, it was hypothesised that following EGFR activation FRET would be detectable in fixed cell samples between F4-Cy3b (a monoclonal to the cytoplasmic domain of the receptor linked to a donor fluorophore, Cy3b) and FB2-Cy5 (an EGFR autophosphorylation site monoclonal linked to an acceptor fluorophore, Cy5). A431 cells were chosen as the test cell line to validate the assay, because of its high EGF receptor expression and its extensive use for nearly 20 years in the analysis of EGFR function. Initially, the specificity of the antibodies F4 and FB2 was tested through western blot of A431 cell lysates (Figure 3.1A). The receptor is specifically detected by the F4 monoclonal, while FB2 recognises both the phosphorylated receptor and two pairs of faster migrating (phospho-) proteins. The degree of immuno-recognition of the receptor by FB2 specifically increased in response to EGF as expected for this phosphotyrosine site-directed monoclonal. Importantly, this immunoreactivity was reduced in a dose-dependent manner by the selective EGFR tyrosine kinase inhibitor AG 1478. It should be noted that in these cells there is basal EGFR phosphorylation consistent with prior data indicating a degree of autocrine receptor activation (Van de Vijver et al., 1991). Moreover, the additional recognition of faster migrating protein species by the FB2 monoclonal does not interfere with the two-site FRET assay reported here, since the specificity of the analysis is determined by F4 (this is an important feature of the two-site IHC assay) (Figure 3.1A).

Fixed A431 cells were employed to test whether in an IHC format, the coincident binding of F4-Cy3b and FB2-Cy5 to phosphorylated EGFR produced a specific FRET signal. Cells were treated with or without EGF, fixed and processed (see Methods Section 2.2.11.4). Employing this assay, it was found that following EGF stimulation there is a marked increase in FRET as illustrated in Figure 3.1B. This is a specific property of the coincident binding of the two fluorescently labelled antibodies, since the lifetime change observed for the donor fluorophore following EGF treatment, is not observed if the antibody-acceptor conjugate is omitted. In the absence of the EGF stimulus there is a reduced degree of FRET, but with lifetimes for the donor in the presence of the acceptor below those observed for donor alone (Figure 3.1B).

To determine whether the EGF-induced increase in FRET reflected an increase in immuno-recognition of tyrosine phosphorylated receptor by the FB2 antibody-acceptor conjugate, cells were pre-treated with AG 1478. At effective doses of this EGFR inhibitor (1.5 and 3.0 μM – Figure 3.1A), FRET was reduced to the basal unstimulated level. Pre-treating the cells with AG 1478 did not reverse the basal degree of FRET. An example of donor Cy3b intensity images and their corresponding average lifetime maps from the same FRET experiment are illustrated in Fig. 3.2A. The average lifetime of F4-Cy3b in these studies decreased from 1.63 ns to 1.50 ns when the acceptor FB2-Cy5 was present and decreased further to 1.38 ns upon EGF stimulation. The changes in lifetime induced by EGF are localised mainly at the plasma membrane as seen from the pseudocolour changes of the lifetime map. This is entirely consistent with the expected increase in tyrosine phosphorylated receptor at the cell surface following a ten-minute stimulation with EGF. Concentrations of 1.5 μM and 3 μM of AG 1478 reversed the donor lifetime to 1.49 ns. The 2-D histograms representing the phase lifetime and modulation can also be represented as average lifetime (the average of phase and modulation lifetimes) in the scatter diagram (See Methods Section 2.2.11.5, Figure 3.2B, Table 3.1A). This type of representation although it loses the information on the individual components of phase and modulation lifetimes, it can be particularly useful in assessing the response of targeted therapy since heterogeneity in terms of responses between cells may be seen. Dose

dependence studies in A431 cells showed that at lower concentrations (0.3 μM and 0.6 μM) FRET was not reversed (Table 3.1B), correlating with the western blot results shown in Figure 3.1A. With higher doses of AG 1478, the lifetimes and average FRET efficiency values were reversed to basal levels.

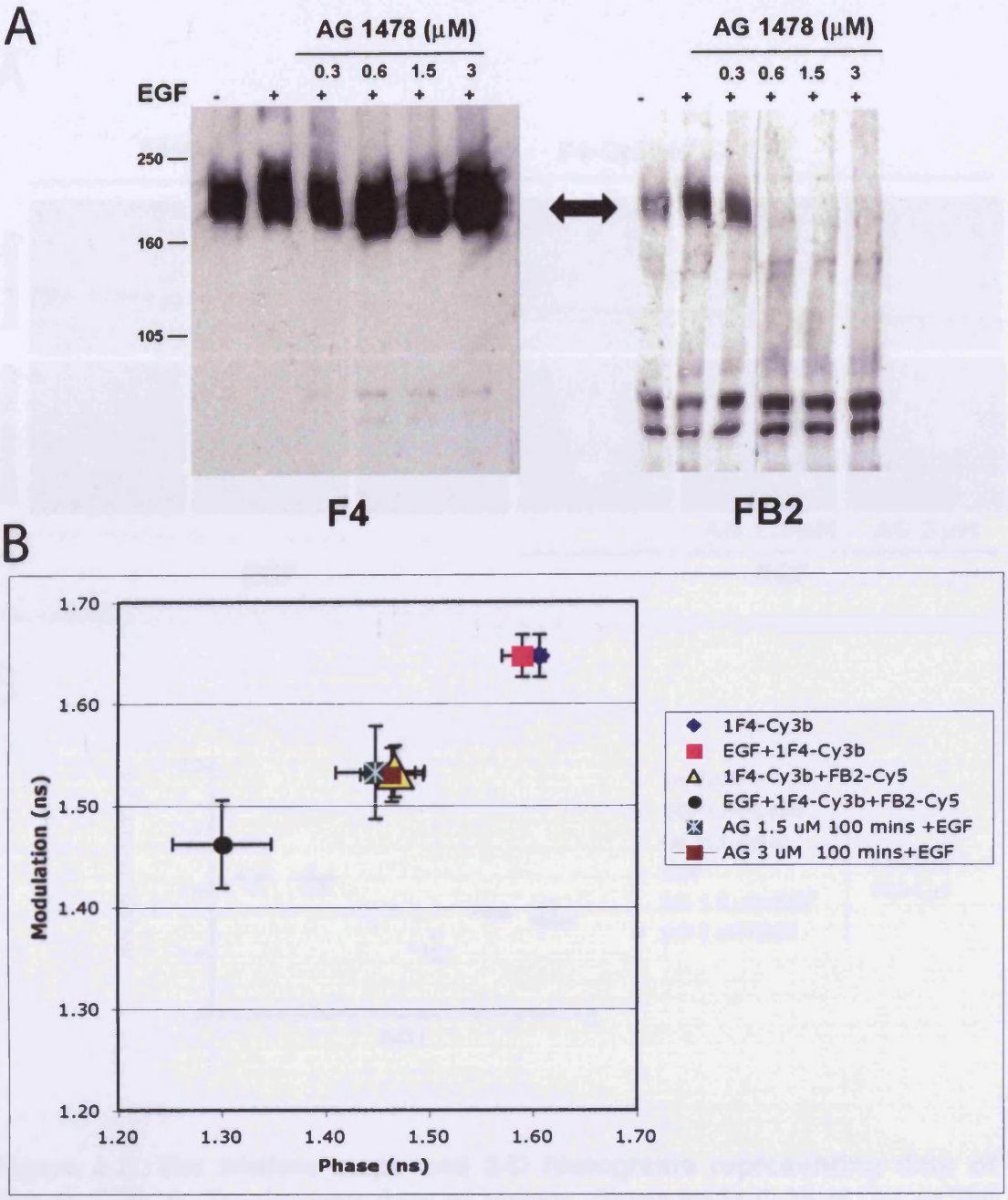

Figure 3.1: EGF induced phosphorylation of the EGFR is prevented by AG 1478 and its activation is monitored by FRET. A, A431 cells were stimulated with 50 ng/ml of EGF for 10 minutes. Cell lysates were probed with F4 (antibody against the cytoplasmic domain of EGFR) and FB2 (EGFR autophosphorylation site monoclonal). The 170 kDa F4 immunoreactive band (EGFR) co-migrates with the major signal from FB2 (arrow). Cells were pre-treated with increasing doses of AG 1478 as indicated and then stimulated with EGF. **B,** The 2-D histogram of phase and modulation lifetimes of F4-Cy3b. A431 cells were incubated with either donor alone (F4-Cy3b) or donor and acceptor (F4-Cy3b+FB2-Cy5) to assess EGFR phosphorylation after pre-treated with AG 1478 with or without EGF stimulation as illustrated. The error bars represent the standard deviations of 5 measurements.

A

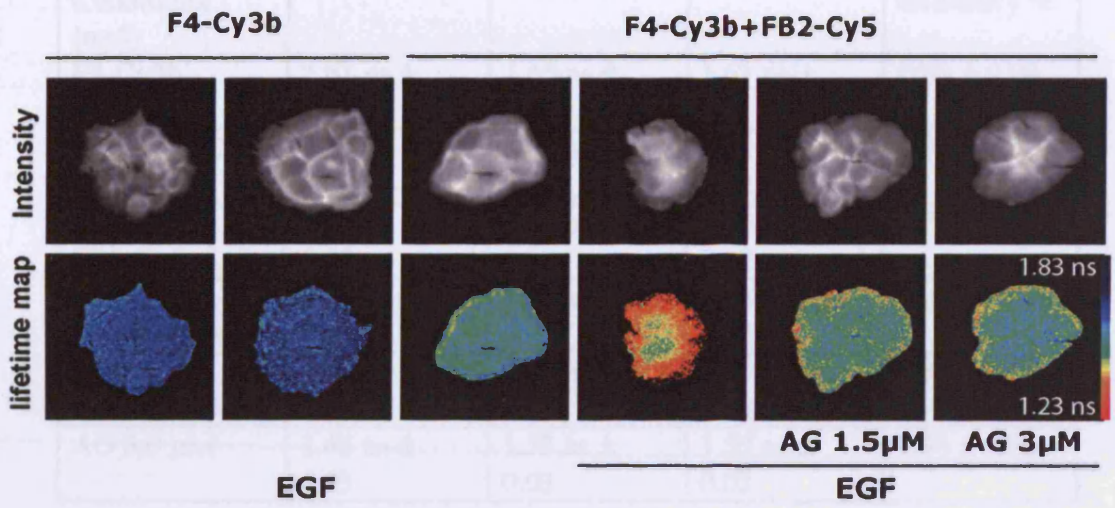

B

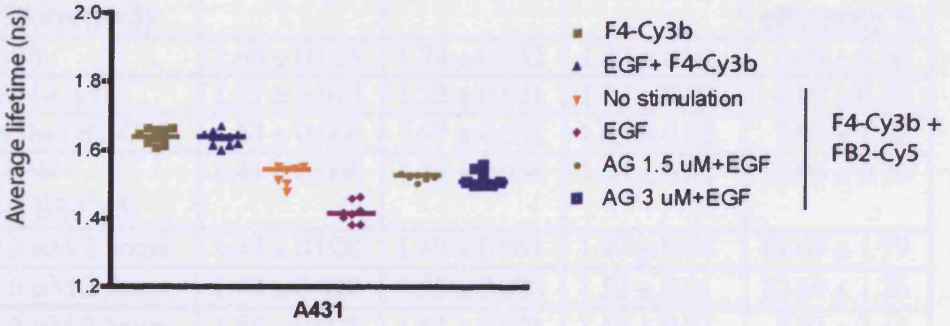

Figure 3.2: The lifetime maps and 2-D histograms representing data of Figure 3.1B. A, The diagrams show an average lifetime for F4-Cy3b of 1.63 ns. The average lifetime remains the same in the presence of EGF but decreases with the acceptor (FB2-Cy5). The decrease in average lifetime to 1.38 ns is most noticeable at the plasma membrane, as seen from the colour changes of the lifetime map. In the presence of AG 1478 (1.5 μM and 3 μM), the average lifetime returns to a higher lifetime of 1.49 ns. **B,** The 2-D histogram representing the phase and modulation lifetimes shown in Figure 3.1B can also be represented as average lifetimes (the average of phase and modulation lifetimes) in the scatter diagram.

A

A431 cells Conditions (n=5)	Phase (ns)	Mod (ns)	Ave (ns)	Ave FRET efficiency %
F4-Cy3b	1.61 ns ± 0.01	1.65 ns ± 0.01	1.63 ns ± 0.01	0.00 ± 0.00
EGF + F4-Cy3b	1.59 ns ± 0.02	1.65 ns ± 0.02	1.62 ns ± 0.02	0.00 ± 2.00
F4-Cy3b + FB2-Cy5	1.47 ns ± 0.03	1.53 ns ± 0.02	1.50 ns ± 0.02	7.79 ± 0.51
EGF + F4-Cy3b+FB2-Cy5	1.30 ns ± 0.05	1.46 ns ± 0.04	1.38 ns ± 0.04	15.11 ± 2.10
AG 1.5 μM	1.45 ns ± 0.04	1.53 ns ± 0.02	1.49 ns ± 0.04	8.39 ± 2.50
AG 3.0 μM	1.46 ns ± 0.03	1.53 ns ± 0.03	1.50 ns ± 0.02	7.96 ± 1.96

B

A431 cells Conditions (n=3)	Phase (ns)	Mod (ns)	Ave (ns)	Ave FRET efficiency %
F4-Cy3b	1.66 ± 0.015	1.74 ± 0.032	1.70 ± 0.02	0.00 ± 0.00
EGF+F4-Cy3b	1.67 ± 0.015	1.72 ± 0.021	1.70 ± 0.02	0.00 ± 0.68
F4-Cy3b+FB2-Cy5	1.63 ± 0.006	1.67 ± 0.032	1.65 ± 0.02	2.93 ± 1.62
EGF +F4-Cy3b+FB2-Cy5	1.41 ± 0.006	1.54 ± 0.036	1.48 ± 0.02	12.96 ± 0.76
AG 0.3 μM 2 hours	1.44 ± 0.020	1.49 ± 0.061	1.47 ± 0.04	13.65 ± 1.99
AG 0.6 μM 2 hours	1.48 ± 0.020	1.55 ± 0.026	1.52 ± 0.01	10.69 ± 1.76
AG 1.5 μM 2 hours	1.56 ± 0.023	1.64 ± 0.021	1.60 ± 0.02	5.87 ± 2.44
AG 3 μM 2 hours	1.55 ± 0.010	1.59 ± 0.044	1.58 ± 0.01	6.48 ± 1.55
AG 9 μM 2 hours	1.59 ± 0.006	1.65 ± 0.053	1.62 ± 0.01	4.42 ± 1.32

Table 3.1: A, The phase, modulation and average lifetimes of F4-Cy3b in different conditions, same experiment as Figure 3.1B. The values in the table represent the average of 5 measurements per condition. **B,** Lifetimes and FRET efficiency values of F4-Cy3b in A431 cells in a dose-dependent study of AG 1478.

To verify that the signal was indeed due to phospho-tyrosine recognition, the protein tyrosine phosphatase from *Yersinia enterocolitica* (YOP) was employed. Pretreatment with YOP abolished both the basal and EGF-induced FRET (Figure 3.3A and 3.3B). This suggests that FRET between F4-Cy3b and FB2-Cy5 in the basal state is not be due to the direct auto-activation of the EGFR receptor (AG 1478 sensitive), but is probably mediated by hetero-dimerisation with other activated epidermal growth factor receptors or by other receptor-associated proteins, which are not inhibited by AG 1478. The observed ligand-induced FRET, the inhibitor dependent reduction of FRET and the defined plasma membrane response, coupled with the specificity of the F4 monoclonal antibody, establishes the use of the F4-FB2 antibody pair to monitor EGFR expression (F4 immuno-reaction) and EGFR activation (F4-FB2 co-incident immunorecognition).

A

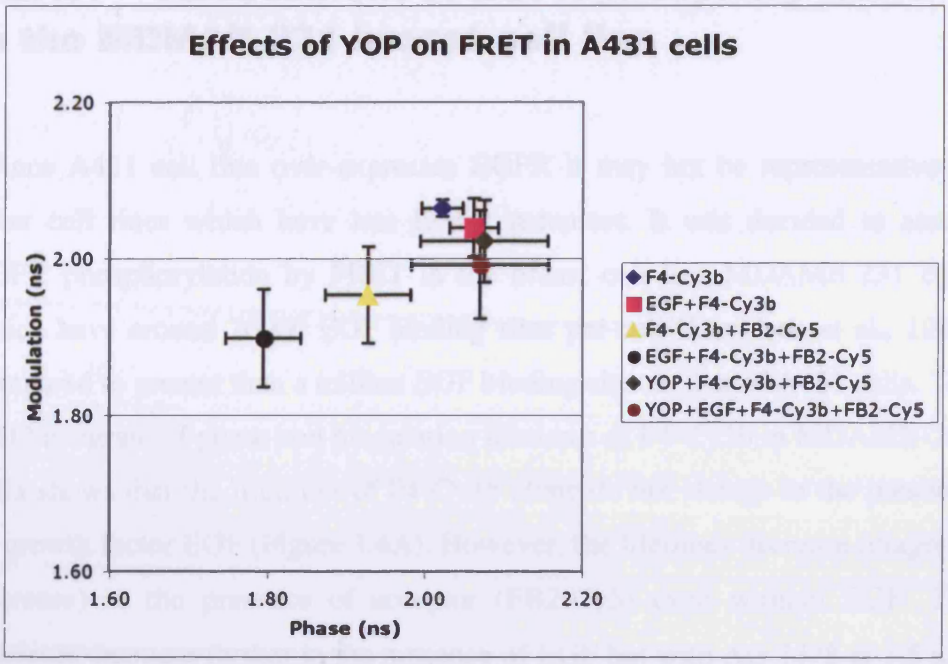

B

A431 cells Conditions (n=10)	Phase lifetime (ns)	Modulation lifetime (ns)	Average lifetime (ns)	Average FRET efficiency
F4-Cy3b	2.02 ± 0.026	2.06 ± 0.011	2.04 ± 0.02	0.00 ± 0.00
EGF+F4-Cy3b	2.06 ± 0.031	2.04 ± 0.037	2.05 ± 0.01	0.00 ± 0.00
F4-Cy3b+FB2-Cy5	1.93 ± 0.055	1.95 ± 0.062	1.94 ± 0.04	5.03 ± 2.27
EGF+F4-Cy3b+FB2-Cy5	1.79 ± 0.047	1.90 ± 0.062	1.85 ± 0.03	9.64 ± 1.53
YOP+F4-Cy3b+FB2-Cy5	2.08 ± 0.081	2.02 ± 0.052	2.05 ± 0.02	0.00 ± 0.74
YOP+EGF+F4-Cy3b+FB2-Cy5	2.07 ± 0.087	1.99 ± 0.069	2.03 ± 0.03	0.00 ± 1.64

Figure 3.3: Treatment with protein tyrosine phosphatase from Yersinia enterocolitica (YOP) diminishes both the basal and EGF induced EGFR phosphorylation in A431 cells. A, The 2-D histogram of phase and modulation lifetimes of F4-Cy3b in A431 cells after the cells were treated with different conditions as illustrated. The diagram shows that YOP reverses the lifetime changes of F4-Cy3b in the presence of the acceptor FB2-Cy5 (with or without EGF stimulation) to that of control F4-Cy3b. **B,** The changes in EGFR phosphorylation indicated by FRET efficiency and lifetimes of F4-Cy3b (representing the data in Figure 3.3A are shown in the table.

3.2.1.1 Assessment of EGFR phosphory-lation in the MDMAB-231 breast cell line

Since A431 cell line over-expresses EGFR it may not be representative of other cell lines which have less EGFR receptors. It was decided to assess EGFR phosphorylation by FRET in the breast cell line MDAMB-231 cells which have around 70000 EGF binding sites per cell (Davidson et al., 1987) compared to greater than a million EGF binding sites in that of A431 cells. The 2-D histogram of phase and modulation lifetimes of F4-Cy3b in MDAMB-231 cells shows that the lifetimes of F4-Cy3b alone do not change in the presence of growth factor EGF (Figure 3.4A). However, the lifetimes decrease (diagonal decrease) in the presence of acceptor (FB2-Cy5) even without EGF. The lifetimes decrease further in the presence of EGF but with AG 1478 at 1.5 μM and 3 μM the lifetimes of Cy3b return to basal level. The values of the lifetimes and FRET efficiency are illustrated in Figure 3.4B. The results are similar to those seen in A431 cells although the basal and EGF induced phosphorylation as indicated by FRET efficiencies are slightly less than A431 cells which have higher levels of EGFR. The experiments indicate that FRET to assess EGFR phosphorylation state may be applied in various cell lines with different amounts of EGFR.

A

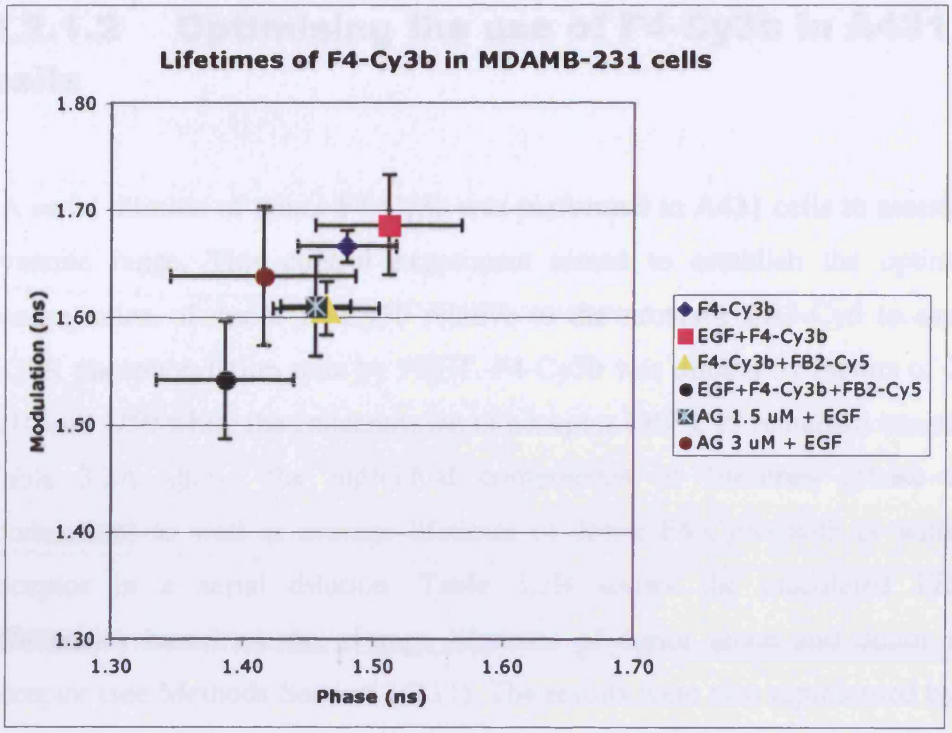

B

MDAMB 231 Conditions (n=5)	Phase lifetime (ns)	Modulation lifetime (ns)	Average lifetime (ns)	Average FRET efficiency
F4-Cy3b	1.48 ± 0.04	1.67 ± 0.02	1.57 ± 0.03	0.00 ± 0.00
EGF+F4-Cy3b	1.51 ± 0.06	1.69 ± 0.05	1.60 ± 0.04	0.00 ± 2.00
F4-Cy3b+FB2-Cy5	1.46 ± 0.04	1.61 ± 0.03	1.54 ± 0.03	2.35 ± 1.75
EGF +F4-Cy3b+FB2-Cy5	1.39 ± 0.05	1.54 ± 0.06	1.46 ± 0.05	6.91 ± 3.37
AG 1.5 μM 2 hours	1.46 ± 0.03	1.61 ± 0.05	1.53 ± 0.03	2.51 ± 3.05
AG 3 μM 2 hours	1.42 ± 0.07	1.64 ± 0.07	1.53 ± 0.06	2.88 ± 4.81

Figure 3.4: AG 1478 diminishes EGF induced EGFR phosphorylation in MDAMB-231 cells. A, The 2-D histogram of phase and modulation lifetimes of F4-Cy3b in MDAMB-231 cells after the cells were treated with different conditions as illustrated and incubated with either donor alone F4-Cy3b or donor and acceptor (F4-Cy3b+FB2-Cy5) to assess EGFR phosphorylation. **B,** The changes in EGFR phosphorylation indicated by FRET efficiency and lifetimes of F4-Cy3b (representing the data in Figure 3.4A) are shown in the table.

3.2.1.2 Optimising the use of F4-Cy3b in A431 cells

A serial dilution of donor F4-Cy3b was performed in A431 cells to assess its dynamic range. This control experiment aimed to establish the optimum concentration of donor F4-Cy3b relative to the acceptor FB2-Cy5 to assess EGFR phosphorylation state by FRET. F4-Cy3b was diluted by factors of 1/5, 1/10 and 1/50 while the concentration of acceptor FB2-Cy5 remained constant. Table 3.2A shows the individual components of lifetimes (phase and modulation) as well as average lifetimes of donor F4-Cy3b with or without acceptor in a serial dilution. Table 3.2B shows the calculated FRET efficiencies based on the average lifetimes of donor alone and donor and acceptor (see Methods Section 2.2.11). The results were also represented by 2-D diagrams of phase and modulation lifetimes of F4-Cy3b shown in Figure 3.5A-C.

A

Dilution factor of F4-Cy3b	Conditions	Phase lifetime (ns)	Modulation lifetime (ns)	Average lifetime (ns)
1/5	F4-Cy3b	1.52 ns ± 0.02	1.43 ns ± 0.08	1.48 ns ± 0.04
1/5	EGF + F4-Cy3b	1.54 ns ± 0.02	1.48 ns ± 0.02	1.51 ns ± 0.02
1/5	F4-Cy3b + FB2-Cy5	1.38 ns ± 0.04	1.37 ns ± 0.03	1.38 ns ± 0.03
1/5	EGF 50 ng/ml	1.16 ns ± 0.04	1.25 ns ± 0.04	1.20 ns ± 0.04
1/10	F4-Cy3b	1.59 ns ± 0.03	1.46 ns ± 0.06	1.52 ns ± 0.04
1/10	EGF+F4-Cy3b	1.41 ns ± 0.03	1.41 ns ± 0.02	1.41 ns ± 0.02
1/10	F4-Cy3b + FB2-Cy5	1.22 ns ± 0.02	1.26 ns ± 0.04	1.24 ns ± 0.03
1/10	EGF 50 ng/ml	1.01 ns ± 0.02	1.13 ns ± 0.04	1.07 ns ± 0.03
1/50	F4-Cy3b	1.42 ns ± 0.03	1.49 ns ± 0.03	1.46 ns ± 0.03
1/50	EGF + F4-Cy3b	1.43 ns ± 0.01	1.41 ns ± 0.08	1.42 ns ± 0.03
1/50	F4-Cy3b + FB2-Cy5	1.14 ns ± 0.02	1.25 ns ± 0.04	1.19 ns ± 0.03
1/50	EGF 50 ng/ml	0.95 ns ± 0.04	1.14 ns ± 0.08	1.04 ns ± 0.06

B

F4-Cy3b Dilution Factor	Basal EGFR phosphorylation (FRET efficiency)	EGF-induced EGFR phosphorylation (FRET efficiency)
1/5	6.8% ± 2.03	18.9% ± 2.7
1/10	18.4% ± 1.97	29.6% ± 1.97
1/50	18.5% ± 2.05	28.8% ± 4.11

Table 3.2: A, The average lifetimes of F4-Cy3b (± standard deviations from three measurements) in A431 cells with different dilution factors of F4-Cy3b. **B,** The changes in EGFR phosphorylation indicated by FRET efficiency (± standard deviations from three measurements) with different dilution factors of F4-Cy3b.

A

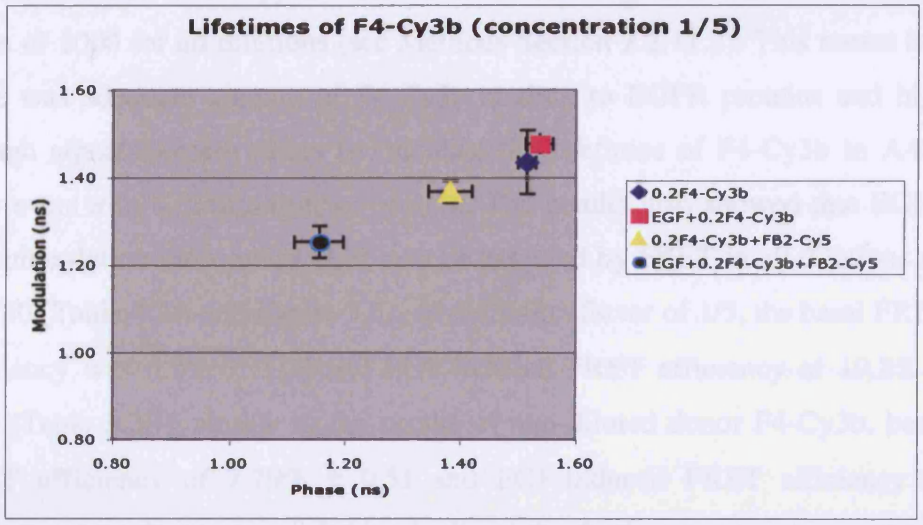

B

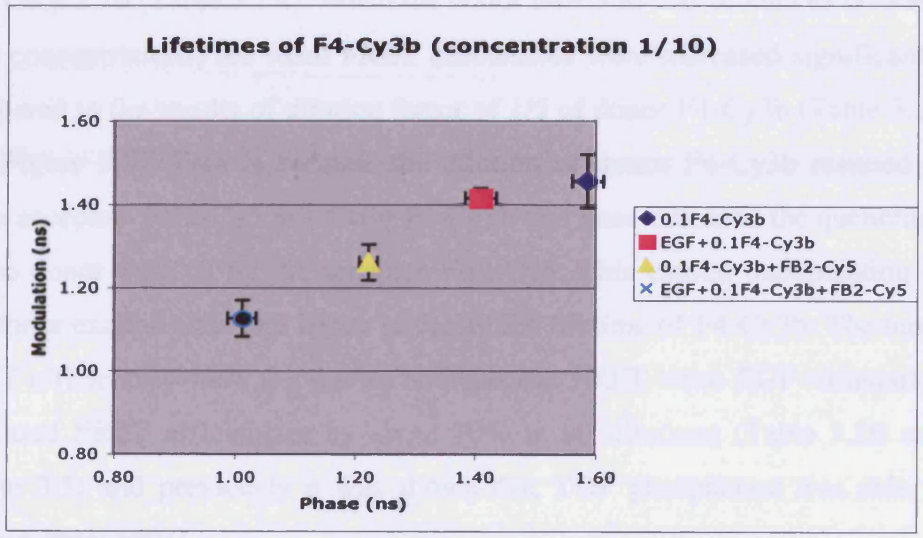

C

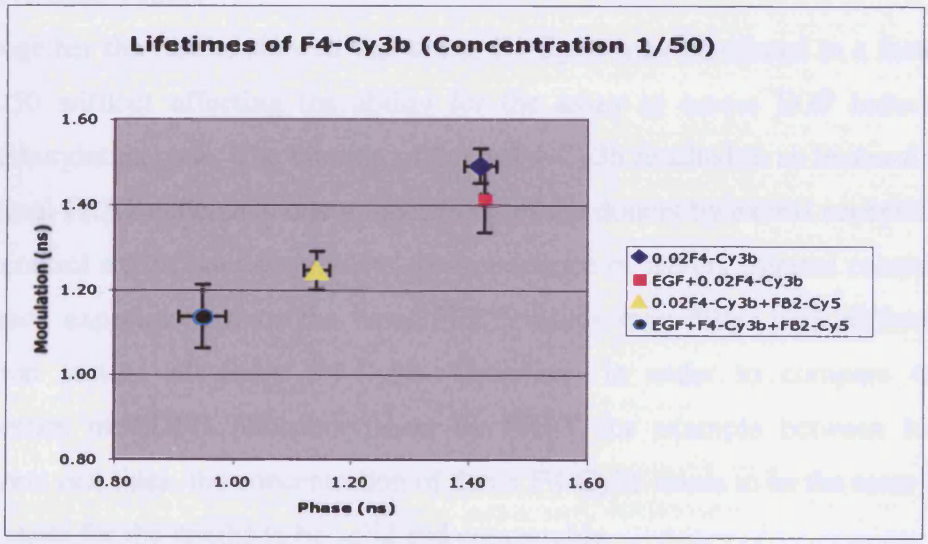

Figure 3.5: The effect of different dilution factors of F4-Cy3b on the lifetimes of F4-Cy3b shown by 2-D histogram. A, Dilution factor of F4-Cy3b 1/5. **B,** Dilution factor of F4-Cy3b 1/10. **C,** Dilution factor of F4-Cy3b

The intensities of F4-Cy3b were observed to be greater than the arbitrary value of 1000 for all dilutions (see Methods Section 2.2.11.2). This meant that there was adequate amount of F4-Cy3b binding to EGFR proteins and high enough signal-to-noise ratios to calculate the lifetimes of F4-Cy3b in A431 cells even with a dilution factor of 1/50. The results also showed that EGFR phosphorylation induced by EGF may be assessed by FRET in all dilutions up to 1/50 (Table 3.2A and Figure 3.5). At a dilution factor of 1/5, the basal FRET efficiency was 6.8% ± 2.03 and EGF-induced FRET efficiency of 19.8% ± 2.70 (Table 3.2B), similar to the results of non-diluted donor F4-Cy3b, basal FRET efficiency of 7.79% ± 0.51 and EGF-induced FRET efficiency of 15.11% ± 2.70 (Table 3.1A). When the donor F4-Cy3b was diluted to 1/10 and 1/50 concentrations, the basal FRET efficiencies were increased significantly compared to the results of dilution factor of 1/5 of donor F4-Cy3b (Table 3.2B and Figure 3.5). This is because the dilution of donor F4-Cy3b resulted in more acceptors FB2-Cy5 per donor F4-Cy3b and thus increased the quenching of the donor F4-Cy3 by the acceptor FB2-Cy5. This caused depopulation of the donor excited state and hence lowering the lifetime of F4-Cy3b. The basal FRET efficiencies were not due to non-specific FRET since EGF stimulation increased FRET efficiencies by about 10% in all dilutions (Table 3.2B and Figure 3.5) and previously it was shown that YOP phosphatase was able to remove basal FRET.

Altogether the results showed that donor F4-Cy3b may be diluted to a factor of 1/50 without affecting the ability for the assay to assess EGF induced phosphorylation state. The dilution of donor F4-Cy3b resulted in an increase in the basal FRET efficiency due to quenching of the donors by excess acceptors. The control experiment emphasises the importance of having internal controls for each experiment since the basal FRET values may differ with different dilution factors of donor F4-Cy3b. Therefore, in order to compare the difference of EGFR phosphorylation by FRET for example between two different cell lines, the concentration of donor F4-Cy3b needs to be the same in both cases for the results to be valid and comparable.

3.2.1.3 A serial dilution of acceptor FB2-Cy5 concentration in A431 cells

A serial dilution of acceptor FB2-Cy5 concentration was also performed in A431 cells to establish the optimum concentration of acceptor FB2-Cy5 relative to donor F4-Cy3b to assess EGFR phosphorylation by FRET. Table 3.3A shows the lifetimes of donor F4-Cy3b and Table 3.3B shows the basal and EGF induced FRET efficiencies with different dilution factors of FB2-Cy5. The results show that as the concentration of acceptor FB2-Cy5 decreased, the amount of basal FRET efficiency decreased (Table 3.3B). However, EGF stimulation induced further FRET (Table 3.3B) indicating that the assay may be used to assess EGF induced EGFR phosphorylation. The decrease of basal FRET efficiency was due to less acceptors FB2-Cy5 per donor F4-Cy3b, resulting in the decreased quenching of the donor F4-Cy3b and increase of donor lifetime. This control experiment again emphasises the importance of using internal control for each experiment and the acceptor concentration needs to be maintained constant to compare FRET efficiencies (e.g. between two cell lines).

A

Conditions	FB2 dilution factor	Phase lifetime (ns)	Modulation lifetime (ns)	Average lifetime (ns)
F4-Cy3b	NA	2.12 ns ± 0.02	2.22 ns ± 0.06	2.17 ns ± 0.02
EGF + F4-Cy3b	NA	2.16 ns ± 0.09	2.22 ns ± 0.02	2.19 ns ± 0.06
F4-Cy3b + FB2-Cy5	1/1	1.84 ns ± 0.04	2.06 ns ± 0.08	1.95 ns ± 0.06
EGF 50 ng/ml	1/1	1.57 ns ± 0.02	1.95 ns ± 0.02	1.76 ns ± 0.01
F4-Cy3b + FB2-Cy5	1/5	1.87 ns ± 0.02	2.12 ns ± 0.03	2.00 ns ± 0.01
EGF 50 ng/ml	1/5	1.77 ns ± 0.02	2.09 ns ± 0.05	1.93 ns ± 0.03
F4-Cy3b + FB2-Cy5	1/10	1.92 ns ± 0.01	2.14 ns ± 0.04	2.03 ns ± 0.02
EGF 50 ng/ml	1/10	1.68 ns ± 0.06	2.05 ns ± 0.08	1.87 ns ± 0.07
F4-Cy3b + FB2-Cy5	1/20	1.92 ns ± 0.03	2.13 ns ± 0.07	2.03 ns ± 0.02
EGF 50 ng/ml	1/20	1.74 ns ± 0.04	2.08 ns ± 0.05	1.91 ns ± 0.04
F4-Cy3b + FB2-Cy5	1/40	1.93 ns ± 0.02	2.14 ns ± 0.04	2.04 ns ± 0.02
EGF 50 ng/ml	1/40	1.85 ns ± 0.04	2.12 ns ± 0.10	1.98 ns ± 0.07

B

FB2-Cy5 Dilution Factor	Basal EGFR phosphorylation (FRET efficiency)	EGF-induced EGFR phosphorylation (FRET efficiency)
1/1	10.1% ± 2.8	18.9% ± 0.5
1/5	7.8% ± 0.5	11.1% ± 1.4
1/10	6.5% ± 0.9	13.8% ± 2.8
1/20	7.3% ± 0.9	12.0% ± 1.8
1/40	6.0% ± 0.9	8.8 % ± 2.8

Table 3.3: A, The average lifetimes of F4-Cy3b (± standard deviations from three measurements) in A431 cells with different dilution factors of FB2-Cy5. **B,** The changes in EGFR phosphorylation indicated by FRET efficiency (± standard deviations from three measurements) with different dilution factors of FB2-Cy5

3.2.1.4 The effect of prolonged incubation periods of acceptor FB2-Cy5 in A431 cells

The effect of incubation periods of acceptor FB2-Cy5 in A431 cells was also assessed to obtain an optimum incubation period of acceptor FB2-Cy5 and to investigate the effect of prolonged incubation with FB2-Cy5 on FRET efficiencies in A431 cells. Table 3.4A shows the lifetimes (phase, modulation and average) and Table 3.4B shows the FRET efficiencies of F4-Cy3b when the cells were incubated with different periods of acceptor FB2-Cy5. As the incubation periods were gradually prolonged, the basal and EGF induced FRET efficiencies increased (Table 3.4B). The results showed that for incubations between two and four hours the basal and EGF-induced FRET efficiencies were relatively constant. The main significant increase of both basal and EGF-induced FRET efficiencies occurred after 8 hours of acceptor incubation. Prolonged acceptor incubation increases quenching of the donor, resulting in a significant decrease of lifetime but non-specific FRET due to non-specific binding as a result of prolonged acceptor incubation cannot be excluded. The results show that the optimum incubation period of acceptor FB2-Cy5 is between 2-4 hours.

A

Conditions	FB2 incubation period	Phase lifetime (ns)	Modulation lifetime (ns)	Average lifetime (ns)
F4-Cy3b	NA	2.12 ns ± 0.02	2.22 ns ± 0.06	2.17 ns ± 0.02
EGF + F4-Cy3b	NA	2.16 ns ± 0.09	2.22 ns ± 0.02	2.19 ns ± 0.06
F4-Cy3b + FB2-Cy5	1 hr	1.87 ns ± 0.01	2.15 ns ± 0.05	2.01 ns ± 0.03
EGF 50 ng/ml	1 hr	1.54 ns ± 0.03	2.11 ns ± 0.06	1.83 ns ± 0.04
F4-Cy3b + FB2-Cy5	2 hrs	1.72 ns ± 0.05	2.06 ns ± 0.04	1.89 ns ± 0.03
EGF 50 ng/ml	2 hrs	1.59 ns ± 0.01	2.02 ns ± 0.02	1.80 ns ± 0.02
F4-Cy3b + FB2-Cy5	4 hrs	1.76 ns ± 0.06	2.09 ns ± 0.02	1.92 ns ± 0.01
EGF 50 ng/ml	4 hrs	1.54 ns ± 0.04	1.95 ns ± 0.06	1.75 ns ± 0.05
F4-Cy3b + FB2-Cy5	8 hrs	1.75 ns ± 0.08	2.00 ns ± 0.01	1.88 ns ± 0.04
EGF 50 ng/ml	8 hrs	1.35 ns ± 0.06	1.88 ns ± 0.06	1.62 ns ± 0.02
F4-Cy3b + FB2-Cy5	18 hrs	1.52 ns ± 0.04	1.86 ns ± 0.06	1.69 ns ± 0.05
EGF 50 ng/ml	18 hrs	1.18 ns ± 0.07	1.67 ns ± 0.04	1.43 ns ± 0.04
F4-Cy3b + FB2-Cy5	28 hrs	1.26 ns ± 0.01	1.79 ns ± 0.04	1.53 ns ± 0.02
EGF 50 ng/ml	28 hrs	1.09 ns ± 0.04	1.58 ns ± 0.03	1.34 ns ± 0.02

B

FB2-Cy5 Incubation periods	Basal EGFR phosphorylation (FRET efficiency)	EGF-induced EGFR phosphorylation (FRET efficiency)
1 hour	7.4 % ± 1.4	15.7% ± 1.8
2 hours	12.9% ± 1.4	17.1% ± 0.9
4 hours	11.5% ± 0.5	19.4% ± 2.3
8 hours	13.4% ± 1.8	25.3% ± 0.9
18 hours	22.1% ± 2.3	34.1% ± 1.8
28 hours	29.5% ± 0.9	38.2% ± 0.9

Table 3.4: A, The average lifetimes of F4-Cy3b (± standard deviations from three measurements) in A431 cells with different incubation periods of FB2-Cy5. **B,** The changes in EGFR phosphorylation indicated by FRET efficiency with different incubation periods of FB2-Cy5 in A431 cells.

3.2.1.5 Assessing the minimum exogenous EGF concentration in inducing FRET

In the section 3.2.1, it was demonstrated that FRET efficiency was increased by exogenous EGF stimulation due to enhanced EGFR phosphorylation, indicating that FRET may be used to assess EGFR phosphorylation. It was intended to assess whether a decrease in the exogenous EGF dose would result in a decrease of FRET efficiency due to inadequate EGFR phosphorylation. This control experiment was important as it would prove that EGF-induced FRET was specific and indicative of EGFR phosphorylation if a decrease in EGF dose also resulted in the loss of EGF-enhanced FRET.

Table 3.5A shows the lifetimes (phase, modulation and average components) and Table 3.5B shows the FRET efficiencies with difference doses of exogenous EGF stimulation in A431 cells. The results show that as the exogenous EGF dose was decreased below 30 ng/ml, the dose became ineffective such that EGF did not induce further FRET compared to basal level (Table 3.5B). EGF concentration was calculated in nanomolar (nM) unit and the relationship between EGF concentration and FRET was plotted in a graph; it was shown that EGF induced FRET (EGFR phosphorylation) was saturated at an EGF concentration between 2.5 nM and 5nM (Table 3.5B).

A

Conditions	Phase lifetime (ns)	Modulation lifetime (ns)	Average lifetime (ns)
F4-Cy3b	2.12 ns ± 0.02	2.22 ns ± 0.06	2.17 ns ± 0.02
EGF+F4-Cy3b	2.16 ns ± 0.09	2.22 ns ± 0.02	2.19 ns ± 0.06
F4-Cy3b +FB2-Cy5	1.86 ns ± 0.01	2.03 ns ± 0.07	1.95 ns ± 0.05
EGF 50 ng/ml	1.57 ns ± 0.02	1.95 ns ± 0.02	1.76 ns ± 0.01
EGF 30 ng/ml	1.62 ns ± 0.03	2.00 ns ± 0.03	1.81 ns ± 0.02
EGF 10 ng/ml	1.77 ns ± 0.06	2.04 ns ± 0.06	1.91 ns ± 0.06
EGF 1 ng/ml	1.87 ns ± 0.05	2.11 ns ± 0.06	1.99 ns ± 0.05
EGF 0.1 ng/ml	1.80 ns ± 0.01	2.08 ns ± 0.04	1.94 ns ± 0.02

B

EGF concentration	EGF-induced EGFR phosphorylation (FRET efficiency)
No EGF (basal)	8.0% ± 2.3
EGF 50 ng/ml	15.5% ± 0.5
EGF 30 ng/ml	15.5% ± 0.9
EGF 10 ng/ml	8.5% ± 2.8
EGF 1 ng/ml	4.5% ± 2.3
EGF 0.1 ng/ml	6.7% ± 0.9

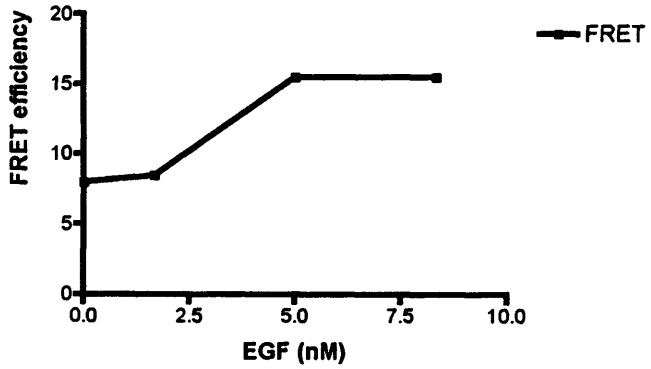

3.2.2 The activation-state of EGFR in head and neck tumours

The series of control experiments established the optimum conditions to assess EGFR phosphorylation by FRET. Furthermore, they illustrated the importance of strict internal controls and constant conditions of the donor and the acceptor for the experiments to obtain meaningful results. The aim was to apply the optimised FRET assay in cells to assess EGFR phosphorylation of tumour cores in paraffin sections of tumour arrays in a high throughput manner by automated FLIM.

The established two-site FRET assay was applied to determine the pattern of EGFR phosphorylation in a series of HNSCC. An archive of head and neck tumour samples from 130 patients embedded in paraffin blocks were converted into three arrays (Figure 3.6). The arrays contained 286 tumour cores (a duplicate of a tumour core from each patient) and several cores comprised normal tonsil tissue as negative controls. These arrays were prepared for FRET experiments using the parameters established in A431 cells.

A duplicate of each array was also prepared. One array was labelled with donor alone (F4-Cy3b) and the other with donor and acceptor (F4-Cy3b + FB2-Cy5). For each tumour core a pair of average lifetimes was obtained, one from the array with donor alone and one from the array that was labelled with donor and acceptor (Figure 3.7). Comparing the two arrays, average FRET efficiency was calculated for each tumour core (See Methods Section 2.2.11.6). Therefore average FRET efficiency was utilised as the main parameter to correlate with the clinical data (Figure 3.8). The survival data of 130 head and neck cancer patients were compared with average FRET efficiency. The average FRET efficiencies of the normal tonsil tissue samples were used as controls. The values of the negative controls ranged from 0% to 8.90% with a median average FRET efficiency of 4.86%. For the tumours, the average FRET efficiencies ranged from 0% to 14.70% and the median was 4.13%. The patients were ranked according to their average FRET efficiency

and the groups split for comparison into (i) upper median versus lower median, (ii) upper tertile versus lower two tertiles, and (iii) upper 10% versus lower 90% range of average FRET efficiency. The Kaplan Meier method was used to compare the survival curves between the groups of patients and log-rank test utilised to calculate the hazard ratios (see method). It was found that higher FRET efficiency was correlated with worse DFS and it was statistically significant in the groups split by upper tertile and upper 10% but not the median. Comparing the patients in the lower two tertiles with the upper tertile, the log-rank test revealed a hazard ratio of 0.57 (95% CI 0.29 to 0.99, p=0.05) (Figure 3.8A). Patients in the lower 90% range of average FRET efficiency had a hazard ratio of 0.43 (95% CI 0.09 to 0.89, p=0.03) compared with the patients in the upper 10% range (Figure 3.8B). However, there was no statistical significance in overall survival between the upper tertile and lower two tertile groups (hazard ratio for lower two tertile = 0.91, 95% CI 0.48 to 1.72, p=0.76) (Figure 3.8C).

To ensure inter-assay validity, the above experiments were repeated in a new set of six tumour arrays, which contained tumour cores from the same patients. New preparations of conjugated antibodies were used and average FRET efficiencies were calculated from each tumour core using automated high throughput FLIM. The automated system was programmed to perform multiple loops and two loops were performed for each array (See Methods). Thus, two measurements were acquired for each process (574 measurements were acquired). The Kaplan Meier survival curves were used to compare between the patients in the upper 10% FRET efficiency and lower 90% efficiency and the log-rank test was used to compare the hazard ratio. The results were similar to the initial study in that the patients in the lower 90% range of average FRET efficiency had a better DFS compared with the upper 10% range (hazard ratio for lower 90% range = 0.38, 95% CI 0.075 to 0.69, p=0.001) (Figure 3.8D). From these FRET efficiency studies it was deduced that phosphorylation of EGFR assessed by high throughput FLIM correlates with DFS. The study illustrated that there was a prominent correlation between EGFR activation and DFS.

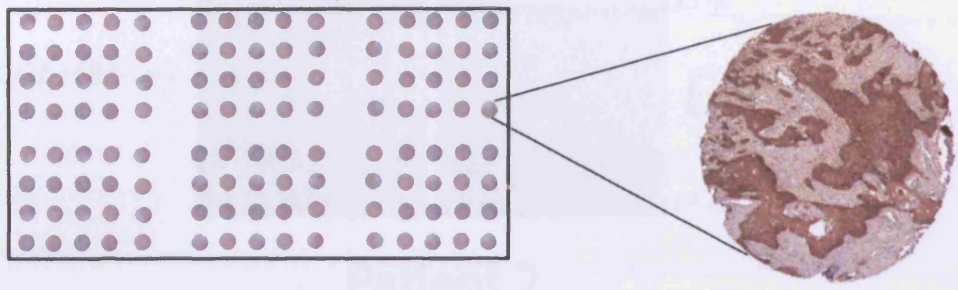

Figure 3.6: Head and neck tissue micro-array (TMA). The left panel shows a diagrammatic representation of a standard Oxford 8 x 15 TMA. The right panel shows an example of a tumour core with conventional EGFR immunostaining of F4 antibody (monoclonal against EGFR cytoplasmic domain, which is the same monoclonal antibody used in FRET experiments).

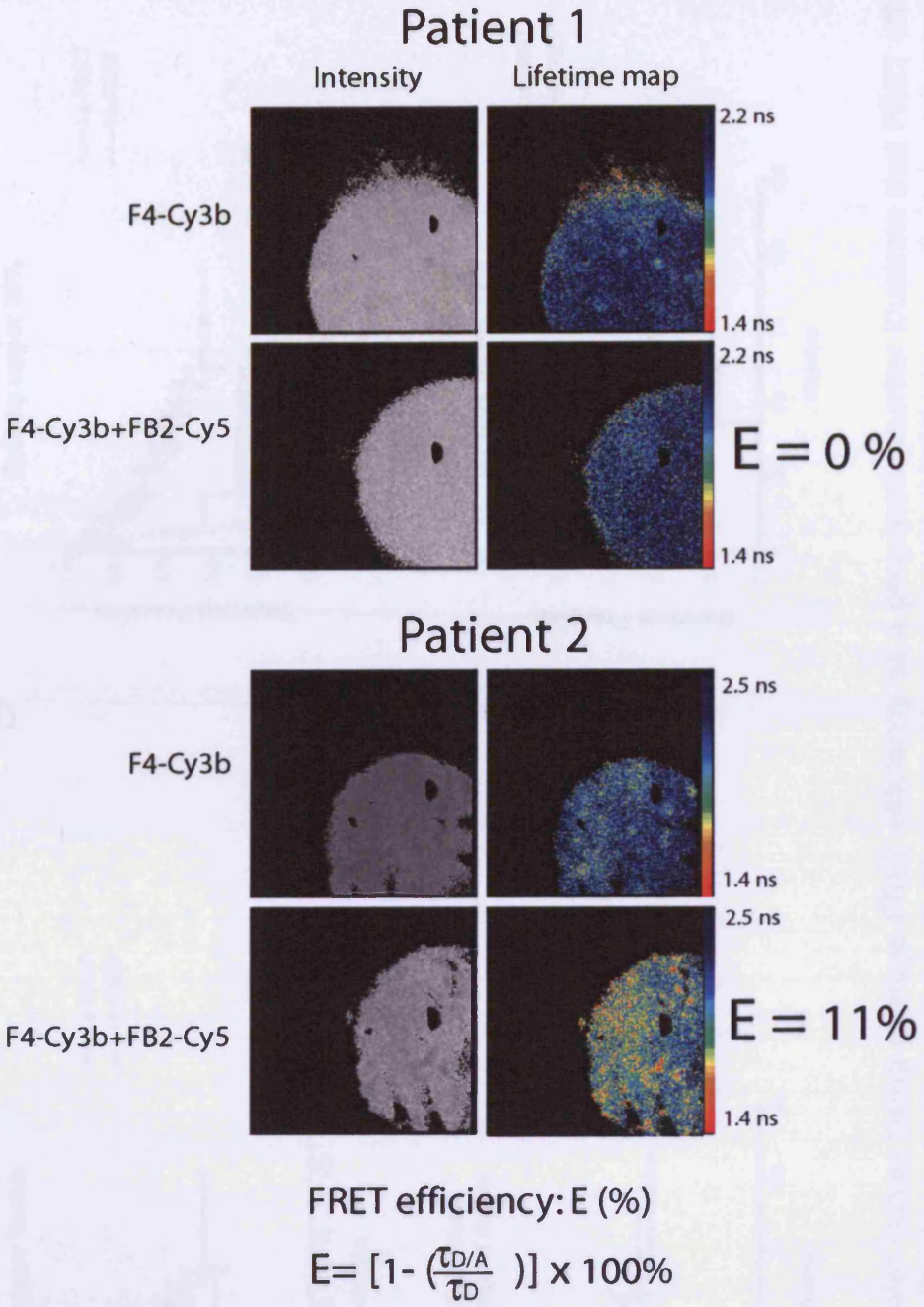

Figure 3.7: EGFR phosphorylation can be mapped by variations in FRET in Head and Neck tumour cores. The left panels show the intensity images of tumour cores from the array. The right panels are lifetime maps of the cores. The upper tumour core of patient 1 was from an array labelled with donor alone (F4-Cy3b). The average donor lifetime of the tumour core was 2.00 ns. The donor and acceptor (F4-Cy3b+FB2-Cy5) core was from a duplicate array. There was no change in the lifetime with a FRET efficiency of 0%. The second set of donor and acceptor cores from patient 2 indicates a further decrease of the average lifetime (2.20 ns to 1.90 ns) with a FRET efficiency of 11%. The decrease in donor lifetime induced by FRET is used to calculate the FRET efficiency.

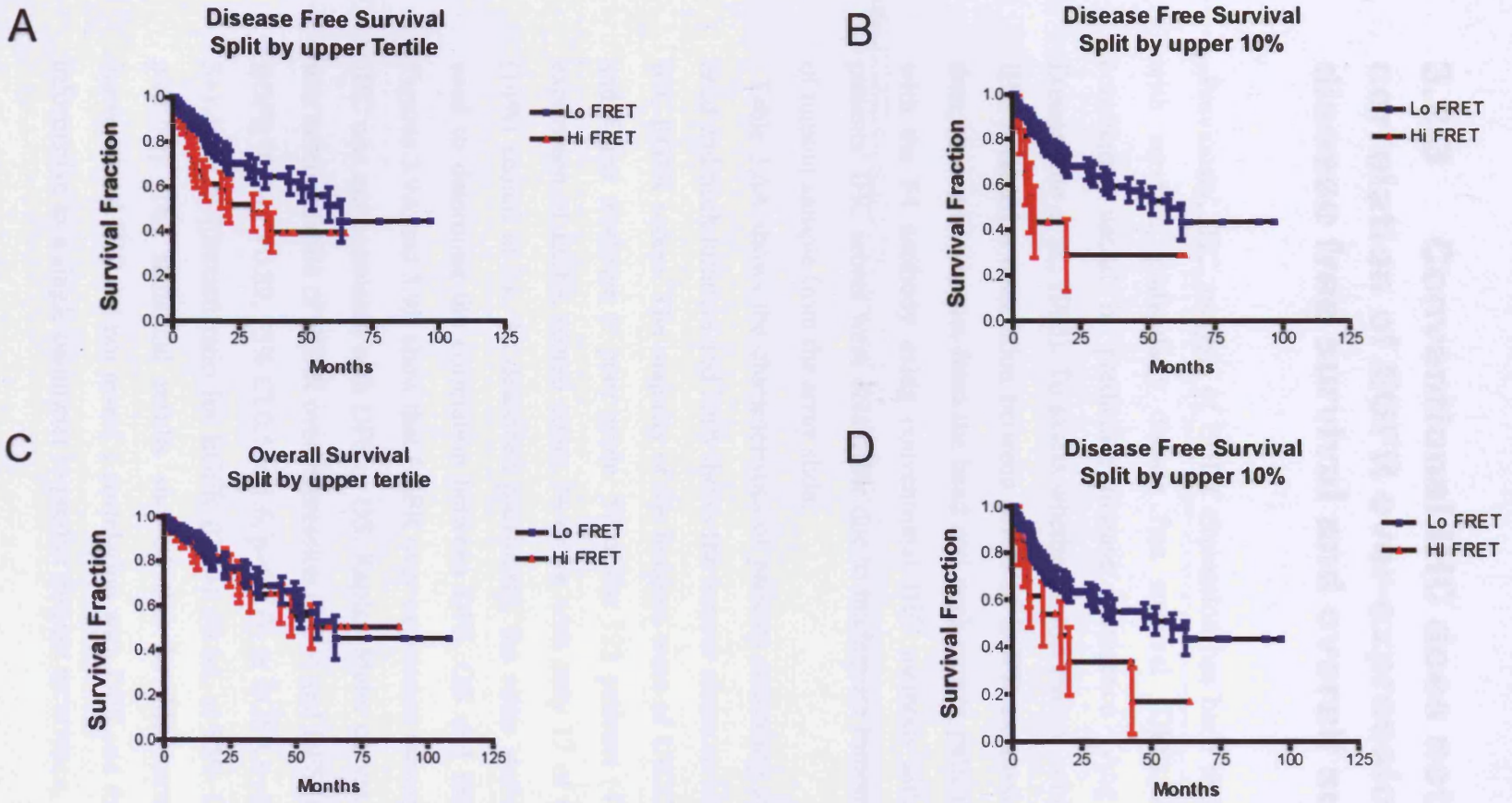

Figure 3.8: Kaplan-Meier curves using average FRET efficiency as a prognostic marker illustrate that FRET efficiency is correlated with disease free survival. **A,** Pilot study: Disease-free survival (DFS) between patients in upper tertile versus the lower two tertiles of average FRET efficiency. **B,** Pilot study: DFS between patients in upper 10% versus lower 90% of average FRET efficiency. **C,** Pilot study: OS between patients in upper 10% versus lower 90% of average FRET efficiency between patients in upper tertile versus the lower two tertiles of average FRET efficiency. **D,** Validation study: DFS curves comparing the upper 10% range with the lower 90% of average FRET efficiency.

3.2.3 Conventional IHC does not reveal a correlation of EGFR over-expression with disease free survival and overall survival

Previously, IHC analysis of EGFR expression has been shown to correlate with survival, particularly disease free survival (DFS) and hence was considered useful in predicting disease recurrence (Ang et al., 2002; Dassonville et al., 1993). To assess whether in this patient cohort conventional IHC revealed a correlation between levels of EGFR expression and survival data, the same tumours from the head and neck cancer patients were labelled with the F4 antibody using conventional IHC methods although only 122 patients' IHC scores were obtainable due to inadequate tumour sample or loss of tumour sample from the array slide.

Table 3.6A shows the characteristics of patients according to the subsites of head and neck tumours and 3.6B shows the tumour characteristics according to IHC EGFR scores. The majority of the tumours were of UICC tumour stage 3 and 4 and moderate to poor grade. 57 of the 122 patients (47%) have over-expression of EGFR scored either 2+ or 3+ with only 17 of the 122 patients (14%) scored at 3+. As described previously, the same statistical tests were used to determine the correlation between DFS, OS and EGFR expression. Figures 3.9A and 3.9B show that EGFR over-expression (scores 2+ and 3+) by IHC was not correlated with DFS or OS. Kaplan-Meier curves show that there was no correlation of EGFR over-expression (2-3+) and DFS [(hazard ratio for EGFR (0-1+) = 0.89, 95% CI 0.5 to 1.6, p=0.67)] or EGFR over-expression (2-3+) and OS [(hazard ratio for EGFR (0-1+) =0.64, at 95% CI 0.35 to 1.05, p=0.74)]. The statistical results showed that in this retrospective study, conventional IHC did not reveal a correlation with DFS and therefore was not informative as a single parameter to predict disease recurrence.

A

Anatomical sites	Male	Female	Median age
Oral cavity (n=38)	19	19	64.5
Oropharynx (n=42)	29	13	53.5
Hypopharynx (n=18)	13	5	64.3
Larynx (n=23)	21	2	62.4
Others (n=1)	1	0	70.1
Total (n=122)	83 (68%)	39 (32%)	58.5

B

EGFR Score	0 (n=36)	1+ (n=29)	2+ (n=40)	3+ (n=17)	Total =122
Tumour Stage					
I	3	0	5	1	9 (7%)
II	6	5	5	2	18 (15%)
III	11	6	9	0	26 (21%)
IV	16	18	21	14	69 (57%)
Grade					
Well	2	4	2	0	8 (7%)
Moderate	17	10	19	8	54 (44%)
Poor	17	15	19	9	60 (49%)

Table 3.6: **A,** The characteristics of patients according to subsites of head and neck tumours. **B,** The characteristics of tumours in relation to immunohistochemistry stains.

A

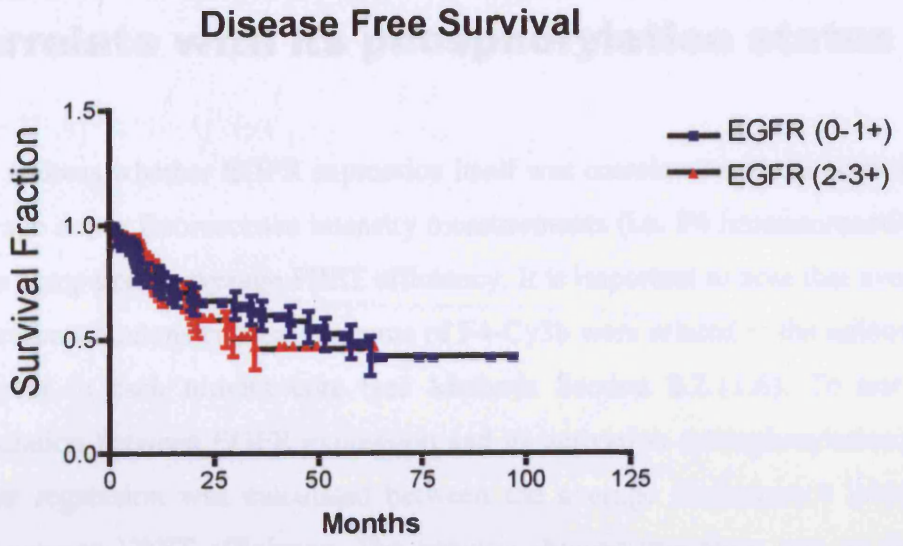

B

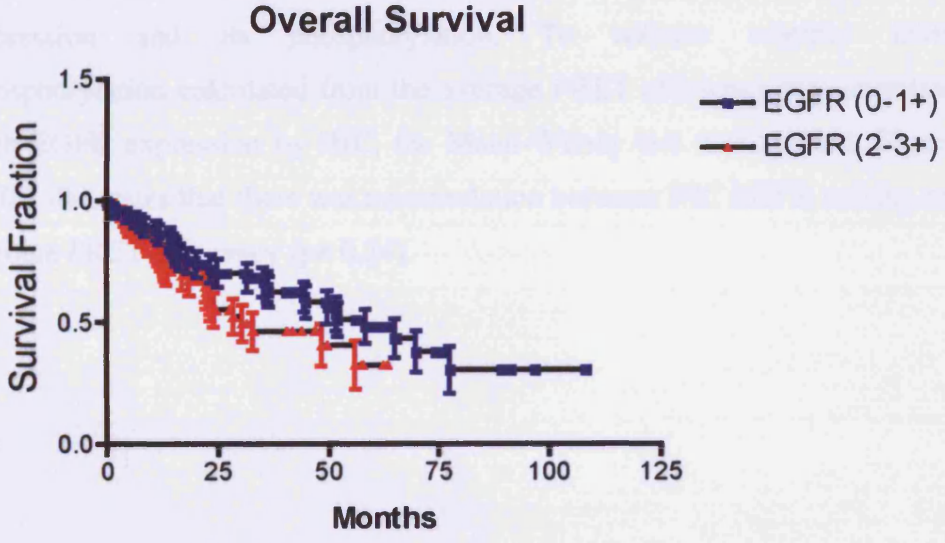

Figure 3.9: EGFR concentration does not reveal a correlation with disease free survival or overall survival. Kaplan-Meier curves were used to compare the disease-free survival (A) and overall survival (B) between EGFR (0-1+) and EGFR (2-3+).

3.2.4 EGFR concentration does not correlate with its phosphorylation status

To address whether EGFR expression itself was correlated with its activation, average donor fluorescence intensity measurements (i.e. F4 immunoreactivity) were compared to average FRET efficiency. It is important to note that average fluorescence intensity measurements of F4-Cy3b were related to the amount of receptor in each tumour core (see Methods Section 2.2.11.6). To test the correlation between EGFR expression and its activation (phosphorylation) the linear regression was calculated between the average fluorescence intensity and average FRET efficiency. The analysis showed that there was no linear relationship between the two parameters [(r^2 = 0) (Figure 3.10A)]. These studies illustrated that there was minimal correlation between EGFR expression and its phosphorylation. To address whether EGFR phosphorylation calculated from the average FRET efficiency was correlated with EGFR expression by IHC, the Mann-Witney test was utilised. Figures 3.10B illustrates that there was no correlation between IHC EGFR scoring and average FRET efficiency (p= 0.24).

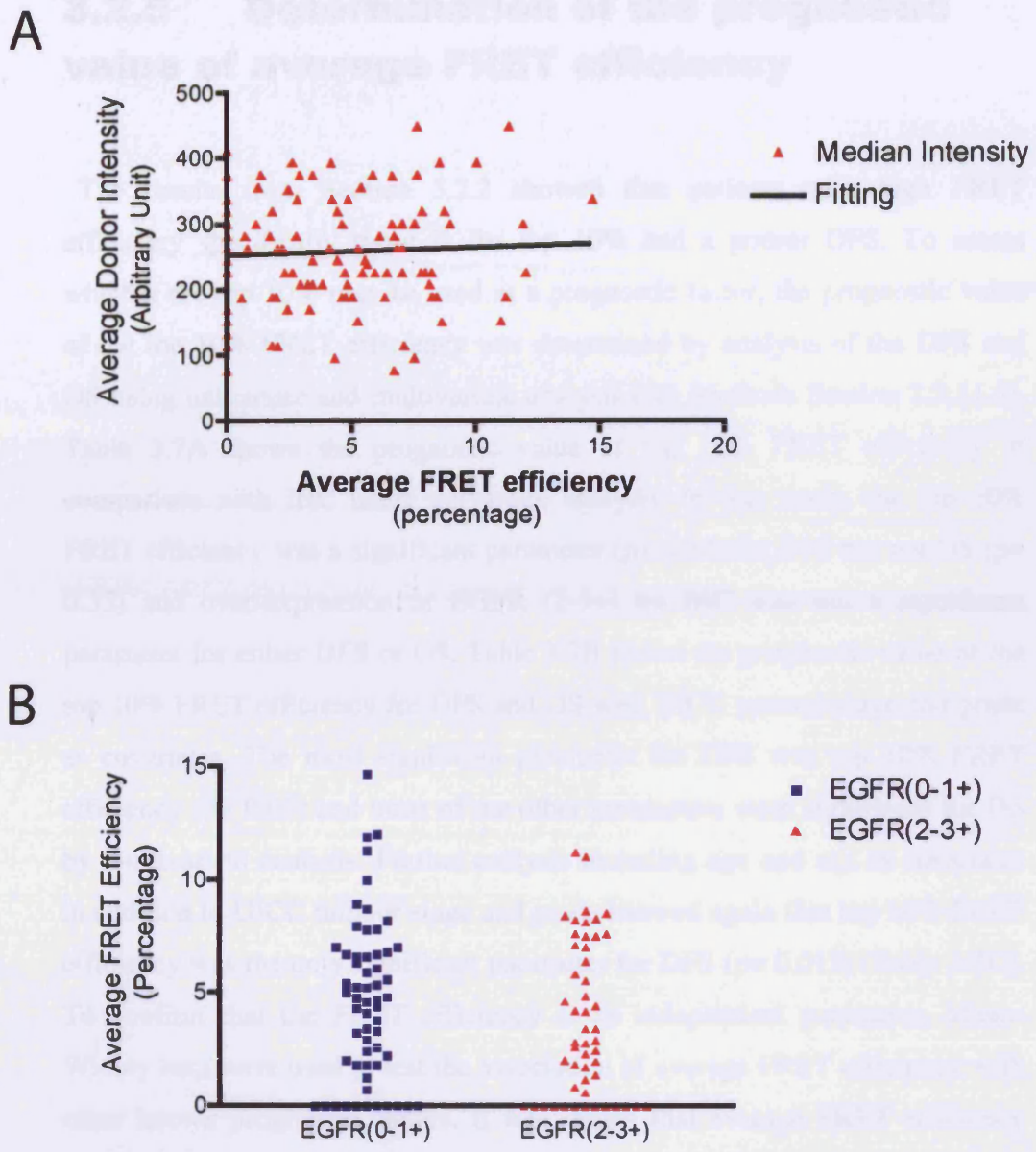

Fig. 3.10: EGFR concentration does not correlate with EGFR phosphorylation. A, The linear regression shows no correlation between donor intensity Cy3b and average FRET efficiency (r2=0). In these studies expression of EGFR is not correlated with its phosphorylation state. **B,** Mann-Witney test illustrates that there is no correlation between average FRET efficiency and EGFR immunochemistry scoring (log-rank test p=0.24).

3.2.5 Determination of the prognostic value of average FRET efficiency

The results from Section 3.2.2 showed that patients with high FRET efficiency specifically those in the top 10% had a poorer DFS. To assess whether the top 10% may be used as a prognostic factor, the prognostic value of the top 10% FRET efficiency was determined by analysis of the DFS and OS using univariate and multivariate analysis (see Methods Section 2.2.11.6). Table 3.7A shows the prognostic value of top 10% FRET efficiency in comparison with IHC using univariate analysis. In this study, the top 10% FRET efficiency was a significant parameter (p= 0.04) for DFS but not OS (p= 0.35) and over-expression of EGFR (2-3+) by IHC was not a significant parameter for either DFS or OS. Table 3.7B shows the prognostic value of the top 10% FRET efficiency for DFS and OS with UICC tumour stage and grade as covariates. The most significant parameter for DFS was top 10% FRET efficiency (p= 0.03) and none of the other parameters were significant for OS by multivariate analysis. Further analysis including age and sex as covariates in addition to UICC tumour stage and grade showed again that top 10% FRET efficiency was the only significant parameter for DFS (p= 0.013) (Table 3.7C). To confirm that the FRET efficiency is an independent parameter, Mann-Witney tests were used to test the association of average FRET efficiency with other known prognostic factors. It was shown that average FRET efficiency was not associated with grade or UICC (International Union Against Cancer) tumour stage (Figure 3.11A and 3.11B).

A

Univariate analysis	Statistical significance value p
Disease-free survival	
EGFR (2-3+) by IHC (n= 122)	0.71
Top 10% FRET efficiency (n= 130)	0.04
Overall Survival	
EGFR (2-3+) by IHC (n=122)	0.08
Top 10% FRET efficiency (n=130)	0.35

B

Multivariate analysis	Statistical significance value p
Disease-free Survival (n =130)	
Top 10% FRET efficiency	0.029
UICC stage 2	0.960
UICC stage 3	0.610
UICC stage 4	0.860
Grade (Linear)	0.190
Grade (Quadratic)	0.970
Overall survival (n=130)	
Top 10% FRET efficiency	0.32
UICC stage 2	0.60
UICC stage 3	0.73
UICC stage 4	0.45
Grade (Linear)	0.84
Grade (Quadratic)	0.36

C

Multivariate analysis	Statistical significance value p
Disease-free Survival (n =130)	
Top 10% FRET efficiency	0.013
UICC stage 2	0.960
UICC stage 3	0.580
UICC stage 4	0.830
Grade (Linear)	0.260
Grade (Quadratic)	0.970
Age	0.240
Sex	0.510

Table 3.7: A, Prognostic value of the top 10% FRET efficiency by univariate analysis as compared to conventional IHC. **B,** Prognostic value of top 10% FRET efficiency by multivariate analysis with UICC tumour stage and grade as covariates. **C,** Prognostic Value of Top 10% FRET efficiency for DFS by multivariate analysis with UICC stage, grade, age and sex as covariates.

A

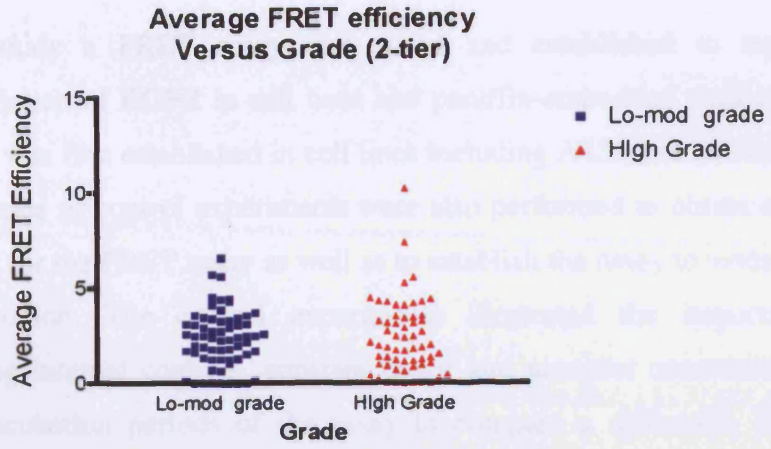

B

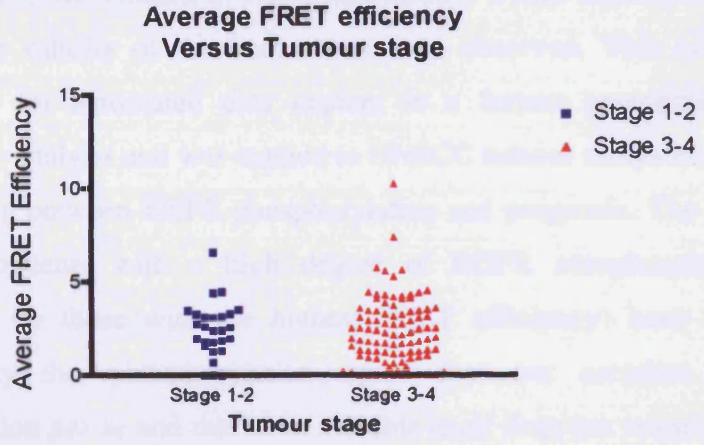

Figure 3.11: A, Mann-Witney tests show that there is no correlation of average FRET efficiency with tumour grade or **B,** UICC tumour stage.

3.3 Discussion

In this study a FRET assay was tested and established to report the phosphorylation of EGFR in cell lines and paraffin-embedded tumour arrays. The assay was first established in cell lines including A431 and MDAMB-231 cells. A series of control experiments were also performed to obtain optimum conditions for the FRET assay as well as to establish the assay to assess EGFR phosphorylation. The control experiments illustrated the importance of maintaining internal controls, constant donor and acceptor concentrations as well as incubation periods of the assay to compare a difference in EGFR phosphorylation either between cell lines or tumour cores by FRET. The assay is designed to provide a two-site assay for phosphorylation of the EGFR using coincidence detection of protein and phospho-site selective monoclonal antibodies, which increases the specificity of the assay. This is of particular importance in the context of tissue microarrays where there is no opportunity to test the validity of the immunoreactions observed. This assay has been developed for automated data capture in a format appropriate for tissue microarray analysis and was applied to HNSCC tumour arrays to determine the relationship between EGFR phosphorylation and prognosis. The study reveals 10% of patients with a high degree of EGFR autophosphorylation (as evidenced by those with the highest FRET efficiency) have a poor DFS. Importantly this phosphorylation status does not correlate with EGFR concentration *per se* and this latter variable itself does not correlate with DFS. However, this retrospective study had a small sample size of 130 patients and 10% of the patients represented only 13 patients and thus a type I error cannot not be excluded.

Several studies have shown a correlation of EGFR expression with OS and DFS (Ang et al., 2002; Dassonville et al., 1993; Gupta et al., 2002; Sheridan et al., 1997). In this retrospective study, conventional immunochemistry scores failed to show the correlation of EGFR expression (2-3+) with DFS and OS as in other prospective studies. This may be due to a small sample size in this retrospective study. But using high throughput FLIM, FRET efficiency was

shown to correlate with DFS in the same group of patients. It is proposed that future IHC experiments may include only those tumours with 3+ expression (i.e. excluding 2+ expression) in the EGFR over-expression group to assess the prognostic value.

The pilot study showed a statistically significant result in the upper tertile range of average FRET efficiency in its correlation with DFS. However, further measurements and validation study only showed statistically significant results in the top 10% range. This means that the exact cut-off points for high FRET efficiency may vary between studies depend on the design of the study. A large prospective trial is needed to determine the cut-off point and to validate the FRET methods for wider clinical use (Hayes et al., 1996; Hayes et al., 1998).

The results presented in this chapter represent a proof of principle that the phosphorylation of EGFR may be assessed by FRET and that such assay may be applied to paraffin sections of tumour arrays to assess the prognosis of cancer patients. It was shown that the assay can be applied to assess EGFR phosphorylation in head and neck tumour arrays in a high throughput manner. It was therefore postulated that the assay may also be applied to assess the phosphorylation of other HER receptors and other signalling pathways in variety of cancers. The ultimate aim is for such assays to be applied to assess phosphorylation of HER receptors in relation to targeted therapies against HER receptors in patients.

4 Activation of alternative HER receptors mediates resistance to tyrosine kinase inhibitors (TKIs) in breast cancer cells

4.1 Introduction

The HER receptors plays a crucial role in breast cancer and many other type of cancers (Yarden and Sliwkowski, 2001). Recently, there has been accelerated use of drugs targeting EGFR and HER2 receptors in breast cancer, including Herceptin (Trastuzumab, a monoclonal antibody for HER2), Iressa (Gefitinib or ZD 1839, a tyrosine kinase inhibitor of EGFR) and Lapatinib (a tyrosine kinase inhibitor of EGFR and HER2) (Baselga, 2002; Piccart-Gebhart et al., 2005; Romond et al., 2005). As discussed in the Introduction, although over-expression of HER receptors has been used to select patients for these drugs, their expression does not necessarily correlate with the response of these drugs (Arteaga, 2006; Chung et al., 2005; Menendez et al., 2006). The underlying mechanisms contributing to the resistance as well as predicting the success of these drugs in cancer patients are still poorly understood.

The response rate to targeted therapies against HER family therapy depends on more than just the receptor concentrations or the mutations of the particular HER receptor (Arteaga, 2006; Chung et al., 2005; Menendez et al., 2006). It is likely that multiple interacting HER receptors and ligands are involved in mediating response to targeted therapy. For example Iressa which targets the EGFR receptor also inhibits the PI3K and PKB pathway via HER3 (Engelman et al., 2005). Moreover, Iressa is also effective in HER2 over-expressing breast cancer cells (Moulder et al., 2001). Therefore, the treatment to reduce the tyrosine kinase activity of EGFR receptors may also affect HER2 and HER3 receptors. Therapy based on receptor concentration, ignoring the activation and

phosphorylation state of the receptor and its interaction with other HER receptors will continue to yield a relatively low response rate (Arteaga, 2002; Kong et al., 2006). Activation of alternative HER receptors through their ligands may mediate resistance to targeted therapy.

Targeting HER2 has been the main focus in breast cancer although increasingly, inhibition of EGFR in combination with HER2 blockage is also seen to be important in breast cancer therapy (Baselga, 2002; Piccart-Gebhart et al., 2005; Romond et al., 2005). *In vitro*, Iressa is effective in HER2 over-expressing breast cancer cells (Moulder et al., 2001). Moreover, EGFR expression had also been shown to play a role in hormone resistant breast cancer patients (Nicholson et al., 1989) and this has led to the use of Iressa with aromatase inhibitors in breast cancer (Polychronis et al., 2005). More recently Lapatinib that targets the tyrosine kinase activities of both EGFR and HER2 has been successfully used in HER2 positive patients who had progressed after Herceptin treatment, confirming the role of EGFR inhibition in breast cancer.

The purpose of this study was to assess the change in activation status of all 4 HER receptors to EGFR tyrosine kinase inhibitors (TKIs) in breast cancer cell lines and their relationship to resistance towards these therapies. Firstly, the establishment of an assay to assess HER2 phosphorylation was performed in A431 cells as a test bed. Secondly, the effect of EGFR TKIs on HER2 phosphorylation by FRET as well as its effect on the dimerisation pattern of other HER receptors with HER2 in breast cancer cells were investigated.

4.2 Results

4.2.1 HER2 phosphorylation state monitored by FRET

The purpose of this study was to assess the response of HER receptors in relation to targeted therapies against EGFR and HER2 in breast cancer cell

lines since inhibition of EGFR together with HER2 is increasingly thought to be important for breast cancer as suggested by the use of the combination inhibitor Lapatinib (Geyer et al., 2006; Konecny et al., 2006). Having established the assessment of EGFR phosphorylation state by FRET in A431 cells (Chapter 3), the method was applied to assess HER2 phosphorylation state in relation to targeted therapy. HER2 is not known to have its own ligand although it is the preferred dimerisation partner for other HER receptors (Graus-Porta et al., 1997). To establish an assay for HER2 phosphorylation, it was necessary to demonstrate HER2 phosphorylation via other HER receptors. A431 cells was chosen as a test bed because of their extensive prior use for the analysis of EGFR and other HER receptors.

To assess HER2 phosphorylation, an anti-HER2 antibody was conjugated to a Cy3b chromophore (HER2-Cy3b) and an anti-phosphoHER2 antibody to Cy5 (pHER2-Cy5). It was hypothesized that upon HER2 phosphorylation, there would be coincident binding of HER2-Cy3b and pHER2-Cy5 inducing Förster resonance energy transfer (FRET). The specific quenching of the donor chromophore Cy3b results in the decrease of lifetime of HER2-Cy3b. Therefore, a decrease in lifetime of HER2-Cy3b would be indicative of HER2 phosphorylation.

To show *in situ* that HER2 could be activated consequent to dimerisation with other members of the HER family, A431 cells were stimulated with EGF, heregulin β (β3 of NRG1, Materials Section 2.1.5) and heregulin-β1 (β1 of NRG1, Materials Section 2.1.5). EGF is the ligand for EGF and heregulin β and heregulin β-1 are both ligands for HER3 and HER4. The average lifetime of the donor HER2-Cy3b alone (detecting HER2 protein) was 2.20 ns and EGF stimulation alone did not affect the donor lifetime (Figure 4.1A). In the presence of acceptor pHER2-Cy5 (detecting phosphorylated HER2), the donor lifetime HER2-Cy3b decreased to 1.75 ns due to basal HER2 phosphorylation. A further decrease of the average lifetime of HER2-Cy3b was measured upon EGF, β and β-1 heregulin (Figure 4.1A). The significant decreases in average lifetime compared to the basal levels ($p<0.01$) indicate an increase in HER2 tyrosine phosphorylation and therefore activation in A431 cells. To verify the measurements were not due to unspecific FRET, the phosphatase YOP was

used after EGF treatment to dephosphorylate the tyrosine on HER2 in the fixed preparations. The average lifetime reverted to the control values (yellow triangles) indicating a loss of FRET. Independently, an increase in HER2 phosphorylation on Tyr1221 and 1222 in a total cell lysate was shown by western blot using a phospho-specific antibody (upper panel) (Figure 4.1B).

As expected, heregulin β and β-1 did not cause EGFR phosphorylation in A431 cells (Figure 4.1C) since HER2 is the preferred dimerisation partner for HER3 and HER4. In this experiment, the cells were incubated with either donor EGFR-Cy3b (F4-Cy3b) or donor and acceptor pEGFR-Cy5 (FB2-Cy5) to assess EGFR phosphorylation (Since several HER pathways will be analysed by FRET in this chapter, F4-Cy3b will be referred to as EGFR-Cy3b and FB2-Cy5 will be termed pEGFR-Cy5). Basal phosphorylation was indicated by a decrease in the median lifetimes from 2.3 ns to 2.1 ns in the presence of the acceptor pEGFR-Cy5. Not surprisingly, EGF caused further EGFR phosphorylation as shown by the significant decrease of lifetime to 1.8 ns ($p < 0.01$). However, heregulin β and heregulin β-1 did not cause a significant decrease in lifetime.

Since A431 cells were used only as a test cell line, three other breast cancer cell lines (MCF-7, MDAMB-453 and SKBR3 cells) were also used for this study. The amount of EGFR and HER2 receptors of A431 cells in relation to the three breast cell lines (MCF-7, MDAMB-453, SKBR3 cells) is illustrated in Figure 4.2A. The assay to assess HER2 phosphorylation was also applied in MCF-7 cells that have 'normal' levels of EGFR and HER2. It was shown that EGF and heregulin β-1 activated HER2, indicated by a decrease in the median lifetimes from a basal level of 1.93 ns to 1.81 ns and 1.86 ns respectively ($p< 0.001$ for both conditions) in MCF-7 cells (Figure 4.2B). Altogether these data indicated that HER2 phosphorylation by ligands for other HER receptors family members could be monitored in intact cells by FRET.

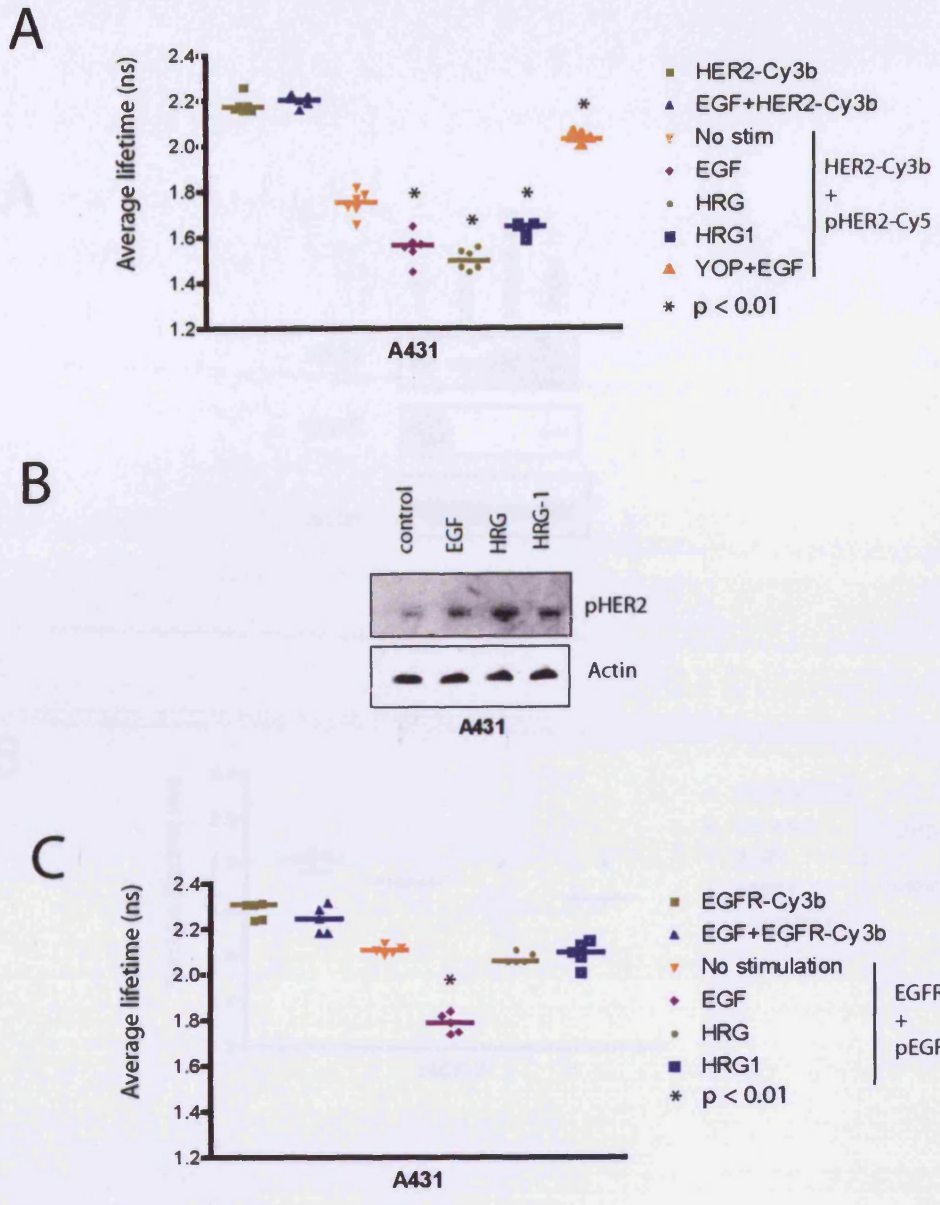

Figure 4.1: HER2 is the preferred dimerisation partner for other HER receptors. A, To assess HER2 phosphorylation in A431 cells by FRET, the cells were incubated with either donor alone (HER2-Cy3b) or donor and acceptor (HER2-Cy3b+pHER2-Cy5) after 10-minute stimulation with either EGF, heregulin beta or heregulin beta-1. To remove phosphotyrosine, the phosphatase YOP was used following stimulation of the cells with EGF. **B,** For western blot, near confluent A431 cells were stimulated with EGF, heregulin beta and heregulin beta-1 for 10 minutes and whole cell lysate was obtained after treated with lysis buffer. 10ng of proteins were used for each lane for western blot analysis and the phosphorylation of HER2 on Tyr 1221/1222 was determined with anti-phosphospecific antibody. **C,** Same experiment as A but A431 cells were incubated with either donor alone (EGFR-Cy3b) or donor and acceptor (EGFR-Cy3b+pEGFR-Cy5) after ligand stimulation to assess EGFR phosphorylation.

A

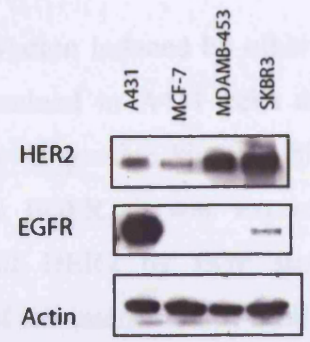

B

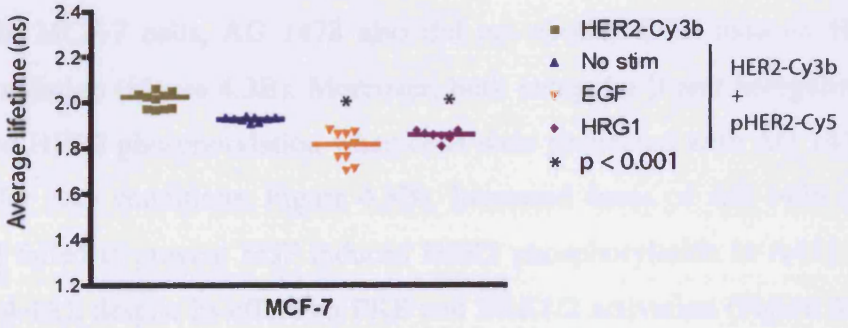

Figure 4.2. A, A431, MCF-7, MDAMB-453 and SKBR3 were grown to near confluency before lysed to assess the total levels of HER2 and EGFR by western blot. **B,** MCF-7 cells were incubated with suitable pair of antibodies to assess HER2 phosphorylation after ligand stimulation.

4.2.2 Effect of tyrosine kinase inhibitors (TKIs) on HER2 activation state

HER2 phosphorylation induced by other HER receptors via their respective ligands was determined in A431 cells and MCF-7 cells while EGFR was inhibited or not with tyrosine kinase inhibitor (TKI) AG 1478. Since A431 cells over-express EGFR, it was expected that AG 1478 would prevent phosphorylation of HER2 by EGF stimulation and to exert a possible inhibitory effect of the interaction of HER2 with HER3 and HER4. However, AG 1478 failed to abolish EGF-induced and heregulin β-induced HER2 phosphorylation in A431 cells (Figure 4.3A). Moreover, it increased HER2 phosphorylation with heregulin β-1, indicated by a decrease in average donor lifetime compared to those with no AG 1478 pre-treatment ($p=0.008$) (Figure 4.3A). In MCF-7 cells, AG 1478 also did not abolish EGF induced HER2 phosphorylation (Figure 4.3B). Moreover, both heregulin β and heregulin β-1 enhanced HER2 phosphorylation when cells were pretreated with AG 1478 ($p < 0.01$ for both conditions; Figure 4.3B). Increased doses of AG 1478 up to 300 μM failed to prevent EGF induced HER2 phosphorylation in A431 cells (Figure 4.4A), despite its effect on PKB and ERK1/2 activation (Figure 4.4B). In MCF-7 cells higher doses of AG 1478 (up to 300 μM) could inhibit EGF-induced HER2 phosphorylation but not the basal HER2 phosphorylation (Figure 4.4C).

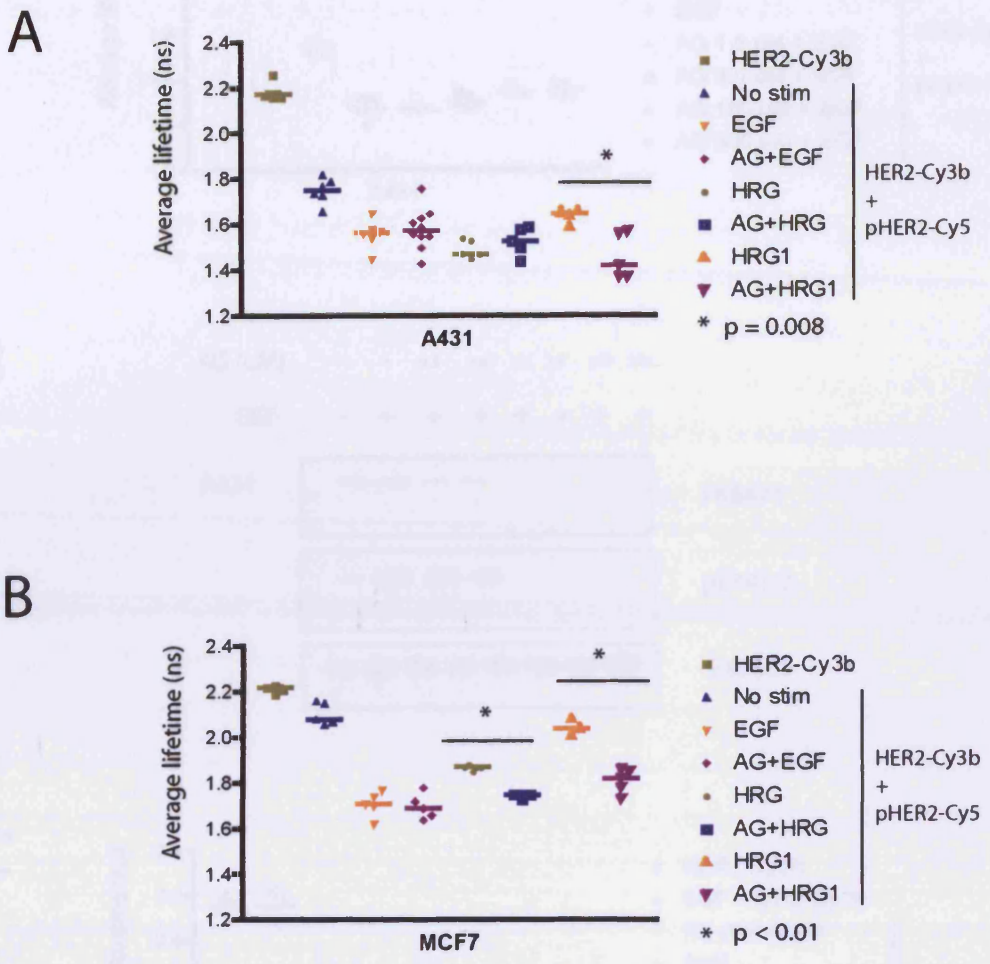

Figure 4.3: AG 1478 does not diminish EGF induced HER2 phosphorylation and enhances heregulin induced HER2 phosphorylation. A, In this experiment, A431 cells were pretreated with tyrosine kinase inhibitor 3μM AG 1478 for two hours before stimulated with either EGF, heregulin beta or heregulin beta-1. The average lifetimes of HER2-Cy3b of those pre-treated with AG 1478 were compared with those without treatment and the medians of the average lifetimes were compared using Mann-Witney test. **B,** The same experiment was also done in MCF-7 cells.

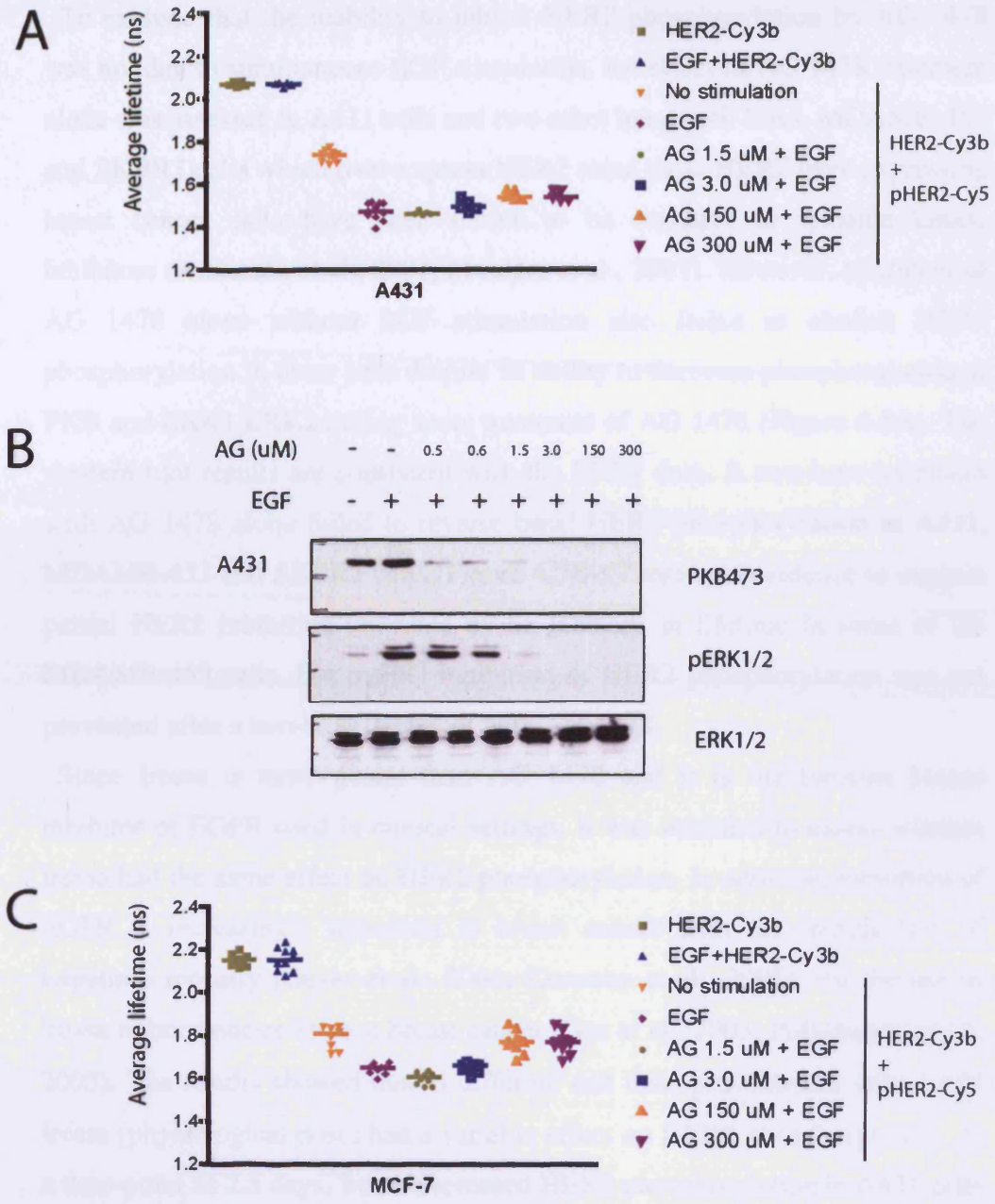

Figure 4.4: Inhibition of EGFR with escalating doses of AG 1478 does not abolish HER2 phosphorylation. **A,** Before being treated with increasing doses of AG 1478 for two hours, A431 cells were stimulated with EGF 100 ng/ml for 10 minutes. The cells were incubated suitable pair of antibodies to assess HER2 phosphorylation. **B,** A431 cells were pretreated with AG 1478 with or without EGF stimulation before treated with lysis buffer and loaded in SDS PAGE. The phosphorylation of PKB on Ser 473 and p44/42 MAP Kinase (Erk1/Erk2) on Thr202/Tyr 204 was determined using phospho-specific antibodies and the total endogenous levels of PKB and p44/42 MAP Kinase were assessed by western blot using anti-PKB and anti-MAPK antibodies. **C,** Same experiment as A but MCF-7 cells were used instead.

To exclude that the inability to inhibit HER2 phosphorylation by AG 1478 was not due to simultaneous EGF stimulation, the effect of AG 1478 treatment alone was assessed in A431 cells and two other breast cell lines, MDAMB-453 and SKBR3 cells which over-express HER2 since these HER2 over-expressing breast cancer cells have been shown to be sensitive to tyrosine kinase inhibitors (Anderson et al., 2001; Moulder et al., 2001). However, treatment of AG 1478 alone without EGF stimulation also failed to abolish HER2 phosphorylation in these cells despite its ability to decrease phosphorylation of PKB and ERK1/ERK2 during acute treatment of AG 1478 (Figure 4.5A). The western blot results are consistent with the FRET data. A two-hour treatment with AG 1478 alone failed to reverse basal HER2 phosphorylation in A431, MDAMB-453 and SKBR3 cells (Figure 4.5B). There was evidence to suggest partial HER2 inhibition indicated by an increase in lifetime in some of the MDAMB-453 cells. But overall inhibition of HER2 phosphorylation was not prevented after a two-hour treatment with AG 1478.

Since Iressa is more potent than AG 1478 and it is the tyrosine kinase inhibitor of EGFR used in clinical settings, it was intended to assess whether Iressa had the same effect on HER2 phosphorylation. In addition, inhibition of EGFR is increasingly important in breast cancer with the introduction of Lapatinib recently (Geyer et al., 2006; Konecny et al., 2006) and the use of Iressa in hormone-resistance breast cancer (Gee et al., 2003; Polychronis et al., 2005). The results showed that in different cell lines pretreatment with 1 μM Iressa (physiological dose) had a variable effect on HER2 phosphorylation. At a time-point of 2.5 days, Iressa decreased HER2 phosphorylation in A431 cells with growth inhibition (Figure 4.6A). On the contrary, MCF-7 cells with normal levels of EGFR, had increased HER2 phosphorylation at 2.5 days of Iressa treatment and cell viability confirmed that cells were highly proliferative at this point; MCF-7 cells were not sensitive to 1 μM Iressa (Figure 4.8B). Some SKBR3 and MDAMB-453 (HER2-over-expressing) cells showed partial HER2 inhibition but the majority of cells showed no suppression of basal HER2 phosphorylation (Figure 4.6A). SKBR3 cells were shown to be sensitive to Iressa with prolonged 1 μM Iressa treatment (Figure 4.8D). Therefore, the

results showed that acute 1 μM Iressa (physiological dose) was not able to abolish basal HER2 phosphorylation in breast cell lines.

Since TKIs including AG 1478 and Iressa failed to decrease basal HER2 phosphorylation in breast cell lines like MCF-7 and SKBR3, it suggested that the persistence of HER2 phosphorylation in these cells was not be due to phosphorylation from EGFR/HER2 dimerisation, but from either HER2/HER3 or HER2/HER4 dimerisation. The fact that EGFR inhibition enhanced HER2 phosphorylation by exogenous heregulin stimulation in MCF-7 cells (Figure 4.3B) suggested that HER2/HER3 and HER2/HER4 dimers occurred to sustain HER2 phosphorylation. However, TKIs abolished HER3 phosphorylation with a corresponding decrease in phospho-PKB and phospho-ERK1/2 (data on AG 1478 shown in Figure 4.6B, data on Iressa shown later Figure 4.13B). The decrease of HER3 phosphorylation but increased HER2 phosphorylation with heregulin (Figure 4.3B) and AG 1478 treatment in MCF-7 cells indicated the involvement of HER4 since heregulin activates both HER3 and HER4. It was postulated that maintenance of HER2 phosphorylation and the additional HER2 phosphorylation by heregulin stimulation following two hour pre-treatment with AG 1478 may be due to activation of HER4 with subsequent HER2 phosphorylation. It was therefore decided to assess HER4 activation and its interaction with HER2 following EGFR inhibition by AG 1478 and Iressa in breast cell lines like MCF-7 and SKBR3.

A

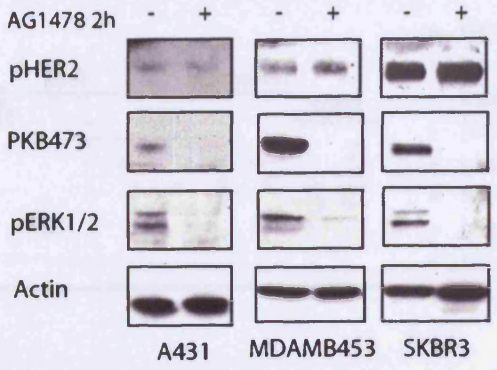

B

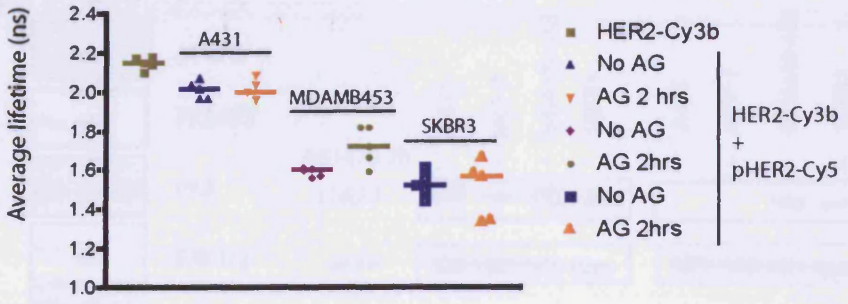

Figure 4.5: The effects of AG 1478 in A431 cells and three breast cell lines. A, A431, MDAMB-453 and SKBR3 were grown to near confluency before lysed to assess the total levels of HER2 and EGFR by western blot. On the right panel, A431 and two breast cell lines were treated with AG 1478 for 2 hours before the cells were lysed for western blot analysis. **B,** A431, MDAMB-453 and SKBR3 cells were incubated with either donor alone (HER2-Cy3b) or donor and acceptor (HER2-Cy3b+pHER2-Cy5) after pretreated the cells with 3μM AG 1478 for 2 hours to assess HER2 phosphorylation by FRET.

A

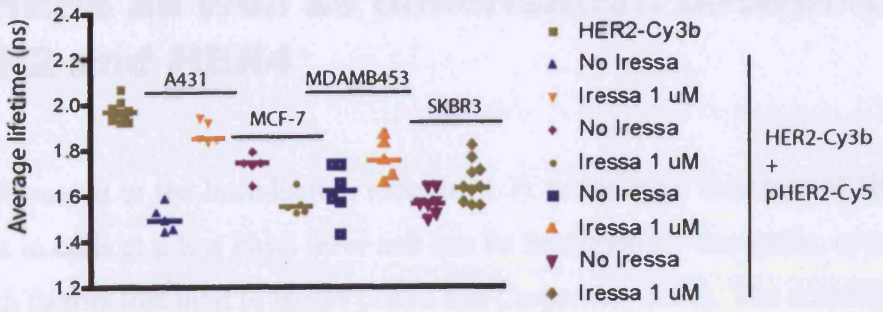

B

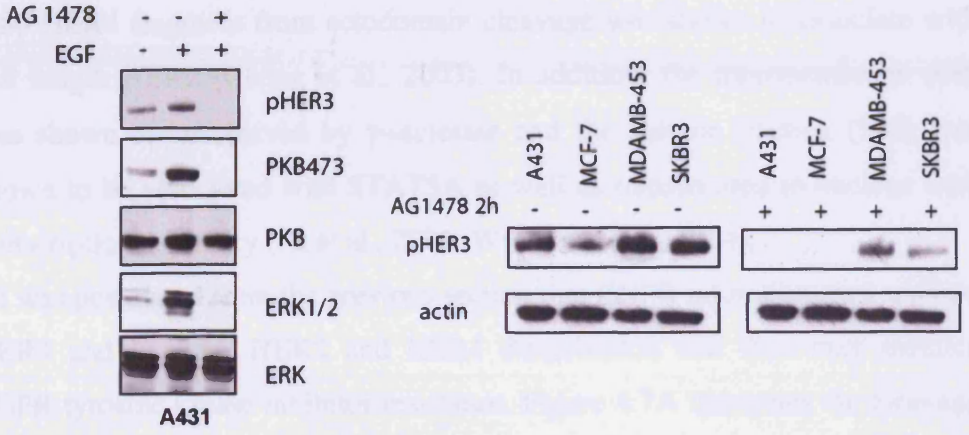

Figure 4.6. A, The effect of Iressa on HER2 phosphorylation state by FRET. A431 cells and three other breast cancer cell lines MCF-7, MDAMB-453 and SKBR3 were incubated with suitable pair of antibodies to assess HER2 phosphorylation after pre-treated with 1 uM Iressa for 2.5 days. **B, The effect of Iressa on pHER3 and downstream signalling pathways by western blot.** On the left panel, A431 cells were pre-treated with AG 1478 with or without EGF stimulation as illustrated before western blot analysis. On the right panels, A431, MCF-7, MDAMB-453 and SKBR3 were lysed for western blot after treated with either 3μM AG 1478 for 2 hours or had no treatment.

4.2.3 TKIs induce proteolytic cleavage of HER4 as well as dimerisation between HER2 and HER4

As discussed in the Introduction (Section 1.3), proteolytic cleavage of HER4 occurs in cells at a low basal level and can be increased by heregulin, or other growth factors that bind to HER4 (Zhou and Carpenter, 2000). The ectodomain cleavage of HER4 is mediated by tumour necrosis factor-∝-converting enzyme (TACE), a transmembrane metalloprotease that produces a membrane-anchored fragment (80 kD) which consists of the entire cytoplasmic and transmembrane domain (Carpenter, 2003; Vecchi and Carpenter, 1997). The m80 HER4 fragment from ectodomain cleavage was shown to associate with full length HER2 (Cheng et al., 2003). In addition, the transmembrane m80 was shown to be cleaved by γ-secretase and the soluble fraction (S80) was shown to be associated with STAT5A as well as translocated to nucleus with transcriptional activity (Ni et al., 2001; Williams et al., 2004).

It was postulated from the previous section that EGFR inhibition may activate HER4 and increase HER2 and HER4 dimerisation and thus may mediate EGFR tyrosine kinase inhibitor resistance. Figure 4.7A illustrates the cleavage of HER4 and production of m80 upon heregulin stimulation in SKBR3 and MCF-7 cells. Moreover, acute treatment with tyrosine kinase inhibitors (TKIs) AG 1478 and Iressa also induced the cleavage of HER4 and production of m80 in both SKBR3 and MCF-7 cells (Figure 4.7A). Upon tyrosine kinase inhibition the m80 fragment accumulation was augmented compared to stimulation with exogenous heregulin. Since HER2 may be the preferred dimerisation partner of HER4, it was therefore postulated that the activation and cleavage of HER4 induced by tyrosine kinase inhibitors may induce dimerisation between HER2 and HER4. Figure 4.7B (upper panels) illustrates the co-immunoprecipitation with intracellular anti-HER4. A similar response to heregulin stimulation was seen with AG 1478 and Iressa which induced dimerisation between HER2 and HER4 in SKBR3 and MCF-7 cells (Figure 4.7B). The co-immunoprecipitation with intracellular anti-HER2 in MCF-7

cells also demonstrated that AG 1478 and Iressa induced dimerisation between HER2 and HER4 (Figure 4.7B, lower panels). In addition, the m80 fragment was shown to dimerise with HER2 upon AG 1478 and Iressa treatments.

In summary, acute treatment with AG 1478 and Iressa inhibited downstream signalling pathways. The inhibition was due to the prevention of EGFR homodimer, EGFR/HER2 and EGFR/HER3 heterodimer formation (Anido et al., 2003; Arteaga et al., 1997; Engelman et al., 2005). However, the proteolytic cleavage of HER4 and heterodimerisation of HER2/HER4 sustained HER2 phosphorylation.

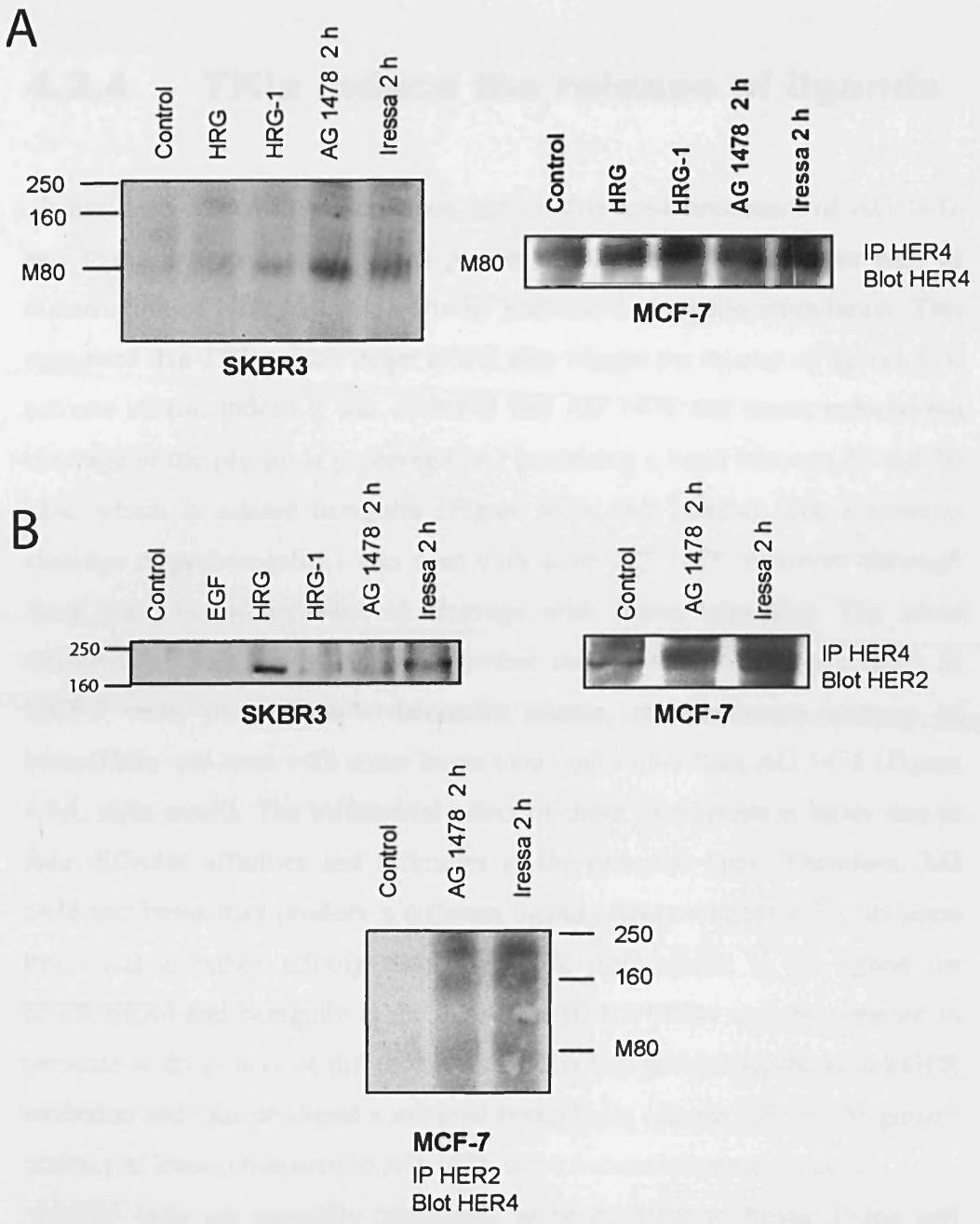

Figure 4.7: AG 1478 and Iressa induce proteolytic cleavage of HER4 as well as dimerisation between HER2 and HER4 in breast cancer cell lines via the release of the ligands. A, Both MCF-7 and SKBR3 were immunoprecipitated with intracellular HER4 antibody after being treated in the conditions as illustrated. Following the immunoprecipitation, the cell lysate without the beads were loaded unto a SDS gel and a western blot analysis was performed. The membrane was probed with anti-HER4 antibody. **B,** In the upper panels, both MCF-7 and SKBR3 were immunoprecipitated with intracellular HER4 antibody after treated with the conditions illustrated before western blot analysis. The membrane was probed with anti-HER2 antibody. In the lower panel, MCF-7 cells near confluency were lysed and immunoprecipitated with intracellular HER2 antibody after treated with either AG 1478 or Iressa. The membrane was probed anti-HER4 antibody.

4.2.4 TKIs induce the release of ligands

It has been shown in the previous section that acute treatment of AG 1478 and Iressa caused activation and proteolytic cleavage of HER4 as well as dimerisation of HER2/HER4, a similar process to heregulin stimulation. This suggested that TKIs which target EGFR may trigger the release of ligands that activate HER4. Indeed it was observed that AG 1478 and Iressa induced the cleavage of the precursor proheregulin-1 producing a band between 35 and 50 kDa, which is mature heregulin (Figure 4.8A, left panels). The maximum cleavage of proheregulin-1 was seen with acute AG 1478 treatment although there was also an increase of cleavage with Iressa treatment. The acute treatment of both drugs increased further the production of betacellulin in MCF-7 cells. In contrast to heregulin release, the maximum increase of betacellulin was seen with acute Iressa treatment rather than AG 1478 (Figure 4.8A, right panel). The differential effect of these two agents is likely due to their different affinities and efficacies in the two cell lines. Therefore, AG 1478 and Iressa may produce a different ligand response in MCF-7 cells since Iressa has a higher affinity than AG 1478. Betacellulin is the ligand for EGFR/HER4 and heregulin is the ligand for HER3/HER4 and their release in response to drugs may be different. AG 1478 is less potent that Iressa in EGFR inhibition and thus produced a minimal betacellulin release. Due to the greater potency of Iressa compared to AG 1478, more betacellulin was induced.

MCF-7 cells are generally considered to be resistant to Iressa. Using cell viability assays it was confirmed that during acute treatment with Iressa, MCF-7 growth was not prevented and furthermore there was an increase in cell proliferation compared to control (Figure 4.8B). In MCF-7 cells, the apparent resistance may be due to the acute Iressa treatment that resulted in enhanced HER2 phosphorylation, with dimerisation between HER2 and HER4. After seven days of treatment, MCF-7 cells were only minimally inhibited by 1μM Iressa and the cleavage of proheregulin-1 persisted after seven days of Iressa treatment. Therefore, the compensatory mechanism from the HER4 activation due to ligand release (including heregulin) and its subsequent dimerisation

with HER2 predicts that Iressa has a minimal cell proliferation inhibitory effect in MCF-7 cells.

In SKBR3 cells which are known to be sensitive to Iressa (Anderson et al., 2001; Moulder et al., 2001), there was also an increase of cleavage of precursor pro-heregulin-1 as well as an increase in betacellulin production induced by two hours of Iressa treatment (Figure 4.8C). However, the release of ligands was not sustained in these sensitive cell lines. Over the seven-day treatment of Iressa, the release of these ligands diminished. The cell viability experiments confirmed that 1μM Iressa decreased the viability of SKBR3 cells to 50% of the control in contrast to MCF-7 cells (Figure 4.8D).

The results showed that the activation and cleavage of HER4 during acute treatment of TKIs of EGFR correlated with the release of ligands including betacellulin and heregulin. The activation of HER4 and dimerisation of HER2/HER4 may mediate primary resistance to Iressa in resistant MCF-7 cells. In sensitive SKBR3 cells, the release of some ligands including betacellulin and mature heregulin-1 diminished with prolonged Iressa treatment.

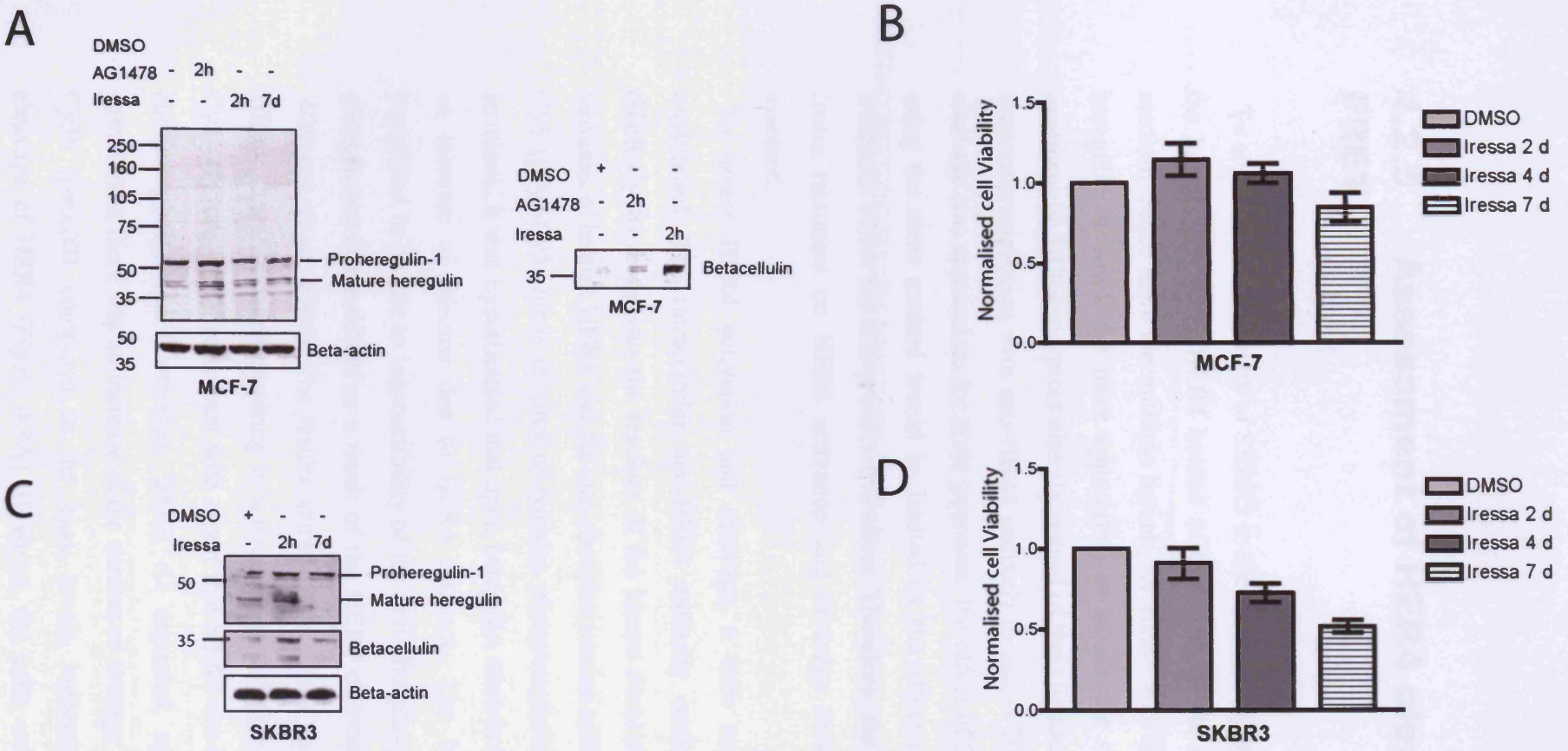

Figure 4.8: AG 1478 and Iressa induce the release of various ligands. **A,** MCF-7 cells were pre-treated with either 3 μM of AG 1478 for 2 hours or 1 μM of Iressa for different durations before the cells were lysed for western blot experiment. 10 ng of protein was loaded in each lane for SDS-gel. The membrane was probed with antibodies recognizing HER4 or proheregulin-1 or betacellulin. The anti-beta-actin antibody was used as loading control. **B,** MCF-7 cells were grown in 24-well plate and left to grow for at least 24 hours before treated with either DMSO or 1 μM Iressa for different durations as illustrated. The viable cells were counted in cell viability analyzer using Trypan blue to stain the dead cells. **C,** Near confluent SKBR3 cells were pre-treated with Iressa or DMSO as illustrated before the cells were lysed for western blot experiment. The membrane was probe with antibodies recognizing proheregulin-1 and betacellulin. **D,** Same experiment as B but SKBR3 cells were used instead of MCF-7 cells.

4.2.5 Assessment of HER4 cleavage by FRET

To attribute the sensitivity of SKBR3 to the decrease of ligands for HER4, all the ligands activating HER4 needed to be tested in the cell lysate and the medium. Since there are multiple ligands for HER4 and multiple isoforms of heregulin, it would be more appropriate to assess the effect of long-term treatment on HER4 receptors directly instead of their ligands. Although the co-immunoprecipitation with anti-HER4 antibody to assess HER4 activation and cleavage was appropriate for acute treatment, the effect of long-term treatment using the same method would be limited by the effect of long-term Iressa treatment which has anti-proliferative effect. Therefore, the effect of long-term Iressa treatment on HER4 activation and cleavage in-situ by FRET was assessed.

To assess HER4 activation and cleavage, a new assay needed to be established. The intracellular anti-HER4 antibody conjugated with Cy3b (HER-Cy3b) recognises the residues of the kinase domain near the carboxy-terminus of human HER4 and the anti-phosphotyrosine antibody conjugated to Cy5 (pTyr-Cy5) binds to sites of tyrosine phosphorylation in the carboxyl-terminus. It was hypothesised that upon heregulin stimulation, there would be an increase of lifetime due to HER4 cleavage. The loss of FRET was postulated to be due to inaccessibility of the anti-phosphotyrosine antibody to phosphotyrosine residues as a result of the HER4 cleavage (Ni et al., 2001; Williams et al., 2004). The results showed that at the basal state there was HER4 phosphorylation resulting in a decrease of average lifetime of HER4-Cy3b (Figure 4.9B), consistent with report that HER4 can homodimerise with autophosphorylation (Carpenter, 2003). As expected, upon heregulin β-1 stimulation, there was an increase of the median of average lifetimes of HER4-Cy3b ($p=0.001$ compared to the basal level), indicating the proteolytic cleavage of HER4 (Figure 4.9A). However, the cells were not sensitive to heregulin β. Although a few cells showed increase of lifetime of HER4-Cy3b,

overall the median of the average lifetime of HER4-Cy3b upon heregulin β stimulation did not change significantly (Figure 4.9A). There are four heregulin (or neuregulin) genes, denoted 1, 2, 3 and 4; and they can exist in different isoforms due to alternative splicing, with different affinities to HER3 and HER4 (Bazley and Gullick, 2005). This particular product heregulin β from Sigma (recognising β3 of NRG1, Materials Section 2.1.5) had been shown to activate mainly HER3 with a crossover ability to activate HER4. This would explain the minimal HER4 cleavage compared with heregulin β stimulation. Heregulin β1 (β1 of NRG1, Materials Section 2.1.5) however, was shown to activate both HER3 and HER4 and would explain the results seen in Figure 4.9A. As a negative control the cells were also stimulated with EGF. An increase of lifetime of HER4-Cy3b was not detected. Unlike the FRET experiment assessing HER2 phosphorylation, the increase of lifetime upon heregulin β-1 stimulation in HER4-FRET experiments did not mean a loss of activation. Instead, it indicated activation of HER4 and cleavage of HER4 tyrosine kinase cytoplasm domain, resulting in the separation between HER4-Cy3b and pTyr-Cy5.

The decrease in lifetime on heregulin β-1 stimulation is due to HER4 cleavage rather than dephosphorylation, as supported by immunoprecipitation results (Figure 4.7) and the literature (Zhou and Carpenter, 2000). Furthermore, phosphatase YOP which dephosphorylated the HER4 phosphorylation could not reverse the change of HER4-Cy3b lifetime significantly following the cleavage of HER4 by heregulin β-1 stimulation compared to EGF and heregulin β which did not cause significant HER4 cleavage (Figure 4.9A and Figure 4.9B)

To further establish the assay for HER4 cleavage by FRET, the cells were pretreated with 100 μM TAPI-1 (TACE inhibitor). The hypothesis was that if the ectodomain cleavage of HER4 is mediated by TACE (Carpenter, 2003; Vecchi and Carpenter, 1997) inducing the loss of FRET (increase of lifetime), then TAPI-1 should reverse the loss of FRET to prove that the assay is specific. MCF-7 and SKBR3 cells were pretreated with 100 μM TAPI-1 or DMSO (as control) for 1 hour before the cells were stimulated with either heregulin β-1 (MCF-7 cells are more sensitive to heregulin β-1 as shown

above) or heregulin β (SKBR3). Figure 4.9C and 4.9D show that while heregulin induced the loss of FRET (increase of lifetime, $p < 0.01$ for both MCF-7 and SKBR3 cells compared to basal condition) due to HER4 cleavage, TAPI-1 reversed the loss of FRET.

The results indicate that activation of HER4 is associated with a decrease in FRET with the reagents employed here and that this correlates with cleavage of HER4. This effect is blocked if cleavage is blocked. Therefore in the case of HER4 and in the context of active TACE, an increase of lifetime can be used as a reporter of its activation and cleavage.

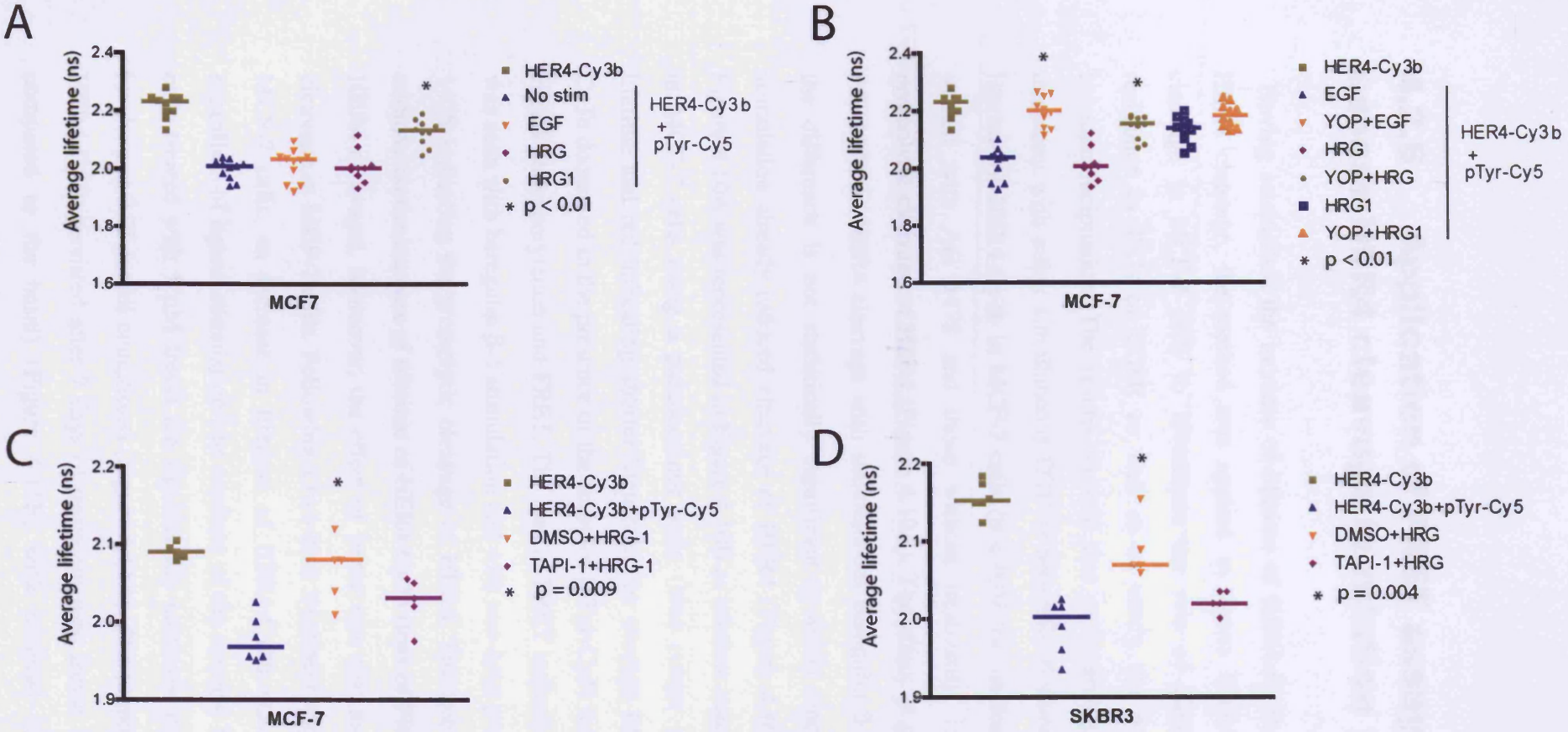

Figure 4.9: Heregulin induces proteolytic cleavage of HER4 in breast cancer cell lines. **A,** MCF-7 cells were incubated with either donor alone (HER4-Cy3b) or donor and acceptor (HER4-Cy3b+pTyr-Cy5) and stimulated with EGF or heregulin beta or heregulin beta-1. **B,** To remove phosphotyrosine, the phosphatase YOP was used following stimulation of the cells with ligands. **C,D,** FRET experiments to assess HER4 cleavage in MCF-7 and SKBR3 cells. The cells were treated with DMSO or TACE inhibitor (TAPI-1) for 1 hour before simulation with heregulin beta-1 (MCF-7 cells) or heregulin beta (SKBR3) and the medians of the lifetimes were compared with the basal condition (without drugs or heregulin stimulation) using Mann-Witney test and the significance value is denoted as *.

4.2.6 Application of FRET assay to assess HER4 cleavage in relation to TKIs

Having established the increase of lifetime of HER4-Cy3b as a reporter of HER4 cleavage, the method was applied to assess HER4 activation and cleavage in MCF-7 cells to investigate the role of HER4 in mediating resistance to TKIs of EGFR as well as to verify the observations from immunoprecipitation. The results showed that pretreatment with AG 1478 treatment with either simultaneous EGF or heregulin β stimulation increased lifetime of HER4-Cy3b in MCF-7 cells ($p < 0.01$ for medians between those treated with AG 1478 and those without treatment), indicative of the proteolytic cleavage of HER4 (Figure 4.10A). The effect of pretreatment with AG 1478 on HER4 cleavage with simultaneous heregulin β-1 is additive but the difference is not statistically significant ($p=0.07$) since heregulin β-1 stimulation already induced cleavage of HER4 (Figure 4.10A). The data of Figure 4.10A was represented in Figure 4.10B as lifetime maps of HER4-Cy3b in MCF-7 cells using a pseudocolour scale (blue colour indicating longer lifetime and red indicating shorter lifetime). The average lifetime of HER4-Cy3b decreased in the presence of the acceptor (pTyr-Cy5) indicating the basal HER4 phosphorylation and FRET. The loss of FRET indicated by blue colour was seen with heregulin β-1 stimulation and with two-hour pretreatment of AG 1478 indicating the proteolytic cleavage of HER4. The two conditions were additive on the increase of lifetime of HER4-Cy3b (loss of FRET, indicative of HER4 cleavage). Moreover, the effect of Iressa was also assessed on HER4 cleavage in MCF-7 cells. Following a two-hour treatment with 1 μM Iressa in MCF-7 cells, an increase in lifetime of HER4-Cy3b was again observed regardless of ligand stimulation (the medians of the average lifetimes of those cells treated with 1 μM Iressa are significantly increased compared to basal levels, $p < 0.01$ for all conditions) (Figure 4.11A). The increase of lifetime of HER4-Cy3b persisted after 7 days of treatment with Iressa 1 μM ($p < 0.001$ compared to the basal) (Figure 4.11B) with minimal inhibition of cell

proliferation (Figure 4.11C). However, increasing the dose of Iressa to 10 μM inhibited the HER4 cleavage with no increase of lifetime of HER4-Cy3b. However, at this dose, DMSO 1:100 concentration was toxic to MCF-7 cells. In addition, 1 μM Iressa is the achievable physiological dose, therefore, the effect of 10 μM Iressa was not pursued further.

FRET was also applied to assess HER4 cleavage in sensitive SKBR3 cells after they were pretreated with Iressa for seven days. Figure 4.12A shows the decrease of average lifetime of HER4-Cy3b in the presence of pHER4-Cy5 from a median of 2.25 ns to a median of 2.1 ns, indicating the basal phosphorylation of HER4. After pretreatment with Iressa 1μM for 2.5 days, there was an increase of average lifetime of HER4-Cy3b indicating activation and proteolytic cleavage of HER4 ($p<0.01$ compared to basal), consistent with immunoprecipitation results (Figure 4.7). However, the amount of HER4 cleavage decreased with seven-days of 1μM Iressa treatment as indicated by the lifetime of HER4-Cy3b returning to basal state ($p=0.32$ compared to basal) (Figure 4.12A). The lifetime map of HER4-Cy3b representing this data is illustrated in Figure 4.12B. The diagram shows an average lifetime for HER4-Cy3b was decreased with the acceptor (pTyr-Cy5) indicating the basal degree of HER4 activation and FRET as illustrated by the change of colour. The increase of lifetime of HER4-Cy3b was seen with 2.5 days of pretreatment with 1μM Iressa. The increase of lifetime of HER4-Cy3b was inhibited when the cells were treated for longer durations with 1 μM Iressa. The results therefore show that there was activation and proteolytic cleavage of HER4 during the acute treatment of Iressa in sensitive SKBR3 but this process diminished after 7 days of treatment (Figure 4.12A and 4.12B) with the decrease in the release of ligands for HER4 including betacellulin and heregulin (Figure 4.8C). The diminished HER4 cleavage would explain why seven-day treatment with 1μM Iressa is able to decrease the proliferation of SKBR3 cells to 50% of that DMSO control in contrast to resistant MCF-7 cells.

In summary, the results showed that the activation and cleavage of HER4 during acute treatment of tyrosine kinase inhibitors of EGFR correlated with the release of ligands including betacellulin and heregulin. The activation of

HER4 and dimerisation of HER2/HER4 may mediate primary resistance to Iressa in resistant MCF-7 cells. In sensitive SKBR3, there was evidence to suggest that the release of some ligands including betacellulin and mature heregulin-1 diminished with prolonged Iressa treatment, correlated with decrease in HER4 cleavage shown by FRET. Therefore, the induction of inactive EGFR homodimers and EGFR/HER2 dimers by Iressa (Arteaga et al., 1997) and the decrease in HER4 activation may explain Iressa sensitivity of SKBR3 cells which over-express HER2 with moderate amount of EGFR. However, since assessment of all the ligands or all types of heregulin are difficult to achieve, it could not excluded that other ligands may remain activated after prolonged Iressa treatment in sensitive SKBR3 cells.

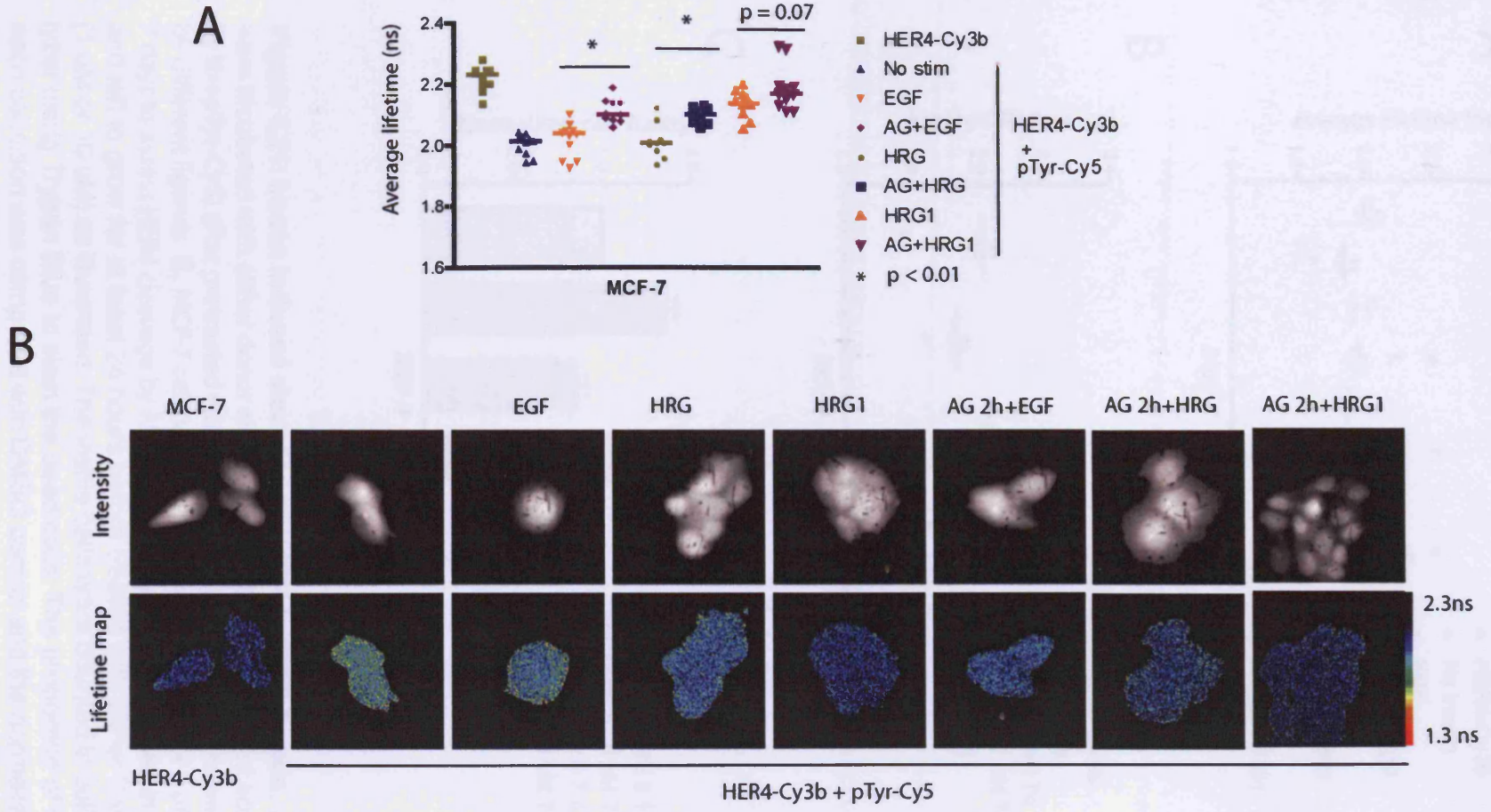

Figure 4.10: The effect of AG 1478 on HER4 cleavage in MCF-7 cells. A, MCF-7 cells were incubated with either donor alone (HER4-Cy3b) or donor and acceptor (HER4-Cy3b+pTyr-Cy5) to assess HER4 cleavage by FRET after stimulated with various ligands with or without two hour pre-treatment of 3 uM AG 1478.

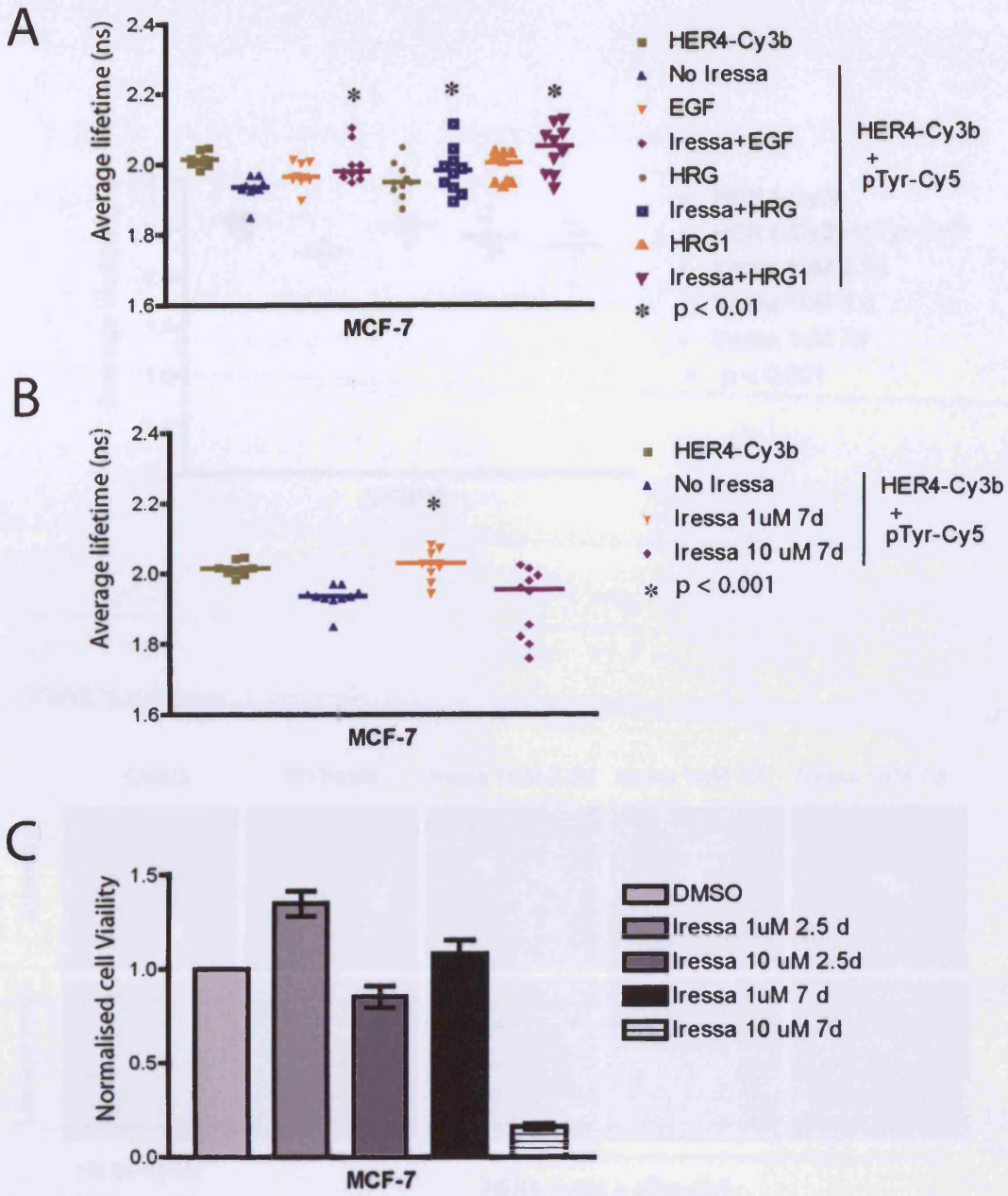

Figure 4.11: Iressa induced cleavage of HER4 in MCF-7 cells. A, MCF-7 cells were incubated with either donor alone (HER4-Cy3b) or donor and acceptor (HER4-Cy3b+pTyr-Cy5) after pretreated with Iressa 1μM for 2 hours while being stimulated by different ligands **B,** MCF-7 cells were treated with Iressa either 1 μM or 10 μM for 7 days to assess HER4 cleavage by FRET **C,** MCF-7 cells were plated in 24-well plate and left to grow for at least 24 hours before treated with either DMSO or Iressa (1 uM or 10 uM) as illustrated. The viable cells were counted in cell viability analyzer using Trypan Blue to stain the dead cells. The proportion of viable cells in each condition was compared with DMSO control and the normalised cell viability was plotted as bar charts above.

A

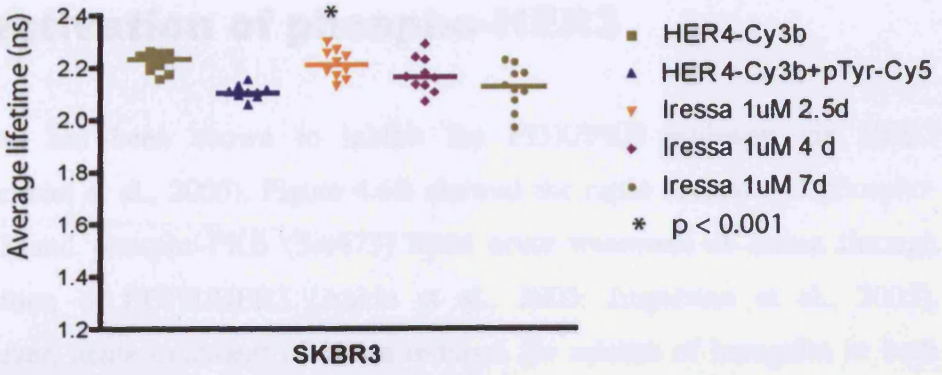

B

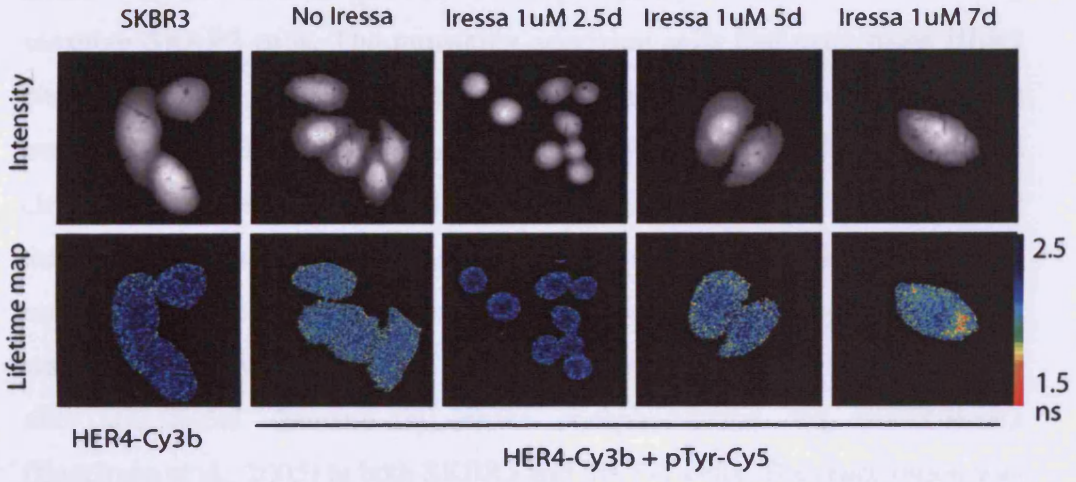

Figure 4.12: Iressa induces proteolytic cleavage of HER4 only during acute setting in SKBR3. **A,** SKBR3 cells were incubated with either donor alone (HER4-Cy3b) or donor and acceptor (HER4-Cy3b+pHER4-Cy5) to assess HER4 proteolytic cleavage by FRET after pretreated with different durations of 1 μM Iressa. **B,** The lifetime maps of HER4-Cy3b in SKBR3 cells using pseudocolour to represent data in A.

4.2.7 Prolonged Iressa treatment caused reactivation of phospho-HER3

Iressa has been shown to inhibit the PI3K/PKB pathway via HER3 (Engelman et al., 2005). Figure 4.6B showed the rapid decrease of phospho-HER3 and phospho-PKB (Ser473) upon acute treatment of Iressa through inhibition of EGFR/HER3 (Anido et al., 2003; Engelman et al., 2005). However, acute treatment of Iressa induced the release of heregulin in both MCF-7 and SKBR3 causing dimerisation of HER2 and HER4 (Figure 4.7 and 4.8). Since heregulin is the ligand for HER3 and HER4, it was thought that acute Iressa treatment may have induced dimerisation of HER2/HER3 as well as HER2/HER4, causing HER2 phosphorylation. Figure 4.13A shows that Iressa was not able to abolish HER2 phosphorylation even in surviving sensitive SKBR3 cells. The remaining surviving cells had even more HER2 phosphorylation compared to basal condition after seven days of Iressa treatment ($p=0.03$) (Figure 4.13A). Since in SKBR3 cells the activation and cleavage of HER4 decreased with prolonged Iressa treatment, it was postulated that the persistent HER2 phosphorylation after seven days of Iressa treatment maybe due to HER2/HER3 dimerisation. Figure 4.13B shows phospho-HER3 was reactivated with prolonged Iressa treatment. The reactivation occurred after the initial decrease in HER3 phosphorylation via EGFR/HER3 (Engelman et al., 2005) in both SKBR3 and MCF-7 cells. The reactivation was not due to the degradation of the drugs since the dose of Iressa was replenished after a few days. There was also a recovery of downstream signalling pathways phospho-PKB (Ser473) and phospho-ERK1/2 within 48 hours (Figure 4.13 B), consistent with activation of alternative HER pathways via the ligands including HER2/HER3 and HER2/HER4.

In summary, the results showed that EGFR inhibition by AG 1478 and Iressa treatment induced the release of multiple ligands including heregulin and betacellulin, which caused cleavage of HER4 and dimerisation of HER2/HER4. However the release of heregulin also caused activation of HER3 and PKB phosphorylation via the HER2/HER3 dimerisation after the

initial inhibition of PKB activation via EGFR/HER3 (Engelman et al., 2005). The release of these ligands mediates primary resistance in MCF-7 cells. In sensitive SKBR3 cells although there is a decrease of HER4 cleavage with prolonged Iressa treatment, the reactivation of phospho-HER3 may mediate secondary resistance to Iressa.

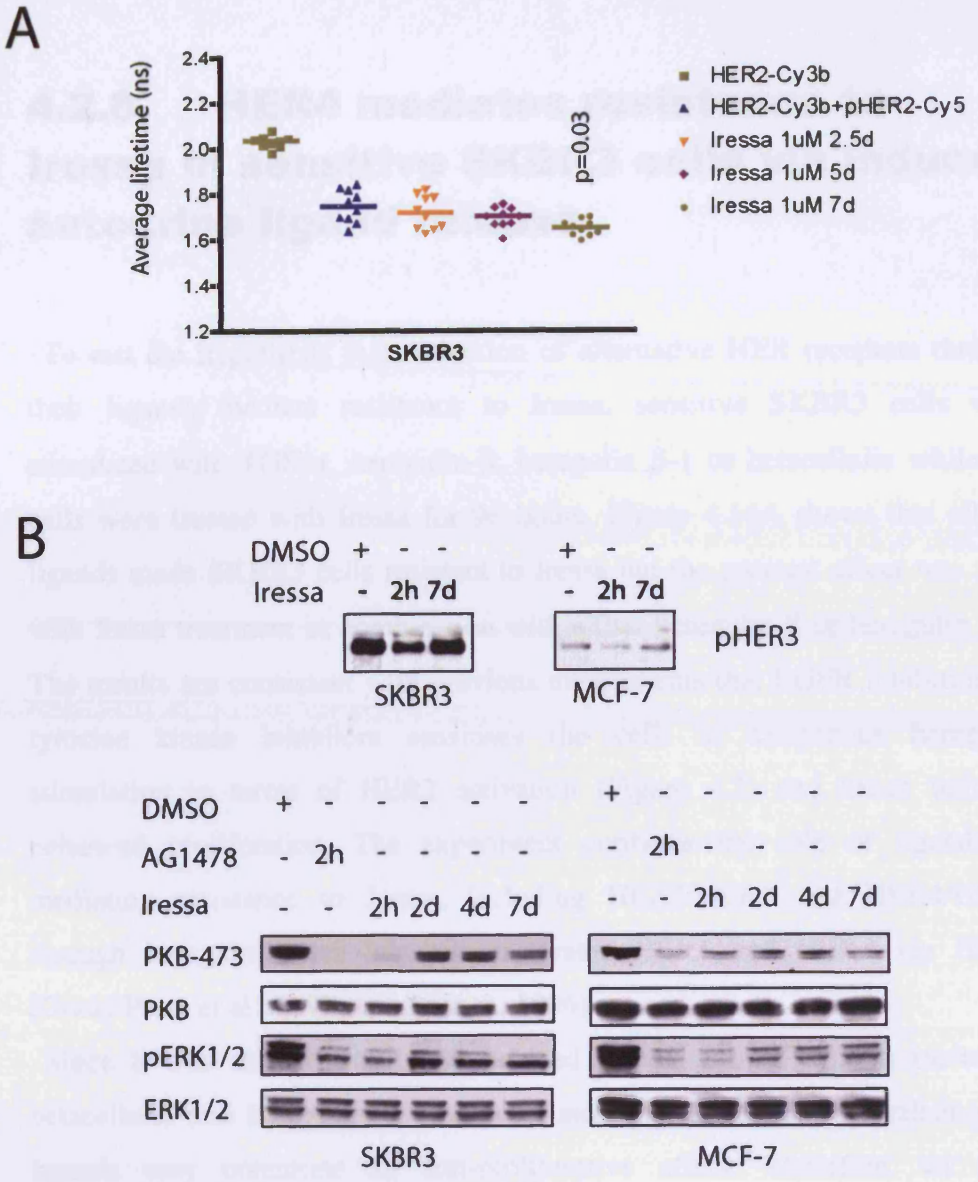

Figure 4.13: Reactivation of HER3 causes persistent HER2 phosphorylation and reactivation of downstream signalling pathways in SKBR3 cells. A, SKBR3 cells were incubated with suitable antibodies to assess HER2 phosphorylation after the cells were treated with 1 μM Iressa for different durations. **B,** In the upper panel, SKBR3 and MCF-7 cells were lysed after treated with either DMSO or Iressa as illustrated for western blot analysis. The phosphorylation of HER3 on Tyr 1289 was determined using phosphospecific antibodies. In the lower panels, the cells were lysed after treated with either DMSO, AG 1478 or Iressa as illustrated. PKB on Ser 473 and MAPK on Thr202/Tyr 204 and the total levels of PKB and ERK1/2 were assessed by western blot using appropriate antibodies.

4.2.8 HER4 mediates resistance to Iressa in sensitive SKBR3 cells via induced autocrine ligand release

To test the hypothesis that activation of alternative HER receptors through their ligands mediate resistance to Iressa, sensitive SKBR3 cells were stimulated with TGF-α, heregulin-β, heregulin β-1 or betacellulin while the cells were treated with Iressa for 96 hours. Figure 4.14A shows that all the ligands made SKBR3 cells resistant to Iressa but the greatest effect was seen with Iressa treatment in combination with either heregulin β or heregulin β-1. The results are consistent with previous experiments that EGFR inhibition by tyrosine kinase inhibitors sensitises the cells to exogenous heregulin stimulation in terms of HER2 activation (Figure 4.2) and hence induced enhanced proliferation. The experiment confirms the role of ligands in mediating resistance to Iressa, including HER3/HER2 and HER4/HER2 through heregulin since heregulin activates HER3 and HER4 via HER2 (Graus-Porta et al., 1997; Lewis et al., 1996).

Since it was shown that Iressa induced the release of ligands including betacellulin and heregulin, it was postulated that antibodies neutralising the ligands may potentiate an anti-proliferative effect. Therefore, an anti-betacellulin antibody (which blocks the effects of betacellulin) was used in combination with Iressa and it was determined that it potentiated the effect of Iressa in an anti-proliferative manner (Figure 4.14B). In summary, HER4 may mediate resistance to Iressa via induced autocrine ligand release.

A

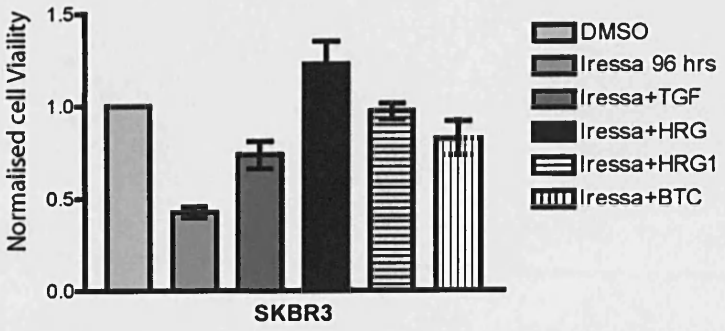

B

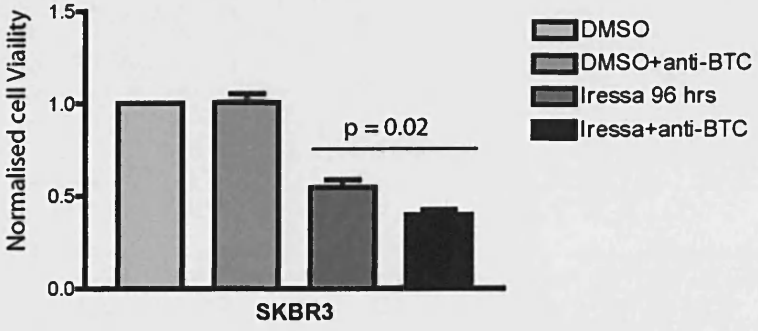

Figure 4.14: Ligands mediate resistance in SKBR3 cells. A, SKBR3 cells were grown in 24-well plates after seeding approximately 25000 cells per well. The cells were left to grow for at least 24 hours before treated with either DMSO (1:1000); Iressa 1 μM alone; or stimulated with either 100 ng/ml TGF, 100 ng/ml heregulin beta, 100 ng/ml heregulin beta-1 or 20 ng/ml betacelluin while pre-treated with Iressa 1 μM. The viable cells were counted in cell viability analyzer after 96 hours using Trypan blue to stain the dead cells. **B,** SKBR3 cells were left to grow in 24 well plate for at least 24 hours before treated with either DMSO or Iressa alone or Iressa in combination with 20 μg/ml anti-betacellulin.

4.2.9 Combined therapy with Iressa and Herceptin is additive in SKBR3

It has been shown that the combined treatment with Herceptin and Iressa in SKBR3 was either additive (Moasser et al., 2001) or synergistic (Normanno et al., 2002) in exerting anti-proliferative effects as well as having enhanced antitumour activity in BT-474 xenografts (Britten, 2004; Moulder et al., 2001). The cell viability experiments confirmed that the combined treatment was more prominent in its anti-proliferative effect than either Iressa or Herceptin treatment alone (Figure 4.15A). FRET was used to assess the effect of combined therapy on EGFR and HER2 phosphorylation in sensitive cells. Figure 4.15B shows the decrease of average lifetime of EGFR-Cy3b with pEGFR-Cy5 from 2.45ns to 2.15ns, indicating basal phosphorylation of EGFR in these cells. Pre-treatment with 1μM Iressa partially suppressed EGFR phosphorylation with the increase of the average lifetime of EGFR-Cy3b from 2.15 ns to 2.3 ns ($p < 0.001$ compared to basal). The incomplete suppression of EGFR phosphorylation by Iressa may be explained by the compensated increase in ligand release (including betacellullin production) induced by Iressa (Figure 4.8). However, combination of 1μM Iressa with 40 μg/ml of Herceptin suppressed EGFR phosphorylation ($p<0.001$ compared to basal) (Figure 4.15B). This result depicts the additive effect of combined therapy in the cell viability experiments (Figure 4.15A). The assessment of HER2 phosphorylation by FRET shows that HER2 phosphorylation increased from basal levels during the first 2.5 days of treatment. However, after five days of treatment we observed a decrease of HER2 phosphorylation (increase in average lifetime of donor HER2-Cy3b), in concordance with an enhanced anti-proliferative effect (Figure 4.15C). And after 7 days of treatment, there are very few cells remaining for FRET analysis.

In summary, combined treatment of cells with Herceptin and Iressa exerts a greater suppression in EGFR and HER2 phosphorylation and induced an enhanced anti-proliferative effect.

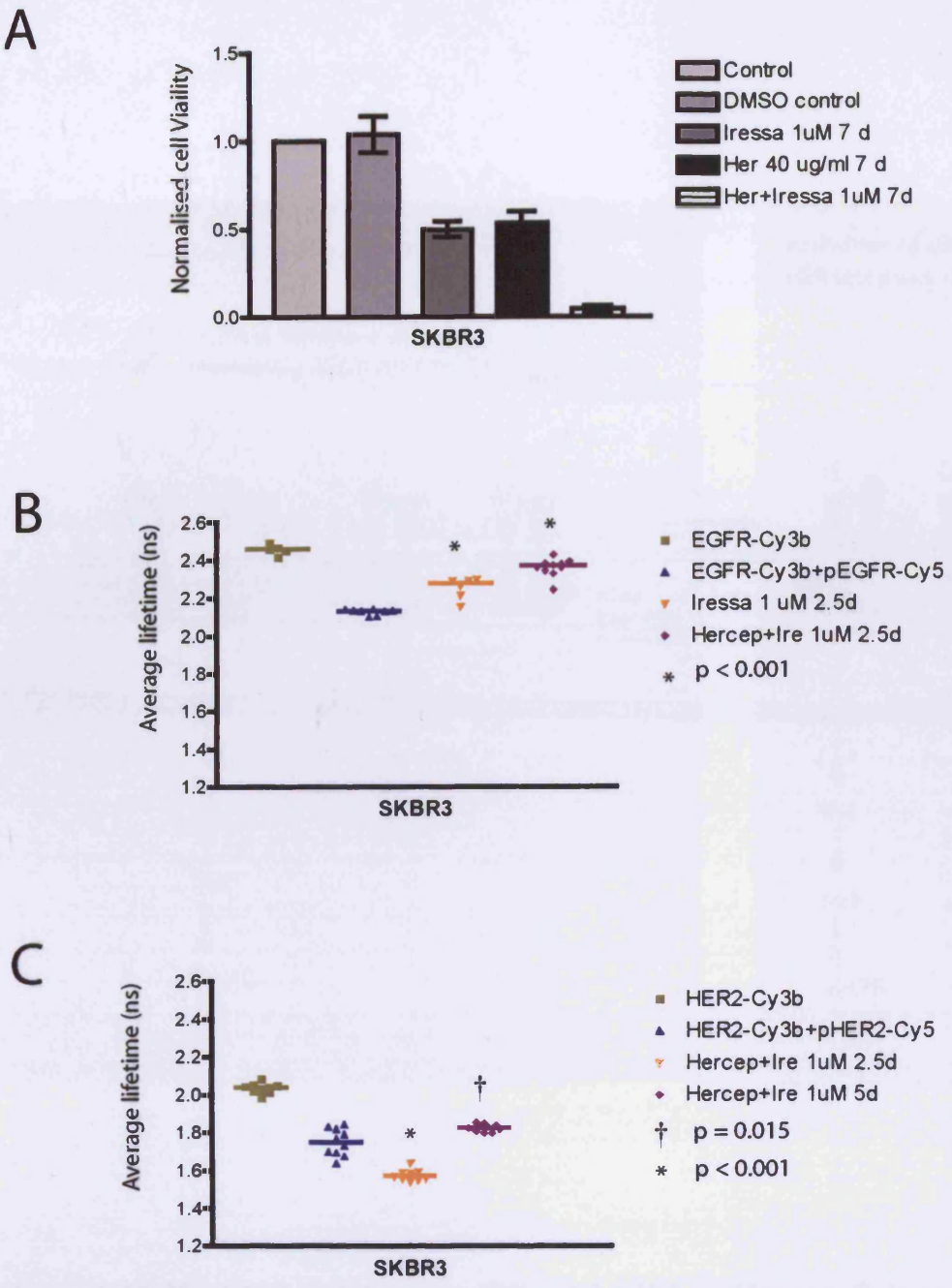

Figure 4.15: Combined therapy of Iressa and Herceptin is additive. A, SKBR3 cells were grown in 24-well plate and left to grow for at least 24 hours before treated with either DMSO or Iressa 1 μM or Iressa 1 μM with Herceptin 40 μg/ml for 7 days. The viable cells were counted in Cell viability analyzer using Trypan blue to stain the dead cells. after seven days of treatment. **B,** SKBR3 were pre-treated with either Iressa 1 μM or combined treatment of Herceptin 40 μg/ml and Iressa 1 μM different durations to assess EGFR phosphorylation by FRET. **C,** After pre-treated the SKBR3 cells with different durations of 40 μg/ml Herceptin and 1 μM Iressa, the cells were incubated with suitable pairs of antibodies to assess either HER2 phosphorylation of by FRET.

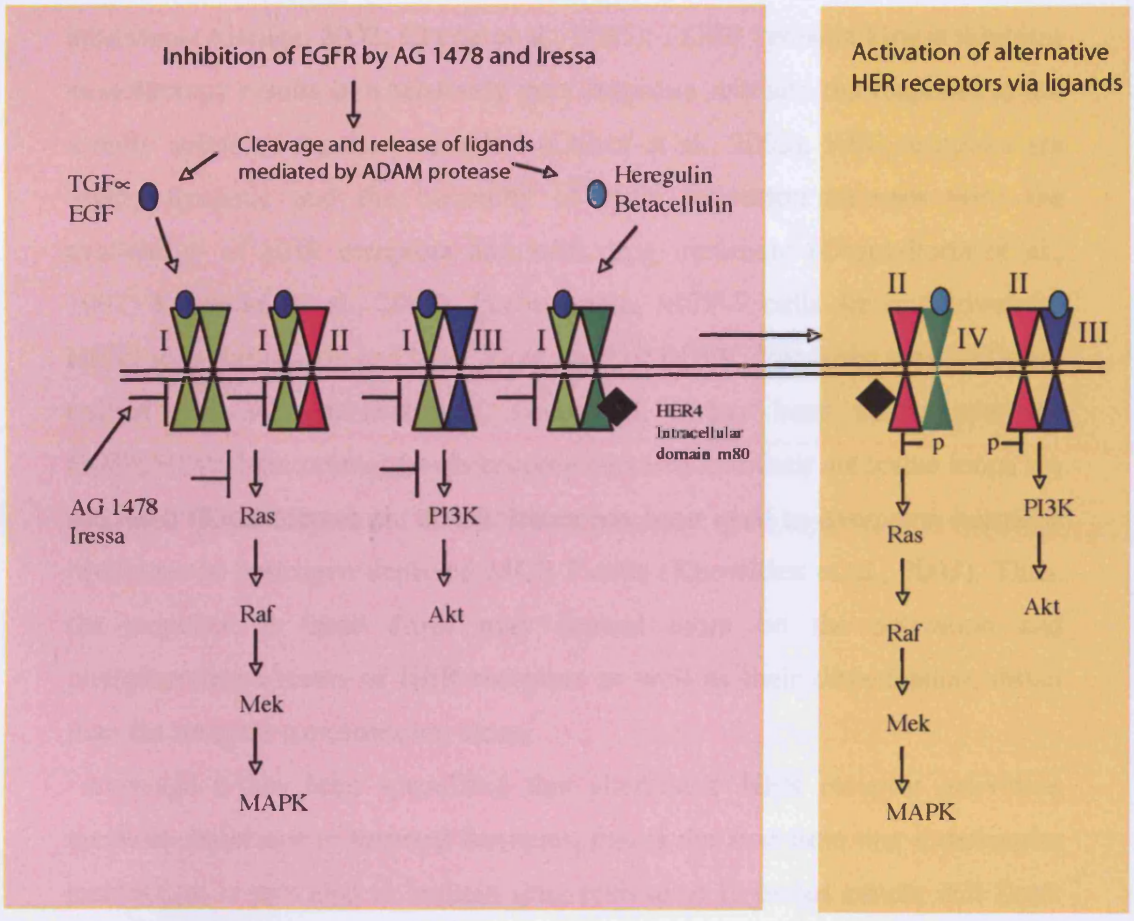

Figure 4.16: Model of resistance to TKIs, AG 1478 and Iressa. Quinazoline tyrosine kinase inhibitors of EGFR have been shown to induce inactive EGFR homodimers, EGFR/HER2 dimer as well as inhibiting EGFR/HER3 dimers, resulting in a decrease in PKB and MAPK activities. However, the inhibition of EGFR activation by AG 1478 and Iressa caused the release of various ligands including heregulin and betacellulin, resulting in HER4 activation and proteolytic cleavage with dimerisation between HER2 and HER4. Moreover, the heregulin release also reactivated HER3 via HER2/HER3 dimers and downstream signalling pathways after the initial decrease of HER3 activation via EGFR/HER3 dimerisation.

4.3 Discussion

The EGFR receptor concentration does not predict the response to EGFR inhibitors (Arteaga, 2002; Chung et al., 2005); EGFR tyrosine kinase inhibitor monotherapy results in a relatively poor response rate and the response is not usually sustained for the responders (Cohen et al., 2003). HER receptors are highly dynamic and the hierarchy of their activation changes with the availability of HER receptors and with drug treatment (Graus-Porta et al., 1997; Knowlden et al., 2003). For example, MCF-7 cells are not driven by HER2 over-expression and have a low level of EGFR. Yet when these cells are treated with the anti-oestrogen, tamoxifen, it has been shown that the EGFR/HER2 heterodimer levels become elevated and their autocrine loops are activated (Knowlden et al., 2003). Iressa has been used to overcome hormone resistance in oestrogen deprived MCF-7 cells (Knowlden et al., 2003). Thus, the response to these drugs may depend more on the activation and phosphorylation status of HER receptors as well as their dimerisation, rather than the receptor concentration alone.

Although it has been speculated that alternative HER receptor activation mediates resistance to targeted therapies, this is the first time that a molecular mechanism is provided to explain drug resistance in breast cancer cell lines. Quinazoline tyrosine kinase inhibitors of EGFR have been shown to induce inactive EGFR homodimers and EGFR/HER2 dimers in EGFR over-expressing cancer cells (Arteaga et al., 1997) as well as inhibits EGFR/HER3 dimers (Engelman et al., 2005). However here, the inhibition of EGFR activation by AG 1478 and Iressa caused the release of various ligands including heregulin and betacellulin. The release of these ligands resulted in dimerisation between HER2 and HER4, and proteolytic cleavage of HER4. Moreover, the heregulin release also reactivated HER3 via HER2/HER3 dimers and downstream signalling pathways after the initial decrease of HER3 activation via EGFR/HER3 dimerisation. These processes offer an explanation for the primary resistance to Iressa in MCF-7 breast cell lines. In Iressa sensitive SKBR3 cells, although there is evidence to suggest that HER2 and HER4 dimerisation decreases with prolonged Iressa treatment, alternative HER

activation including HER2/HER3 dimers may mediate secondary resistance to Iressa, despite the initial anti-proliferative effect from the inhibition of EGFR homodimers, EGFR/HER2 and EGFR/HER3. The model of resistance to Iressa is shown in Figure 4.16.

The current literature seems to suggest that HER2 phosphorylation is abolished by TKIs in HER2 over-expressing breast cancer cell lines (Anido et al., 2003; Moasser et al., 2001). The study presented here does not contradict the current literature, rather the FRET provides a novel insight into the present knowledge of HER receptor activation. FRET has the unique ability to specifically monitor the phosphorylation status of proteins at the single cell level. For example, it can often detect HER2 phosphorylation in individual cells even when the HER2 phosphorylation signal is below the detection limits of western blot. In cell lines which are sensitive to Iressa, chronic Iressa treatment may actually cause down-regulation of EGFR and HER2 levels and thus HER2 phosphorylation maybe below detection limit of western analysis for the whole cell lysate even though HER2 remains activated in the individual cells and may be monitored by FRET. The apparent difference from the current literature is also more an issue of different experimental conditions of EGFR inhibitor treatments. For example, in Moasser et al (2001), the experiments on HER2 phosphorylation were a dose dependent study of Iressa on SKBR3 cells (Moasser et al., 2001). HER2 phosphorylation was only partially suppressed by 1 μM Iressa and only fully abolished when the dose was increased to 10 μM. Similar experiments were performed here but 10 μM drug was found to be toxic to cells in part through the vehicle.

In a recent paper by Zhou et al (2006) the authors found that among various genes examined in 44 different non-small cell lung cancer cell lines, only the expression of heregulin significantly correlated with insensitivity to Iressa (Zhou et al., 2006). Although HER3 expression was only very weakly correlated with Iressa sensitivity, the authors concluded that it is the heregulin-induced HER3 activation rather than the level causing insensitivity to Iressa (Zhou et al., 2006). It has been shown in this study that HER3 phosphorylation was suppressed by Iressa upon immediate treatment in three breast cancer cell lines as well as A431 cells through suppression of EGFR/HER3 dimerisation. However, the release of ligands (including heregulin and betacellulin) induced

by Iressa treatment resulted in dimerisation between HER4 and HER2 as well as HER3 and HER2. The effects of these dimerisations were the reactivation of phospho-HER3 and phospho-PKB (Ser473).

Sergina et al (2007) also observed the reactivation of phospho-HER3 with prolonged Iressa treatment (Sergina et al., 2007). The reactivation of HER3 may occur within several hours of Iressa treatment after the initial suppression of HER3 activation. The group explained that the reactivation of HER3 with prolonged Iressa treatment was due to a compensatory shift in the HER3 phosphorylation-dephosphorylation equilibrium as a result of increased HER3 expression and reduced phosphatase activity (Sergina et al., 2007) without giving consideration to the importance of ligand release. The results on activation of the alternative HER receptors have contributed to the gaps in understanding the mechanisms of resistance to these targeted therapies.

Although exogenous heregulin enhanced aggregation (Tan et al., 1999) and increased invasiveness in breast cell lines (Xu et al., 1997), it has been reported to have an anti-proliferative effect (Sartor et al., 2001) and thus may challenge the role of HER4 in mediating resistance to Iressa. Aguilar et al (1999) reported that some of the disparity on various effects of heregulin is due to variations in the cell lines, ligand dosage and the methodologies used between different investigators (Aguilar et al., 1999). The group found no evidence that heregulin had any growth-inhibitory effects in human epithelial cells after using several different *in vitro* and *in vivo* assays in nine different cell lines. The study presented here has also shown that exogenous heregulin induced proliferation rather than exerting an anti-proliferative effect upon Iressa treatment, confirming the role of heregulin in mediating resistance to tyrosine kinase inhibitors of EGFR. Moreover, the role of HER4 in mediating resistance to Iressa was confirmed since anti-betacellulin antibody potentiated the anti-proliferative effect in combination with Iressa treatment.

The combined therapy of Herceptin and Iressa is additive in suppression of EGFR and HER2 phosphorylation as well as exerting its anti-proliferative effect, consistent with the report that a combination of targeted therapies against both EGFR and HER2 is more effective that single agents in breast cancer (Normanno et al., 2002). There are other signalling pathways such as VEGF that are independent but interrelated to EGFR. For instance EGF and

TGF-α both induce VEGF expression but EGFR inhibition does not block VEGF and tumour angiogenesis is maintained (Tabernero, 2007). VEGF upregulation may contribute to resistance to EGFR inhibition and both pre-clinical and clinical studies have confirmed the additive effects of VEGF and EGFR inhibitors. This example also presents a rationale for using combined therapies for cancer patients (Ciardiello et al., 2006; Tabernero, 2007). The results here indicate how apparent targeted therapies for breast cancer patients have complex effects, offering treatment opportunities to overcome resistance in patients. It is anticipated that future therapy for breast cancer may involve targeting various HER receptors, their ligands (Zhou et al., 2006) as well as metalloproteinases that mediate the cleavage of the ligands (Fridman et al., 2007).

5 TACE-mediated ligand release induces activation of alternative HER receptors in response to Trastuzumab (Herceptin) treatment in breast cancer cells

5.1 Introduction

Herceptin, a humanised murine monoclonal antibody against HER2, is now used in the adjuvant treatment of breast cancer (Piccart-Gebhart et al., 2005; Romond et al., 2005). It binds to the domain IV of the juxtamembrane region of HER2 (Cho et al., 2003). As discussed in the Introduction (Section 1.5), there have been several proposals of mechanisms of Herceptin to explain its clinical benefits. These include HER2 receptor downregulation and inhibition of aberrant receptor tyrosine kinase activity (Cuello et al., 2001; Sliwkowski et al., 1999); activation of antibody-dependent cellular cytotoxicity (Clynes et al., 2000; Cooley et al., 1999); activation of pTEN (Nagata et al., 2004); inhibition of basal and activated HER2 ectodomain cleavage in breast cancer cells (Molina et al., 2001); increased $p27^{Kip1}$ levels and interaction with CDK2, resulting in decreased CDK2 activity (Lane et al., 2001). However, the exact mechanisms of action are still unknown. Moreover, the reasons why some patients are resistant and the responders eventually develop resistance to Herceptin have not been explained through experimental procedures.

Here using established FRET methods and western blot to assess phosphorylation status of HER receptors, the study assessed the change in activation status of all 4 HER receptors in relation to Herceptin treatment in breast cancer cell lines.

5.2 Results

5.2.1 The effects of Herceptin on HER2 receptors and phosphorylation status in SKBR3 cells

In the previous chapter, it was shown that Iressa failed to diminish HER2 phosphorylation due to activation of alternative HER3 and HER4 receptors via various ligands. Since Herceptin targets the HER2 receptor, it was decided to investigate whether Herceptin would abolish HER2 phosphorylation in SKBR3 cells. Assessing HER2 phosphorylation by FRET, the decrease of average lifetime of HER2-Cy3b with pHER2-Cy5 from 2.15 ns to 1.5ns indicates the basal phosphorylation of HER2 in SKBR3 (Figure 5.1A). After two days of Herceptin treatment, there was suppression of HER2 phosphorylation (increase of average lifetime) with an increase in its median compared to basal phosphorylation ($p=0.03$) but the difference was not significant after five days. There was however a considerable amount of heterogeneity between cells, with suppression of HER2 phosphorylation in some cells (yellow box) although the phosphorylation of HER2 was maintained in the majority of cells (Figure 5.1A). After 10 days of Herceptin treatment, the remaining treated surviving cells still had persistent HER2 phosphorylation (Figure 5.1A). The heterogeneity of responses to Herceptin shown in Figure 5.1A was presented as lifetime maps of HER2-Cy3b in SKBR3 cells using pseudocolour; some cells showed reversal of HER2 phosphorylation (indicated by blue colour) and paradoxically in other cells HER2 phosphorylation was increased (indicated by red colour) and two examples of each condition are shown in the Figure 5.1B. The inability of Herceptin to abolish HER2 phosphorylation after 10 days of Herceptin treatment was also confirmed by western blot despite the effect on the viability of SKBR3 cells (Figure 5.2A and 5.2B). However, after 10 days treatment of

SKBR3 cells with Herceptin, the HER2 receptors were downregulated (Figure 5.2B).

In summary, the results showed that although Herceptin downregulated HER2 receptors in HER2 over-expressing SKBR3 breast cancer cells, the remaining surviving cells had persistent HER2 phosphorylation. The downregulation of HER2 receptors would result in the decrease of HER2 homodimers which are known to cause ligand independent activation in these cells (Worthylake et al., 1999). Therefore, the continued HER2 phosphorylation in these cells would imply that HER2 phosphorylation may be maintained by other HER receptors, e.g. EGFR/HER2, HER3/HER2 and HER4/HER2 since Herceptin binds to HER2 receptors without affecting their dimerisation with other HER receptors.

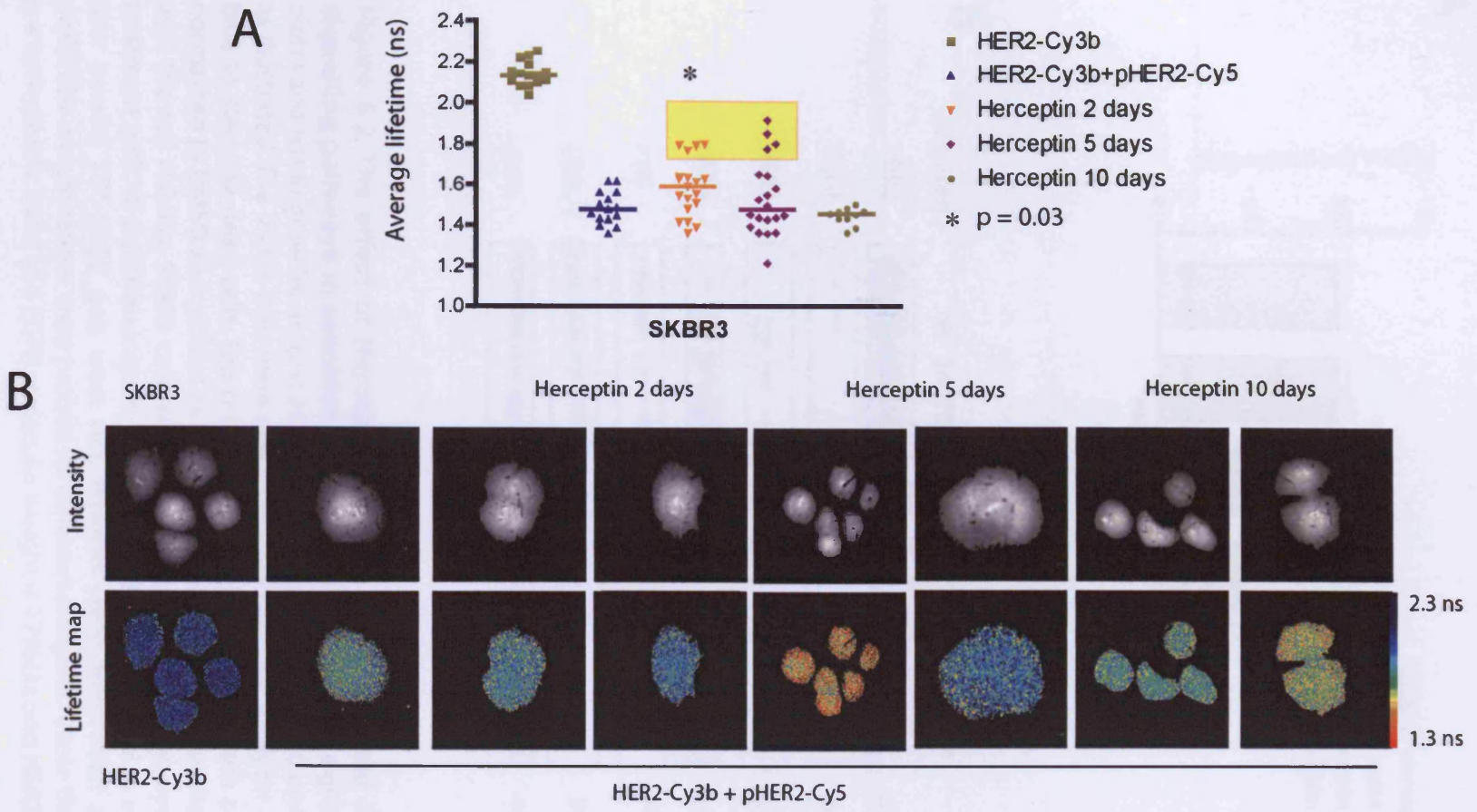

Figure 5.1: Effect of Herceptin on HER2 phosphorylation by FRET. A, SKBR3 cells were incubated with suitable pair of antibodies to assess HER2 phosphorylation by FRET after pretreated with 40 µg/ml Herceptin as illustrated. **B,** The lifetime maps of HER2-Cy3b in SKBR3 cells using pseudocolour. Two examples of different HER2 responses induced by Herceptin are shown in the diagrams.

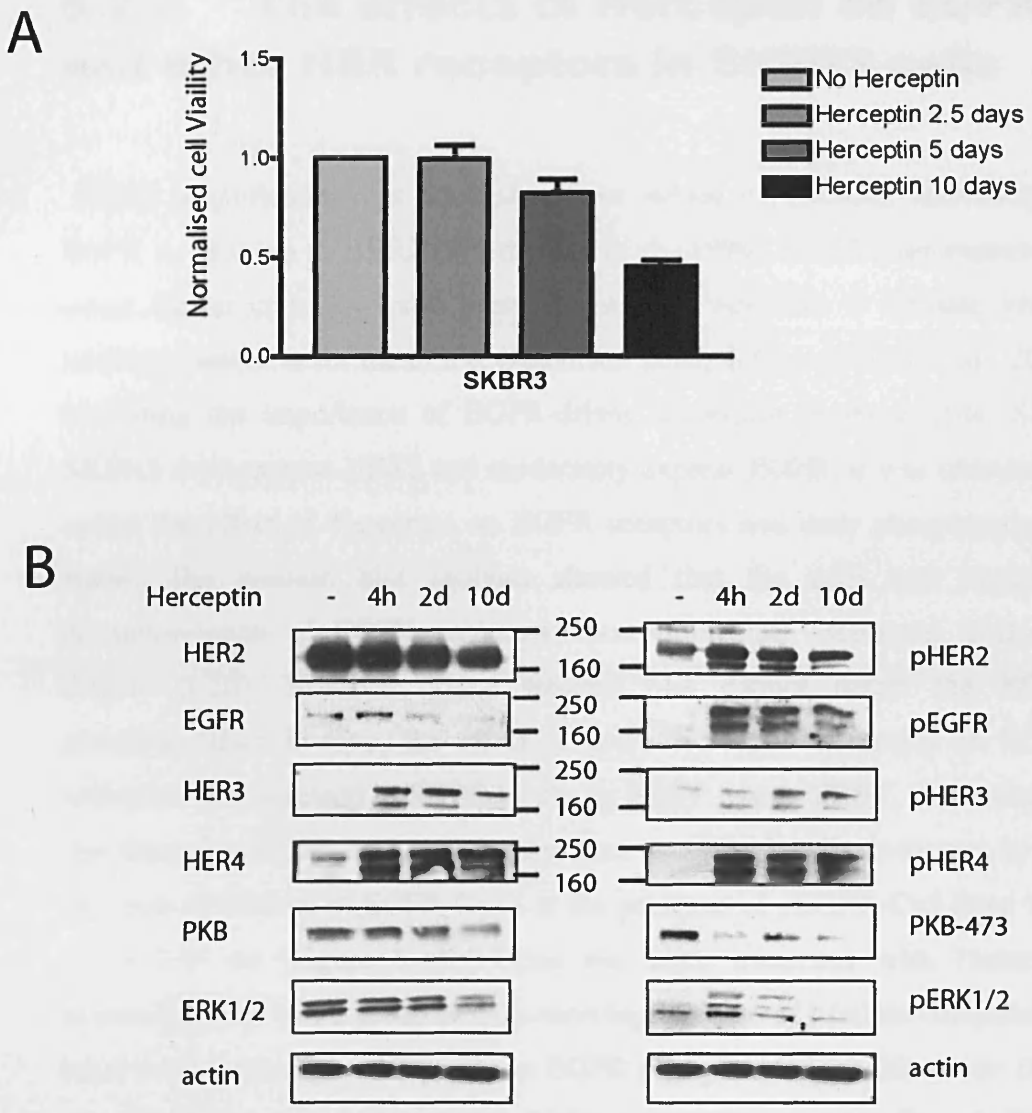

Figure 5.2: The effect of Herceptin on HER receptors and downstream signalling pathways in sensitive SKBR3. A, SKBR3 cells were grown in 24-well plates and left to grow for at least 24 hours before treated with 40 µg/ml Herceptin as illustrated. The viable cells were counted in cell viability analyzer using Trypan Blue to stain the dead cells. The proportion of viable cells in each condition was normalised to DMSO and plotted as bar chart above **B,** In the parallel experiment with the cell viability, SKBR3 cells were lysed for western blot analysis after pre-treatment with 40 µg/ml Herceptin. 10 ng of protein was loaded in each lane and four parallel SDS-PAGE gels were run. Proteins were transferred and different molecular weight ranges were probed for different antigens. (Note that at 160 kDa is a non-specific band and EGFR molecular weight is 175kDa and HER2 is 185 kDa).

5.2.2 The effects of Herceptin on EGFR and other HER receptors in SKBR3 cells

HER2 amplification has been shown to induce constitutive activation of EGFR in addition to HER2 (Worthylake et al., 1999). HER2 over-expressing breast cancer cells have also been shown to be sensitive to tyrosine kinase inhibitors selective for the EGFR (Anderson et al., 2001; Moulder et al., 2001) indicating the importance of EGFR-driven activation in these cells. Since SKBR3 over-express HER2 and moderately express EGFR, it was intended to assess the effect of Herceptin on EGFR receptors and their phosphorylation status. The western blot analysis showed that the cells had increased phosphorylation of EGFR receptors upon immediate Herceptin treatment (Figure 5.2B). However, since western blot cannot detect the EGFR phosphorylation in vivo, the effect of acute Herceptin treatment on EGFR activation was assessed in SKBR3 cells by FRET. Using FRET, it was shown that there was EGFR basal phosphorylation in SKBR3 cells, indicated by the decrease of lifetime of EGFR-Cy3b in the presence of pEGFR-Cy5 from 2.45 ns to 2.15 ns (Figure 5.3A). Upon the acute treatment with Herceptin treatment, there was a group of cells showing increase of lifetime compared to basal level (indicative of decrease in EGFR phosphorylation). However, there was another group of cells where EGFR activation was not affected. These cells in fact had increased EGFR phosphorylation compared to basal level, suggesting that these cells were not affected by the inhibitory effect of HER2 by Herceptin. Long-term treatment of Herceptin downregulated EGFR to an undetectable level in western blot and this had occurred in concordance with downregulation of HER2 receptors and an effect on the cell viability (Figure 5.2A and 5.2B).

The western blot analysis also showed that there was increased activation of phospho-HER3 and phospho-HER4 (Figure 5.2B). In the previous chapter, it was shown that Iressa induced activation and proteolytic cleavage of HER4 as well as dimerisation of HER2/HER4. It was intended to assess whether Herceptin also induced similar processes in SKBR3. Using

immunoprecipitation it was demonstrated that there was an increased cleavage of HER4 as well as dimerisation between HER2 and HER4 induced by acute Herceptin treatment (Figure 5.3B). Using the established method to assess HER4 cleavage by FERT, it was shown that Herceptin induced the cleavage of HER4 indicated by increase of lifetime of HER4-Cy3b, which persisted over 1 week treatment with Herceptin (Figure 5.3C).

In summary, the results showed that although Herceptin downregulated EGFR and HER2 receptors in SKBR3 which are known to have constitutive activation of EGFR and HER2, the phosphorylation of EGFR and HER2 was not abolished in the treated surviving cells. In addition, these cells have increased HER3 and HER4 levels. Furthermore, Herceptin induced the cleavage of HER4 as well as HER2/HER4 dimerisation in these cells.

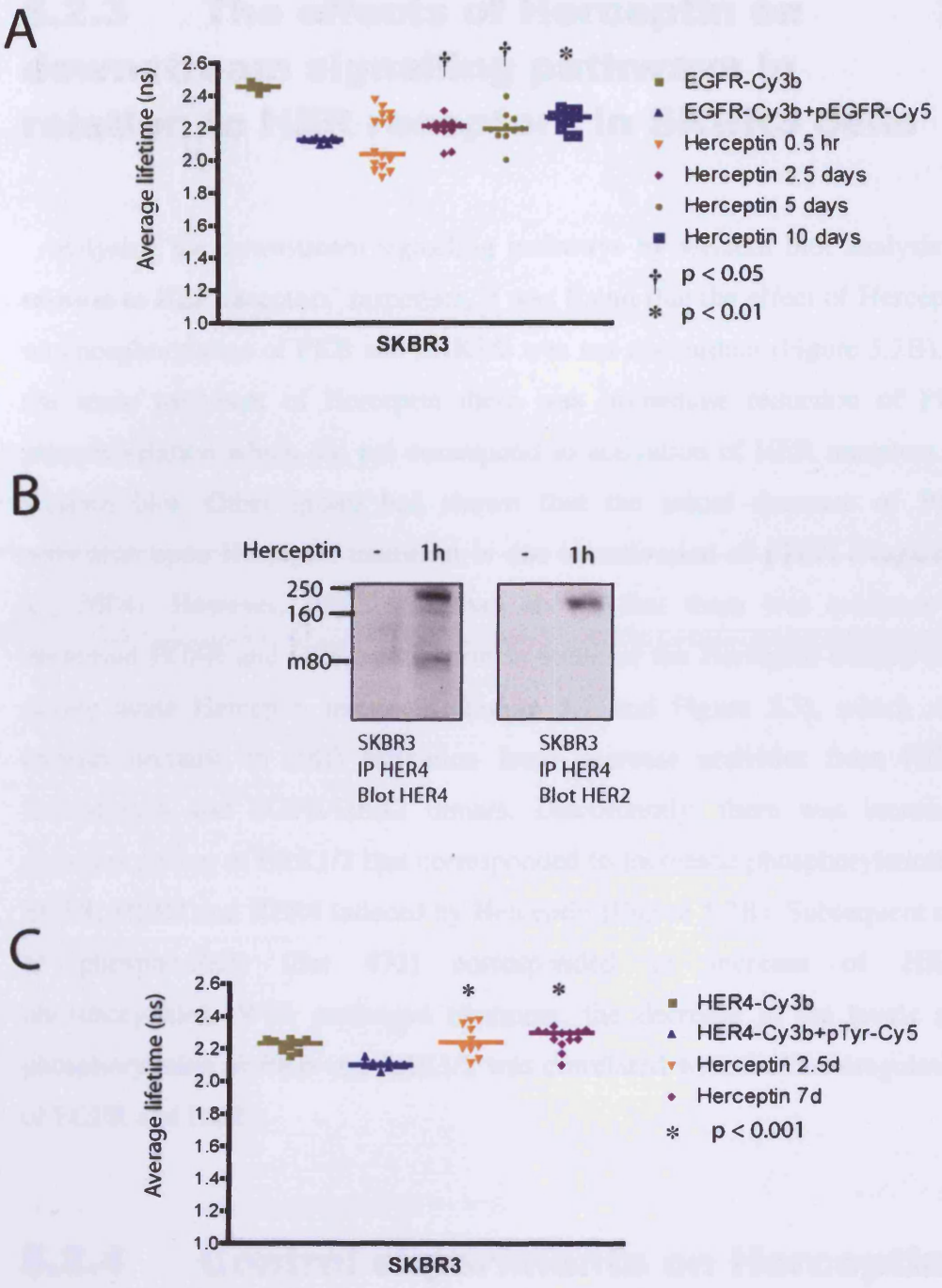

Figure 5.3: The effect of Herceptin on EGFR and HER4 activation/cleavage. A, SKBR3 cells were pretreated with different durations of 40 µg/ml Herceptin to assess EGFR phosphorylation by FRET. **B,** SKBR3 cells were immunoprecipitated with intracellular HER4 antibody. Following the immunoprecipitation, the cell lysate without the beads were loaded unto a SDS gel and a western blot analysis was performed. The membrane was probed with either anti-HER4 antibody (left panel) or anti-HER2 antibody (right panel). **C,** SKBR3 cells were pretreated with 40 µg/ml Herceptin as illustrated to assess HER4 cleavage by FRET.

5.2.3 The effects of Herceptin on downstream signalling pathways in relation to HER receptors in SKBR3 cells

Analysing the downstream signalling pathways by western blot analysis in relation to HER receptors' responses, it was found that the effect of Herceptin on phosphorylation of PKB and ERK1/2 was not concordant (Figure 5.2B). In the acute treatment of Herceptin there was immediate reduction of PKB phosphorylation which did not correspond to activation of HER receptors by western blot. Other group had shown that the initial decrease of PKB activation upon Herceptin treatment is due to activation of pTEN (Nagata et al., 2004). However, FRET data had shown that there was evidence of decreased EGFR and HER2 activation in some of the Herceptin treated cells during acute Herceptin treatment (Figure 5.1 and Figure 5.3), which may explain decrease in PKB activation from decrease activities from HER2 homodimers and EGFR/HER2 dimers. Discordantly, there was increased phosphorylation of ERK1/2 that corresponded to increased phosphorylation of EGFR, HER2 and HER4 induced by Herceptin (Figure 5.2B). Subsequent rise of phospho-PKB (Ser 473) corresponded to increase of HER3 phosphorylation. With prolonged treatment, the decrease in the levels and phosphorylation of PKB and ERK1/2 was correlated with the downregulation of EGFR and HER2.

5.2.4 Control experiments on Herceptin

The results from Section 5.2.1 to 5.2.3 have shown that Herceptin induced activation of all HER receptors and such mechanism may mediate its resistance in breast cell lines. To conclude such results, several control experiments were done to exclude other possibilities.

It was shown that the loss of pTEN predicts Herceptin resistance (Nagata et al., 2004). The study however did not find such evidence in SKBR3 and MCF-

7 cells (Figure 5.4A). Moreover, it was possible that the degradation of Herceptin would diminish its effect, resulting in its resistance in breast cell lines. To exclude the degradation of Herceptin over the treatment period, a western blot analysis was performed on the medium containing SKBR3 cells treated with 40 μg/ml Herceptin as well as medium containing 40 μg/ml Herceptin that was kept in incubator for up to 10 days. The medium was denatured in SDS and was loaded in SDS PAGE. The membrane was probed with monoclonal anti-human immunoglobulin antibody that recognizes the Fc component of Herceptin. The results showed that degradation of Herceptin did not happen for up to 10 days in the experiments (Figure 5.4B). As control, the effect of Herceptin on HER2 phosphorylation in normal breast cell line MCF-12F was also assessed. Even though Herceptin was unable to abolish HER2 phosphorylation in SKBR3 cells due to activation of alternative HER pathways, it caused almost complete reversal of HER2 phosphorylation (shown by increase of lifetime) in MCF-12F (Figure 5.4B).

These control experiments confirmed that the activation of HER receptors in SKBR3 cells seen in Section 5.2.1 to 5.2.3 was not due to loss of pTEN or degradation of drugs. Moreover, the inability for Herceptin to abolish HER2 phosphorylation was only seen in SKBR3 cells and not normal breast cells, MCF-12F.

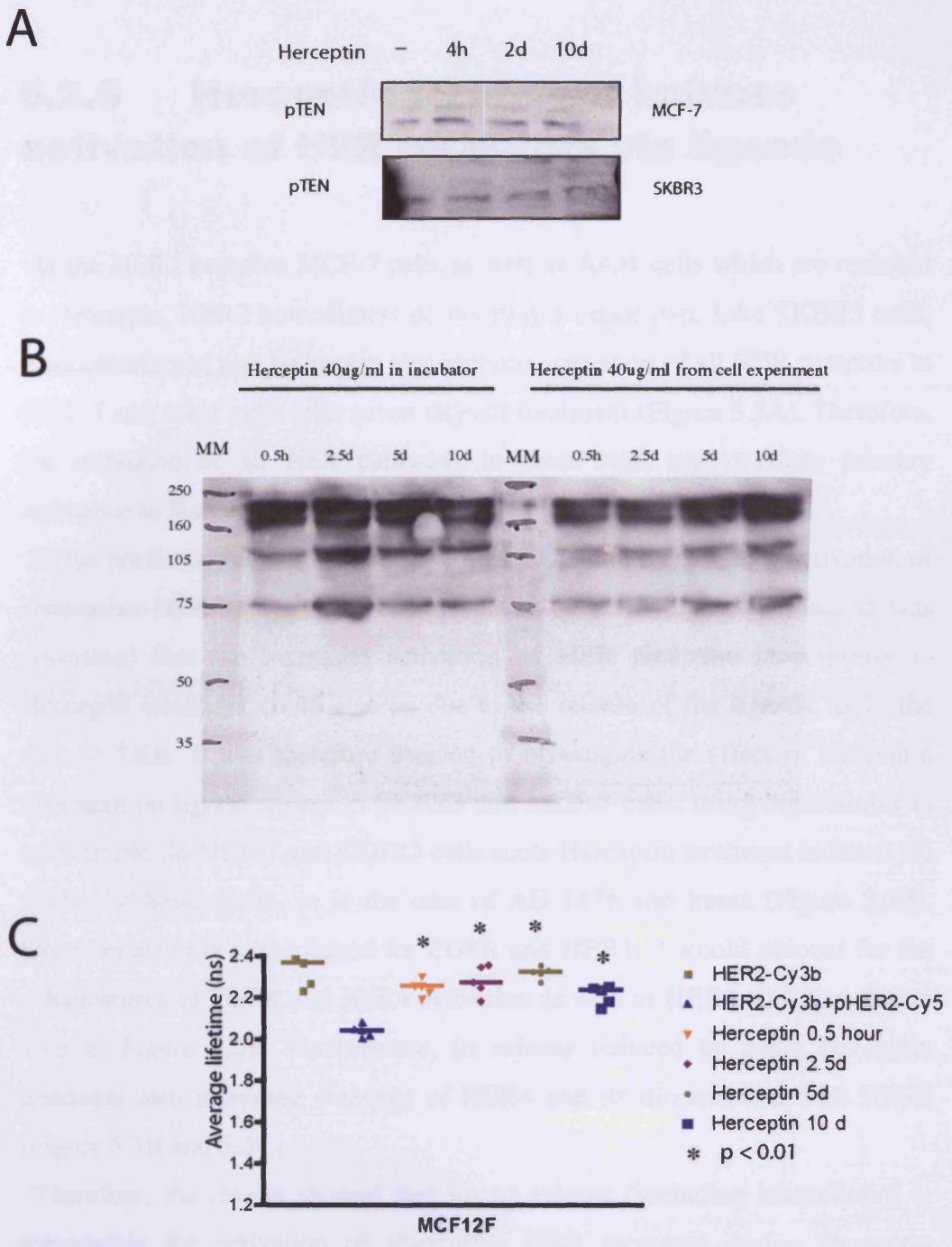

Figure 5.4: Control experiments of Herceptin. A, SKBR3 and MCF-7 cells were treated with 40 ug/ml Herceptin for different durations before the cells were lysed for western blot analysis and the membrane was blotted with anti-pTEN antibody. **B,** Western blot experiment using the medium from the SKBR3 cells treated with 40 mg/ml Herceptin as well as medium containing 40 mg/ml Herceptin that was kept in incubator for up to 10 days. The medium was denatured with SDS-PAGE and boiled for 10 minutes and 40µl was loaded in each lane of SDS-PAGE gel. The membrane was probed with monoclonal anti-human immunoglobulin antibody which recognizes the Fc component of Herceptin. **C,** MCF-12F were incubated with suitable pair of antibodies to assess HER2 phosphorylation by FRET after pretreated with different durations of 40 µg/ml Herceptin.

5.2.5 Herceptin treatment induces activation of HER receptors via ligands

In the HER2 negative MCF-7 cells as well as A431 cells which are resistant to Herceptin, HER2 homodimers do not play a major part. Like SKBR3 cells, it was confirmed that Herceptin also induced activation of all HER receptors in MCF-7 and A431 cells after seven days of treatment (Figure 5.5A). Therefore, the activation of all HER pathways in these cells may mediate primary resistance to Herceptin.

In the previous chapter, it was shown that TKIs treatment induce activation of alternative HER receptors in breast cancer cells via ligand release. It was postulated that the increased activation of HER receptors in response to Herceptin treatment could also be due to the release of the ligands, as in the case of TKIs. It was therefore decided to investigate the effect of Herceptin treatment on ligand release in SKBR3 and MCF-7 cells, using betacellulin as an example. In MCF-7 and SKBR3 cells acute Herceptin treatment induced the release of betacellulin, as in the case of AG 1478 and Iressa (Figure 5.5B). Since betacellulin is the ligand for EGFR and HER4, it would account for the enhancement of EGFR and HER4 activation as well as HER2 phosphorylation seen in Figure 5.2B. Furthermore, its release induced by acute Herceptin treatment also increased cleavage of HER4 and its dimerisation with HER2 (Figure 5.3B and 5.3C).

Therefore, the results showed that ligand release (including betacellulin) is responsible for activation of alternative HER receptors during Herceptin treatment in breast cancer cells, a similar process to the treatment with TKIs of EGFR. Despite its anti-viability effects, the activation of alternative HER receptors may mediate resistance to Herceptin in SKBR3 cells.

5.2.6 The release of ligands induced by Herceptin is mediated by TACE

The release of ligands from their membrane-anchored precursors (ectodomain shedding) has been shown to be mediated by TACE (Shirakabe et al., 2001; Sunnarborg et al., 2002). Since it was shown that Herceptin induces the activation of HER receptors via the release of their respective ligands, it was postulated that TACE inhibitors would decrease HER2 phosphorylation by inhibiting ligand release. Assessing HER2 phosphorylation by FRET, the decrease of average lifetime of HER2-Cy3b with pHER2-Cy5 indicates the basal phosphorylation of HER2 in SKBR3 cells and MCF-7 cells (Figure 5.6A and B). Acute Herceptin treatment did not reverse lifetime change in SKBR3 and MCF-7 cells (Figure 5.6A and B). However, with concurrent treatment of Herceptin and TAPI-1, there was increased suppression of HER2 phosphorylation (increase of average lifetime) with an increase in its median compared to basal phosphorylation in both SKBR3 and MCF-7 cells (Figure 5.6A and B).

The results therefore confirmed that the activation of HER receptors in response to Herceptin in breast cancer cells is due to TACE-mediated ligand release.

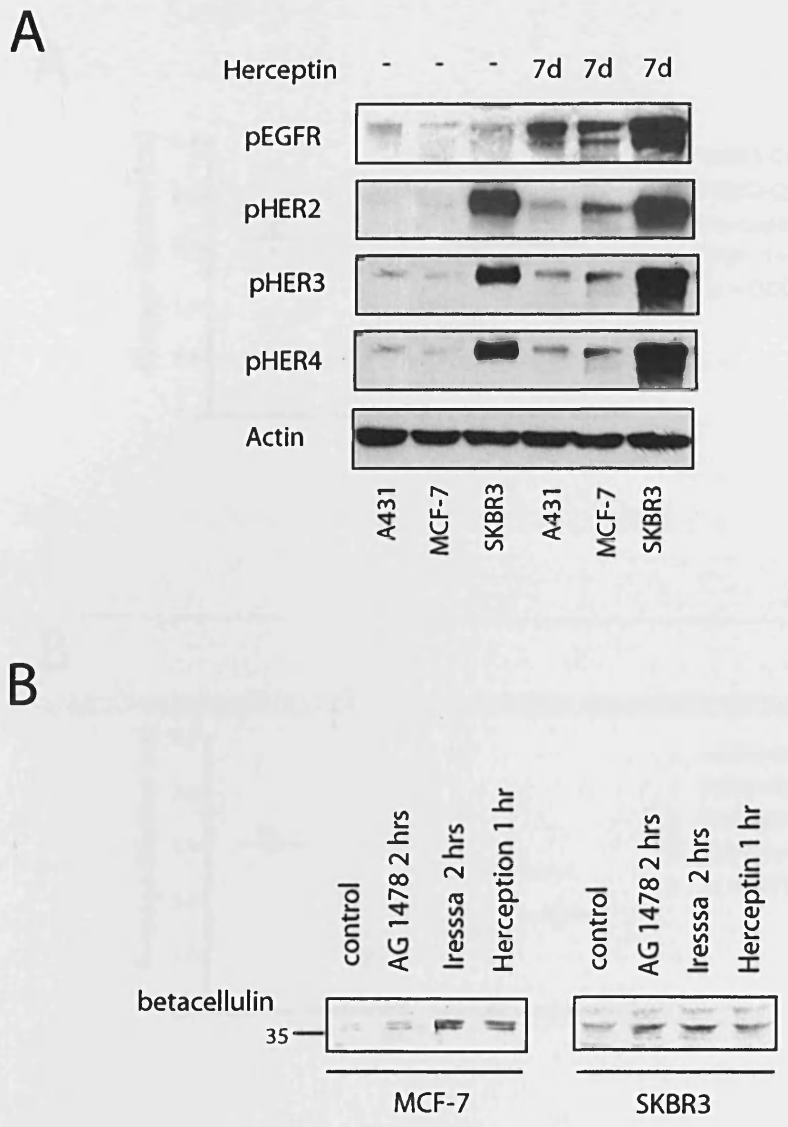

Figure 5.5: The effect of Herceptin on HER receptors and ligand release. **A,** A431 cells, MCF-7 and SKBR3 cells were treated with either nothing or 40 ug/ml Herceptin for 7 days before western blot analysis. The phosphorylation of EGFR on Tyr 845, HER2 on Tyr 1221/1222, HER3 on Tyr 1289 and HER4 on Tyr 1284 were assessed using appropriate antibodies. **B,** MCF-7 cells were pretreated with either 3 uM AG 1478 or 1 uM Iressa or 40 ug/ml Herceptin as illustrated before the cells were lysed for western blot experiment. The membrane was probed with anti-betacellulin antibody.

A

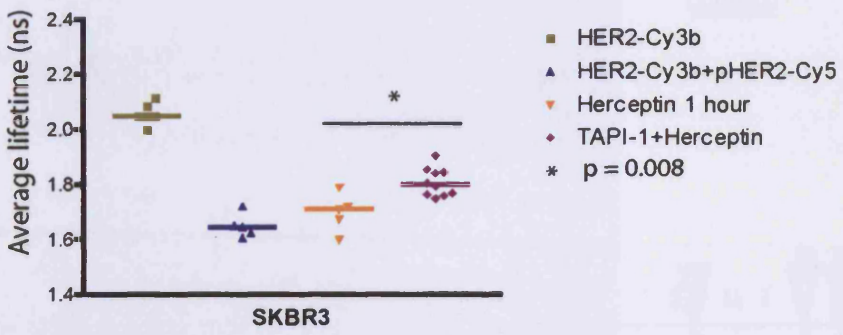

B

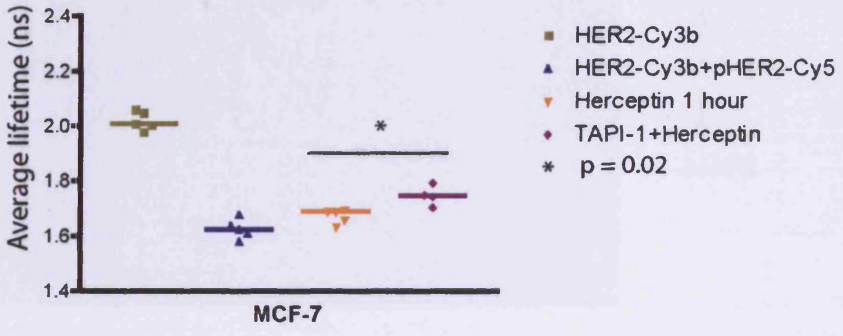

Figure 5.6 TACE inhibitor decreases HER2 phosphorylation maintained by activation of alternative HER receptors induced by Herceptin treatment. A and B, FRET experiments to assess HER2 phosphorytlation in SKBR3 and MCF-7cells. The cells were treated with 40 ug/ml Herceptin for 1 hour with or without TACE inhibitor (TAPI-1). The medians of the lifetimes were compared with the basal condition using Mann-Witney test and the significance value is denoted as *.

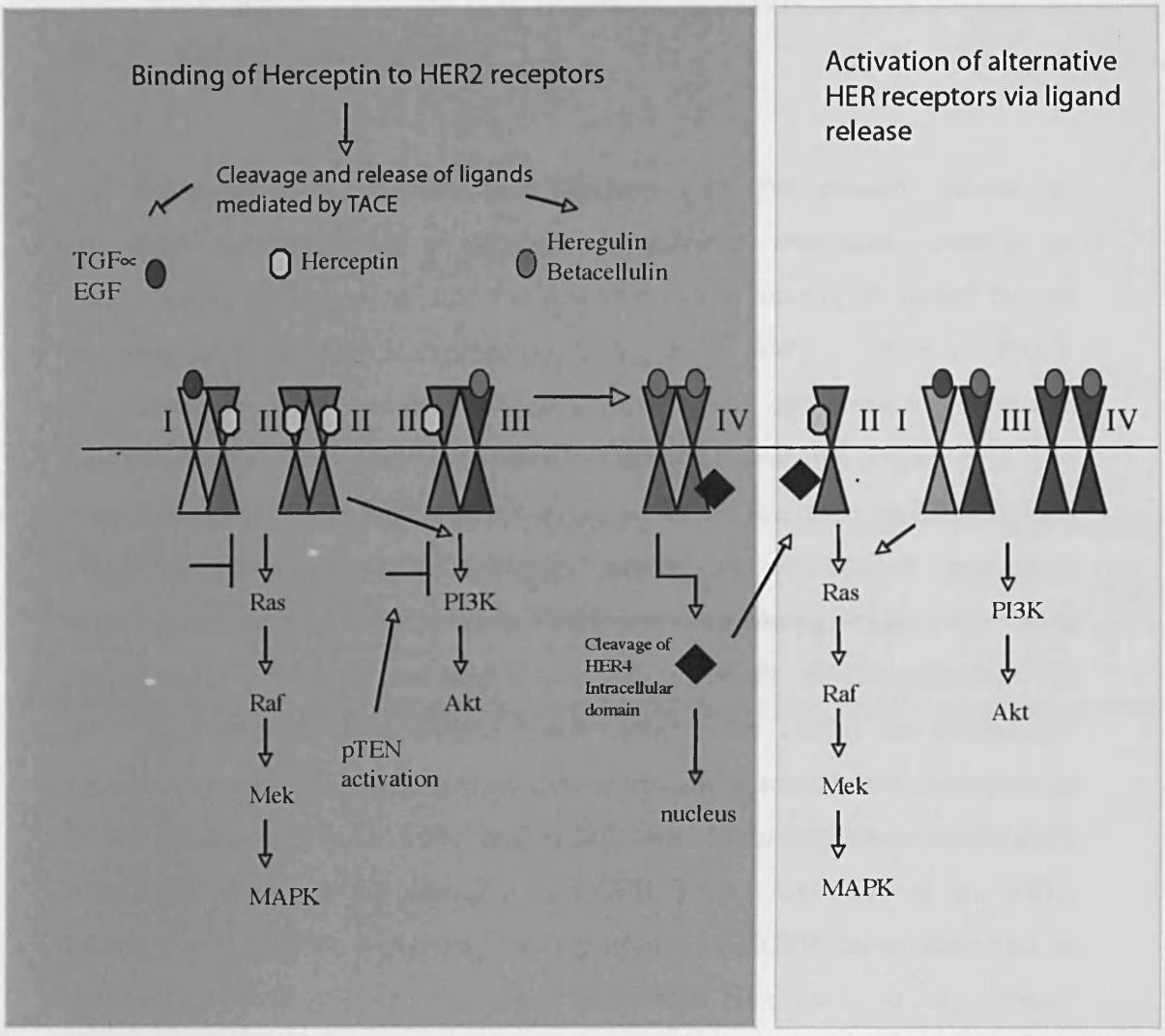

Figure 5.7: Herceptin (Trastuzumab) induces the activation of HER receptors via TACE mediated ligand release. Herceptin downregulates EGFR and HER2 receptors in HER2 over-expressing SKBR3 breast cancer cells with decreased EGFR and HER2 activation in some cells (most likely through an effect on HER2 homodimers or EGFR/HER2 dimers). However, the treated cells have increased total HER3 and HER4 protein with increased phosphorylation of all HER receptors, suggesting the activation of these receptors via alternative dimers in the surviving cells, e.g. EGFR/HER3 and HER3/HER4 as well as HER4 cleavage and HER2/HER4 dimers. The increased activation of all HER receptors is due to TACE-mediated ligand release. In the acute Herceptin treatment, an immediate reduction of PKB phosphorylation has been shown to be due to activation of pTEN by other group. However, it may also be due to decreased activation from EGFR/HER2 or HER2/HER2 dimers. Discordantly, Herceptin increases ERK1/2 phosphorylation, corresponding to increased phosphorylation of EGFR, HER2 and HER4 receptors (and formation of alternative dimers including HER2/HER4 dimers) induced by Herceptin treatment. Subsequent rise of PKB phosphorylation corresponds to an increase of the HER3 phosphorylation induced by Herceptin treatment.

5.3 Discussion

As discussed in the Introduction (Section 1.1), the present criteria for Herceptin treatment based on receptor concentration treatment results in an unsatisfactory response rate and the response is not usually sustained for the responders for Herceptin monotherapy (Cohen et al., 2003; Vogel et al., 2002). The study here has presented evidence from breast cell lines to propose a model of how the secondary resistance to Herceptin develops (Figure 5.7). The results showed that Herceptin down-regulated HER2 receptors in SKBR3 cells consistent with report that Herceptin induces the endocytosis and down regulation of HER2 homodimers in HER2 over-expressing breast cancer cells (Menard et al., 2003). It was also shown that Herceptin downregulated EGFR in HER2 over-expressing SKBR3 breast cancer cells. This is not unpredicted since HER2 amplification has been shown to induce constitutive activation of EGFR (Worthylake et al., 1999) and HER2 over-expressing breast cancer cells have been shown to be sensitive to EGFR TKIs (Anderson et al., 2001; Moulder et al., 2001), indicating the importance of EGFR driven activities in these cell. On the contrary to current belief that Herceptin reduces tyrosine kinase activity of HER2 and other HER receptors, western blot results showed that Herceptin treatment increased the activation of all HER receptors in SKBR3 cells despite the down-regulation of EGFR and HER2. However, analyzing the effects of Herceptin by FRET showed great heterogeneity between cells. There is evidence that Herceptin decreased EGFR and HER2 activation in some of these cells (probably through effect on HER2 homodimers or EGFR/HER2 dimers), correlated with decreased cell viability in Herceptin-treated SKBR3 cells. But overall, there was activation of EGFR and HER2 receptors despite the down-regulation of these receptors in the treated cells. Furthermore, the treated cells had increased total HER3 and HER4 protein with increased phosphorylation of all HER receptors. The increased activation of all HER receptors was found to be due to TACE mediated ligand release, consistent with report that unlike Pertuzumab, Herceptin does not prevent dimerisation of HER2 with other receptors (Agus

et al., 2002). The activation of downstream signalling pathways (Section 5.2.3) in relation to HER receptors is also illustrated in Figure 5.7. This model of secondary resistance to Herceptin explain why Herceptin as monotherapy is seldom tumouricidal despite a response in HER2 positive tumours since ligand mediated activation of other HER receptors through TACE will rescue the signalling pathway lost by HER2 homodimers or EGFR/HER2 dimers. The model is further supported by the fact that TACE inhibitor diminished persistent HER2 phosphorylation in surviving SKBR3 cells. In the HER2 negative MCF-7 cells which are resistant to Herceptin, HER2 homodimers do not play a major part. Herceptin induces activation of all HER pathways through TACE-mediated ligand release and may mediate primary resistance to Herceptin with no effect on cell viability.

It was shown that Herceptin decreases the viability of treated SKBR3 cells to less than 50% of that control. However, the surviving cells continued to have HER2 phosphorylation with activation of alternative HER pathways. There are two possible explanations. Firstly, breast cancers are a heterogeneous group of diseases with different gene expression and protein levels between different cell lines as well as within the same cell type (Sorlie et al., 2003). Therefore in a pool of SKBR3 cells, there may already be some cells which are resistant to Herceptin at the outset and they undergo clonal expansion while the sensitive cells undergo apoptosis. The other possibility is that the surviving cells represent those that have adapted the environment by shifting the dependence of EGFR/HER2 pathway to other pathways. The results suggest that both of these two explanations maybe true. Upon Herceptin treatment there were immediately two responses on EGFR activation (Figure 5.3A), which highlights the possibility of heterogeneous group of cells and the difference in their genetic expression, that determine the difference in response to drugs. But the results also illustrated here that Herceptin treatment induces the release of ligands through TACE and cause activation and dimerisation of alternative HER receptors to compensate the drug effect. It seems that Herceptin treatment has eliminated the cells that are highly dependent on EGFR activation or HER2 homodimers, and the surviving cells have shifted the dependence to HER3 and HER4 signalling pathways.

Lapatinib in combination with Capecitabine was found to be superior in women with HER2 positive breast cancer that has progressed after chemotherapy and Herceptin (Geyer et al., 2006). The results presented here may explain why this is the case. Herceptin treatment in HER2 over-expressing breast cancer cell may result in activation of all HER receptors regardless of response, including activation of EGFR and HER2. This explains why Lapatinib which inhibits tyrosine kinase activity of EGFR and HER2, is effective in HER2 positive patients who have progressed on Herceptin. However, all these patients will invariably progress, implying that other pathways like HER3 and HER4 may play a part in the escaping mechanisms.

In this and previous chapters, FRET was applied to assess activation of HER receptors in relation to Herceptin and Iressa treatments in breast cancer cells, revealing the possible mechanisms of resistance to these drugs. The next chapter describes the use of FRET to assess HER2 phosphorylation in xenografts and in breast tumour arrays.

6 Assessing HER2 phosphorylation state by FRET in xenograft tumours and breast tumour arrays

6.1 Introduction

In Chapter 4, an assay to assess HER2 phosphorylation status by FRET was established in cell lines. The long-term aim is to apply such an assay in stratification of breast cancer patients for targeted therapies in the prospective trials. To apply such assay to prospective trials, optimisation of the assays needed to be performed in cell lines, xenograft models and archives of paraffin-embedded breast tumour arrays. The optimisation will enable problems to be identified before applying this novel method to assess HER2 phosphorylation in breast cancer patients.

The first objective was to assess the effect of antigen-retrieval in cell lines, in particular whether the detection of HER2 phosphorylation by FRET would be increased by antigen retrieval through recovery of the epitopes since antigen retrieval is routinely applied to paraffin-embedded tumour arrays in IHC. The second objective was to assess whether the phosphorylated HER2 epitopes of xenograft tumours would be preserved after being removed from Severe Combined Immune Deficiency (SCID) mice and being embedded into paraffin tissues or whether the phosphorylated epitopes would decay rapidly after removal. If the phosphorylated epitopes were to degrade rapidly, FRET would not be useful in monitoring the phosphorylation status of HER receptors in tumours. Knowing the extent of this decay will also help to develop guidelines for the handling of tumours in future prospective trials used for FRET experiments. The differences between IHC and FRET in detecting HER2 phosphorylation also were determined also. Although formalin is used routinely to preserve human tissues before the

tumours are paraffin-embedded, it was intended to assess whether liquid nitrogen could also be used in preserving the epitopes of phosphorylated HER2. In addition, the impact of the delay in fixation on the pHER2 antigen would be assessed since it is possible that this delay may occur when the tumours are removed surgically. The method of fixation (either by formalin or liquid nitrogen) and the effect of delay in fixation as well as the differences between IHC and FRET in detecting HER2 phosphorylation will be described in this chapter. The third objective was to assess the differences in HER2 phosphorylation between different regions of heterogeneous breast tissues (tumour area versus stromal area) and between HER2 positive and HER2 negative breast tumour slides. The FRET assay was also applied to assess HER2 phosphorylation in a set of breast tumour arrays (containing a mixture of HER2 positive and HER2 negative breast tumour cores) using automated FLIM. The optimisation of automated FLIM on archives of paraffin-embedded breast arrays is essential before its application to prospective trials. Lastly the assay was applied to a HER2 positive breast tumour array and it was intended to assess whether FRET to assess HER2 phosphorylation could be used to stratify HER2 positive patients further into different prognostic groups. The variation in HER2 phosphorylation between IHC and FRET in breast tumour arrays was determined.

6.2 Results

6.2.1 Effect of antigen retrieval on HER2 phosphorylation in cell lines

Antigen retrieval is routinely performed to recover the epitopes from the formalin-fixed, paraffin-embedded tumour arrays during IHC processing. However, before FRET could be applied to assess HER2 phosphorylation in xenograft tumours and paraffin-embedded tumour arrays, the effect of antigen retrieval on HER2 phosphorylation was assessed in cell lines. It was intended to

assess whether the detection of HER2 phosphorylation by FRET would be increased by the recovery of the epitopes through antigen retrieval.

A431 cells and MCF-7 cells were treated with an additional antigen retrieval process following fixation with 4% PFA and then incubated with either donor HER2-Cy3b with or without acceptor pHER2-Cy5. Figure 6.1 shows the lifetimes of HER2-Cy3b with or without prior EGF stimulation to assess HER2 phosphorylation in A431 cells. The lifetimes and FRET efficiencies obtained were compared with the non-antigen retrieval (Figure 4.1) and the results are shown in Figure 6.1B. The antigen retrieval increased the detection of basal phosphorylation due to recovery of epitopes compared to the non-antigen retrieval process (Figure 6.1B). At the basal level, the lifetime of HER2-Cy3b in A431 cells decreased from 2.2 ns to 1.41 ns in the presence of acceptor (a FRET efficiency of 37.1%), in contrast to a decrease of lifetime from 2.19 ns to 1.75 ns in the case of non-antigen-retrieval process (a FRET efficiency of 19.8%) (Figure 6.1B). EGF stimulation induced further phosphorylation, decrease of lifetime from 1.4 ns to 1.28 ns (FRET efficiency 42.9%) compared with non-antigen retrieval process (lifetime decreased from 1.75 ns to 1.56 ns with EGF stimulation, a FRET efficiency of 37.1%) (Figure 6.1B). Similar patterns were observed in MCF-7 cells (Figure 6.1C and Figure 4.1C).

In summary the results showed that antigen retrieval increased the detection of HER2 phosphorylation by FRET through the recovery of the epitopes.

A

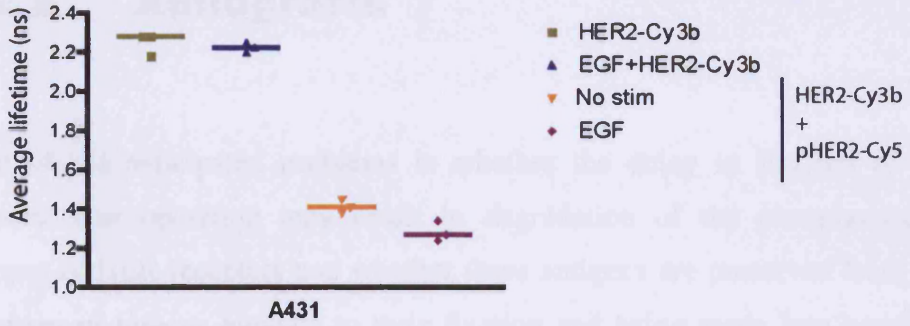

B

A431 (n=5)	HER2-Cy3b (ns)	EGF+HER2-Cy3b (ns)	HER2-Cy3b+pHER2-Cy5 (ns)	EGF+HER2-Cy3b+pHER2-Cy5 (ns)
Non-antigen retrieval	2.19 ± 0.4	2.20 ± 0.02	1.75 ± 0.06	1.56 ± 0.06
Antigen retrieval	2.25 ± 0.05	2.22 ± 0.02	1.41 ± 0.04	1.28 ± 0.05

	Non-antigen retrieval	Antigen retrieval
Basal FRET efficiency	19.8% ± 2.1	37.1% ± 0.9
EGF induced FRET efficiency	28.7% ± 3.3	42.9% ± 1.5

C

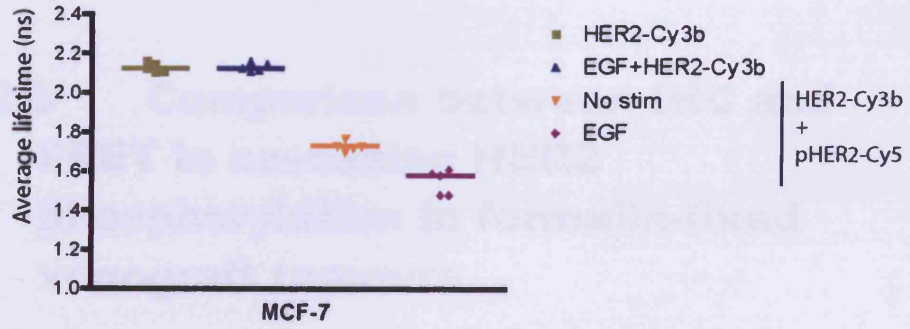

Figure 6.1: Effects of antigen retrieval on detection of HER2 phosphorylation by FRET. A, A431 cells were treated with antigen retrieval after fixation with 4% PFA to assess HER2 phosphorylation by FRET after stimulation with 50 ng/ml EGF. **B,** The average lifetimes and FRET efficiencies were compared between the non-antigen retrieval and antigen retrieval conditions. **C,** Same experiment of A done in MCF-7 cells.

6.2.2 Xenografts

One of the anticipated problems is whether the delay in fixation of the tumours after operation may result in degradation of the phosphorylated epitopes of HER receptors and whether these antigens are preserved from the processes of tumour removal to their fixation and being made into paraffin-embedded tumour arrays. The assumption was that phosphorylated antigens are preserved after the tumours are made into paraffin sections and thus anti-phosphospecific antibodies will be useful in determining the phosphorylation status of the tumours. To test this assumption, HER2 over-expressing breast cancer cell lines (SKBR3 and MDAMB-453 cells) were inoculated in nude mice. Unfortunately, the tumours did not grow successfully in nude mice. The same experiment was later repeated in SCID mice but only MDMAB-453 cell lines were grown successfully and SKBR3 cells were found to be non tumourigenic in SCID mice. It was intended to assess whether the phosphorylated HER2 epitopes (pHER2) of the xenograft tumour would decrease by delaying the fixation process. Both formalin and the liquid nitrogen were used for tumour fixation to compare the phosphorylation status of HER2 by IHC and FRET.

6.2.3 Comparison between IHC and FRET in assessing HER2 phosphorylation in formalin-fixed xenograft tumours

The largest tumour from one SCID mouse was cut into three parts (see Methods): one was fixed immediately with formalin (NBF) and another was left at room temperature for 1 hour and the third one was left on ice for 1 hour before fixation with formalin. These tumours were processed according to the standard protocol and made into paraffin-embedded slides. To perform IHC staining, the slides were dewaxed and the antigen-retrieval process was

performed according to the guidelines from New England Biolabs' protocols on anti-pHER2 IHC staining (see Methods Section 2.2.9). Figure 6.2A shows anti-pHER2 IHC staining of the MDAMB-453 xenograft tumour slides. The anti-pHER2 staining shown by the brown membranous staining was present in all three slides. However, differences in intensity or percentage of cell staining between the three slides could not be detected (Figure 6.2A). The control slide without primary pHER2 antibody (stained only with rabbit secondary antibody) does not show membranous staining (Figure 6.2A). Therefore, the results demonstrated that the phosphorylated antigens of HER2 were retained up to an hour of delay in fixation with formalin and differences could not be detected between the three conditions using IHC method.

To compare IHC and FRET methods, duplicate paraffin slides from the three conditions were prepared. The same procedure for dewaxing and antigen-retrieval was used. For each condition, a pair of slides were used, one labelled with donor HER2-Cy3b alone and the other with donor HER2-Cy3b and acceptor pHER2-Cy5 to assess HER2 phosphorylation. The lifetimes of donor alone and donor with acceptor were obtained. The FRET efficiency for each condition was calculated (see Methods Section 2.2.11). HER2 phosphorylation indicated by the FRET efficiency was different in the three conditions. Figure 6.2B shows a median FRET efficiency of about 15% in a tumour, which was fixed immediately by NBF. And in the two tumour samples, which were left for 1 hour either at room temperature or on ice, showed a lower FRET efficiency, indicative of a decrease in HER2 phosphorylation (Figure 6.2B).

A

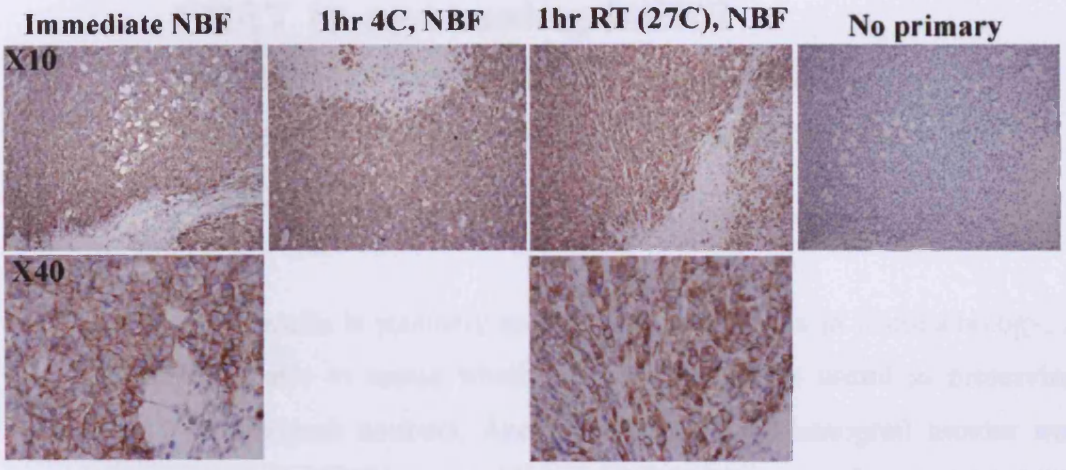

B

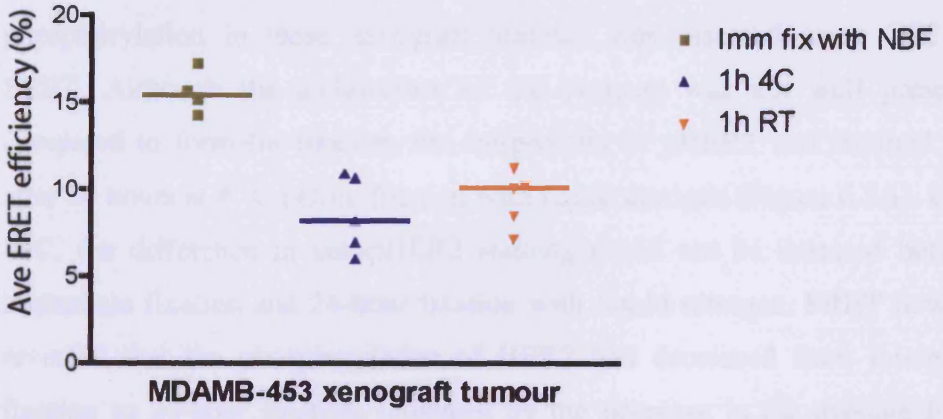

Figure 6.2: Comparison between assessment of HER2 phosphorylation by IHC and FRET in MDAMB-453 Xenograft tumour fixed with formalin (NBF). **A, A** MDMAB-453 xenograft tumour was removed and cut into three parts to be fixed in three ways: (1) fixed immediately by NBF, (2) left on ice at 4 degree C for I hour before NBF fixation, (3) left at 1 hour room temp before NBF fixation. The tumours were made into paraffin-embedded tumour slides. The tumour slides were subjected to antigen-retrieval as per protocol before anti-pHER2 staining was done on all slides. Rabbit seconday antibody was used following primary antibody staining. One slide without primary pHER2 antibody was stained with only with rabbit secondary antibody as control. **B,** Duplicate slides were labelled with either donor alone (HER2-Cy3b) or donor and acceptor (HER2-Cy3b +pHER2-Cy5) to assess HER2 phosphorylation by FRET.

6.2.4 Comparison between IHC and FRET in assessing HER2 phosphorylation status of the xenograft tumours fixed with liquid nitrogen

Although formalin is routinely used to fix the tumours in histopathology, it was intended also to assess whether liquid nitrogen is useful in preserving pHER2 in xenograft tumours. Another MDMAB-453 xenograft tumour was removed from the SCID mice and it was sectioned into two parts (see Methods Section 2.2.8): one was fixed immediately by liquid nitrogen and another was left at 4 ^{0}C before fixation with liquid nitrogen. The effect of delay in fixation with liquid nitrogen fixation (immediate versus 24 hours) on HER2 phosphorylation in these xenograft tumours was assessed using IHC and FRET. Although the architecture of the tumours was not well preserved compared to formalin fixation, the antigenicity of pHER2 was retained even after 24 hours at 4 ^{0}C before fixation with liquid nitrogen (Figure 6.3A). Using IHC, the difference in anti-pHER2 staining could not be detected between immediate fixation and 24-hour fixation with liquid nitrogen. FRET however revealed that the phosphorylation of HER2 had decreased from immediate fixation to 24-hour fixation, indicated by the decrease in the average FRET efficiency from a median of 7.5 % to about 5% (Figure 6.3B).

All together the xenograft experiments showed that the variations in HER2 phosphorylation due to delay in fixation with either formalin or liquid nitrogen may be detected by FRET, which would otherwise not be quantified by IHC.

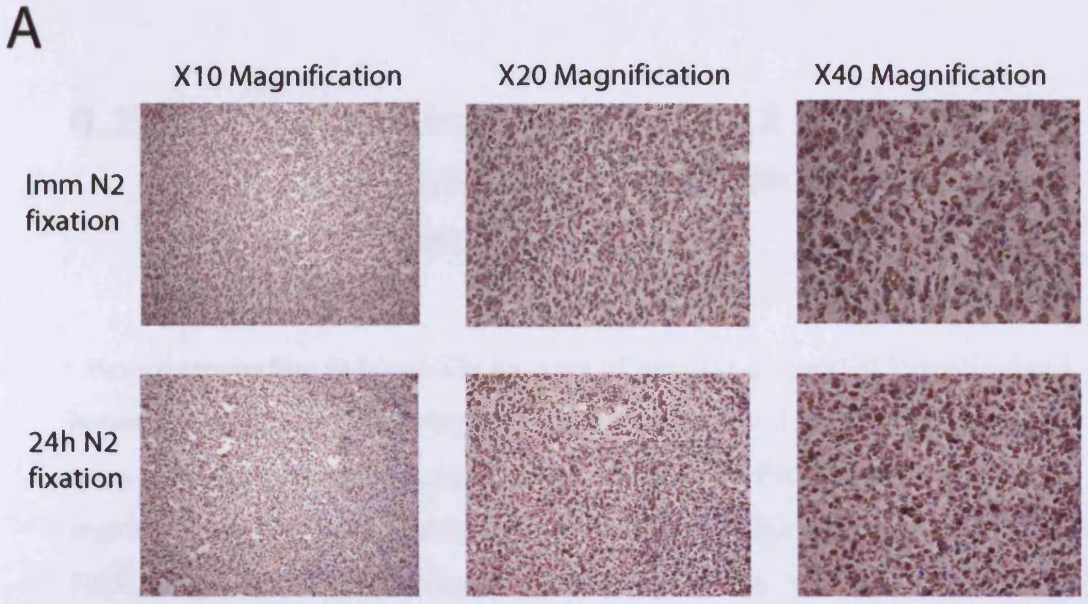

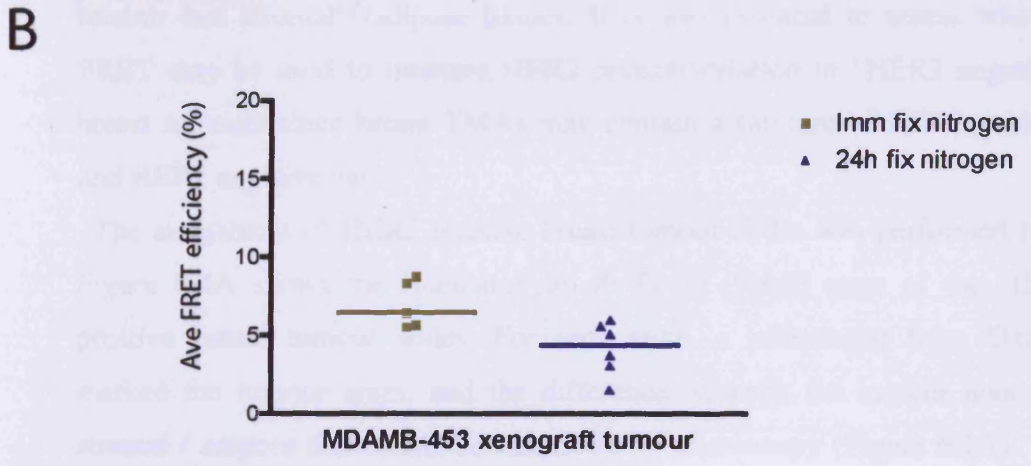

Figure 6.3: Comparison between assessment of HER2 phosphorylation by IHC and FRET in MDAMB-453 Xenograft tumour fixed with liquid nitrogen. **A,** A MDMAB-453 xenograft tumour was obtained and cut into two parts. They were fixed either immediately in liquid nitrogen or left at 4 degree C for 24 hours before fixation with liquid nitrogen. The tumours in the two conditions were then made into tumour slides and stored in - 80 degree C. On the day of experiment, the slides were thawed before being stained with anti-pHER2 antibody. **B,** The tumour slides were prepared in the same manner as A. But after thawing, the slides were labelled with either donor alone (HER2-Cy3b) or donor and acceptor (HER2-Cy3b + pHER2-Cy5) to assess HER2 phosphorylation.

6.2.5 Determination of HER2 phosphorylation by FRET in breast tumour slides

Before proceeding to breast TMAs, a set of paraffin-embedded formalin-fixed breast tumour slides containing both HER2 positive and HER2 negative cases were obtained to assess the variation in lifetimes by FRET between different regions of the breast tumour tissues and between HER2 positive tumours and HER2 negative tumours. The understanding of the variation in lifetimes between different regions will be useful for interpretation of TMAs since it is not uncommon for tumour cores in the TMAs to differ in the composition of tumour and stromal / adipose tissues. It is also essential to assess whether FRET may be used to measure HER2 phosphorylation in "HER2 negative" breast tumours since breast TMAs may contain a mixture of HER2 positive and HER2 negative cases.

The assessment of HER2 positive breast tumour slides was performed first. Figure 6.4A shows the Haematoxylin & Eosin (H&E) stain of the HER2 positive breast tumour slides. For each slide, a pathologist from Oxford marked the tumour areas, and the difference between the tumour area and stromal / adipose tissues can be visualised by microscopy (Figure 6.4A). The variations in the lifetimes of HER2-Cy3b (indicating HER2 phosphorylation) between different regions of a HER2 positive breast tumour slide are shown in Table 6.1A. The average lifetimes taken from the tumour areas were below 1.5ns, whereas the average lifetimes of the stromal areas were in the region of 2 ns. Figure 6.4B shows examples of these differences represented by lifetime maps. The figures show the donor intensity images (left panels), DC images (middle panels) and the lifetime maps (right panels) of HER2-Cy3b of a tumour region and a stromal region from a HER2 positive tumour slide. In the upper panels, the images were acquired from a tumour region and even within this region there were differences in donor intensities (indicative of HER2 expression). As shown (Figure 6.4B, upper panels), only the lifetimes from the

area with adequate signal-to-noise ratio may be obtained, as represented by the pseudo-colour of the lifetime map (red indicates shorter lifetimes). In the lower panels, the images were acquired from a stromal region of the tumour slide. The average lifetime of the region of interest was higher (i.e. lower HER2 phosphorylation) as indicated by pseudo-colour of the lifetime map (blue indicates higher lifetimes). All together, the data show that the tumour regions have a higher HER2 phosphorylation compared to stromal area, as indicated by lower lifetimes of HER2-Cy3b.

HER2 phosphorylation by FRET was also assessed in HER2 negative (IHC 0 or 1+) breast tumour slides. Table 6.1B exemplifies the lifetimes of HER2-Cy3b in several tumour areas of a HER2 negative breast tumour slide. In a HER2-negative slide the tumour areas had longer lifetimes than the HER2 positive cases (Table 6.1A), i.e. lower HER2 phosphorylation. However, in some areas, bright spots were noted (an example from tumour area 2 shown in Figure 6.5A, upper panels), indicating a high HER2 intensity (concentration). If the region of interest included this area, the overall lifetime of HER2-Cy3b decreased from 2.1 ns to 1.91 ns (tumour area 2, Table 6.1B). Figure 6.5 shows the diagrams of tumour area 2 (representing the data in table 6.1B). It shows that there were differences in the maximum intensities of the donor HER2-Cy3b within the tumour region. The left upper panel shows a very bright region (indicating high HER2 expression) within the tumour area. The lifetime map shows that the lifetime of this bright region is below 1.5 ns indicating high HER2 phosphorylation. However, average the lifetime of the whole region of interest resulted in an average lifetime of 1.91 ns. When the bright spot was excluded the average lifetime increased to 2.1 ns.

In summary, the experiments showed that the tumour areas of the HER2 positive slide had a higher HER2 phosphorylation than the stromal area. The tumour areas of HER2 positive slide also had a higher HER2 phosphorylation compared to the tumour areas from a HER2 negative slide. In addition it also illustrated that the "so-called" HER2 negative breast tumour may be heterogeneous and contain areas that have high HER2 concentration with an increased HER2 phosphorylation status. Therefore, the results showed the importance of selecting an appropriate region for the TMAs since the amount

of breast tumour versus stromal tissues may influence the results significantly and introduce sample heterogeneity.

A

HER2 positive tumour slide	Phase lifetime (ns)	Modulation lifetime (ns)	Average lifetime (ns)
Tumour area 1	0.85 ± 0.35	1.30 ± 0.58	1.08
Tumour area 2	1.03 ± 0.20	0.79 ± 0.28	0.91
Tumour area 3	0.93 ± 0.15	1.35 ± 0.25	1.14
Tumour area 4	0.82 ± 0.13	1.07 ± 0.24	0.95
Stromal area 1	1.68 ± 0.30	2.27 ± 0.35	1.98
Stromal area 2	1.68 ± 0.44	2.83 ± 0.50	2.26

B

HER2 negative tumour slide	Phase lifetime (ns)	Modulation lifetime (ns)	Average lifetime (ns)
Tumour area 1	1.74 ± 0.60	2.15 ± 0.65	1.95
Tumour area 2 (including bright spot)	1.56 ± 0.37	2.25 ± 0.49	1.91
Tumour area 2 (excluding bright spot)	1.79 ± 0.15	2.40 ± 0.39	2.10
Tumour area 3 (including bright spot)	1.24 ± 0.16	1.93 ± 0.27	1.59
Tumour area 3 (excluding bright spot)	1.79 ± 0.44	2.81 ± 0.49	2.3

Table 6.1: A, The average lifetimes of HER2-Cy3b in tumour areas and stromal areas of a HER2 positive breast tumour slide. **B,** The average lifetimes of HER2-Cy3b in tumour areas of a HER2 negative breast tumour slide.

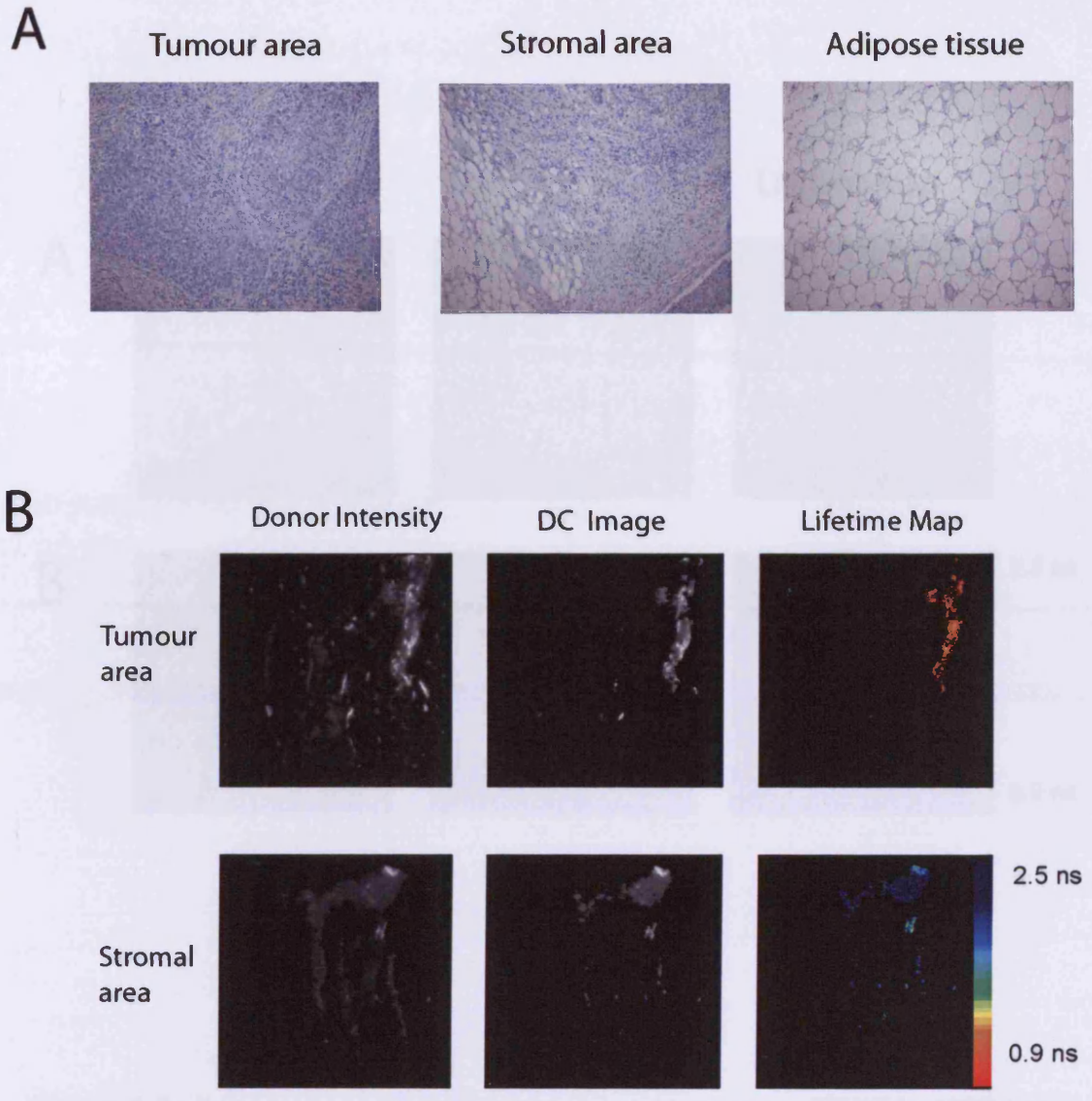

Figure 6.4: Assessment of HER2 phosphorylation by FRET in HER2 positive breast tumour slides. Formalin-fixed and paraffin-embedded HER2 positive tumour slides were labelled with donor HER2-Cy3b and acceptor pHER2-Cy5 after antigen retrieval as per protocol. **A,** The tumour slides were marked for tumour regions and stromal regions (stromal and adipose tissue) after H&E stain, so that the lifetimes of the different regions within the tumour slide could be assessed. **B**, The diagrams from one tumour slide. The left panels show the donor intensity images, the middle panels show DC images and the right panels are lifetime maps. In the upper panels, the images were taken from a tumour region indicated by H & E stain. In the lower panels, the images were taken from a stromal area.

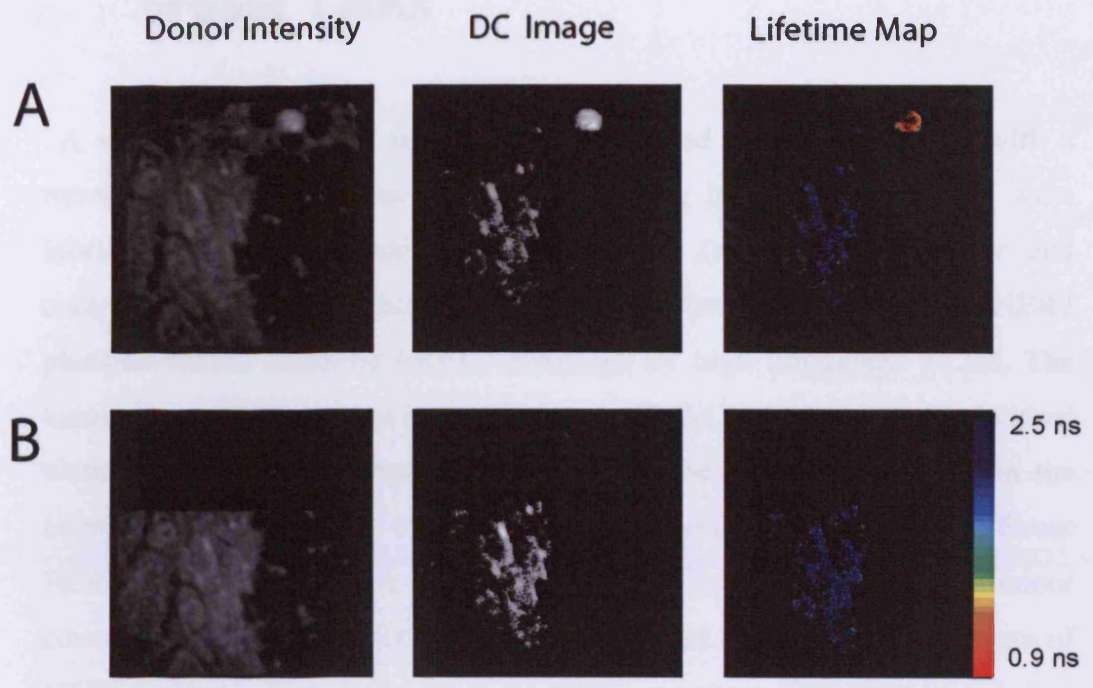

Figure 6.5: Assessment of HER2 phosphorylation by FRET in HER2 negative breast tumour slides. A, Formalin-fixed and paraffin-embedded HER2 negative tumour slides were labelled with donor HER2-Cy3b and acceptor pHER2-Cy5 after antigen retrieval as per protocol. The diagrams were taken from the tumour region of one tumour slide. The left panels show the donor intensity images of tumour region, the middle panels show DC images and the right panels are lifetime maps of the cores. **B**, Excluding the bright spot in the region of interest.

6.2.6 Assessment of the HER2 phosphorylation status in mixed HER2 breast TMAs

A set of breast tumour arrays (which contained 230 tumour cores with a mixture of HER2 positive and HER2 negative breast tumour cores) were labelled with either donor HER2-Cy3b alone (as control) or donor and acceptor pHER2-Cy5 according to the protocol to assess the HER2 phosphorylation status by FRET, monitored by high throughput FLIM. The tumour cores were mapped in the automated FLIM and lifetimes of individual tumours cores were obtained. The results showed great heterogeneity in the intensity of donor HER2-Cy3b between the tumour cores due to different HER2 expression between them. In the mixed breast TMAs, some tumour cores had very low level of HER2 expression and thus very little amounts of HER2-Cy3b would have bound to the HER2 receptors. This would result in a low signal to noise ratio and the intensity from such sample would be too low relative to the background scattering foil to calculate the lifetime (See Methods Section 2.2.11). Such problems however did not occur in the tumour cores with high HER2 expression. The heterogeneity problem was further highlighted when different exposure times of the excitation source were used since the tumour cores with high expression of HER2 only required a very short exposure time while the tumour cores with low HER2 expression would require a longer exposure time to reach an adequate signal to noise ratio. Moreover, when exposed to a longer exposure time, the tumour cores with high HER2 expression may reach a saturated intensity (> arbitrary threshold value of 4900) for the software to calculate the lifetime (See Methods Section 2.2.11).

Due to the heterogeneity problem in the intensity between the tumour cores, cores were initially exposed manually to different exposure times to optimise and calibrate the automated FLIM instrument. Figure 6.6 shows the diagrams from the optimisation in a tumour core. When the exposure time of pulsed laser excitation was 2000ms, the intensities of both tumour core and

background were high and the average lifetime of donor HER2-Cy3b was 2.04 ns (Figure 6.6A). When the exposure times were decreased to 1500ms and 1000ms, the contrast of the donor intensity between the tumour core and the background was more obvious and the average lifetimes were 2.04 ns and 2.01 ns respectively (Figure 6.6B and 6.6C). When the exposure time was decreased to 500 ms, the maximum intensity of the donor HER2-Cy3b had decreased to a threshold of about 1000 (arbitrary value) and the signal-to-noise ratio was too low to calculate the lifetime of HER2-Cy3b. In another tumour core, the intensity of the donor fluorescence was saturated with 2000 ms exposure (> arbitrary value of 4095), resulting in an inability to calculate lifetimes (Figure 6.7A). However, when the exposure times were decreased, the lifetimes could be calculated (Figure 6.7A). In some of the tumour cores, the donor intensities of the tumour core were saturated even with an exposure time of 1000 ms and lifetime was only obtained when the exposure was decreased to 500 ms (Figure 6.7B).

In summary while processing the mixed breast TMAs, it was found that there was a great heterogeneity problem between the intensity of the tumour cores making it difficult to process the TMAs in a high throughput manner by the FLIM. To optimise the instrument, a calibration curve was plotted so that the relationship between exposure times and maximum intensities of donor HER2-Cy3b of the breast tumour cores could be determined.

To obtain the calibration curve, several breast tumour cores were manually exposed to different exposure times and the intensities of the donor HER2-Cy3b were recorded. Figure 6.8 shows examples of four tumour cores (TA15DA0001, 0003, 0005 and 0011) and the maximum intensities of the donor HER2-Cy3b (y-axis) were plotted against the exposure times (x-axis) of the tumour cores. In TA15DA0001 and 0011, the intensities were already saturated at an exposure time around 700 ms. Therefore, using an exposure time greater than 1000 ms would result in not being able to calculate the lifetime of HER2-Cy3b. There was however a linear relationship between exposure times and maximum intensities below 700 ms. For tumour cores TA15DA0003 and 0005, the maximum intensities relative to the exposure times were linear although the intensities decreased below the threshold of 1000 if the exposure time was less than 500 ms (Figure 6.8). The maximum

intensity was not saturated even with an exposure time of greater than 2000 ms (Figure 6.8).

Therefore, at this stage the lifetimes of the arrays with a mixture of HER2 positive and HER2 negative breast tumour cores could not be acquired by FLIM automatically, due to heterogeneity in the intensities of HER2-Cy3b as a result of variable HER2 expression among the tumour cores. The calibration curve however provided the relationship between the exposure times and the maximum intensities of the tumour cores and this information was used for further automation of the instrument which will be discussed in the next section.

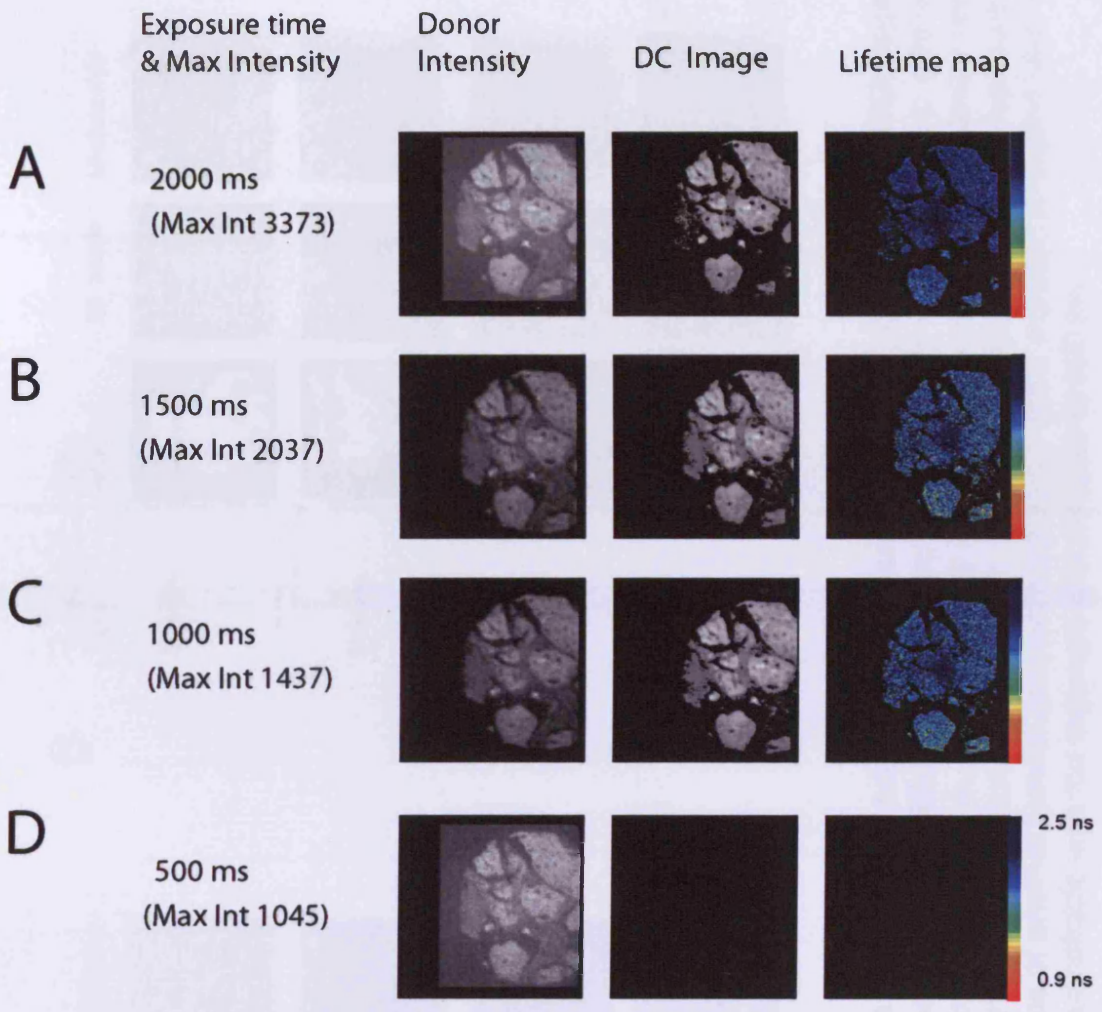

Figure 6.6: Optimisation of exposure times for a TMA containing a mixture of HER2 positive and HER2 negative tumour cores. Breast tumour cores labelled with donor HER2-Cy3b and acceptor pHER2-Cy5 were exposed to different durations of pulsed laser excitation: 2000 ms (A), 1500 ms (B), 1000 ms (C) and 500 ms (D).

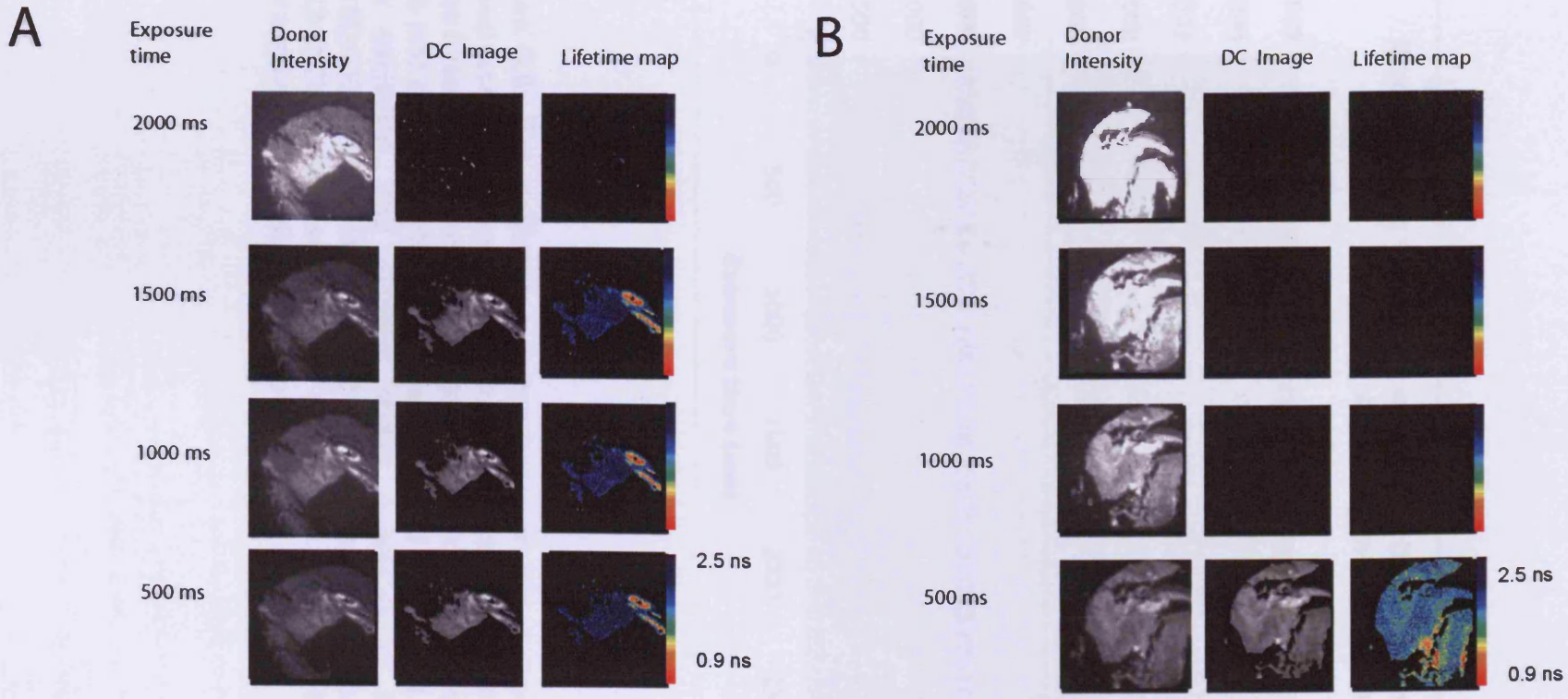

Figure 6.7: Optimisation of exposure times for an array containing a mixture of HER2 positve and HER2 negative breast tumour cores. Breast tumour cores labelled with donor HER2-Cy3b and acceptor pHER2-Cy5 were exposed to different durations of pulsed laser excitation. Two examples are illustrated here. **A**, The intensity of the donor fluoresecence of a tumour core was saturated in the case of 2000 ms exposure and the lifetime of donor HER2-Cy3b was not quantifiable until the exposure times were decreased to 1500 ms. **B,** The donor intensities of another tumour core were saturated when exposed to pulsed laser excitation of greater than 1000 ms and lifetimes were not quantifiable until the exposure was reduced to 500 ms.

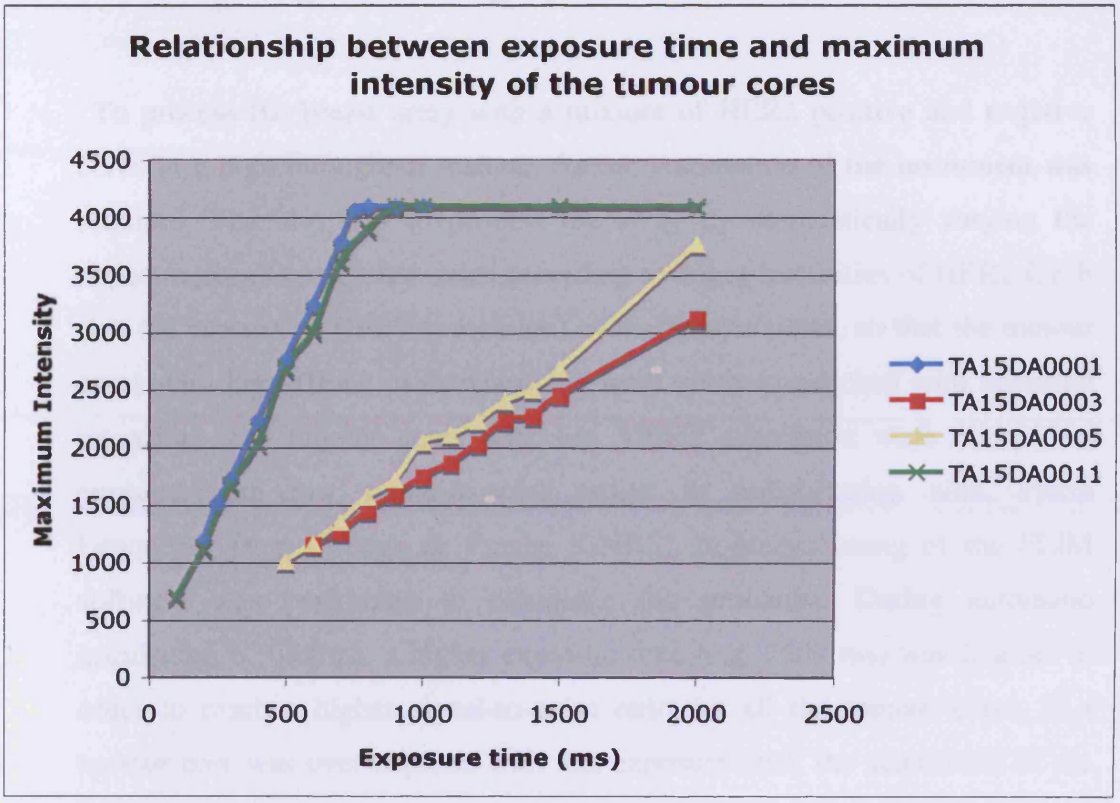

Figure 6.8: The calibration curve between the exposure times of the pulsed laser excitation and the maximum intensities of donor HER2-Cy3b of the breast tumour cores. Breast tumour cores labelled with donor HER2-Cy3b and acceptor pHER2-Cy5 were exposed to different durations of pulsed laser excitation. The diagram shows examples of four tumour cores (TA15DA0001, 0003, 0005 and 0011). The maximum intensities of the donor HER2-Cy3b (y-axis) were plotted against the exposure times of the pulsed laser excitation (X-axis).of the tumour cores.

6.2.7 Automation of the exposure times for high throughput FLIM

To process the breast array with a mixture of HER2 positive and negative cores in a high throughput manner, further automation of the instrument was required. The aim was to process the array by automatically varying the exposure times for tumour cores according to donor intensities of HER2-Cy3b (i.e. the amount of HER2 expression) of the tumour cores, so that the tumour cores with high HER2 over-expression were not over-exposed with saturated intensities and tumour cores with low HER2 expression were not under-exposed with low signal-to-noise ratios. In collaboration with, Pierre Leboucher from College de France (CNRS), re-programming of the FLIM software was performed to overcome the problems. During automatic acquisition of lifetime, a higher exposure time (e.g. 2000 ms) was first set in order to reach a higher signal-to-noise ratio for all the tumour cores. If a tumour core was over-exposed with this exposure time, the acquisition of the lifetime of that tumour core would be repeated with a lower exposure time (e.g. 1900 ms). The cycle (i.e. acquisition with a lower exposure time) would continue to eliminate over-exposure of the tumour cores. Before acquisition, the operator needed to choose the maximum and minimum acceptable intensities (e.g. arbitrary value of 4000 for maximum intensity and 2000 for minimum intensity) as well as the interval of decrease in exposure time (e.g. 100 ms) so that the exposure time would decrease according to a pre-set interval during each re-run when the tumour cores were over-exposed. With this re-evaluation of the automation software, the tumour arrays with a mixture of HER2 positive and negative cases could be processed automatically by FLIM. However, out of the 234 tumour cores, only 71 samples could be analysed since the lifetimes of most tumour cores were still unobtainable despite adequate intensities of the tumour cores. This was because in some cases, the tumour and the background had similar intensities and by increasing the exposure times, the intensity of the background increased with the tumour

so that the lifetime could not obtained. The Kaplan-Meier survival curves of those 71 were plotted using average FRET efficiency as a prognostic marker (split by median). The statistically significant differences the DFS and OS between the two groups were not obtained although there was a trend for patients with high FRET to have lower DFS (p=0.41) (Figure 6.9).

The automation of the FLIM is an ongoing project in the laboratory and is constantly upgraded by Pierre Leboucher and Banafshe Larijani. Since the last experiment shown in this section, the automated FLIM is now able to set suitable exposure times according to the intensity of HER2-Cy3b of a tumour core after the initial run at a low exposure time and the lifetimes of low HER2 tumour cores can now be obtained. This will enable the arrays to be processed in a high throughput manner regardless of HER2 expression of the tumour cores.

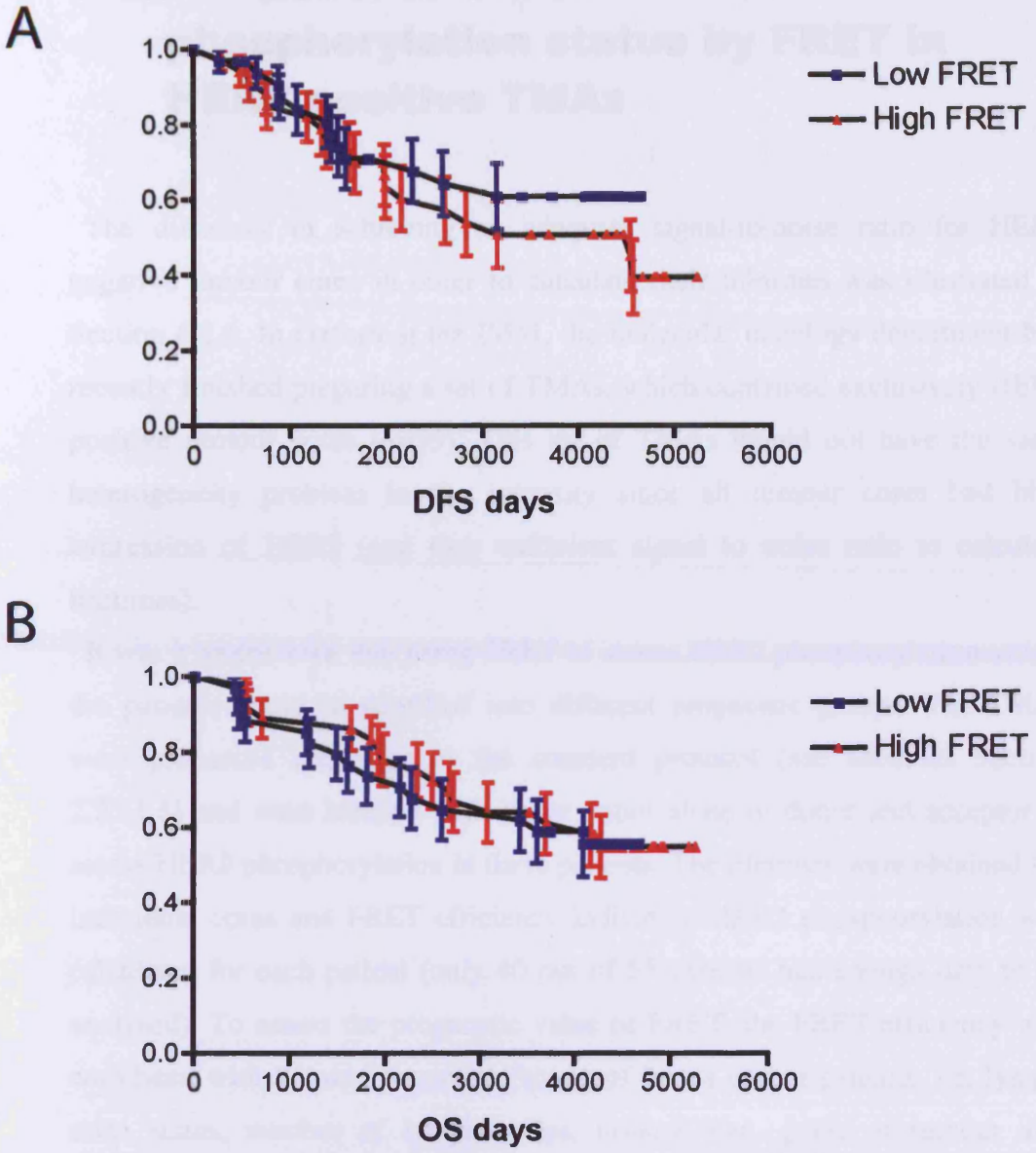

Figure 6.9: Kaplan-Meier curves using average FRET efficiency as a prognostic marker in a set of breast tumour arrays which contained both HER2 positive and HER2 negative cores. A, Disease-free survival (DFS) between patients in upper median versus the lower median of average FRET efficiency. **B,** Overall survival (DFS) between patients in upper median versus the lower median of average FRET efficiency.

6.2.8 Assessment of the HER2 phosphorylation status by FRET in HER2 positive TMAs

The difficulty in achieving an adequate signal-to-noise ratio for HER2 negative tumour cores in order to calculate their lifetimes was illustrated in Section 6.2.6. In Oxford at the IMM, the molecular oncology department had recently finished preparing a set of TMAs, which contained exclusively HER2 positive tumour cores (n=55). This set of TMAs would not have the same heterogeneity problem in the intensity since all tumour cores had high expression of HER2 (and thus sufficient signal to noise ratio to calculate lifetimes).

It was hypothesized that using FRET to assess HER2 phosphorylation status, the patients could be stratified into different prognostic groups. The TMAs were processed according to the standard protocol (see Methods Section 2.2.11.6) and were labelled with either donor alone or donor and acceptor to assess HER2 phosphorylation in these patients. The lifetimes were obtained for individual cores and FRET efficiency indicating HER2 phosphorylation was calculated for each patient (only 40 out of 55 patients had enough data to be analysed). To assess the prognostic value of FRET, the FRET efficiency was correlated with known prognostic factors of breast cancer patients, i.e. lymph node status, number of lymph nodes, tumour size, grade of tumour and hormone status of the tumour. Figure 6.10 and 6.11 show that increased HER2 phosphorylation status indicated by high FRET efficiency was associated with poor prognostic factors in HER2 positive patients. Amongst the HER2 positive patients split by median, patients with high FRET efficiency had poorer prognostic factors, with greater proportions of patients having node-positive disease, 4 or more lymph nodes positive, tumours greater than 4 cm, high-grade tumours and ER negative disease (Figure 6.10 and Figure 6.11). To further determine the prognostic value of FRET, the data was also correlated with the survival data of these breast cancer patients. Using average FRET efficiency as a prognostic marker, Kaplan-Meier curves illustrate that high

FRET efficiency (indicating high HER2 phosphorylation) had a trend towards a poorer disease-free survival (DFS) and overall survival (OS), although the number of patients was too low to reach statistical significance (p=0.4 for DFS and p=0.38 for OS between low FRET and high FRET) (Figure 6.12).

In summary, the results showed that using FRET to assess HER2 phosphorylation, HER2 positive breast cancer patients could be stratified further into different prognostic groups.

A

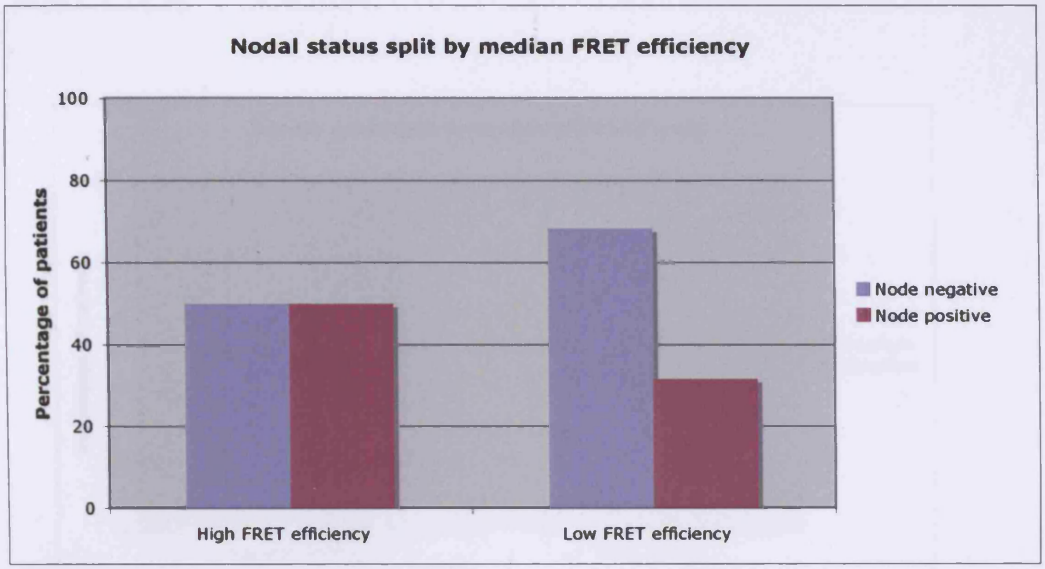
Nodal status split by median FRET efficiency
Percentage of patients
100
80
60
40
20
0
High FRET efficiency
Low FRET efficiency
Node negative
Node positive

B

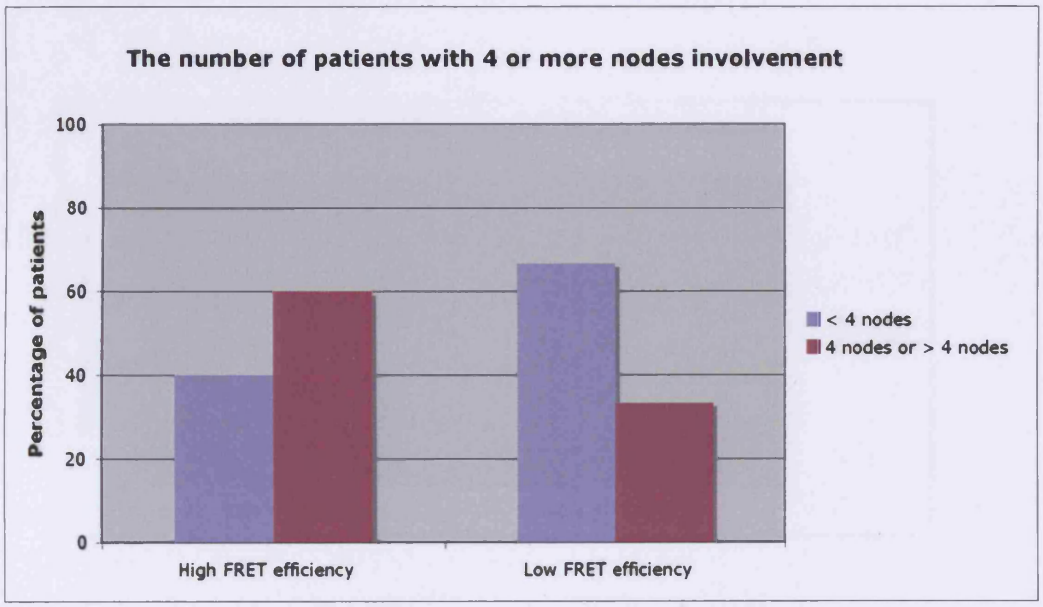
The number of patients with 4 or more nodes involvement
Percentage of patients
100
80
60
40
20
0
High FRET efficiency
Low FRET efficiency
< 4 nodes
4 nodes or > 4 nodes

C

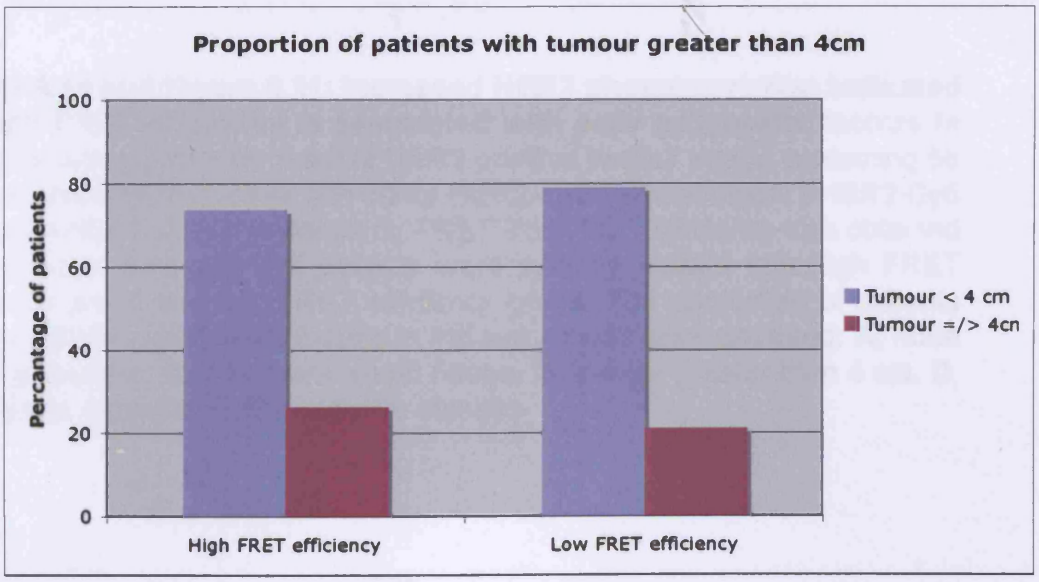
Proportion of patients with tumour greater than 4cm
Percantage of patients
100
80
60
40
20
0
High FRET efficiency
Low FRET efficiency
Tumour < 4 cm
Tumour =/> 4cn

D

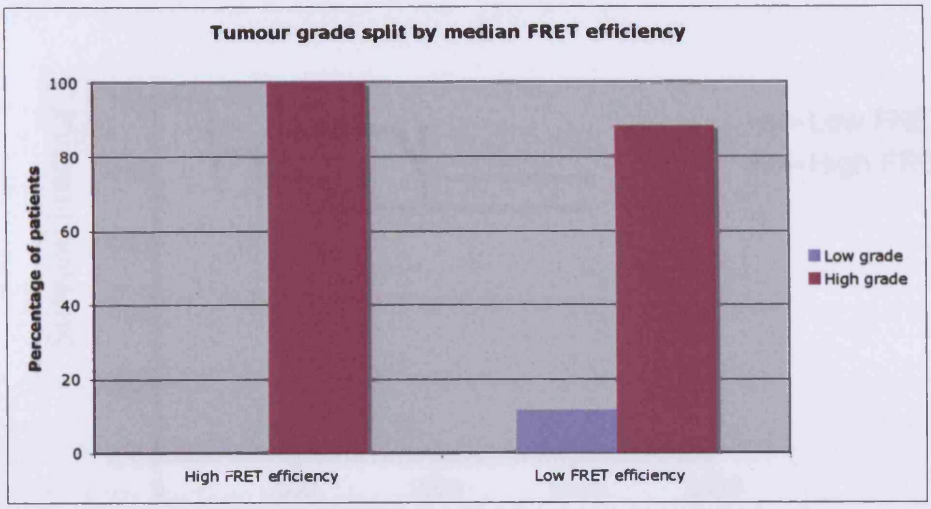

E

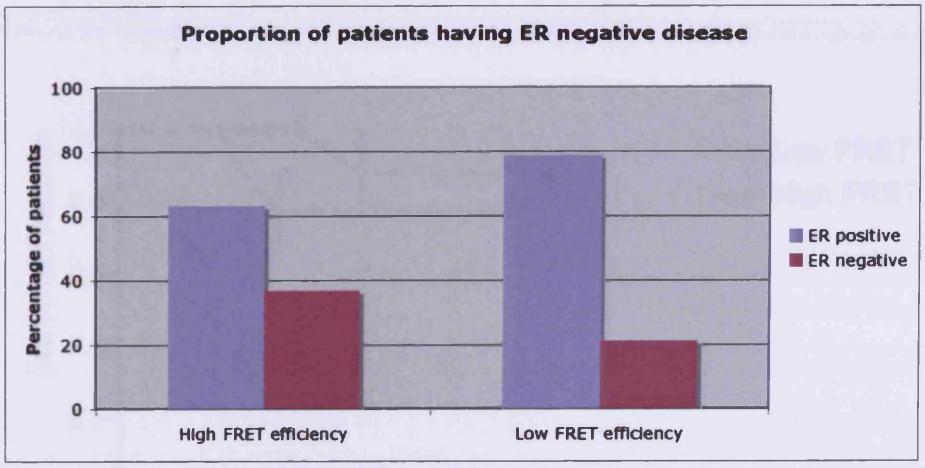

Figure 6.10 and Figure 6.11: Increased HER2 phosphorylation indicated by high FRET efficiency is associated with poor prognostic factors in HER2 positive patients. A set of HER2 positive tumour arrays containing 55 tumour cores were labelled with donor HER2-Cy3b and acceptor pHER2-Cy5 to assess HER2 phosphorylation by FRET. The FRET efficiency was obtained for individual core and the patients were split by median into high FRET efficiency group and low FRET efficiency group. The proportion of patients having different prognostic factors in the two groups were analysed: **A,** node positive disease, **B**, 4 or more lymph nodes. **C**, tumour greater than 4 cm. **D**, high grade tumours. **E,** ER negative disease

A

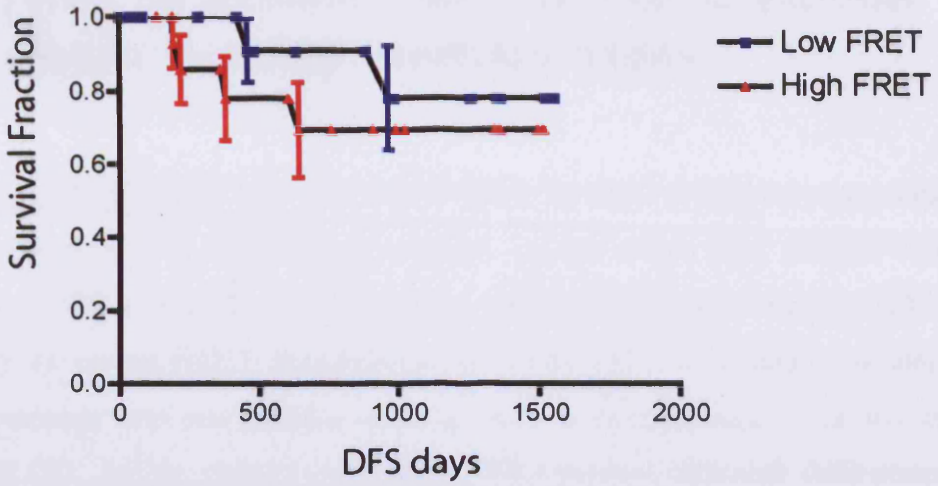

B

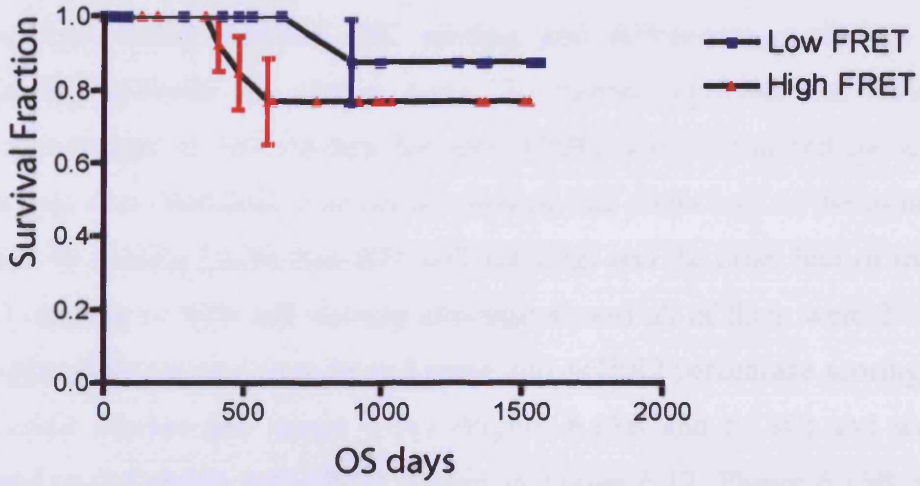

Figure 6.12: : Kaplan-Meier curves using average FRET efficiency as a prognostic marker in a set of HER2 positive breast tumour arrays which contained 55 tumour cores. A, Disease-free survival (DFS) between patients in upper median versus the lower median of average FRET efficiency. **B,** Overall survival (DFS) between patients in upper median versus the lower median of average FRET efficiency.

6.2.9 Correlation of IHC method with FRET to assess HER2 phosphorylation status in HER2 positive TMAs

The focus of the study was to assess whether the IHC would correlate with FRET efficiency. The HER2 positive breast tumour arrays were stained with either anti-HER2 antibody (to confirm the presence of HER2) or anti-pHER2 antibody (to assess HER2 phosphorylation) using IHC. An example of anti-HER2 staining and anti-pHER2 staining from a tumour core is shown in Figure 6.13A. All the tumour cores were HER2 positive although differences between tumour cores were observed (These tumour cores were all previously assigned to be HER2 positive by HercepTest which is based on the intensity of HER2 staining). For anti-pHER2 staining, all the tumour cores had a similar intensity (2+) using standard IHC scoring and differences could not be distinguished between the tumour cores. To further subdivide the tumour cores, percentages of cell staining for anti-pHER2 was determined for each tumour core (See Methods). The results showed that about half of the tumour cores had 4+ scoring (more than 80% cell staining) and the other half of them had 1-3+scoring (< 80% cell staining although almost all of them were 2-3+). The Kaplan Meier curves were plotted using anti-pHER2 percentage scoring as a prognostic marker (4+ versus 2-3+) (Figure 6.13B and 6.13C) and were compared to the results with FRET shown in Figure 6.12, Figure 6.13B and 6.13C. These data show that the differences between the two groups were not significant for DFS (p=0.7) although there was a trend for the patients with 4+ scoring to have a lower OS (not statistically significant, p=0.1).

To further assess the difference between FRET and IHC, the Mann Witney test was used to compare the medians of the average FRET efficiency between the two groups (IHC pHER2 scorings 2-3+ versus 4+). Figure 6.14A shows that the median of tumour cores with a score of 4+ was higher than with a lower score although the difference was not statistically significant probably because of low number of tumour cores (p=0.27). The correlation of HER2

level with FRET efficiency was also explored using the percentage of cell staining for anti-HER2 by IHC. The median of the FRET efficiency of tumour cores with a score of 4+ was higher than with a lower score ($p=0.03$, Figure 6.14B).

In summary, the experiments on HER2 positive breast tumour array showed that FRET maybe used to stratify HER2 positive breast cancer patients into different prognostic groups. The difference in the intensity of anti-pHER2 staining between different tumour cores using IHC was not significant. Further subdividing these patients by the percentage of cell staining using IHC showed that there was a trend for the tumour cores with > 80% cell staining (4+) to have a lower OS. These tumour cores also had higher FRET efficiency. Moreover, tumour cores with high percentage of anti-HER2 cell staining (> 80%) had a higher FRET efficiency.

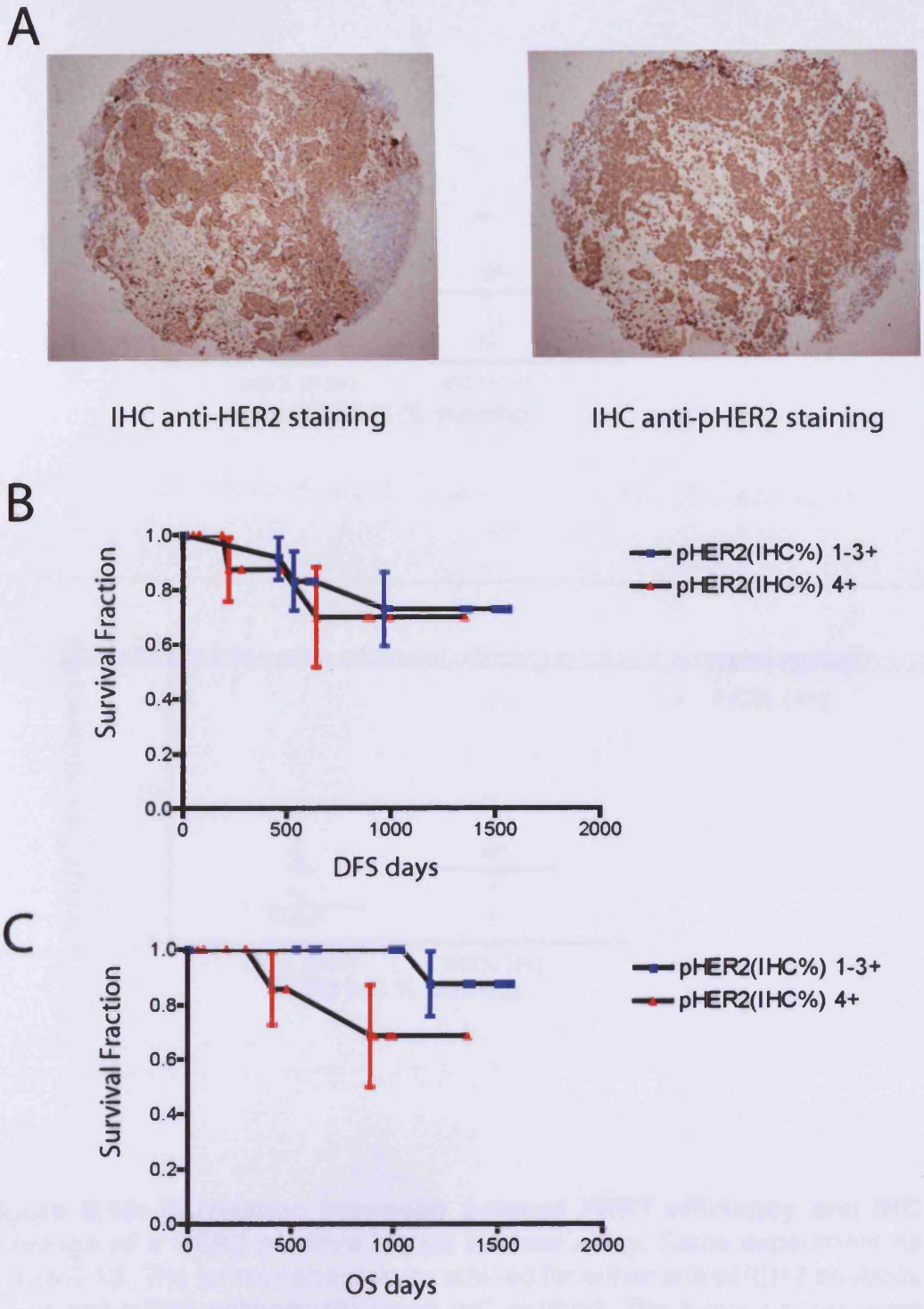

Figure 6.13: Kaplan-Meier curves using anti-pHER2 staining as a pronostic marker in a set of HER2 positive breast tumour arrays which contained 55 tumour cores. A, IHC of anti-HER2 staining and anti-pHER2 staining of a tumour core. **B,** Disease-free survival (DFS) between patients with 4+ percentage of cell staining versus 1-3+ percentage of cell staining. **C,** Overall survival (OS) between patients with 4+ percentage of cell staining versus 1-3+ percentage of cell staining

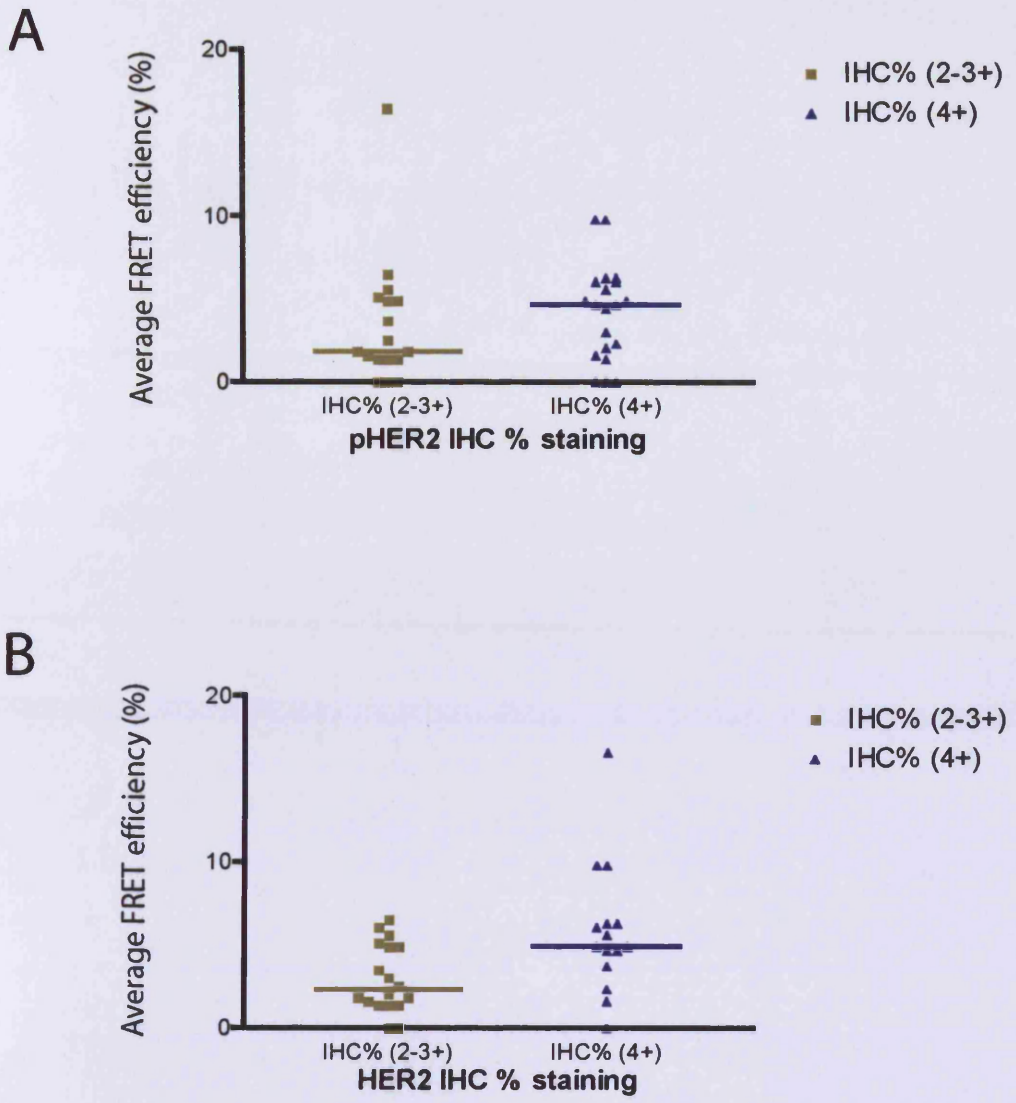

Figure 6.14: Correlation betweeen average FRET efficiency and IHC scorings of a HER2 positive breast tumour array. Same experiment as Figure 6.13. The tumour arrays were stained for either anti-pHER2 antibody (A) or anti-HER2 antibody (B) using IHC method. The tumour cores were split into two groups: more than 80% percentage staining (4+) or less than 80% (2-3+). The medians of the average FRET efficiency were compared betweem two groups for both anti-pHER2 staining and anti-HER2 staining.

6.3 Discussion

In this chapter, HER2 phosphorylation status by FRET was established in MDAMB-453 xenograft tumours and breast TMAs, to test for the assay to be applied for use in the future prospective trials. The assessment of HER2 phosphorylation by FRET was compared with IHC in MDAMB-453 xenograft tumours and in archives of paraffin-embedded and formalin-fixed breast tumour arrays. The results showed that the phospho-antigen of HER2 was retained for tumours fixed immediately with formalin, after 1 hour on ice and at room temperature before fixation. Using IHC, anti-pHER2 staining was present in all three conditions and differences between them could not be detected. Using FRET to assess HER2 phosphorylation however revealed a decrease in FRET efficiency after 1 hour of delay in formalin fixation either on ice or at room temperature. The most likely explanation of the difference between IHC and FRET is that IHC depends on the subjective interpretation of the intensity of the membranous staining and the human eye does not have the dynamic range a camera has to enable a distinction. While the variation between the HER2 phosphorylation is small, the differences may be difficult to detect in a precise manner with the naked eye. Moreover, IHC can be affected by background staining which is less of a problem in FRET due to the use of two-site assay that increases the specificity of the method. The data therefore illustrate that variations in phosphorylation of HER2 can be detected by FRET whereas these differences cannot be quantified by IHC. The preservation of pHER2 was also assessed in MDAMB-453 xenografts using liquid nitrogen, either fixed immediately or left at 4°C for 24 hours before liquid nitrogen fixation. It was shown that FRET was more precise in determining HER2 phosphorylation status since IHC could not detect the difference that was shown by FRET. HER2 phosphorylation decreased with delay in liquid nitrogen fixation but was retained up to 24 hours at 4^0 C before fixation. This is important considering that there maybe delays in the operating theatre when the tumours are removed. It is important to note that the experiments to assess HER2 phosphorylation status by IHC and FRET were performed in parallel in

duplicate sets of tumour arrays. The processes for antigen-retrieval and the fixation of the tumour arrays with either formalin (NBF) or liquid nitrogen were therefore identical. It is speculated that the phosphotyrosine is retained may be in part because activated receptors will recruit SH2 domain adaptors/effectors that will help to protect the phosphotyrosine from dephosphorylation.

Although IHC staining for phosphorylated HER receptors is possible, the two-site FRET assay is more precise than IHC staining. The reason being that IHC may be affected by various factors including non-specific staining and concentration of the antibodies. HER2 is expressed in normal epithelial cells as well as some breast tumour cells. Background staining may be a problem in IHC when the concentration of primary antibodies is too high since the anti-HER2 or anti-pHER2 antibodies may bind to both normal cells and breast tumour cells. In contrast, background staining is not a problem in the two-site FRET assay. However, if the concentration of primary antibody is too low this may result in a low "signal-to-noise" ratio that in turn results in not being able to calculate the lifetime. The calculation of lifetime may also be affected by the concentration of the receptors. For example, in breast tumours with low HER2 concentration, the intensity of HER2-Cy3b was found to be too low for the lifetime to be calculated as shown in section 6.2.6. In this case, the "signal-to-noise" ratio may be low regardless of the concentration of the primary antibody.

Proteins are unstable and one particular study has shown that the variability in the type of fixatives, duration of fixation, tissue processing and IHC techniques including antigen retrieval processes may all affect the sensitivity and specificity of IHC (Vincent-Salomon et al., 2003). The same study however showed that a high accuracy of HER2 assessment by IHC maybe achieved by using a calibration processes which include antigen retrieval procedure, high dilutions of anti-HER2 antibody (to reduce background staining) and the use of specific controls. This recommendation can also apply to FRET experiments to assess HER2 phosphorylation in tumour arrays since the process of tissue processing is essentially similar to IHC. Various antigen retrieval processes may be performed to assess whether it affects the detection of HER2 phosphorylation status by FRET.

The quantity of tumour versus stromal components in tumour cores of TMAs may vary depend on how the tumour cores are collected and processed. In IHC, this variation of the stromal component may affect the IHC results since the scorings of IHC depends on the intensity of the staining as well as the percentage of staining cancer cells. In this chapter, using FRET, a variation of lifetime (indicating HER2 phosphorylation) was observed between the stromal component and tumour component of breast tumour slides. When selecting a region of interest that includes tumour and stromal areas, the intensity of the tumour area is much greater than the stromal area. The lifetime calculation will be based mainly on the area with greater intensity (i.e. the tumour area), and the stromal contribution may be minimal unless the tumour core contains minimal tumour tissue.

As discussed in the Introduction, determining a cut-off point for HER2 status by IHC and FISH is problematic and yet extremely important since the selection of patients for Herceptin is based on IHC (3+) or FISH (> 6 HER2 gene copies per nucleus, or ratio > 2.2). Selecting a cut-off point for "high" HER2 phosphorylation by FRET is also not straightforward. FRET efficiency is a continuous variable and selecting a cut-off point may be based on either prognosis of breast cancer patients or prediction for targeted therapy. Nevertheless, this needs to be done using the data from a prospective trial to have significance. In the small series (n=55) of HER2 positive breast cancer cases (n=55) presented in this chapter, the median FRET efficiency was used as a cut-off point in the first instance. The results were encouraging in that FRET was shown to be able to stratify patients further into different prognostic group among HER2 positive cases (IHC 2-3+). However, further validation of the cut-off points for FRET need to be performed in a large prospective trial.

Since HER2 has been shown to be the preferred dimerisation partner for other HER receptors, it is possible that HER2 may be activated through over-expression of other HER receptors or one of the ligands. It has been shown that Herceptin and Cisplatin were synergistic in MCF-7 cells (non HER2 over-expressing) engineered to over-express heregulin. One of the reasons for Herceptin to be effective in these cells is thought to be due to activation of HER2 via HER2/HER3 dimerisation as a result of heregulin over-expression (Arteaga, 2006; Menendez et al., 2006). This implies that patients without

HER2 over-expressing breast tumours may also respond to Herceptin in combination with chemotherapy. Using FRET may potentially be useful to select patients for Herceptin treatment regardless of the concentration status of HER2 by IHC or FISH and may be particularly useful in equivocal cases of IHC and FISH cases.

In this chapter, it is shown that FRET may be used to assess HER2 phosphorylation in paraffin sections as well as liquid-nitrogen frozen sections. Moreover, it may be used to stratify HER2 positive breast cancer patients into different prognostic groups. However, the results presented in this chapter are only a pilot study and further work needs to be performed on another set of HER2 positive tumour arrays. More patients will be needed in order to achieve enough power to detect statistically significant differences between the high FRET group and low FRET group. Further validation may need to be performed in large prospective trials. The future aim is that the prognostic and predictive values of FRET as well as a cut-off value may eventually be determined from the prospective trials.

7 Final Discussion

7.1 Overview

As discussed in the Introduction, the HER (ErbB) receptors are implicated in the pathogenesis of several cancers, including EGFR in head and neck cancer and HER2 in breast cancer (Salomon et al., 1995). Targeted therapies against EGFR and HER2 receptors are gaining an increasingly important role in the treatment of various cancers. For example, Herceptin was originally recommended by NICE to use only for metastatic breast cancer with HER2 over-expression due to the clinical benefits shown in a randomised trial (Slamon et al., 2001). Since the publication of the three trials in 2005 (NSABP B-31, NCCTG N9831, HERA) which showed a survival benefit for Herceptin to be given as adjuvant treatment during the early course of breast cancer (Piccart-Gebhart et al., 2005; Romond et al., 2005), there has been a worldwide increased use of Herceptin as adjuvant treatment in early breast cancer. The cost of adding this new drug to the management of breast cancer can be significant. It has been estimated that the cost of Herceptin is around £25 000 per patient per year (Dent and Clemons, 2005) and that treating early breast cancer for 75 patients would cost a hospital trust £1.9 millions on drug cost alone and £ 2.3 million when including other costs like pathology testing and cardiac monitoring for the drugs (Barrett A, 2006). Needless to say that the demand for this drug will have a lot of financial as well as ethical issues in the UK, with possible diversion of resources from other diseases. This is reflected by the constant debate among health care workers (Barrett A, 2006; Editorial, 2005) as well as in the public domain (in several BBC news' headlines) about the use of this drug since the publication of the three trials. Aside from the costs of the drugs and unpredictable response, up to 5-10% patients may have worsening cardiac function if given this drug with chemotherapy (Piccart-Gebhart et al., 2005). To correctly select cancer patients for these drugs in

order to exclude patients who will not benefit is a challenge for clinicians and scientists.

As discussed in the Introduction, over-expression and high levels of HER receptors do not necessarily reflect the functional state of their pathways, e.g. recent studies indicate that IHC reporting on EGFR expression levels is inconsistent in its predictions of disease recurrence and notably response to treatment (Arteaga, 2002; Dei Tos AP, 2005). EGFR inhibitors including Iressa are now given to patients without assessment of EGFR receptor concentration since EGFR has a poor predictive value (Chung et al., 2005). For breast cancer patients, despite the selection of patients by HER2 status (using either IHC or FISH), only about one third of these patients respond to Herceptin monotherapy (Vogel et al., 2002) and non-HER2 over-expressing breast tumours may also respond to Herceptin (Arteaga, 2006; Menendez et al., 2006). This emphasizes the need to understand at a higher level of detail the functional status of candidate markers employed in diagnostic, prognostic and therapeutic settings.

Monitoring response to treatment is of increasing importance with respect to trials of new molecular-directed therapeutics, as well as in seeking to optimise the use of those reaching the clinic. It is well accepted that the use of biomarkers in the development of new agents is important and it is implicit that these markers reflect the action of the target (whether direct or through a validated surrogate) and not simply its presence. The logic applied to the targeting and monitoring of inhibition for these targets is no less relevant to the question of prognostic indicators in relation to disease. The need to be able to determine the functional status of potential therapeutic targets or prognostic indicators is essential. Therefore, there is a need for a quantitative and objective method for assessing HER receptor phosphorylation to complement the current methods of HER receptor concentration testing by IHC.

7.2 Assessing HER receptor phosphorylation by FRET

In this thesis, the assessment of EGFR phosphorylation by FRET was first established in cell lines. These established reagents were applied to head and neck tumour arrays using a high throughput automated FLIM. It was shown that increased FRET (indicative of EGFR phosphorylation) was correlated with disease recurrence and prognosis of the patients. Moreover, the results showed that EGFR concentration and phosphorylation determined by FRET in these patients were not correlated. This is not surprising given that a number of mechanisms other than over-expression of EGFR receptors may cause increased activation of EGFR, including over-expression of ligands for EGFR and other HER receptors, dimerisation with HER2 receptors to induce cellular signalling as well as constitutive activated mutant EGFR receptors (Arteaga, 2002; Dei Tos AP, 2005). Other studies have shown that the response rate for EGFR inhibitors in head and neck cancer patients with over-expression of EGFR is only around 10% (Baselga et al., 2005; Cohen et al., 2003; Herbst et al., 2005) and patients without EGFR over-expression are also found to be responsive to Cetuximab in colon cancer (Chung et al., 2005). All these emphasise the importance of assessing EGFR phosphorylation rather than just concentration in these patients.

Currently the most accurate predictor of disease recurrence for HNSCC is the Tumour Node Metastasis (TNM) stage, particularly the lymph node status. There have been several studies seeking to find prognostic markers that can complement clinico-pathological information to predict survival and recurrence in HNSCC, e.g. EGFR over-expression level (Ang et al., 2002), TGF-α / EGFR mRNA (Dassonville et al., 1993) and p53 status (Boyle et al., 1993; Brennan et al., 1995). At present, an elevated level of TGF-∝ seems to be as important or even more important in classifying prognostic groups than EGFR expression level (Chung et al., 2004; Endo et al., 2000; Rubin Grandis et al., 1998; Todd et al., 1989; Wen et al., 1996). It is implicit that the ligand is engaging and activating its receptor and hence the assessment of activation status should be informative and indeed the data in this chapter supports this contention. The activation of the receptor measured by FRET gives prognostic information that is not available from analysing EGFR in the conventional way or even with phospho-antibodies as indicated by Chung et al 2004 (Chung et al., 2004).

FRET to assess HER2 phosphorylation was also established in A431 cells and breast cell lines. The assay was applied to assess HER2 phosphorylation in MDAMB-453 xenograft tumours. The results showed that variation in HER2 phosphorylation could be detected by FRET in xenograft tumours whereas these differences could not be quantified to the same extent by IHC that relies on subjective interpretation of the intensity staining. The FRET assay to assess HER2 phosphorylation was also applied to determine HER2 phosphorylation in a set of breast tumour arrays that was determined to be HER2 positive by IHC method. However, it was shown that FRET maybe used to stratify these HER2 positive breast cancer patients further into different prognostic groups, demonstrating the superiority of FRET over IHC.

7.3 Resistance to targeted therapies in breast cancer

Monotherapy with either EGFR and HER2 inhibitors (e.g. Iressa and Herceptin treatment), often results in a relatively poor response rate and the response is not usually sustained for the responders (Cohen et al., 2003; Vogel et al., 2002) due to primary and secondary resistance to these drugs. The FRET assay was used in breast cell lines, to measure the effect of these drugs on HER receptor phosphorylation. The method was established in cells prior to using it in clinical setting to stratify patients for targeted therapy. It was hypothesised that EGFR inhibition should abolish HER2 phosphorylation if HER2 is the preferred dimerisation partner for other HER receptors. This was however not the case. Using FRET to monitor HER2 phosphorylation, the responses of HER receptors in breast cancer cell lines were investigated when the cells were treated with targeted therapies. It was shown that the specific tyrosine kinase inhibitors of EGFR (HER1), AG1478 and Iressa decreased EGFR and HER3 phosphorylation through inhibition of EGFR/HER3 dimerisation, but induced activation and cleavage of HER4. It is implied that the dimerisation between HER2 and HER4 leads to HER2 phosphorylation. These drug–induced processes were mediated by the release of ligands

including heregulin and betacellulin that activate HER3 and HER4 via HER2. Whereas anti-betacellulin antibody in combination with Iressa increased the anti-proliferative effect, ligands like heregulin and betacellulin rendered sensitive SKBR3 resistant to Iressa. These results confirmed the role of ligands and activation of alternative HER receptors in mediating resistance to Iressa. It was also shown that Herceptin which targets the extra-cellular domain of HER2, induced the phosphorylation of HER2 receptors and cleavage of HER4 in SKBR3 cells through their ligands despite the ability to downregulate EGFR and HER2 in the long term. Therefore the results in cell lines provided a molecular mechanism for the resistance to Iressa and Herceptin through ligands-induced activation of alternative HER pathways. Both of these results highlight the complexity of action of targeted therapies and may indicate alternative strategies to investigate intervention.

The release of ligands from their membrane-anchored precursors (ectodomain shedding) is mediated by different metalloproteinases (including the ADAM family). For example, precursors of TGF-α are released by TACE (ADAM 17) (Sunnarborg et al., 2002) and precursors of neuregulin (heregulin) β-1 and β-4 are mediated by ADAM 19 (Shirakabe et al., 2001). However, many questions remain unanswered, including biosynthesis and activation of these metalloproteinases like TACE in the secretory pathway, their trafficking in different compartments, the regulation/specificity of TACE and other metalloproteinases in the processing and shedding of HER ligands and the exact cleavage sites of the ligand precursors (Dempsey et al., 2002). The specificity of metalloproteinases is particularly important since for example TACE has many substrates including the precursors of amphiregulin, TGF-α and heparin-binding EGF (Hinkle et al., 2004) as well as the HER 4 receptor (Carpenter, 2003; Vecchi and Carpenter, 1997). The complexities associated with the regulation of ectodomain shedding of these ligands by the metalloproteinases make it difficult to ascertain a definite role for a particular metalloproteinase in the processing of a HER ligand. Therefore, understanding the cleavage and activation of ligands by the metalloproteinases is key to providing further therapeutic intervention. Furthermore, investigating how this ectodomain shedding of the ligands is influenced by targeted therapy is also crucial. For example to understand the mechanisms of how betacellulin and

heregulin are released through the inhibition of EGFR may provide a strategy to overcome resistance to Iressa via activation of alternative HER receptors. The common understanding is that EGFR inhibitors like Iressa must switch off all tyrosine kinase activities of EGFR but it was suggested that Iressa may inactivate inhibitory kinase like GAK kinase and thus antagonise the inhibitory effect of the drug on EGFR signalling (Brehmer et al., 2005). The question of whether this inactivation of GAK kinase by Iressa is related to the regulation and production of ligands like betacellulin and heregulin remains to be answered. INCB3619, a potent inhibitor of ADAM 10 and ADAM 17, is effective in preventing the cleavage of heregulin and other ligands mediated by these two ADAM family members (Zhou et al., 2006) and it is currently being evaluated in the clinic (Fridman et al., 2007). However, INCB3619 being an inhibitor of ADAM 10 and ADAM 17, may not be effective in preventing the cleavage of ligands by other metalloproteinases, e.g. ADAM 19 which mediates heregulin β-1 and β-4 (Shirakabe et al., 2001).

7.4 Future prospects

It has been shown in this thesis that FRET may be used to assess phosphorylation of HER receptors quantitatively, in contrast to IHC which is semi-quantitative and may be subjective (Dei Tos AP, 2005). FRET uses a two-site assay, overcoming the problems of non-specificity of single antibody in IHC. The assay has been adapted to assess activation and phosphorylation of HER receptors in various cell lines as well as paraffin-embedded formalin-fixed tumour slides and arrays. The long-term aim is to exploit the strength of the FRET method to assess phosphorylation of HER receptors in relation to resistance and sensitivity to targeted therapies. This methodology (complementary to current methods, IHC and FISH) may be applied to select cancer patients who will respond to targeted therapies like Herceptin, and to determine potential resistance mechanisms and develop new treatment strategies or rational combinations of therapy. The method can also be used to assess HER dimerisation patterns if a suitable pair of antibodies were used, e.g.

conjugation of Cy3b to anti-HER2 and Cy5 to anti-HER3 to assess dimerisation of HER2/HER3. The dimerisation patterns of HER receptors are increasingly known to be important for the prognosis of several cancers and may predict sensitivity and resistance to targeted therapies. For example it was shown that HER2/HER4 and HER2/HER3 dimerisation partners maybe important in mediating resistance to EGFR inhibitors. Therefore, FRET may be exploited to assess phosphorylation of HER receptors as well as their dimerisation patterns to determine mechanisms of sensitivity and resistance to targeted therapies in breast cancer.

Since the studies in HNSCC and breast arrays presented in this thesis are only retrospective exploratory assessments of patients' survival, a prospective protocol driven assessment for validation and determination of performance characteristics needs to be performed using FRET as described by Hayes et al (Hayes et al., 1996; Hayes et al., 1998) in order to validate the FRET methods for wider clinical use. This strategy will allow the assays to be utilised for prospective stratification of patients in randomised trials of EGFR and HER2 inhibition.

The results from breast tumour arrays showed that FRET may be used to stratify patients further among HER2 positive patients, justifying the decision to apply this methodology to assess phosphorylation of HER2 and other HER receptors in a prospective breast cancer trial including adjuvant Herceptin (HERA) trial (Piccart-Gebhart et al., 2005; Smith et al., 2007). HERA trial is an international, multicenter, randomised trial compared one or two years of Herceptin given in HER2-positive breast cancer patients who had completed surgery, radiotherapy and chemotherapy (Piccart-Gebhart et al., 2005; Smith et al., 2007). It has been proposed that future work may involve assessing FRET as a prognostic tool and a predictive tool for DFS and OS in Herceptin and non Herceptin-treated patients of the (HERA) trial. In addition, the trial may also be used to validate the methodology as well as to select a cut-off point for FRET efficiency. The cut-off point may then be used to separate patients into good and bad prognostic groups and early relapse or late/non-relapse patients in the HERA trial. The cut-off point may be applied for other future trials once it is validated in this trial. This present investigation has shown that phosphorylation of alternative HER receptors may mediate resistance to

targeted therapies in breast cancer cells. Therefore, the hypothesis may be tested further in human breast cancer samples from HERA trial by investigating whether time to relapse on Herceptin in these patients is related to activation of alternative HER receptors and their dimerisation patterns. The relapse rate and the onset of relapse may also be correlated with gene expression arrays between the control arm and the treated arm in the HERA trial to assess the factors that determine who will benefit from Herceptin in breast cancer. The overall aim for the proposed works in the HERA trial is to assess whether FRET may be used as a diagnostic parameter to assess functional status of HER2. The accuracy of this putative diagnostic parameter may be exploited to identify breast cancer patients at presentation that may benefit from Herceptin and other targeted therapies and exclude non-responders from the potential side effects of the drugs. Similar strategies may also be applied to other prospective trials using the same methodology to assess the phosphorylation of HER2 and other HER receptors in breast cancer and other types of cancers in relation to targeted therapies.

Future research can also be done to further analyse the mechanisms of resistance to targeted therapies like Iressa, Herceptin and Lapatinib in hormone sensitive and resistant breast cell lines and in xenograft models. EGFR activation has been shown to play a role in hormone resistant breast cancer patients (Gee et al., 2003; Knowlden et al., 2003; Polychronis et al., 2005). Furthermore, HER receptors have been shown to interact with hormone receptors and contribute to resistance to hormone therapies in hormone-resistant breast cancer lines (Dowsett et al., 2005; Johnston et al., 2003; Martin et al., 2005; Martin et al., 2003). Future work may involve assessing EGFR and HER2 activation (as well as the dimerisation patterns of HER receptors) by FRET in hormone resistant MCF-7 cell lines with or without Iressa and Lapatinib treatment (acute versus long-term) in vitro and investigate their interaction with hormone receptors.

It has been shown that reactivation of HER3 occurs in prolonged Iressa treatment (Sergina et al., 2007) and heregulin mediated HER3 activation may play a role in mediating resistance to Iressa (Zhou et al., 2006). In this thesis it was demonstrated that acute treatment with Iressa and Herceptin (acute and up to 10 days of treatment) may induce activation of alternative HER receptors

(including HER3 phosphorylation) in breast cell lines. The goal for future investigation may be to assess phosphorylation and dimerisation patterns of HER receptors by FRET in relation to targeted therapies, e.g. acute and long-term treatment with Herceptin, Iressa and Lapatinib in breast cell lines and in xenograft models. Particularly HER3 phosphorylation and its dimerisation pattern with HER2 should be assessed. These results will be correlated with downstream signalling pathways like PKB and ERK1/2 phosphorylation using FRET to understand further the mechanisms of resistance to these drugs. These experiments can also be performed on human samples by for example conducting neoadjuvant Herceptin and Lapatinib trials, in order to understand the mechanisms of resistance to these drugs in human patients.

7.5 Concluding remarks

In this investigation, a novel method using FRET to assess HER receptor phosphorylation was established in both TMAs and cells. It was shown that the two-site assay FRET to assess HER phosphorylation is specific and may be applied to paraffin-embedded formalin-fixed head and neck as well as breast tissue arrays. Moreover, FRET may be used to stratify HER2 positive breast cancer patients into different prognostic groups. Using this method to assess HER receptors, it was demonstrated that Iressa and Herceptin treatment in breast cancer cells induced activation of alternative HER pathways, providing an insight into the mechanisms of resistance to these targeted therapies in breast cancer, and hence offering treatment opportunities to overcome resistance in patients. It is proposed to utilise this assay for prospective stratification of patients in randomised trials of EGFR and HER2 inhibition. Since it is applicable to paraffin sections, retrospective analysis of trials of EGFR and HER2 inhibitors will also be possible to define those who gain most, besides the patients with EGFR and HER2 mutations. In the longer term, the identification of these patients at presentation should provide guidance on more aggressive treatment or more specifically on appropriate targeted therapies. The methodology shows great promise and can also be applied to

assess the activation of other signalling pathways (e.g. PKB and MAPK) in relation to various cancer treatments.

References

Adams, E. J., Green, J. A., Clark, A. H., and Youngson, J. H. (1999). Comparison of different scoring systems for immunohistochemical staining. J Clin Pathol *52*, 75-77.

Aguilar, Z., Akita, R. W., Finn, R. S., Ramos, B. L., Pegram, M. D., Kabbinavar, F. F., Pietras, R. J., Pisacane, P., Sliwkowski, M. X., and Slamon, D. J. (1999). Biologic effects of heregulin/neu differentiation factor on normal and malignant human breast and ovarian epithelial cells. Oncogene *18*, 6050-6062.

Agus, D. B., Akita, R. W., Fox, W. D., Lewis, G. D., Higgins, B., Pisacane, P. I., Lofgren, J. A., Tindell, C., Evans, D. P., Maiese, K., *et al.* (2002). Targeting ligand-activated ErbB2 signaling inhibits breast and prostate tumor growth. Cancer Cell *2*, 127-137.

Agus, D. B., Sweeney, C. J., Morris, M. J., Mendelson, D. S., McNeel, D. G., Ahmann, F. R., Wang, J., Derynck, M. K., Ng, K., Lyons, B., *et al.* (2007). Efficacy and safety of single-agent pertuzumab (rhuMAb 2C4), a human epidermal growth factor receptor dimerization inhibitor, in castration-resistant prostate cancer after progression from taxane-based therapy. J Clin Oncol *25*, 675-681.

Alcor D, C. V. a. L. B. (2007). Revealing signalling in single cells by single and two-photon fluorescence imaging microscopy).

Anderson, N. G., Ahmad, T., Chan, K., Dobson, R., and Bundred, N. J. (2001). ZD1839 (Iressa), a novel epidermal growth factor receptor (EGFR) tyrosine kinase inhibitor, potently inhibits the growth of EGFR-positive cancer cell lines with or without erbB2 overexpression. Int J Cancer *94*, 774-782.

Ang, K. K., Berkey, B. A., Tu, X., Zhang, H. Z., Katz, R., Hammond, E. H., Fu, K. K., and Milas, L. (2002). Impact of epidermal growth factor receptor expression on survival and pattern of relapse in patients with advanced head and neck carcinoma. Cancer Res *62*, 7350-7356.

Anido, J., Matar, P., Albanell, J., Guzman, M., Rojo, F., Arribas, J., Averbuch, S., and Baselga, J. (2003). ZD1839, a specific epidermal growth factor receptor (EGFR) tyrosine kinase inhibitor, induces the formation of inactive

EGFR/HER2 and EGFR/HER3 heterodimers and prevents heregulin signaling in HER2-overexpressing breast cancer cells. Clin Cancer Res *9*, 1274-1283.

Arteaga, C. L. (2002). Epidermal growth factor receptor dependence in human tumors: more than just expression? Oncologist *7 Suppl 4*, 31-39.

Arteaga, C. L. (2006). Can trastuzumab be effective against tumors with low HER2/Neu (ErbB2) receptors? J Clin Oncol *24*, 3722-3725.

Arteaga, C. L., Ramsey, T. T., Shawver, L. K., and Guyer, C. A. (1997). Unliganded epidermal growth factor receptor dimerization induced by direct interaction of quinazolines with the ATP binding site. J Biol Chem *272*, 23247-23254.

Barrett A, R. T., Small M, Smith R (2006). How much will Herceptin really cost? BMJ *333*, 1118-1120.

Baselga, J. (2002). Combined anti-EGF receptor and anti-HER2 receptor therapy in breast cancer: a promising strategy ready for clinical testing. Ann Oncol *13*, 8-9.

Baselga, J., Trigo, J. M., Bourhis, J., Tortochaux, J., Cortes-Funes, H., Hitt, R., Gascon, P., Amellal, N., Harstrick, A., and Eckardt, A. (2005). Phase II multicenter study of the antiepidermal growth factor receptor monoclonal antibody cetuximab in combination with platinum-based chemotherapy in patients with platinum-refractory metastatic and/or recurrent squamous cell carcinoma of the head and neck. J Clin Oncol *23*, 5568-5577.

Baulida, J., Kraus, M. H., Alimandi, M., Di Fiore, P. P., and Carpenter, G. (1996). All ErbB receptors other than the epidermal growth factor receptor are endocytosis impaired. J Biol Chem *271*, 5251-5257.

Bazley, L. A., and Gullick, W. J. (2005). The epidermal growth factor receptor family. Endocr Relat Cancer *12 Suppl 1*, S17-27.

Beerli, R. R., and Hynes, N. E. (1996). Epidermal growth factor-related peptides activate distinct subsets of ErbB receptors and differ in their biological activities. J Biol Chem *271*, 6071-6076.

Bei, R., Budillon, A., Masuelli, L., Cereda, V., Vitolo, D., Di Gennaro, E., Ripavecchia, V., Palumbo, C., Ionna, F., Losito, S., *et al.* (2004). Frequent overexpression of multiple ErbB receptors by head and neck squamous cell carcinoma contrasts with rare antibody immunity in patients. J Pathol *204*, 317-325.

Bennasroune, A., Gardin, A., Aunis, D., Cremel, G., and Hubert, P. (2004). Tyrosine kinase receptors as attractive targets of cancer therapy. Crit Rev Oncol Hematol *50*, 23-38.

Bertram, J. S. (2000). The molecular biology of cancer. Mol Aspects Med *21*, 167-223.

Blume-Jensen, P., and Hunter, T. (2001). Oncogenic kinase signalling. Nature *411*, 355-365.

Bonner, J. A., Harari, P. M., Giralt, J., Azarnia, N., Shin, D. M., Cohen, R. B., Jones, C. U., Sur, R., Raben, D., Jassem, J., *et al.* (2006). Radiotherapy plus cetuximab for squamous-cell carcinoma of the head and neck. N Engl J Med *354*, 567-578.

Boyle, J. O., Hakim, J., Koch, W., van der Riet, P., Hruban, R. H., Roa, R. A., Correo, R., Eby, Y. J., Ruppert, J. M., and Sidransky, D. (1993). The incidence of p53 mutations increases with progression of head and neck cancer. Cancer Res *53*, 4477-4480.

Brehmer, D., Greff, Z., Godl, K., Blencke, S., Kurtenbach, A., Weber, M., Muller, S., Klebl, B., Cotten, M., Keri, G., *et al.* (2005). Cellular targets of gefitinib. Cancer Res *65*, 379-382.

Brennan, J. A., Mao, L., Hruban, R. H., Boyle, J. O., Eby, Y. J., Koch, W. M., Goodman, S. N., and Sidransky, D. (1995). Molecular assessment of histopathological staging in squamous-cell carcinoma of the head and neck. N Engl J Med *332*, 429-435.

Britten, C. D. (2004). Targeting ErbB receptor signaling: a pan-ErbB approach to cancer. Mol Cancer Ther *3*, 1335-1342.

Calleja, V., Alcor, D., Laguerre, M., Park, J., Vojnovic, B., Hemmings, B. A., Downward, J., Parker, P. J., and Larijani, B. (2007). Intramolecular and Intermolecular Interactions of Protein Kinase B Define Its Activation In Vivo. PLoS Biol *5*, e95.

Carpenter, G. (2003). ErbB-4: mechanism of action and biology. Exp Cell Res *284*, 66-77.

Chan-Hui, P. Y., Stephens, K., Warnock, R. A., and Singh, S. (2004). Applications of eTag trade mark assay platform to systems biology approaches in molecular oncology and toxicology studies. Clin Immunol *111*, 162-174.

Chen, S., and Parmigiani, G. (2007). Meta-analysis of BRCA1 and BRCA2 penetrance. J Clin Oncol *25*, 1329-1333.

Cheng, Q. C., Tikhomirov, O., Zhou, W., and Carpenter, G. (2003). Ectodomain cleavage of ErbB-4: characterization of the cleavage site and m80 fragment. J Biol Chem *278*, 38421-38427.

Cho, H. S., Mason, K., Ramyar, K. X., Stanley, A. M., Gabelli, S. B., Denney, D. W., Jr., and Leahy, D. J. (2003). Structure of the extracellular region of HER2 alone and in complex with the Herceptin Fab. Nature *421*, 756-760.

Chung, C. H., Ely, K., McGavran, L., Varella-Garcia, M., Parker, J., Parker, N., Jarrett, C., Carter, J., Murphy, B. A., Netterville, J., *et al.* (2006). Increased epidermal growth factor receptor gene copy number is associated with poor prognosis in head and neck squamous cell carcinomas. J Clin Oncol *24*, 4170-4176.

Chung, C. H., Parker, J. S., Karaca, G., Wu, J., Funkhouser, W. K., Moore, D., Butterfoss, D., Xiang, D., Zanation, A., Yin, X., *et al.* (2004). Molecular classification of head and neck squamous cell carcinomas using patterns of gene expression. Cancer Cell *5*, 489-500.

Chung, K. Y., Shia, J., Kemeny, N. E., Shah, M., Schwartz, G. K., Tse, A., Hamilton, A., Pan, D., Schrag, D., Schwartz, L., *et al.* (2005). Cetuximab shows activity in colorectal cancer patients with tumors that do not express the epidermal growth factor receptor by immunohistochemistry. J Clin Oncol *23*, 1803-1810.

Ciardiello, F., Troiani, T., Bianco, R., Orditura, M., Morgillo, F., Martinelli, E., Morelli, M. P., Cascone, T., and Tortora, G. (2006). Interaction between the epidermal growth factor receptor (EGFR) and the vascular endothelial growth factor (VEGF) pathways: a rational approach for multi-target anticancer therapy. Ann Oncol *17*, vii109-vii114.

Citri, A., Skaria, K. B., and Yarden, Y. (2003). The deaf and the dumb: the biology of ErbB-2 and ErbB-3. Exp Cell Res *284*, 54-65.

Citri, A., and Yarden, Y. (2006). EGF-ERBB signalling: towards the systems level. Nat Rev Mol Cell Biol *7*, 505-516.

Clynes, R. A., Towers, T. L., Presta, L. G., and Ravetch, J. V. (2000). Inhibitory Fc receptors modulate in vivo cytoxicity against tumor targets. Nat Med *6*, 443-446.

Cohen, E. E., Rosen, F., Stadler, W. M., Recant, W., Stenson, K., Huo, D., and Vokes, E. E. (2003). Phase II trial of ZD1839 in recurrent or metastatic squamous cell carcinoma of the head and neck. J Clin Oncol *21*, 1980-1987.

Cooley, S., Burns, L. J., Repka, T., and Miller, J. S. (1999). Natural killer cell cytotoxicity of breast cancer targets is enhanced by two distinct mechanisms of antibody-dependent cellular cytotoxicity against LFA-3 and HER2/neu. Exp Hematol *27*, 1533-1541.

Cuello, M., Ettenberg, S. A., Clark, A. S., Keane, M. M., Posner, R. H., Nau, M. M., Dennis, P. A., and Lipkowitz, S. (2001). Down-regulation of the erbB-2 receptor by trastuzumab (herceptin) enhances tumor necrosis factor-related apoptosis-inducing ligand-mediated apoptosis in breast and ovarian cancer cell lines that overexpress erbB-2. Cancer Res *61*, 4892-4900.

Cunningham, D., Humblet, Y., Siena, S., Khayat, D., Bleiberg, H., Santoro, A., Bets, D., Mueser, M., Harstrick, A., Verslype, C., *et al.* (2004). Cetuximab monotherapy and cetuximab plus irinotecan in irinotecan-refractory metastatic colorectal cancer. N Engl J Med *351*, 337-345.

Dassonville, O., Formento, J. L., Francoual, M., Ramaioli, A., Santini, J., Schneider, M., Demard, F., and Milano, G. (1993). Expression of epidermal growth factor receptor and survival in upper aerodigestive tract cancer. J Clin Oncol *11*, 1873-1878.

Davidson, N. E., Gelmann, E. P., Lippman, M. E., and Dickson, R. B. (1987). Epidermal growth factor receptor gene expression in estrogen receptor-positive and negative human breast cancer cell lines. Mol Endocrinol *1*, 216-223.

de Bono, J. S., Bellmunt, J., Attard, G., Droz, J. P., Miller, K., Flechon, A., Sternberg, C., Parker, C., Zugmaier, G., Hersberger-Gimenez, V., *et al.* (2007). Open-label phase II study evaluating the efficacy and safety of two doses of pertuzumab in castrate chemotherapy-naive patients with hormone-refractory prostate cancer. J Clin Oncol *25*, 257-262.

Dei Tos AP, E. I. (2005). Assessing epidermal growth factor receptor expression in tumours : What is the value of current test methods? European Journal of Cancer *41*, 1383-1392.

Dempsey, P. J., Garton, K., and Raines, E. W. (2002). Emerging roles of TACE as a key protease in ErbB ligand shedding. Mol Interv *2*, 136-141.

Dent, R., and Clemons, M. (2005). Adjuvant trastuzumab for breast cancer. Bmj *331*, 1035-1036.

Depowski, P. L., Rosenthal, S. I., and Ross, J. S. (2001). Loss of expression of the PTEN gene protein product is associated with poor outcome in breast cancer. Mod Pathol *14*, 672-676.

Downward, J. (2006). Signal transduction. Prelude to an anniversary for the RAS oncogene. Science *314*, 433-434.

Downward, J., Yarden, Y., Mayes, E., Scrace, G., Totty, N., Stockwell, P., Ullrich, A., Schlessinger, J., and Waterfield, M. D. (1984). Close similarity of epidermal growth factor receptor and v-erb-B oncogene protein sequences. Nature *307*, 521-527.

Dowsett, M., Martin, L. A., Smith, I., and Johnston, S. (2005). Mechanisms of resistance to aromatase inhibitors. J Steroid Biochem Mol Biol *95*, 167-172.

Editorial (2005). Herceptin and early breast cancer: a moment for caution. Lancet *366*, 1673.

Elenius, K., Choi, C. J., Paul, S., Santiestevan, E., Nishi, E., and Klagsbrun, M. (1999). Characterization of a naturally occurring ErbB4 isoform that does not bind or activate phosphatidyl inositol 3-kinase. Oncogene *18*, 2607-2615.

Endo, S., Zeng, Q., Burke, N. A., He, Y., Melhem, M. F., Watkins, S. F., Lango, M. N., Drenning, S. D., Huang, L., and Rubin Grandis, J. (2000). TGF-alpha antisense gene therapy inhibits head and neck squamous cell carcinoma growth in vivo. Gene Ther *7*, 1906-1914.

Engelman, J. A., Janne, P. A., Mermel, C., Pearlberg, J., Mukohara, T., Fleet, C., Cichowski, K., Johnson, B. E., and Cantley, L. C. (2005). ErbB-3 mediates phosphoinositide 3-kinase activity in gefitinib-sensitive non-small cell lung cancer cell lines. Proc Natl Acad Sci U S A *102*, 3788-3793.

Fan, Y. S., Davis, L. M., and Shows, T. B. (1990). Mapping small DNA sequences by fluorescence in situ hybridization directly on banded metaphase chromosomes. Proc Natl Acad Sci U S A *87*, 6223-6227.

Fitzgibbons, P. L., Page, D. L., Weaver, D., Thor, A. D., Allred, D. C., Clark, G. M., Ruby, S. G., O'Malley, F., Simpson, J. F., Connolly, J. L., *et al.* (2000). Prognostic factors in breast cancer. College of American Pathologists Consensus Statement 1999. Arch Pathol Lab Med *124*, 966-978.

Förster, V. (1948). Zwischenmolekulare Energlewanderung undFluoreszenz (Intermolecular energy migration and fluorescence). Annalen Der Physik *2*, 55-75.

Franklin, M. C., Carey, K. D., Vajdos, F. F., Leahy, D. J., de Vos, A. M., and Sliwkowski, M. X. (2004). Insights into ErbB signaling from the structure of the ErbB2-pertuzumab complex. Cancer Cell *5*, 317-328.

Fridman, J. S., Caulder, E., Hansbury, M., Liu, X., Yang, G., Wang, Q., Lo, Y., Zhou, B. B., Pan, M., Thomas, S. M., *et al.* (2007). Selective inhibition of ADAM metalloproteases as a novel approach for modulating ErbB pathways in cancer. Clin Cancer Res *13*, 1892-1902.

Fukuoka, M., Yano, S., Giaccone, G., Tamura, T., Nakagawa, K., Douillard, J. Y., Nishiwaki, Y., Vansteenkiste, J., Kudoh, S., Rischin, D., *et al.* (2003). Multi-institutional randomized phase II trial of gefitinib for previously treated patients with advanced non-small-cell lung cancer (The IDEAL 1 Trial) [corrected]. J Clin Oncol *21*, 2237-2246.

Gee, J. M., Harper, M. E., Hutcheson, I. R., Madden, T. A., Barrow, D., Knowlden, J. M., McClelland, R. A., Jordan, N., Wakeling, A. E., and Nicholson, R. I. (2003). The antiepidermal growth factor receptor agent gefitinib (ZD1839/Iressa) improves antihormone response and prevents development of resistance in breast cancer in vitro. Endocrinology *144*, 5105-5117.

Generali, D., Leek, R., Fox, S. B., Moore, J. W., Taylor, C., Chambers, P., and Harris, A. L. (2007). EGFR mutations in exons 18-21 in sporadic breast cancer. Ann Oncol *18*, 203-205.

Geyer, C. (2006). A Phase III Randomized, Open-Label, International Study Comparing Lapatinib and Capecitabine Vs. Capecitabine in Women With Refractory Advanced Metastatic Breast Cancer (EGF100151). American Society of Clinical Oncology 2006 Annual Meeting (ASCO) Late Breaker Presentation.

Geyer, C. E., Forster, J., Lindquist, D., Chan, S., Romieu, C. G., Pienkowski, T., Jagiello-Gruszfeld, A., Crown, J., Chan, A., Kaufman, B., *et al.* (2006). Lapatinib plus capecitabine for HER2-positive advanced breast cancer. N Engl J Med *355*, 2733-2743.

Gordon, M. S., Matei, D., Aghajanian, C., Matulonis, U. A., Brewer, M., Fleming, G. F., Hainsworth, J. D., Garcia, A. A., Pegram, M. D., Schilder, R. J., *et al.* (2006). Clinical activity of pertuzumab (rhuMAb 2C4), a HER dimerization inhibitor, in advanced ovarian cancer: potential predictive relationship with tumor HER2 activation status. J Clin Oncol *24*, 4324-4332.

Grander, D. (1998). How do mutated oncogenes and tumor suppressor genes cause cancer? Med Oncol *15*, 20-26.

Graus-Porta, D., Beerli, R. R., Daly, J. M., and Hynes, N. E. (1997). ErbB-2, the preferred heterodimerization partner of all ErbB receptors, is a mediator of lateral signaling. Embo J *16*, 1647-1655.

Gupta, A. K., McKenna, W. G., Weber, C. N., Feldman, M. D., Goldsmith, J. D., Mick, R., Machtay, M., Rosenthal, D. I., Bakanauskas, V. J., Cerniglia, G. J., *et al.* (2002). Local recurrence in head and neck cancer: relationship to radiation resistance and signal transduction. Clin Cancer Res *8*, 885-892.

Hanahan D, W. R. e. a. (2000). The hallmarks of cancer. Cell *100*, 57-70.

Hartmann, L. C., Ingle, J. N., Wold, L. E., Farr, G. H., Jr., Grill, J. P., Su, J. Q., Maihle, N. J., Krook, J. E., Witzig, T. E., and Roche, P. C. (1994). Prognostic value of c-erbB2 overexpression in axillary lymph node positive breast cancer. Results from a randomized adjuvant treatment protocol. Cancer *74*, 2956-2963.

Hayes, D. F., Bast, R. C., Desch, C. E., Fritsche, H., Jr., Kemeny, N. E., Jessup, J. M., Locker, G. Y., Macdonald, J. S., Mennel, R. G., Norton, L., *et al.* (1996). Tumor marker utility grading system: a framework to evaluate clinical utility of tumor markers. J Natl Cancer Inst *88*, 1456-1466.

Hayes, D. F., Trock, B., and Harris, A. L. (1998). Assessing the clinical impact of prognostic factors: when is "statistically significant" clinically useful? Breast Cancer Res Treat *52*, 305-319.

Herbst, R. S. (2004). Review of epidermal growth factor receptor biology. Int J Radiat Oncol Biol Phys *59*, 21-26.

Herbst, R. S., Arquette, M., Shin, D. M., Dicke, K., Vokes, E. E., Azarnia, N., Hong, W. K., and Kies, M. S. (2005). Phase II multicenter study of the epidermal growth factor receptor antibody cetuximab and cisplatin for recurrent and refractory squamous cell carcinoma of the head and neck. J Clin Oncol *23*, 5578-5587.

Hinkle, C. L., Sunnarborg, S. W., Loiselle, D., Parker, C. E., Stevenson, M., Russell, W. E., and Lee, D. C. (2004). Selective roles for tumor necrosis factor alpha-converting enzyme/ADAM17 in the shedding of the epidermal growth factor receptor ligand family: the juxtamembrane stalk determines cleavage efficiency. J Biol Chem *279*, 24179-24188.

Hirsch, F. R., Varella-Garcia, M., Bunn, P. A., Jr., Di Maria, M. V., Veve, R., Bremmes, R. M., Baron, A. E., Zeng, C., and Franklin, W. A. (2003). Epidermal growth factor receptor in non-small-cell lung carcinomas: correlation between gene copy number and protein expression and impact on prognosis. J Clin Oncol *21*, 3798-3807.

Jares-Erijman, E. A., and Jovin, T. M. (2003). FRET imaging. Nat Biotechnol *21*, 1387-1395.

Johnston, S. R., Head, J., Pancholi, S., Detre, S., Martin, L. A., Smith, I. E., and Dowsett, M. (2003). Integration of signal transduction inhibitors with endocrine therapy: an approach to overcoming hormone resistance in breast cancer. Clin Cancer Res *9*, 524S-532S.

Kakar, S., Puangsuvan, N., Stevens, J. M., Serenas, R., Mangan, G., Sahai, S., and Mihalov, M. L. (2000). HER-2/neu assessment in breast cancer by immunohistochemistry and fluorescence in situ hybridization: comparison of results and correlation with survival. Mol Diagn *5*, 199-207.

Kersemaekers, A. M., Fleuren, G. J., Kenter, G. G., Van den Broek, L. J., Uljee, S. M., Hermans, J., and Van de Vijver, M. J. (1999). Oncogene alterations in carcinomas of the uterine cervix: overexpression of the epidermal growth factor receptor is associated with poor prognosis. Clin Cancer Res *5*, 577-586.

King, R. (2000). Cancer Biology, Second Edition edn: Pearson Education Limited).

Knowlden, J. M., Hutcheson, I. R., Jones, H. E., Madden, T., Gee, J. M., Harper, M. E., Barrow, D., Wakeling, A. E., and Nicholson, R. I. (2003). Elevated levels of epidermal growth factor receptor/c-erbB2 heterodimers mediate an autocrine growth regulatory pathway in tamoxifen-resistant MCF-7 cells. Endocrinology *144*, 1032-1044.

Knudson, A. G., Jr. (1971). Mutation and cancer: statistical study of retinoblastoma. Proc Natl Acad Sci U S A *68*, 820-823.

Konecny, G. E., Pegram, M. D., Venkatesan, N., Finn, R., Yang, G., Rahmeh, M., Untch, M., Rusnak, D. W., Spehar, G., Mullin, R. J., *et al.* (2006). Activity of the dual kinase inhibitor lapatinib (GW572016) against HER-2-overexpressing and trastuzumab-treated breast cancer cells. Cancer Res *66*, 1630-1639.

Kong, A., Leboucher, P., Leek, R., Calleja, V., Winter, S., Harris, A., Parker, P. J., and Larijani, B. (2006). Prognostic value of an activation state marker for epidermal growth factor receptor in tissue microarrays of head and neck cancer. Cancer Res *66*, 2834-2843.

Kris, M. G., Natale, R. B., Herbst, R. S., Lynch, T. J., Jr., Prager, D., Belani, C. P., Schiller, J. H., Kelly, K., Spiridonidis, H., Sandler, A., *et al.* (2003). Efficacy of gefitinib, an inhibitor of the epidermal growth factor receptor tyrosine kinase, in symptomatic patients with non-small cell lung cancer: a randomized trial. Jama *290*, 2149-2158.

Kwak, E. L., Jankowski, J., Thayer, S. P., Lauwers, G. Y., Brannigan, B. W., Harris, P. L., Okimoto, R. A., Haserlat, S. M., Driscoll, D. R., Ferry, D., *et al.* (2006). Epidermal growth factor receptor kinase domain mutations in esophageal and pancreatic adenocarcinomas. Clin Cancer Res *12*, 4283-4287.

Lakowicz, J. R. (1999). Principles of Fluorescence Spectroscopy (New York: Kluewer Academic/Plenum Publishers).

Lane, H. A., Motoyama, A. B., Beuvink, I., and Hynes, N. E. (2001). Modulation of p27/Cdk2 complex formation through 4D5-mediated inhibition of HER2 receptor signaling. Ann Oncol *12 Suppl 1*, S21-22.

Larijani, B. (2006). Biological applications of single- and two-photon fluorescence: John Wiley & Sons, Ltd).

Larijani, B., Allen-Baume, V., Morgan, C. P., Li, M., and Cockcroft, S. (2003). EGF regulation of PITP dynamics is blocked by inhibitors of phospholipase C and of the Ras-MAP kinase pathway. Curr Biol *13*, 78-84.

Lee, E. Y., To, H., Shew, J. Y., Bookstein, R., Scully, P., and Lee, W. H. (1988). Inactivation of the retinoblastoma susceptibility gene in human breast cancers. Science *241*, 218-221.

Lee, J. W., Soung, Y. H., Seo, S. H., Kim, S. Y., Park, C. H., Wang, Y. P., Park, K., Nam, S. W., Park, W. S., Kim, S. H., *et al.* (2006). Somatic

mutations of ERBB2 kinase domain in gastric, colorectal, and breast carcinomas. Clin Cancer Res *12*, 57-61.

Lenferink, A. E., Pinkas-Kramarski, R., van de Poll, M. L., van Vugt, M. J., Klapper, L. N., Tzahar, E., Waterman, H., Sela, M., van Zoelen, E. J., and Yarden, Y. (1998). Differential endocytic routing of homo- and hetero-dimeric ErbB tyrosine kinases confers signaling superiority to receptor heterodimers. Embo J *17*, 3385-3397.

Lewis, G. D., Lofgren, J. A., McMurtrey, A. E., Nuijens, A., Fendly, B. M., Bauer, K. D., and Sliwkowski, M. X. (1996). Growth regulation of human breast and ovarian tumor cells by heregulin: Evidence for the requirement of ErbB2 as a critical component in mediating heregulin responsiveness. Cancer Res *56*, 1457-1465.

Lichtner, R. B., Menrad, A., Sommer, A., Klar, U., and Schneider, M. R. (2001). Signaling-inactive epidermal growth factor receptor/ligand complexes in intact carcinoma cells by quinazoline tyrosine kinase inhibitors. Cancer Res *61*, 5790-5795.

Loeffler-Ragg, J., Witsch-Baumgartner, M., Tzankov, A., Hilbe, W., Schwentner, I., Sprinzl, G. M., Utermann, G., and Zwierzina, H. (2006). Low incidence of mutations in EGFR kinase domain in Caucasian patients with head and neck squamous cell carcinoma. Eur J Cancer *42*, 109-111.

Lynch, T. J., Bell, D. W., Sordella, R., Gurubhagavatula, S., Okimoto, R. A., Brannigan, B. W., Harris, P. L., Haserlat, S. M., Supko, J. G., Haluska, F. G., *et al.* (2004). Activating mutations in the epidermal growth factor receptor underlying responsiveness of non-small-cell lung cancer to gefitinib. N Engl J Med *350*, 2129-2139.

Marks, J. R., Humphrey, P. A., Wu, K., Berry, D., Bandarenko, N., Kerns, B. J., and Iglehart, J. D. (1994). Overexpression of p53 and HER-2/neu proteins as prognostic markers in early stage breast cancer. Ann Surg *219*, 332-341.

Martin, L. A., Farmer, I., Johnston, S. R., Ali, S., and Dowsett, M. (2005). Elevated ERK1/ERK2/estrogen receptor cross-talk enhances estrogen-mediated signaling during long-term estrogen deprivation. Endocr Relat Cancer *12 Suppl 1*, S75-84.

Martin, L. A., Farmer, I., Johnston, S. R., Ali, S., Marshall, C., and Dowsett, M. (2003). Enhanced estrogen receptor (ER) alpha, ERBB2, and MAPK signal

transduction pathways operate during the adaptation of MCF-7 cells to long term estrogen deprivation. J Biol Chem *278*, 30458-30468.

McMenamin, M. E., Soung, P., Perera, S., Kaplan, I., Loda, M., and Sellers, W. R. (1999). Loss of PTEN expression in paraffin-embedded primary prostate cancer correlates with high Gleason score and advanced stage. Cancer Res *59*, 4291-4296.

Menard, S., Pupa, S. M., Campiglio, M., and Tagliabue, E. (2003). Biologic and therapeutic role of HER2 in cancer. Oncogene *22*, 6570-6578.

Mendelsohn, J., and Baselga, J. (2003). Status of epidermal growth factor receptor antagonists in the biology and treatment of cancer. J Clin Oncol *21*, 2787-2799.

Mendelsohn, J., and Baselga, J. (2006). Epidermal growth factor receptor targeting in cancer. Semin Oncol *33*, 369-385.

Menendez, J. A., Mehmi, I., and Lupu, R. (2006). Trastuzumab in combination with heregulin-activated Her-2 (erbB-2) triggers a receptor-enhanced chemosensitivity effect in the absence of Her-2 overexpression. J Clin Oncol *24*, 3735-3746.

Mere, L., Bennett, T., Coassin, P., England, P., Hamman, B., Rink, T., Zimmerman, S., and Negulescu, P. (1999). Miniaturized FRET assays and microfluidics: key components for ultra-high-throughput screening. Drug Discov Today *4*, 363-369.

Mitchell, M. S., and Press, M. F. (1999). The role of immunohistochemistry and fluorescence in situ hybridization for HER2/neu in assessing the prognosis of breast cancer. Semin Oncol *26*, 108-116.

Miyawaki, A. (2003). Visualization of the spatial and temporal dynamics of intracellular signaling. Dev Cell *4*, 295-305.

Moasser, M. M., Basso, A., Averbuch, S. D., and Rosen, N. (2001). The tyrosine kinase inhibitor ZD1839 ("Iressa") inhibits HER2-driven signaling and suppresses the growth of HER2-overexpressing tumor cells. Cancer Res *61*, 7184-7188.

Molina, M. A., Codony-Servat, J., Albanell, J., Rojo, F., Arribas, J., and Baselga, J. (2001). Trastuzumab (herceptin), a humanized anti-Her2 receptor monoclonal antibody, inhibits basal and activated Her2 ectodomain cleavage in breast cancer cells. Cancer Res *61*, 4744-4749.

Moscatello, D. K., Holgado-Madruga, M., Godwin, A. K., Ramirez, G., Gunn, G., Zoltick, P. W., Biegel, J. A., Hayes, R. L., and Wong, A. J. (1995). Frequent expression of a mutant epidermal growth factor receptor in multiple human tumors. Cancer Res *55*, 5536-5539.

Moulder, S. L., Yakes, F. M., Muthuswamy, S. K., Bianco, R., Simpson, J. F., and Arteaga, C. L. (2001). Epidermal growth factor receptor (HER1) tyrosine kinase inhibitor ZD1839 (Iressa) inhibits HER2/neu (erbB2)-overexpressing breast cancer cells in vitro and in vivo. Cancer Res *61*, 8887-8895.

Nagata, Y., Lan, K. H., Zhou, X., Tan, M., Esteva, F. J., Sahin, A. A., Klos, K. S., Li, P., Monia, B. P., Nguyen, N. T., *et al.* (2004). PTEN activation contributes to tumor inhibition by trastuzumab, and loss of PTEN predicts trastuzumab resistance in patients. Cancer Cell *6*, 117-127.

Ni, C. Y., Murphy, M. P., Golde, T. E., and Carpenter, G. (2001). gamma - Secretase cleavage and nuclear localization of ErbB-4 receptor tyrosine kinase. Science *294*, 2179-2181.

Nicholson, R. I., Gee, J. M., and Harper, M. E. (2001). EGFR and cancer prognosis. Eur J Cancer *37 Suppl 4*, S9-15.

Nicholson, S., Sainsbury, J. R., Halcrow, P., Chambers, P., Farndon, J. R., and Harris, A. L. (1989). Expression of epidermal growth factor receptors associated with lack of response to endocrine therapy in recurrent breast cancer. Lancet *1*, 182-185.

Normanno, N., Campiglio, M., De, L. A., Somenzi, G., Maiello, M., Ciardiello, F., Gianni, L., Salomon, D. S., and Menard, S. (2002). Cooperative inhibitory effect of ZD1839 (Iressa) in combination with trastuzumab (Herceptin) on human breast cancer cell growth. Ann Oncol *13*, 65-72.

Okamoto, I., Araki, J., Suto, R., Shimada, M., Nakagawa, K., and Fukuoka, M. (2006). EGFR mutation in gefitinib-responsive small-cell lung cancer. Ann Oncol *17*, 1028-1029.

Olayioye, M. A., Neve, R. M., Lane, H. A., and Hynes, N. E. (2000). The ErbB signaling network: receptor heterodimerization in development and cancer. Embo J *19*, 3159-3167.

Paez, J. G., Janne, P. A., Lee, J. C., Tracy, S., Greulich, H., Gabriel, S., Herman, P., Kaye, F. J., Lindeman, N., Boggon, T. J., *et al.* (2004). EGFR

mutations in lung cancer: correlation with clinical response to gefitinib therapy. Science *304*, 1497-1500.

Parra, H. S., Cavina, R., Latteri, F., Zucali, P. A., Campagnoli, E., Morenghi, E., Grimaldi, G. C., Roncalli, M., and Santoro, A. (2004). Analysis of epidermal growth factor receptor expression as a predictive factor for response to gefitinib ('Iressa', ZD1839) in non-small-cell lung cancer. Br J Cancer *91*, 208-212.

Parsons, M., Vojnovic, B., and Ameer-Beg, S. (2004). Imaging protein-protein interactions in cell motility using fluorescence resonance energy transfer (FRET). Biochem Soc Trans *32*, 431-433.

Pauletti, G., Dandekar, S., Rong, H., Ramos, L., Peng, H., Seshadri, R., and Slamon, D. J. (2000). Assessment of methods for tissue-based detection of the HER-2/neu alteration in human breast cancer: a direct comparison of fluorescence in situ hybridization and immunohistochemistry. J Clin Oncol *18*, 3651-3664.

Pawson, T., and Scott, J. D. (1997). Signaling through scaffold, anchoring, and adaptor proteins. Science *278*, 2075-2080.

Perez-Soler, R., Chachoua, A., Hammond, L. A., Rowinsky, E. K., Huberman, M., Karp, D., Rigas, J., Clark, G. M., Santabarbara, P., and Bonomi, P. (2004). Determinants of tumor response and survival with erlotinib in patients with non--small-cell lung cancer. J Clin Oncol *22*, 3238-3247.

Piccart-Gebhart, M. J., Procter, M., Leyland-Jones, B., Goldhirsch, A., Untch, M., Smith, I., Gianni, L., Baselga, J., Bell, R., Jackisch, C., *et al.* (2005). Trastuzumab after adjuvant chemotherapy in HER2-positive breast cancer. N Engl J Med *353*, 1659-1672.

Polverini, P. J., and Nor, J. E. (1999). Apoptosis and predisposition to oral cancer. Crit Rev Oral Biol Med *10*, 139-152.

Polychronis, A., Sinnett, H. D., Hadjiminas, D., Singhal, H., Mansi, J. L., Shivapatham, D., Shousha, S., Jiang, J., Peston, D., Barrett, N., *et al.* (2005). Preoperative gefitinib versus gefitinib and anastrozole in postmenopausal patients with oestrogen-receptor positive and epidermal-growth-factor-receptor-positive primary breast cancer: a double-blind placebo-controlled phase II randomised trial. Lancet Oncol *6*, 383-391.

Press, M. F., Hung, G., Godolphin, W., and Slamon, D. J. (1994). Sensitivity of HER-2/neu antibodies in archival tissue samples: potential source of error in immunohistochemical studies of oncogene expression. Cancer Res *54*, 2771-2777.

Rae, J. M., Scheys, J. O., Clark, K. M., Chadwick, R. B., Kiefer, M. C., and Lippman, M. E. (2004). EGFR and EGFRvIII expression in primary breast cancer and cell lines. Breast Cancer Res Treat *87*, 87-95.

Ramos-Vara, J. A. (2005). Technical aspects of immunohistochemistry. Vet Pathol *42*, 405-426.

Robinson, D. R., Wu, Y. M., and Lin, S. F. (2000). The protein tyrosine kinase family of the human genome. Oncogene *19*, 5548-5557.

Romond, E. H., Perez, E. A., Bryant, J., Suman, V. J., Geyer, C. E., Jr., Davidson, N. E., Tan-Chiu, E., Martino, S., Paik, S., Kaufman, P. A., *et al.* (2005). Trastuzumab plus adjuvant chemotherapy for operable HER2-positive breast cancer. N Engl J Med *353*, 1673-1684.

Rosen, P. P., Lesser, M. L., Arroyo, C. D., Cranor, M., Borgen, P., and Norton, L. (1995). Immunohistochemical detection of HER2/neu in patients with axillary lymph node negative breast carcinoma. A study of epidemiologic risk factors, histologic features, and prognosis. Cancer *75*, 1320-1326.

Ross, J. S., and Fletcher, J. A. (1999). HER-2/neu (c-erb-B2) gene and protein in breast cancer. Am J Clin Pathol *112*, S53-67.

Rubin Grandis, J., Melhem, M. F., Barnes, E. L., and Tweardy, D. J. (1996). Quantitative immunohistochemical analysis of transforming growth factor-alpha and epidermal growth factor receptor in patients with squamous cell carcinoma of the head and neck. Cancer *78*, 1284-1292.

Rubin Grandis, J., Melhem, M. F., Gooding, W. E., Day, R., Holst, V. A., Wagener, M. M., Drenning, S. D., and Tweardy, D. J. (1998). Levels of TGF-alpha and EGFR protein in head and neck squamous cell carcinoma and patient survival. J Natl Cancer Inst *90*, 824-832.

Salido, M., Tusquets, I., Corominas, J. M., Suarez, M., Espinet, B., Corzo, C., Bellet, M., Fabregat, X., Serrano, S., and Sole, F. (2005). Polysomy of chromosome 17 in breast cancer tumors showing an overexpression of ERBB2: a study of 175 cases using fluorescence in situ hybridization and immunohistochemistry. Breast Cancer Res *7*, R267-273.

Salomon, D. S., Brandt, R., Ciardiello, F., and Normanno, N. (1995). Epidermal growth factor-related peptides and their receptors in human malignancies. Crit Rev Oncol Hematol *19*, 183-232.

Saltz, L. B., Meropol, N. J., Loehrer, P. J., Sr., Needle, M. N., Kopit, J., and Mayer, R. J. (2004). Phase II trial of cetuximab in patients with refractory colorectal cancer that expresses the epidermal growth factor receptor. J Clin Oncol *22*, 1201-1208.

Sartor, C. I., Zhou, H., Kozlowska, E., Guttridge, K., Kawata, E., Caskey, L., Harrelson, J., Hynes, N., Ethier, S., Calvo, B., and Earp, H. S., 3rd (2001). Her4 mediates ligand-dependent antiproliferative and differentiation responses in human breast cancer cells. Mol Cell Biol *21*, 4265-4275.

Scher, H. I., Sarkis, A., Reuter, V., Cohen, D., Netto, G., Petrylak, D., Lianes, P., Fuks, Z., Mendelsohn, J., and Cordon-Cardo, C. (1995). Changing pattern of expression of the epidermal growth factor receptor and transforming growth factor alpha in the progression of prostatic neoplasms. Clin Cancer Res *1*, 545-550.

Schilder, R. J., Sill, M. W., Chen, X., Darcy, K. M., Decesare, S. L., Lewandowski, G., Lee, R. B., Arciero, C. A., Wu, H., and Godwin, A. K. (2005). Phase II study of gefitinib in patients with relapsed or persistent ovarian or primary peritoneal carcinoma and evaluation of epidermal growth factor receptor mutations and immunohistochemical expression: a Gynecologic Oncology Group Study. Clin Cancer Res *11*, 5539-5548.

Schlessinger, J. (2002). Ligand-induced, receptor-mediated dimerization and activation of EGF receptor. Cell *110*, 669-672.

Schulze, W. X., Deng, L., and Mann, M. (2005). Phosphotyrosine interactome of the ErbB-receptor kinase family. Mol Syst Biol *1*, 2005 0008.

Seelig, S. (1999). Fluorescence in situ hybridization versus immunohistochemistry: importance of clinical outcome. J Clin Oncol *17*, 3690-3692.

Sergina, N. V., Rausch, M., Wang, D., Blair, J., Hann, B., Shokat, K. M., and Moasser, M. M. (2007). Escape from HER-family tyrosine kinase inhibitor therapy by the kinase-inactive HER3. Nature *445*, 437-441.

Shepherd, F. A., Rodrigues Pereira, J., Ciuleanu, T., Tan, E. H., Hirsh, V., Thongprasert, S., Campos, D., Maoleekoonpiroj, S., Smylie, M., Martins, R.,

et al. (2005). Erlotinib in previously treated non-small-cell lung cancer. N Engl J Med *353*, 123-132.

Sheridan, M. T., O'Dwyer, T., Seymour, C. B., and Mothersill, C. E. (1997). Potential indicators of radiosensitivity in squamous cell carcinoma of the head and neck. Radiat Oncol Investig *5*, 180-186.

Shirakabe, K., Wakatsuki, S., Kurisaki, T., and Fujisawa-Sehara, A. (2001). Roles of Meltrin beta /ADAM19 in the processing of neuregulin. J Biol Chem *276*, 9352-9358.

Slamon, D. J., Clark, G. M., Wong, S. G., Levin, W. J., Ullrich, A., and McGuire, W. L. (1987). Human breast cancer: correlation of relapse and survival with amplification of the HER-2/neu oncogene. Science *235*, 177-182.

Slamon, D. J., Leyland-Jones, B., Shak, S., Fuchs, H., Paton, V., Bajamonde, A., Fleming, T., Eiermann, W., Wolter, J., Pegram, M., *et al.* (2001). Use of chemotherapy plus a monoclonal antibody against HER2 for metastatic breast cancer that overexpresses HER2. N Engl J Med *344*, 783-792.

Sliwkowski, M. X., Lofgren, J. A., Lewis, G. D., Hotaling, T. E., Fendly, B. M., and Fox, J. A. (1999). Nonclinical studies addressing the mechanism of action of trastuzumab (Herceptin). Semin Oncol *26*, 60-70.

Smith, I., Procter, M., Gelber, R. D., Guillaume, S., Feyereislova, A., Dowsett, M., Goldhirsch, A., Untch, M., Mariani, G., Baselga, J., *et al.* (2007). 2-year follow-up of trastuzumab after adjuvant chemotherapy in HER2-positive breast cancer: a randomised controlled trial. Lancet *369*, 29-36.

Songyang, Z., Shoelson, S. E., Chaudhuri, M., Gish, G., Pawson, T., Haser, W. G., King, F., Roberts, T., Ratnofsky, S., Lechleider, R. J., and et al. (1993). SH2 domains recognize specific phosphopeptide sequences. Cell *72*, 767-778.

Sorkin, A., Di Fiore, P. P., and Carpenter, G. (1993). The carboxyl terminus of epidermal growth factor receptor/erbB-2 chimerae is internalization impaired. Oncogene *8*, 3021-3028.

Sorkin, A., McClure, M., Huang, F., and Carter, R. (2000). Interaction of EGF receptor and grb2 in living cells visualized by fluorescence resonance energy transfer (FRET) microscopy. Curr Biol *10*, 1395-1398.

Sorlie, T., Tibshirani, R., Parker, J., Hastie, T., Marron, J. S., Nobel, A., Deng, S., Johnsen, H., Pesich, R., Geisler, S., *et al.* (2003). Repeated observation of

breast tumor subtypes in independent gene expression data sets. Proc Natl Acad Sci U S A *100*, 8418-8423.

Stryer, L., and Haugland, R. P. (1967). Energy transfer: a spectroscopic ruler. Proc Natl Acad Sci U S A *58*, 719-726.

Sunnarborg, S. W., Hinkle, C. L., Stevenson, M., Russell, W. E., Raska, C. S., Peschon, J. J., Castner, B. J., Gerhart, M. J., Paxton, R. J., Black, R. A., and Lee, D. C. (2002). Tumor necrosis factor-alpha converting enzyme (TACE) regulates epidermal growth factor receptor ligand availability. J Biol Chem *277*, 12838-12845.

Suthers, G. K. (2007). Cancer risks for Australian women with a BRCA1 or a BRCA2 mutation. ANZ J Surg *77*, 314-319.

Tabernero, J. (2007). The role of VEGF and EGFR inhibition: implications for combining anti-VEGF and anti-EGFR agents. Mol Cancer Res *5*, 203-220.

Tan, M., Grijalva, R., and Yu, D. (1999). Heregulin beta1-activated phosphatidylinositol 3-kinase enhances aggregation of MCF-7 breast cancer cells independent of extracellular signal-regulated kinase. Cancer Res *59*, 1620-1625.

Tannock, I., Hill, R., Bristow, R., and Harrington, L. (2005). The basic science of oncology: The McGraw-Hill Companies).

Taub, R., Kirsch, I., Morton, C., Lenoir, G., Swan, D., Tronick, S., Aaronson, S., and Leder, P. (1982). Translocation of the c-myc gene into the immunoglobulin heavy chain locus in human Burkitt lymphoma and murine plasmacytoma cells. Proc Natl Acad Sci U S A *79*, 7837-7841.

Todd, R., Donoff, B. R., Gertz, R., Chang, A. L., Chow, P., Matossian, K., McBride, J., Chiang, T., Gallagher, G. T., and Wong, D. T. (1989). TGF-alpha and EGF-receptor mRNAs in human oral cancers. Carcinogenesis *10*, 1553-1556.

Toth, P. T., Ren, D., and Miller, R. J. (2004). Regulation of CXCR4 receptor dimerization by the chemokine SDF-1alpha and the HIV-1 coat protein gp120: a fluorescence resonance energy transfer (FRET) study. J Pharmacol Exp Ther *310*, 8-17.

Valeur, B. (2002). Molecular Fluorescence : Principles and Applications, In (Wiley-vch).

Van de Vijver, M. J., Kumar, R., and Mendelsohn, J. (1991). Ligand-induced activation of A431 cell epidermal growth factor receptors occurs primarily by an autocrine pathway that acts upon receptors on the surface rather than intracellularly. J Biol Chem *266*, 7503-7508.

van der Geer, P., Hunter, T., and Lindberg, R. A. (1994). Receptor protein-tyrosine kinases and their signal transduction pathways. Annu Rev Cell Biol *10*, 251-337.

van der Geer, P., and Pawson, T. (1995). The PTB domain: a new protein module implicated in signal transduction. Trends Biochem Sci *20*, 277-280.

Vecchi, M., and Carpenter, G. (1997). Constitutive proteolysis of the ErbB-4 receptor tyrosine kinase by a unique, sequential mechanism. J Cell Biol *139*, 995-1003.

Vincent-Salomon, A., MacGrogan, G., Couturier, J., Arnould, L., Denoux, Y., Fiche, M., Jacquemier, J., Mathieu, M. C., Penault-Llorca, F., Rigaud, C., *et al.* (2003). Calibration of immunohistochemistry for assessment of HER2 in breast cancer: results of the French multicentre GEFPICS study. Histopathology *42*, 337-347.

Vogel, C. L., Cobleigh, M. A., Tripathy, D., Gutheil, J. C., Harris, L. N., Fehrenbacher, L., Slamon, D. J., Murphy, M., Novotny, W. F., Burchmore, M., *et al.* (2002). Efficacy and safety of trastuzumab as a single agent in first-line treatment of HER2-overexpressing metastatic breast cancer. J Clin Oncol *20*, 719-726.

Vogt, P. K. (1993). Cancer genes. West J Med *158*, 273-278.

Vousden, K. H., and Prives, C. (2005). P53 and prognosis: new insights and further complexity. Cell *120*, 7-10.

Walker, R. A. (2006). Quantification of immunohistochemistry--issues concerning methods, utility and semiquantitative assessment I. Histopathology *49*, 406-410.

Wallasch, C., Weiss, F. U., Niederfellner, G., Jallal, B., Issing, W., and Ullrich, A. (1995). Heregulin-dependent regulation of HER2/neu oncogenic signaling by heterodimerization with HER3. Embo J *14*, 4267-4275.

Wang, S., Saboorian, M. H., Frenkel, E., Hynan, L., Gokaslan, S. T., and Ashfaq, R. (2000). Laboratory assessment of the status of Her-2/neu protein and oncogene in breast cancer specimens: comparison of

immunohistochemistry assay with fluorescence in situ hybridisation assays. J Clin Pathol *53*, 374-381.

Wang, S. E., Narasanna, A., Perez-Torres, M., Xiang, B., Wu, F. Y., Yang, S., Carpenter, G., Gazdar, A. F., Muthuswamy, S. K., and Arteaga, C. L. (2006). HER2 kinase domain mutation results in constitutive phosphorylation and activation of HER2 and EGFR and resistance to EGFR tyrosine kinase inhibitors. Cancer Cell *10*, 25-38.

Wen, Q. H., Miwa, T., Yoshizaki, T., Nagayama, I., Furukawa, M., and Nishijima, H. (1996). Prognostic value of EGFR and TGF-alpha in early laryngeal cancer treated with radiotherapy. Laryngoscope *106*, 884-888.

Wiley, E. L., and Diaz, L. K. (2004). High-quality HER-2 testing: setting a standard for oncologic biomarker assessment. Jama *291*, 2019-2020.

Williams, C. C., Allison, J. G., Vidal, G. A., Burow, M. E., Beckman, B. S., Marrero, L., and Jones, F. E. (2004). The ERBB4/HER4 receptor tyrosine kinase regulates gene expression by functioning as a STAT5A nuclear chaperone. J Cell Biol *167*, 469-478.

Wood, E. R., Truesdale, A. T., McDonald, O. B., Yuan, D., Hassell, A., Dickerson, S. H., Ellis, B., Pennisi, C., Horne, E., Lackey, K., *et al.* (2004). A unique structure for epidermal growth factor receptor bound to GW572016 (Lapatinib): relationships among protein conformation, inhibitor off-rate, and receptor activity in tumor cells. Cancer Res *64*, 6652-6659.

Wolff, A. C., Hammond, M. E., Schwartz, J. N., Hagerty, K. L., Allred, D. C., Cote, R. J., Dowsett, M., Fitzgibbons, P. L., Hanna, W. M., Langer, A., *et al.* (2007). American Society of Clinical Oncology/College of American Pathologists guideline recommendations for human epidermal growth factor receptor 2 testing in breast cancer. J Clin Oncol *25*, 118-145.

Worthylake, R., Opresko, L. K., and Wiley, H. S. (1999). ErbB-2 amplification inhibits down-regulation and induces constitutive activation of both ErbB-2 and epidermal growth factor receptors. J Biol Chem *274*, 8865-8874.

Wu, P., and Brand, L. (1994). Resonance energy transfer: methods and applications. Anal Biochem *218*, 1-13.

Xu, F. J., Stack, S., Boyer, C., O'Briant, K., Whitaker, R., Mills, G. B., Yu, Y. H., and Bast, R. C., Jr. (1997). Heregulin and agonistic anti-p185(c-erbB2) antibodies inhibit proliferation but increase invasiveness of breast cancer cells

that overexpress p185(c-erbB2): increased invasiveness may contribute to poor prognosis. Clin Cancer Res *3*, 1629-1634.

Yamanaka, Y., Friess, H., Kobrin, M. S., Buchler, M., Beger, H. G., and Korc, M. (1993). Coexpression of epidermal growth factor receptor and ligands in human pancreatic cancer is associated with enhanced tumor aggressiveness. Anticancer Res *13*, 565-569.

Yarden, Y., and Sliwkowski, M. X. (2001). Untangling the ErbB signalling network. Nat Rev Mol Cell Biol *2*, 127-137.

Yasuda, R. (2006). Imaging spatiotemporal dynamics of neuronal signaling using fluorescence resonance energy transfer and fluorescence lifetime imaging microscopy. Curr Opin Neurobiol *16*, 551-561.

Yaziji, H., Goldstein, L. C., Barry, T. S., Werling, R., Hwang, H., Ellis, G. K., Gralow, J. R., Livingston, R. B., and Gown, A. M. (2004). HER-2 testing in breast cancer using parallel tissue-based methods. Jama *291*, 1972-1977.

Zhou, B. B., Peyton, M., He, B., Liu, C., Girard, L., Caudler, E., Lo, Y., Baribaud, F., Mikami, I., Reguart, N., *et al.* (2006). Targeting ADAM-mediated ligand cleavage to inhibit HER3 and EGFR pathways in non-small cell lung cancer. Cancer Cell *10*, 39-50.

Zhou, W., and Carpenter, G. (2000). Heregulin-dependent trafficking and cleavage of ErbB-4. J Biol Chem *275*, 34737-34743.